Faculty of Engineering
Department of Architecture and Built Environment

Digital Modelling, Analysis and Fabrication of Deployable Structures for Kinetic Architecture

Daniel Enrique Gómez Lizcano

Architect, MSc in Construction

A thesis submitted to the University of Nottingham

for the degree of Doctor of Philosophy [PhD]

February 2021

ACKNOWLEDGEMENTS

This research was funded in Colombia by the Administrative Department of Science, Technology, and Innovation COLCIENCIAS[1], through a forgivable educative loan for supporting doctoral studies abroad: Call No 728 of 2015.

I gratefully acknowledge my PhD supervisory team at the University of Nottingham: Prof. Paolo Beccarelli, Prof. Davide De Focatiis, and the Emeritus Prof. John Chilton for their scientific expertise and guidance. I would also like to recognise my master's thesis supervisor in Colombia: Maria Claudia Villate for the essential education in the topic of deployable structures. Next, thanks to my dearest friends for their continuous motivation, and finally, special recognition for my family's unconditional support.

[1] On the 5th of December 2019, COLCIENCIAS was officially converted into the Ministry of Science, Technology, and Innovation MINCIENCIAS.

ABSTRACT

As a result of the human mobility needs and the progressive technological advances over time, varied deployable structures utilising scissors and sliding mechanisms have evolved for transformable and transportable functionalities. In recent decades, this topic has piqued the interest of professionals within several fields - the Arts, Industrial Design, Architecture and Engineering - leading to an extensive database of publications in journals, conference proceedings, books, and patents.

Gaps between theory and practice can sometimes restrict prospective applications due to structural complexities compromising the material capacities during installation, service, or dismantling. This thesis aims to develop alternative solutions for stabilising the angular distortions of quadrangular expandable grids, controlling the deflection limits, and enhancing the structural behaviour of large-span constructions requiring transitory processes, with a rapid installation or a frequent relocation.

The expertise given by other authors in the literature review is the framework to understand and recreate a variety of concepts. This work employs the latest digital modelling tools to evaluate complex projects from the early design phases, collecting real-time data from parametric environments, movement simulations, and simplified structural predictions. In addition, physical to-scale models are created by additive manufacturing and standard portable tools, granting rapid testing.

A holistic and reciprocal method is necessary to obtain an overall spatial evaluation, validity, and reliability. The geometry is categorised into eight cases to study the viability of automatically offering proper strength, safety, and rigidity through diagonal stress-free mechanisms, rectifying the primary instabilities during the size and shape transitions.

On the other side, although permanent and static structures follow the Eurocodes & related building standards, temporary and mobile variants may require identical severe conditions. A hypothetical transportable tent compares the stabilisation of diagonal scissors and triangulations by passive cables; later, tensioned locking devices target to control climate loads deflection limits at the deployed position.

As a result of this research, a complete design process contributed to developing successful solutions for mobile architectural applications, maintaining a degree of freedom. After discussing the efficiency of the setting-up procedures, the suggested active-cables outline demonstrated superior structural performance to every load scenario, can prevent excessive time usage during manual locking and facilitates the components adjusting task from the ground level. Related transformable umbrellas may adopt the proposed structural analysis methodology; however, researchers should correlate detailed engineering studies and full-scale testing to validate practical results.

CONTENTS

LIST OF FIGURES

1 INTRODUCTION

Over history, civil constructions have transcended from static objects to dynamic systems integrating architecture and the environment. Whereas a large context relates the motion experience in the built form and space: *portable, flexible, or adaptive architecture*, the scientific concept of a *deployable structure* comprises various prefabricated systems and their capacity to change from a compact to an expanded configuration. Size and shape variations can occur, thus offering movement transitions towards an operational state where it can withstand its own weight in addition to external loads (Gantes, 2011).

Typical examples include: scissor mechanisms, origami, cable-membrane coverings, inflatable/pneumatic devices, and some tensegrity structures, among many others. According to the chronological and critical review given by Fenci and Curie (2017), a consistent classification of the existent family types remains in constant evolution and diversification, regardless of the efforts to associate these structures over the past decades. Likewise, Hanaor and Levy (2001) created the most exhaustive and cited work, although more modern developments and technologies are lacking.

Elmokadem, et al. (2018) reported three main application categories regarding the kinetic architecture: *I structure systems, II interiors,* and *III facades*. Users can dismount *transportable* buildings to a compact bundle, and *transformable* solutions [e.g., a roof or a façade] may have a permanent location but produce an adaptive response to the changing weather conditions (Rodriguez & Chilton, 2004; 2006).

This thesis considers *deployable kinetic structures using scissors and sliding mechanisms*. It is motivated by producing lightweight geometries with pliable or variable formats, the opportunity to keep a single degree of freedom, and the speed of installation for mobile and temporary applications at a large scale. Besides, the modularity and the industrialised production fosters recycling, reuse, diminish the generation of building waste, and avoid the need for new resources.

An intrinsic requirement is to pre-design their dual functionality for obtaining a precise and efficient performance (Alegria Mira, et al., 2012): (*I*) during deployment or folding to produce the size and shape alterations (*kinematic mechanism*), and (*II*) at the end state to bear and transfer loads (*structural system*). An additional -*inactive state*- occurs when closed in a compact size, easing transportation or storage.

The mutual relationship between geometry/kinematics/structural response is assessed for early project stages through experimental work in the most recent computational & manufacturing methods, thus facilitating future detailed research.

1.1 Deployable structures using scissors and sliding mechanisms

A deployable structure incorporating scissors and sliding mechanisms could benefit from maintaining a single degree of freedom [1DOF], transmitting the movement simultaneously and uniformly between its components. In agreement with Villate (2008, p. 43 & 69), the geometry principles can be generalised by at least two basic polygons:

- A deformable triangle with hinged bars, plus a slidable component.

- Quadrilaterals with all bars articulated. The geometry becomes fixed if an additional bar is incorporated to triangulate the mechanism.

Figure 1.1 shows planar linkages preserving a single degree of freedom. These are explained further by the Grübler–Kutzbach equation in Chapter 3.2.1; however, the mobility design cannot be guaranteed straightforward in all three-dimensional linkages.

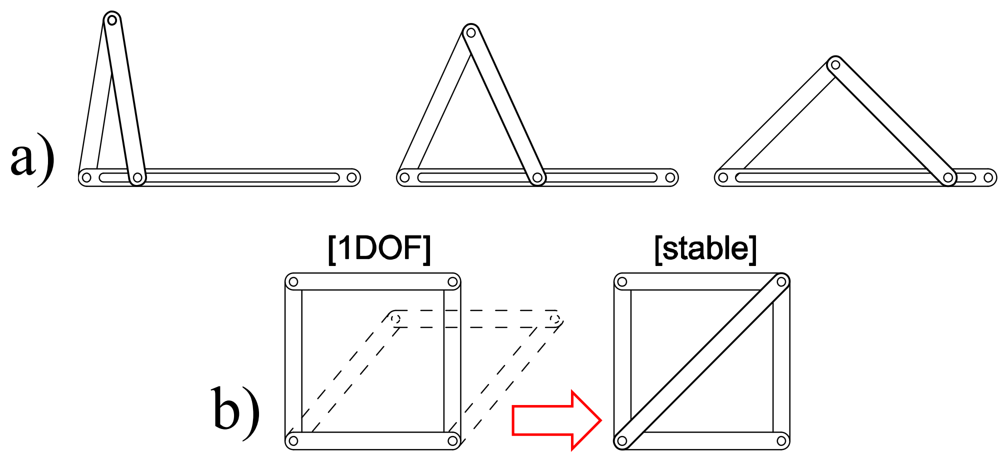

Figure 1.1 *Deformable polygons: (a) Triangles, (b) Quadrilaterals.*

The slidable triangle assemblage does not have many applications for deployable structures, but Hernandez (1987) indicated a relevant umbrella shape category for its understanding; likewise, the deformable quadrilaterals criterion can be associated with a series of scissor components. Both mechanisms are complementary and may be used to produce telescopic legs or a mast to elevate the covering textile in a scissor structure tent.

Notwithstanding the advantages that scissors and sliding mechanisms can offer, the theoretical possibilities encountered over more than 50 years of evolution has not produced many projects at a large scale. The primary limitations are attributable to the kinetic performance of specific geometries, the covering fabric compatibility, the lack of specifications for temporal vs permanent structures within the existing international building codes, and the high manufacturing cost throughout the second half of the twentieth century (Pellegrino & Guest, 2000; De Temmerman, 2007; Alegria Mira, 2014).

Nowadays, it is feasible to examine these complexities from early design phases through Digital Fabrication methods: *Computer-Aided Design* [CAD], *Computer-Aided Engineering* [CAE], and *Computer-Aided Manufacturing* [CAM]. In the challenging decision-making process, it is worth integrating 3D modelling and movement simulations, examining the correct transmission of forces between components, defining the covering textile characteristics, recreating environmental parameters on virtual models, and further testing in physical models.

There is an opportunity to continue updating the construction sector with advanced technological innovations. Deployable systems can be understood not only as a structural skeleton but as the whole building, incorporating slim components with a high degree of part complexity, evaluating the use of lightweight materials, and offering viable mechanisms for different use and size conditions.

Figure 1.2 synthesises the evolution of the most relevant Information Technology [IT] tools for digital manufacturing processes and the correlated scissors concept, as it covers a broader category for the present study in deployable structures:

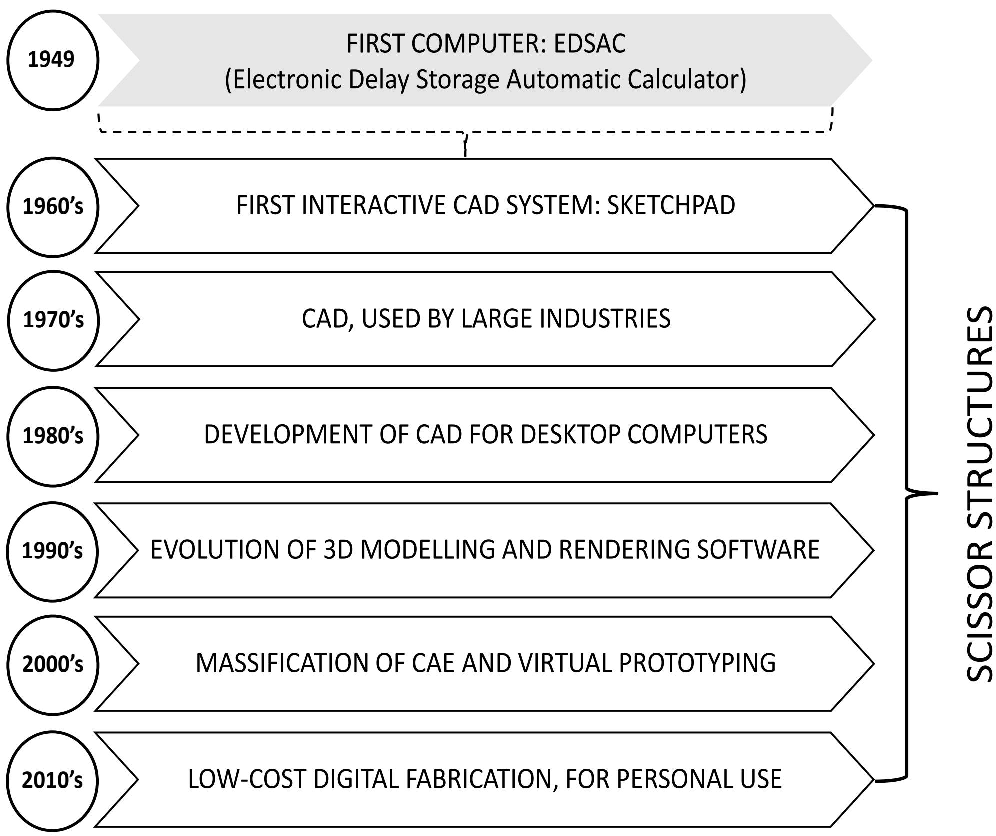

Figure 1.2 *Correlation between relevant IT tools and scissor structures evolution.*

1.2 Scope and research questions

1.2.1 Scope

My interest in deployable structures through scissors and sliding mechanisms arose during prior research experiences, searching through the change of form, function and use of buildings, attractive criteria to adapt human activity and satisfying societies' habitability needs regarding the built environment. Several typologies were replicated in software and scale models based on a comprehensive literature review, among other personal proposals (Gómez Lizcano, 2012; 2013). After this process, I understood the complexity and the existing limitations between theory and constructability.

On the one side, angulated scissors (Hoberman, 1990) can offer compatible movements and size variations that maintain the figure's radius. However, I decided to keep them out of the scope of the current study since their low compactness against polar and translational scissors would restrict the transportation capacity.

Following Gantes classification (Gantes, 2011), this work focuses on earth-based deployable structures, primarily used for temporary/relocatable construction and emergencies. Instead of the *self-locking* or *bi-stable* scissors, I prefer stress-free mechanisms in the collapsed, moving, and the final deployed position, so manual locking is necessary to fix the desired configuration. (Gantes, et al., 1989).

Since digital fabrication methods became more accessible during the 2010s (Figure 1.2), it is explored in virtual environments and scale models the functionality of the main mechanical components, the structural capacities, and the constructive determinants in terms of conceptual design. On the other hand, it is tested the covering membrane compatibility during movements, but the material specifications and the load interaction with the scissor structure are not examined in depth.

The data collected is reviewed from an architectural perspective and is an introductory analysis of early project phases. It is intended to be a decision-making source for further detailed engineering methods, according to precise needs, and before its implementation on a full scale.

1.2.2 Research questions

Although some of the existing scissor structure products incorporate the concept of the bi-stable or self-locking mechanism, the use of flexible material technologies increases the system complexity during the incompatible deployment/folding processes and lower the load-bearing capacity in the open conformation. In contrast, small to medium-scale geometries with a quadrangular subdivision and stress-free scissors are often complemented through diagonal cables acting in the final state exclusively, or with additional post-installed bars for overcoming the lack of in-plane triangulation.

Estimating structural efficiency and reliability over the expected life cycle is essential in constructions with larger scales, especially on transitory usages demanding a frequent re-location or rapid installation. Besides, as the stability problems can be extreme during the size and shape transitions, the system requires proper strength, safety and rigidity to prevent failures.

Finding new ways to incorporate stress-free stiffening components using cross-braced scissors or simply by articulated bars may simplify the structural analysis procedure, optimise the installation time, and reduce the working at heights risk when adjusting all the components. Moreover, complementary tensioned locking devices could effectively control climate loads deflection limits, bringing major serviceability strength at the deployed position and fulfilling the building codes when appropriate.

1.3 Aims and objectives

By exploring the fundaments of classic quadrangular expandable grids featuring a stress-free motion, and with the support of Digital Fabrication methods, this thesis aims to develop alternative solutions for stabilising the angular distortions, controlling the deflection limits, and enhancing the structural behaviour of large-span constructions exposed to transitory usages. The intention is to integrate 1DOF deployable structures on transportable and transformable architecture, such as a temporary shelter or an umbrella roof.

The main objectives are:

1. To review the literature regarding deployable structures using scissors & sliding mechanisms, identifying the strengths and weaknesses in architectural contexts.

2. To describe key principles for obtaining 1DOF structures and the methods for granting rapid testing & validation of the study from the early design phases.

3. To examine the kinematical functionality of the proposed geometries, employing 2D & 3D modelling, parametric design, and mechanical simulation.

4. To produce scale models by 3D printing & low-cost manufacturing and provide elemental considerations for full-scale constructions based on the potential outcomes.

5. To carry out preliminary analysis methods by specialised structural engineering software, tailoring the main components according to conceptual design conditions and the locking devices for controlling moving out of position when subjected to external forces.

1.4 Research outline

Chapter 2 introduces a comprehensive characterisation of deployable structures using scissors and sliding mechanisms. It provides a historical context summary by citing a list of authors and their work, comments on the experimental prototypes, associated products, and patents to determine the fundamental variables for the thesis exploration.

Chapter 3 describes the mechanical formulation of pantograph structures, the digital modelling methods to simplify the understanding of geometrical kinematics, the employed manufacturing resources to test reduced models, and the early-design parametric structural assessment conditions, considering European technical standards in construction.

Chapter 4 studies eight cases, starting from prior-art representative quadrangular base prisms. The conceptualisation procedure emphasises two- and three-dimensional sketches on AutoCAD/Rhinoceros®, the parametric design environment Grasshopper™ and movement simulation via the assembly environment of Autodesk Inventor. The patterns connectivity is further commented for producing spatially rigidised geometries.

Chapter 5 inspects the fabricated scale models and documents the advantages or disadvantages of each situation. It envisages potential architectural uses for roofs, transportable tents, or transformable umbrellas, designed from flat, simple or double curvature surfaces. Later, it is provided with a synthesis of the complementary criteria for full-scale buildings.

Chapter 6 conducts preliminary static load simulations through Finite Element Analysis in the structural engineering tool provided by the plug-in Karamba3D. Predictions are compared to a scale-model load testing and later evaluated on full-scale theoretic structures. In the end, a generalised methodology for supplementary evaluations or similar conceptual design improvements is included.

Chapter 7 presents the main thesis conclusions given the objectives achievement, contributions to the research field, lessons learned, limitations and recommendations for further work.

2 REVIEW OF LITERATURE

2.1 Introduction

The purpose of this chapter is to revise relevant prior research, relating the primary deployable structure notions for transformable and transportable functionalities: (I) Sliding-pantograph mechanisms to umbrellas, and (II) Scissor structures to roofs or shelters. It is organised in chronological order, bearing in mind mobile and rapidly assembled architecture since ancient times; Sánchez & Escrig (1997) indicated specific examples, among others:

- Sunlight parasols in ancient Egypt over 3 thousand years ago and waterproof leather umbrellas discovered in 11th century BC China.
- Folding chairs or stools in the Nordic Bronze Age, Ancient Egypt, Minoan Greece, and Ancient Rome.
- Portable Yurts by nomadic groups in Central Asia.
- Military siege machines and load lifting artefacts in the Middle Ages.
- Machines, mobile bridges, and umbrellas in the Renaissance by Leonardo Da Vinci.

The umbrellas included in this thesis could integrate both main principles governing 1DOF deformable polygons mentioned in Chapter 1: slidable triangles and articulated quadrilaterals. A series of two-dimensional sliding-pantograph mechanisms around a concentric axis or pole produces a typical geometry; the contour remains non-connected, so the set is laterally unstable.

When anchored to the ground, they require a detailed structural analysis to withstand the impact of different wind loads and avoid the overturning effect caused by possible overexertions at the base. Figure 2.1 represents the most regularly used fixed and transportable umbrellas.

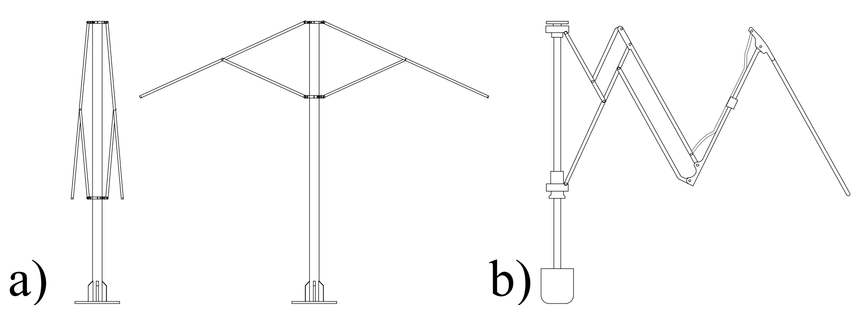

Figure 2.1 *Umbrella-like geometries: (a) Standard folding ribs, (b) Multi folding ribs.*

Likewise, a scissor unit consists of bar pairs connected at an intermediate node through a revolute joint, allowing single-axis rotation, no translation, or sliding linear motion. In scissor linkages, each bar is then interconnected to others through pivots at their end nodes, maintaining a synchronised mechanical movement; these deployable structures are alternatively denominated Lazy-Tongs, Pantographs or Scissor-Like Elements [SLEs] by authors.

Varying the bars length, shape, and the scissors intermediate node positioning can produce different configurations. Figure 2.2 shows the most common two-dimensional scissor structures with an architectural utility:

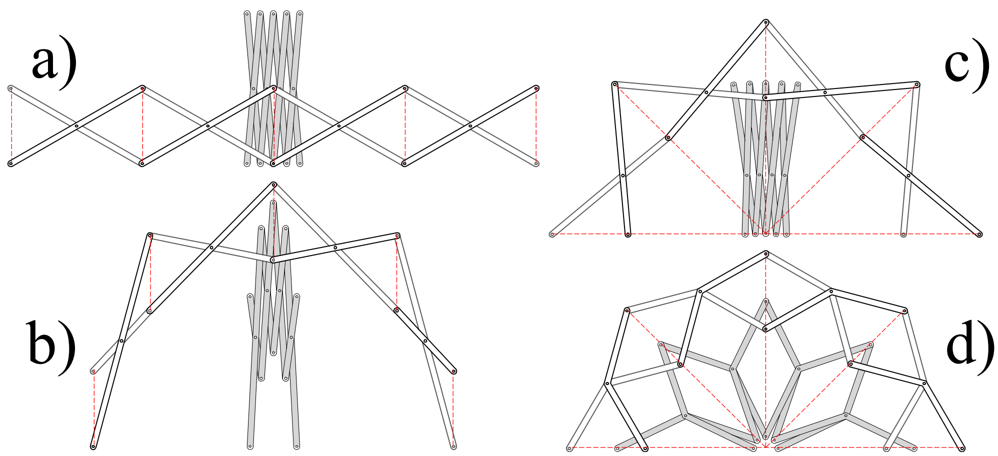

Figure 2.2 *Main two-dimensional scissor linkages with architectural utility: (a) Plane translational units, (b) Curved translational units, (c) Polar units, (d) Angulated units.*

Plane translational units: It comprises pairs of straight beams with equal length, pivoted on its middle node. The imaginary unit lines linking the upper and lower end nodes stay parallel during rectilineal deployments.

Curved translational units: It comprises pairs of straight beams with unequal length, which are pivoted on its middle node. The imaginary unit lines linking the upper and lower end nodes stay parallel during slanted or curved deployments.

Polar units*:* It comprises pairs of straight beams with equal length, which are eccentrically pivoted. The imaginary unit lines linking the upper and lower end nodes intersect at a point, with an angle that varies during curved deployments.

Angulated units*:* It comprises pairs of beams that are characterised for having a specific kink angle, equal length, and pivots on its middle node. The imaginary unit lines linking the upper and lower end nodes intersect at a point, with a constant angle during curved deployments.

Note: The general description of the scissor unit types above refers to the graphic and may differ from other less used variations.

2.2 Representative modern variations of traditional umbrellas

Contrasting the classic umbrellas having a bowl configuration, George H. Peake patented a collapsible hyperbolic paraboloid (Peake, 1966). The creation claimed to be an improved solution due to resisting high wind gusts and keeping the membrane in proper tension, avoiding the possibility of getting an inverted shape [Figure 2.3]. The frame has the capacity of being reconfigurable to vary the curvature depth by including elongated rods or tubes, in addition to joints with rotational movement.

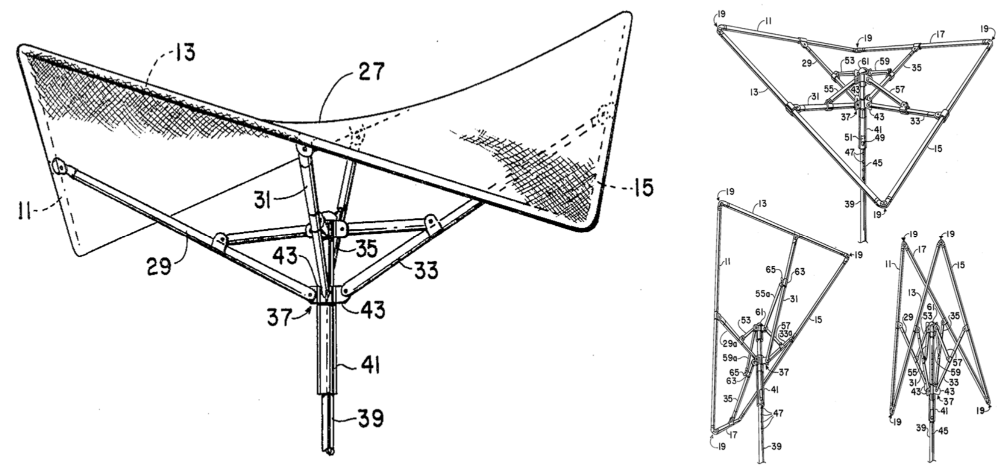

Figure 2.3 *Collapsible hyperbolic paraboloid umbrella. (Peake, 1966)*

Despite the fact that there are no known commercial references of Peake's invention, it is now possible to find diverse Hypar or Sail-like shape parasols using standard pantographs. An example was proposed by Gendriesch, et al. (2004) and is known as *STRUCTURELAB S1* (StructureLab GmbH, 2006-2010). The invention placed the canopy area below the supporting structure, alternating high and low points to create a clean ceiling for the observer; however, the wind and vertical load resistance is limited due to the absence of contour rigidisation.

Figure 2.4 illustrates an embodiment possibility.

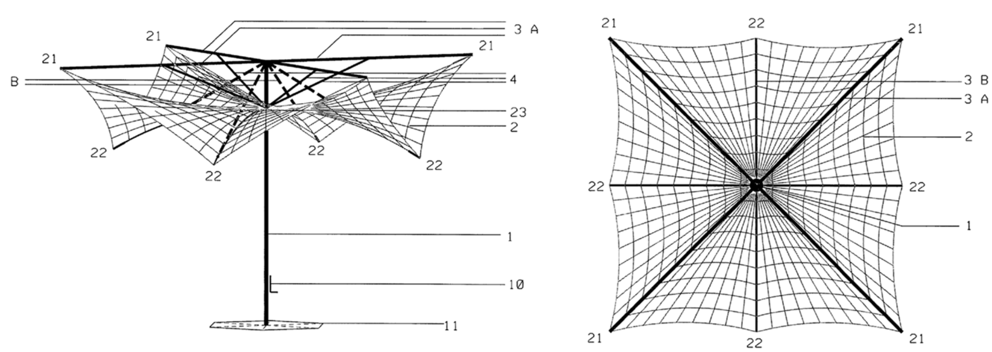

Figure 2.4 *A regular square with eight vertices: perspective and top view. (Gendriesch, et al., 2004)*

On the other hand, Frei Otto, and Bodo Rash as the project director, constructed the first large-scale convertible umbrella for the Federal Garden Exhibition in 1971 [Figure 2.5]. It corresponds to a 19m wide and 9.5m height design with a novel shape feature on the ribs system to reduce the arms-length telescopically. The controlled curved trajectory allowed independent movement sequences between umbrellas, even when overlapping (Otto & Rasch, 1995).

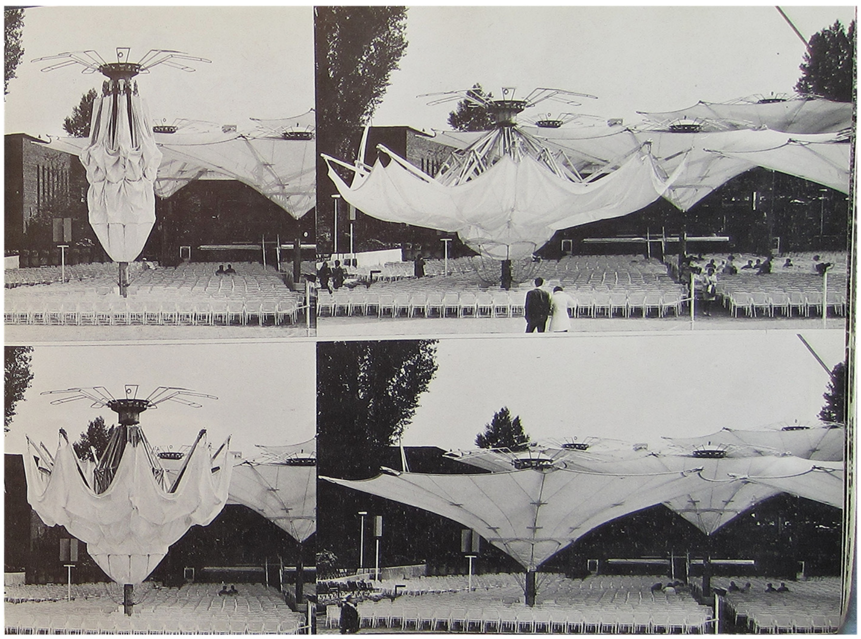

Figure 2.5 *Federal Garden Exhibition umbrellas. (Otto, 1972)*

Bodo Rasch and his team continued for several years later in the company *SL Rasch GmbH*, combining a telescopic mast solution with optional variations in the arms folding system. Their advanced construction engineering has produced umbrellas of different sizes, structural geometry, and ornamentation.

Figure 2.6 represents different folding system trajectories.

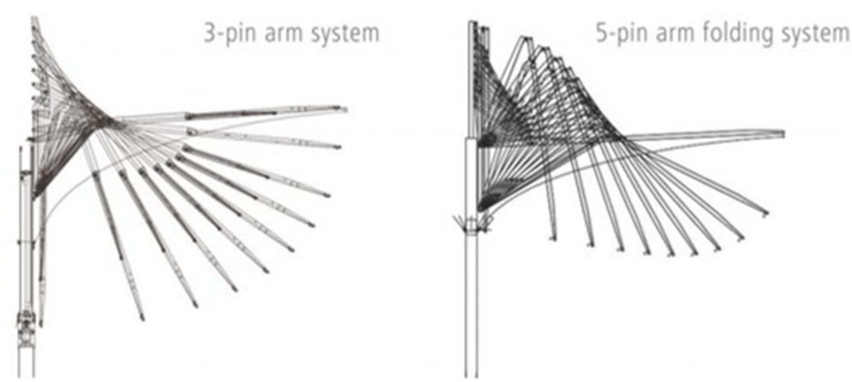

Figure 2.6 *Folding system types. (SL-Rasch GmbH Special & Lightweight Structures, 2018)*

Continuous improvements have led them to apply for related international patents (Rasch, 1989; 2010), (Rasch & Bradatsch, 1995; 2007), (Willim, et al., 2004). Projects in Saudi Arabia like the 5x5m solar-powered prototypes in 1987, or the 17x18m forked arms umbrellas in 1992 for the Prophet´s Holy Mosque at Madinah, were early applied examples of their climate-control innovations [Figure 2.7].

a)  b) 

Figure 2.7 *(a) Solar cells built into the umbrella arms (b) Umbrellas at the inner courtyard of the Prophet's Holy Mosque Madinah. (Otto & Rasch, 1995)*

Depending on the dimensions, the environment and the surrounding objects, detailed engineering should be performed to simultaneously evaluate the global forces acting on umbrellas [drag forces, lift forces and overturning moment at the base of the mast], including computer simulations, wind tunnel experiments on models and full-scale prototypes. Related research has been performed by Haug, et al. (2003), Michalski, et al. (2007; 2011; 2015).

Figure 2.8 displays the largest and most challenging project so far:

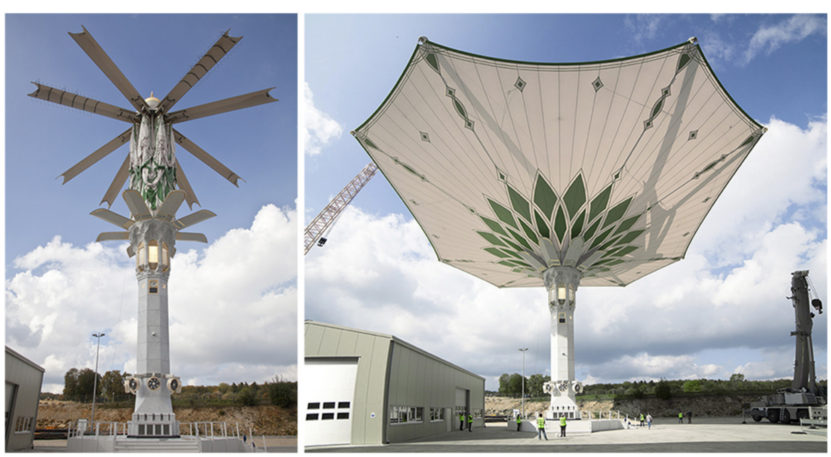

Figure 2.8 *An umbrella with a diameter of over 50 meters. (SL-Rasch GmbH Special & Lightweight Structures, 2018)*

Instead of the umbrellas that remain permanently anchored in situ, Klaus Becher theorised a tilting mechanism to facilitate the transport and standing of a large shelter [Figure 2.9]. The rigidity of the supporting post is guaranteed, and the forces are correctly transferred to the linked platform, providing a high degree of safety during the entire elevation or lowering ranges. An easy and quick covering can be built by a single person or a maximum of two, regardless of its relative weight and size (Becher, 1977).

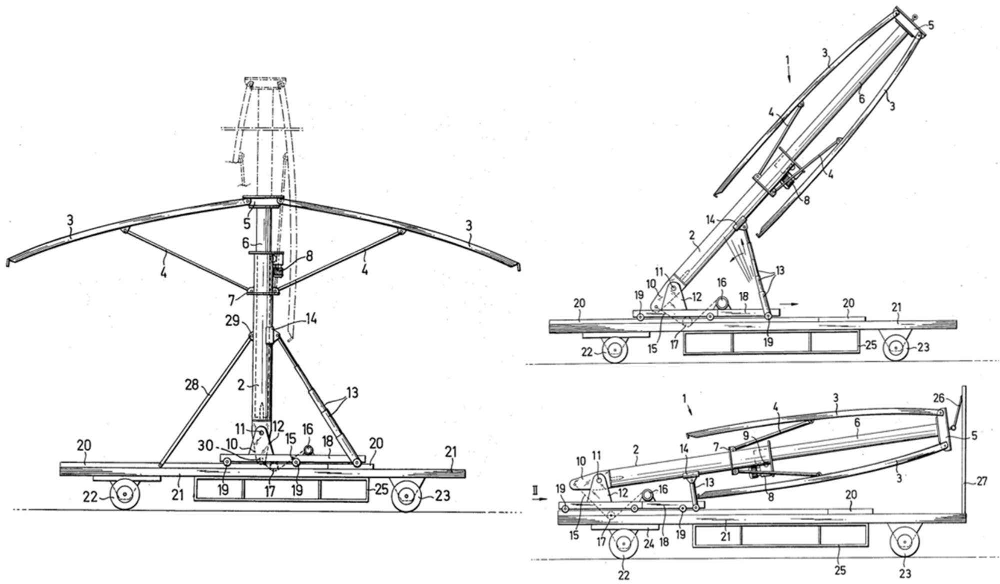

Figure 2.9 *Large shelter umbrella. (Becher, 1977)*

The Austrian specialised company in open-air gastronomy products, *J. Meissl GmbH*, has adopted a similar technique for rapidly obtaining sophisticated transportable bars and giant umbrellas with up to 113 m² of covered area. This mobility capacity proves to be mainly advantageous for temporal constructions in exhibitions and fairs.

As seen in Figure 2.10, a removable trailer helps to re-locate and tilt the structure using a hydraulic lift. At the same time, the bar flooring deck and the furniture brings support as stabiliser and counterweight, so avoiding the need for foundations.

Figure 2.10 *Umbrella bars with Giant Umbrellas. (J. Meissl GmbH, 2019)*

Alternatively, an extensive covered area from 25 to 36 m² can be installed by human force. A wheeled bar facilitates the transportation method, with the umbrella compactly packaged [Figure 2.11].

Figure 2.11 *Mobile Bar. (J. Meissl GmbH, 2019)*

Under the trademark *ROBUS* ®, a new product is being produced combining the properties of pantographs and umbrellas. *ROBUS Inc.* is a Canadian -based Company founded in 2016, operating from Canada/London/New York offices, and partnership with manufacturing facilities worldwide. This company has divisions for the military, commercial interests, hunting, disaster relief, medical care, and outdoor events.

Figure 2.12 shows the installation process through a packaged trailer and hydraulic power, as it was reported in the WIPO [PCT] patent application. For diameters under 20m, it can be operational in 5 to 10 minutes with the assistance of 1-2 workers and can withstand winds up to 120km/h; sizes up to 45m in diameter are possible with further technical specifications (Robus Shelters Inc., 2019).

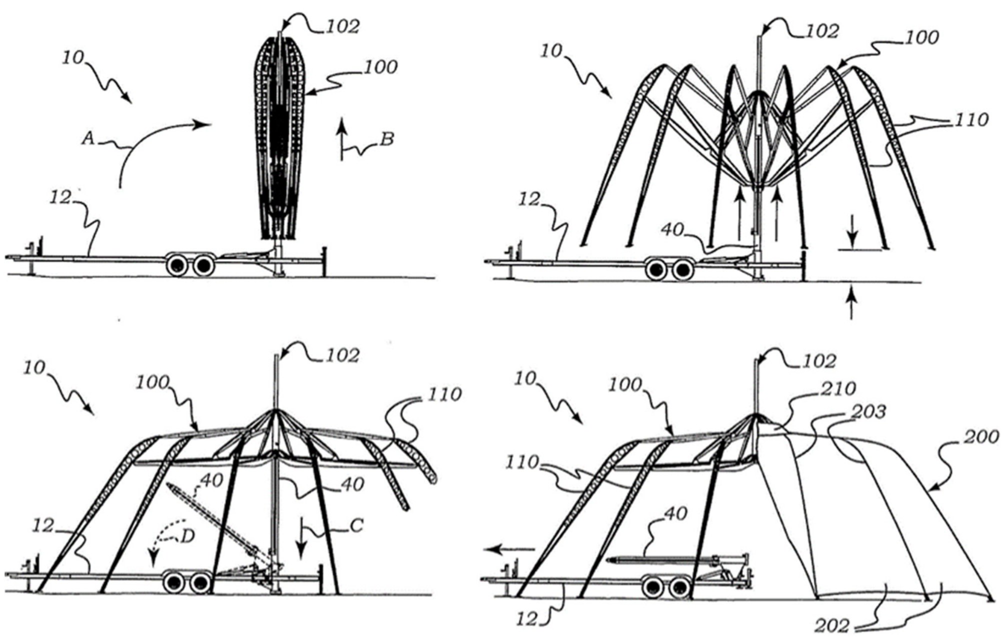

Figure 2.12 *Mobile shelter comprising an umbrella-like collapsible marquee. (Bouchard, 2004)*

2.3 Selected authors in scissor structures and realisations

2.3.1 Early developments

From the 20th century, the first remarkable author is Guy St Barbe Sladen Watkins and the patent "Improvement Supports for Tents Marquees Temporary Bridges and other Portable Structures" (Watkins, 1914), [Figure 2.13]. The described advantage is to produce obstruction-free articulated constructions, avoiding the need for internal poles or other vertical supports that might affect the usable area.

Instead of keeping a straight line of an ordinary lattice formation, the crossed paired members are pivoted in such a way that gradually forms a curved roof. Tension or compression resisting devices between the ridge and the eaves rigidise the structure; alternatively, the arch bars can be locked when they abut to others. The resulting geometry is deployable only in two dimensions and needs extra working on-site for bracing and tying all the arches.

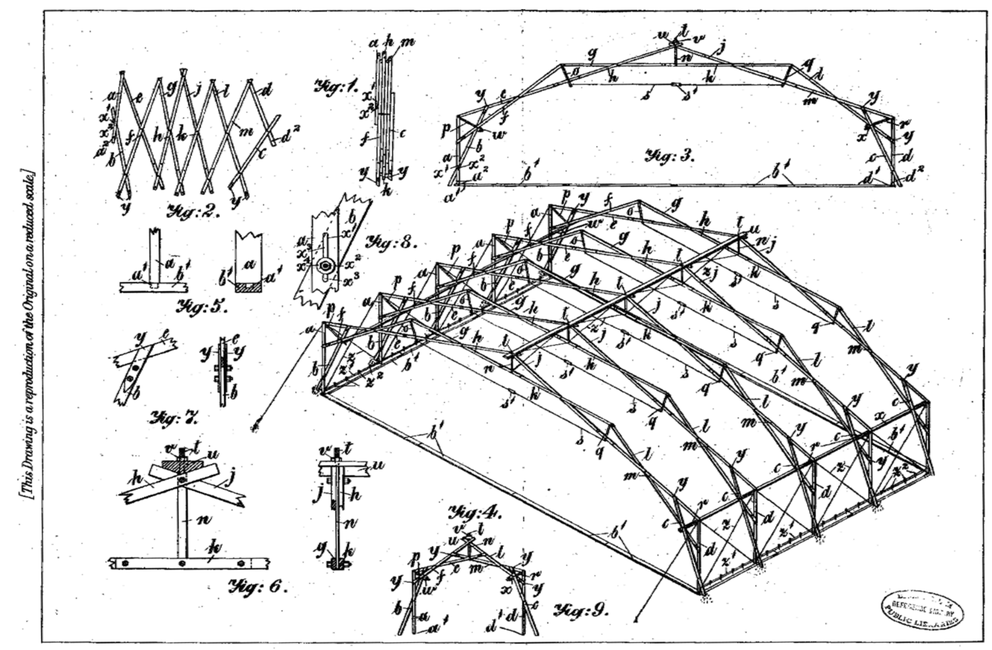

Figure 2.13 *Drawings from the patent "Improvement Supports for Tents Marquees Temporary Bridges and other Portable Structures". (Watkins, 1914)*

2.3.2 Emilio Pérez Piñero

The contributions made by the Spanish architect Emilio Pérez Piñero during the 1960s became a source of inspiration for many others working in the field of mobility for space grids. In Pérez Belda (2013), the differences between geometries of squared or triangular meshes formed by three or four bars converging around a coupling are described [Figure 2.14a], in which the central or eccentric position of the intermediate pivot compared to its upper and lower ends, enables flat or curved shapes [Figure 2.14b].

Thanks to Pérez Piñero's work, the understanding, the evolution and popularisation of Pantograph Structures or Scissor-Like Elements [SLE] were afterwards possible.

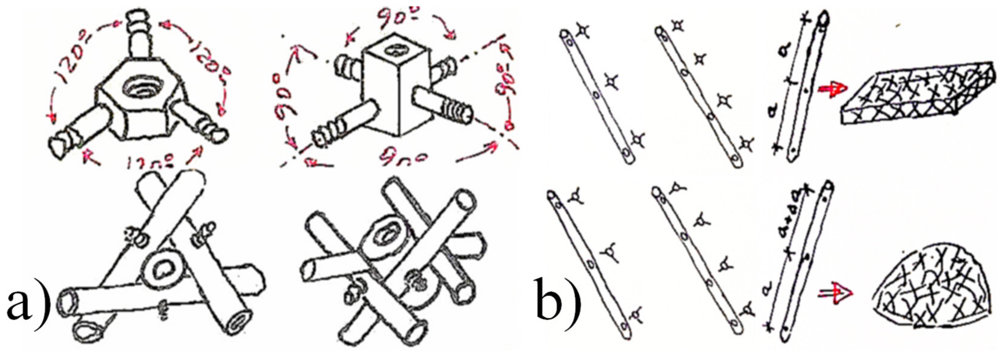

Figure 2.14 *(a) Types of deployable structure nodes, (b) Types of rods. ©Emilio Pérez Piñero Foundation (Pérez Belda, 2013)*

Despite the enounced principles, there was a compatibility problem with his double curvature proposals made from triangular joints [e.g., dome], caused by bending moments on the rods during the deployment. For this reason, a resource was given in the patent ES266801A1 (Pérez Piñero, 1961) using pre-bent rods; moreover, according to L. Puertas del Rio, those mechanisms had three rotational degrees of freedom (Puertas del Rio, 1991). In contrast, flat configurations based on squared nodes had only one degree of freedom, which is very effective for the structure's integrity.

The arrangement of the rods on a single coupler restricts the opening capacity, as the spatial proximity of the elements creates a similar positioning to a reciprocal frame. This last characteristic translates in the use of svelte bars from the design process for both cases, as can be seen in Figure 2.15:

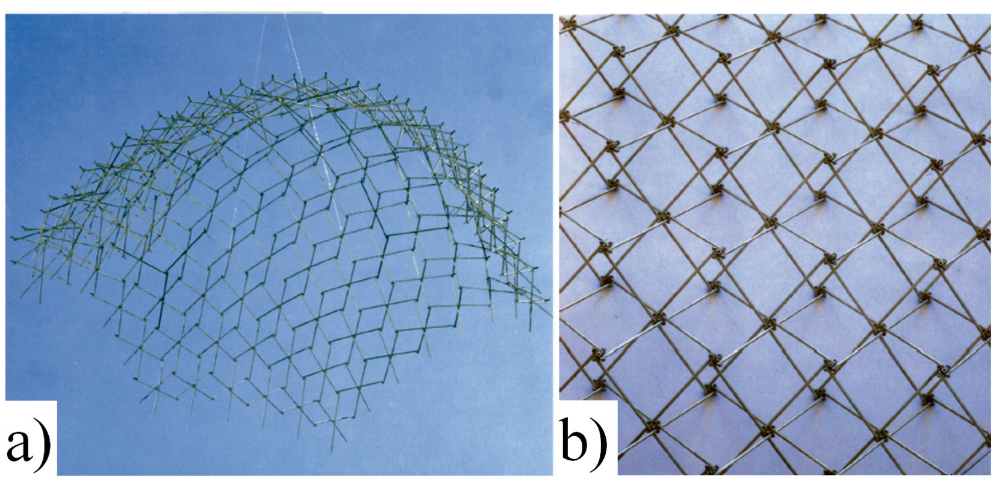

Figure 2.15 *(a) Model for a portable theatre exhibited in London, 1961, (b) Model for the roof of the 25 Years of Peace Pavillion, 1964. (Calvo López & Sanz Alarcón, 2011)*

2.3.3 Theodore Zeigler

By the mid-1970s, the North American Theodore Zeigler studied new collapsible arch-like geometries [e.g., vault] or semi-spherical shapes [e.g., geodesic domes], [Figure 2.16]. Scissors were used to introduce a self-locking or self-stabilised feature derived from specific constraints in the length and shape of the bars, avoiding the use of additional elements such as cables or any locking device (Zeigler, 1976; 1981). As a result, geometric incongruences exist during deployment, and the structure does not behave as a pure mechanism.

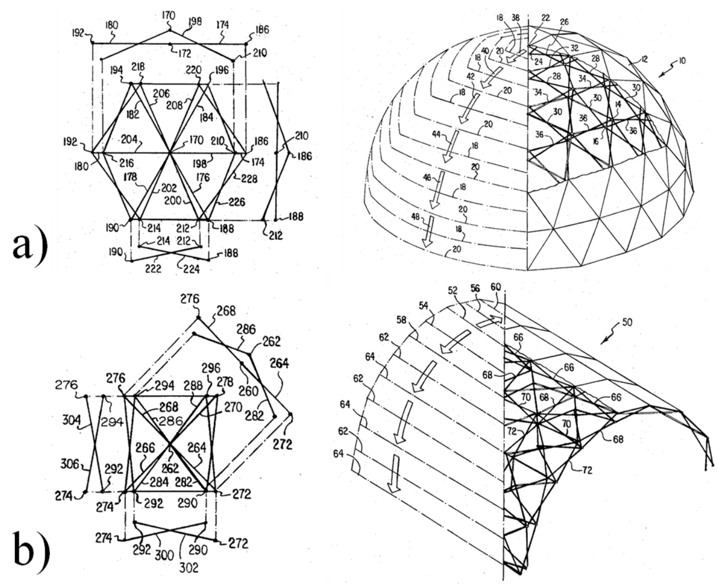

Figure 2.16 *(a) Geodesic Dome, (b) Vault. (Zeigler, 1981)*

Some variations in the shape and type of connections are indicated in Figure 2.17 to control the produced snap-through behaviour. The alternative (b) is the simplest form, where the rod elements have enough resiliency to bow; this requires an applied effort to achieve deformations both in the deployment and in the fold. Gantes (2011) stated that these structures were more susceptible to buckling under service loads due to twisted or bent elements in the final deployed configuration.

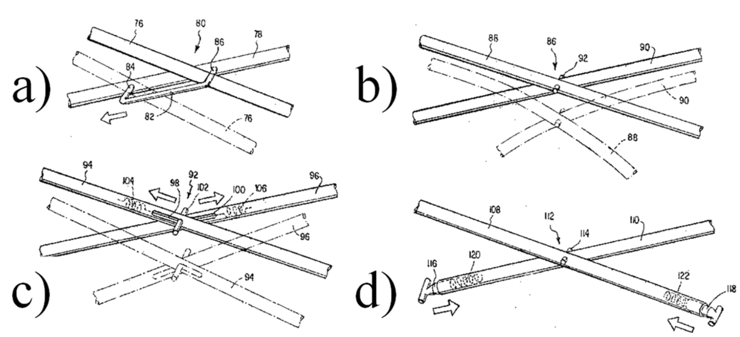

Figure 2.17 *Various ways of achieving the limited sliding control, and fixed, pivotal connections. (Zeigler, 1981)*

Despite the reduction of load-bearing capacity due to residual stresses in the deployed conformation, it is not always essential to get high structural specifications; for instance, "*Nomadic Display*", the first portable pop-up display system for exhibitors, patented by Zeigler (1985), [Figure 2.18]. Furthermore, equivalent technical features to those defined by Zeigler (1987) [Figure 2.19] can be identified in Prusmack (2007), and remain valid in products known as *DRASH®: Deployable Rapid Assembly Shelter.* In practice, these constructions must also be fixed to the ground and usually be secured with cables to counteract wind loads.

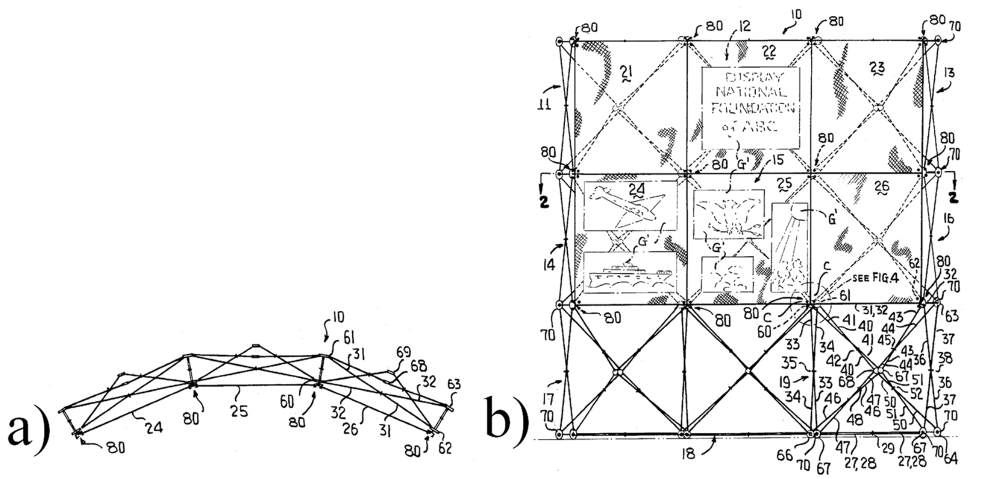

Figure 2.18 *Display panel mounting clip: (a) Top view, (b) Front view. (Zeigler, 1985)*

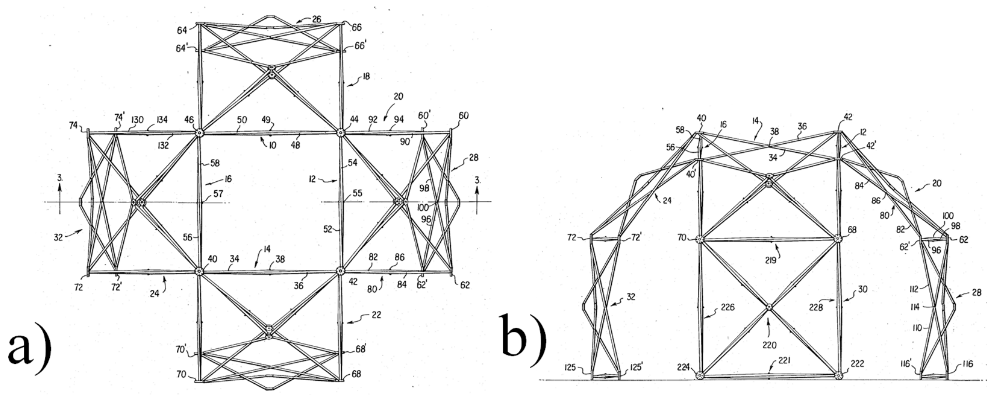

Figure 2.19 *Portable shelter assemblies: (a) Top view, (b) Front view. (Zeigler, 1987)*

Zeigler (2000) registered one more patent on scissor structures for military tents, commercially known as *Base-X® Shelters*. Instead of the self-locking or self-stabilised feature, it includes manual locking, diagonal cables for added rigidity, and the system has more than 1DOF due to the structure's legs.

The resulting roofing geometries can be locked in lower levels before raising the structure with human force; this procedure can be completed in a short time but demands training for a step by step deployment, as depicted in Figure 2.20.

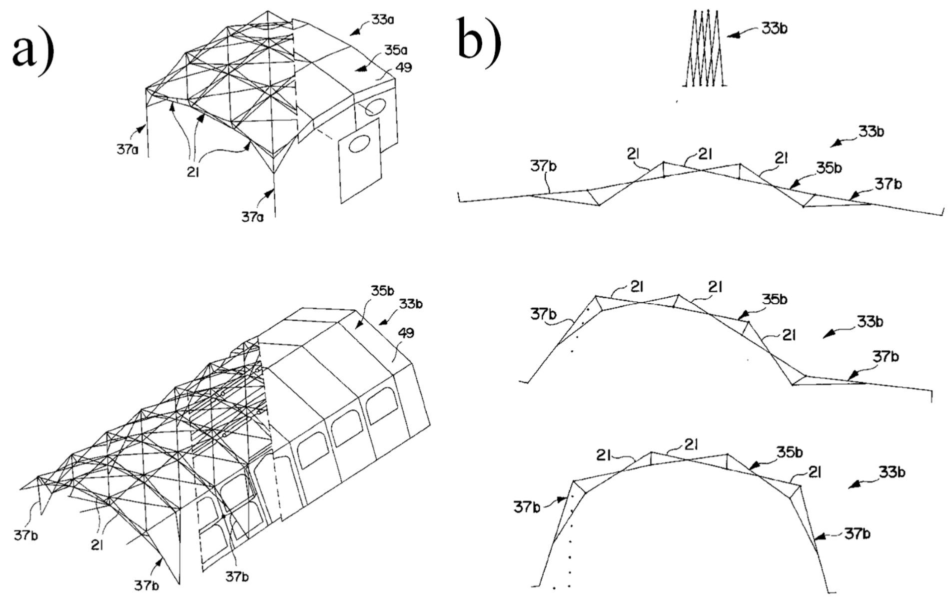

Figure 2.20 *Folding frame system with foldable leg assembly and method of erecting a folding frame system: (a) Dome and vault-like geometries, (b) Deployment process. (Zeigler, 2000)*

2.3.4 Félix Escrig

In the '80s, the Spanish architect Felix Escrig set out new ideas at the University of Seville, where he had a teaching career. Often in co-operation with Juan Pérez Valcárcel and Jose Sanchez, the research was focused on analysing a wide variety of flat, clastic and synclastic surfaces. The first possibilities can be found in the patent ES532,117 (Escrig Pallarés, 1984b), which were gradually complemented and summarised through time by Escrig (1993; 2012), among many other scientific publications.

The most elementary flat models are illustrated in Figure 2.21

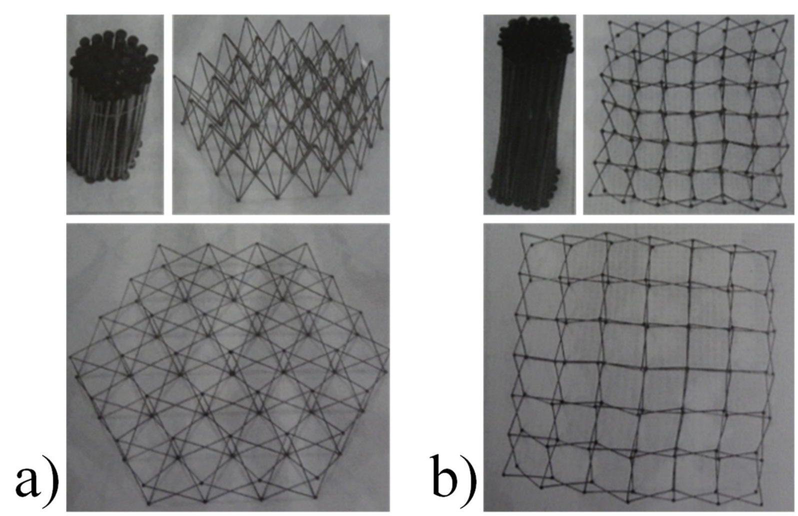

Figure 2.21 *Flat geometries: (a) Triangular, (b) Squared. (Escrig Pallarés, 1993)*

Escrig & P. Valcárcel (1986) utilised basic patterns to achieve umbrellas and sun shelters covering large areas. In 1988, flat meshes with a triangular subdivision were potentially considered for the San Francisco Square and the Maestranza Bullring at Seville, although these projects were never constructed. On the other hand, flat grids of squares can be shaped with fewer beams and simpler joints. However, they have lateral instability and for this reason, tensioning cables or diagonal stiffeners are required once the structure is open. Because of the issues that could be produced during the system deployment, substitute explorations continued in convex and concave solutions.

When configuring a cylindrical vault by combining plane translational and polar scissors, restrictions were revealed on three-direction curvatures as it causes warping on bars during deployments, limiting its prospective usage on larger scales [Figure 2.22]. In grids of squares, an inner diagonal bracing was initially studied in the scale models of Figure 2.23a. After, an outer diagonalisation of a transportable arch with a 15m span associates two complementary and simultaneous patents by Escrig & Sanchez (2007a; 2007b), [Figure 2.23b].

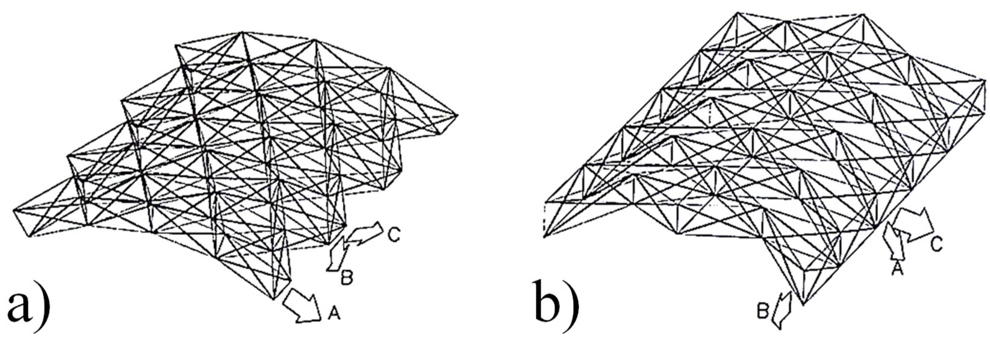

Figure 2.22 *Two options for triangular cylindrical geometries. (Escrig Pallarés, 1993)*

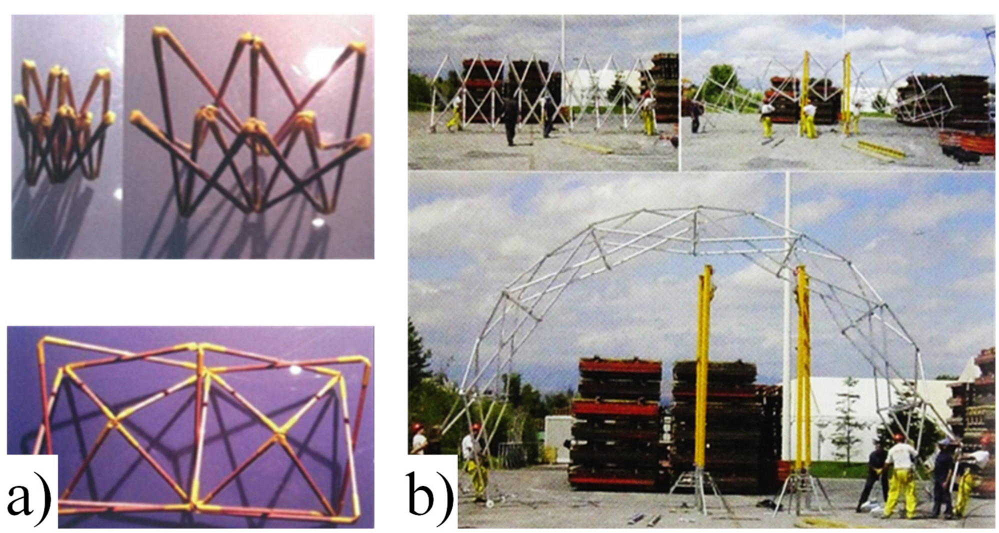

Figure 2.23 *Diagonal stiffeners: (a) Scale model, (b) Prototype. (Escrig, 2012)*

Many other double curvature investigations were made with different functionality criteria; the following description lists some of them:

- An original tessellation method was designed to obtain partitions from arbitrary spatial points, which considerably improves the regularity between bars; nonetheless, the geometry describes compatibility in the open and fold state, but not on intermediate positions. Deformations could be controlled while the resulting structure is self-stabilised [Figure 2.24].

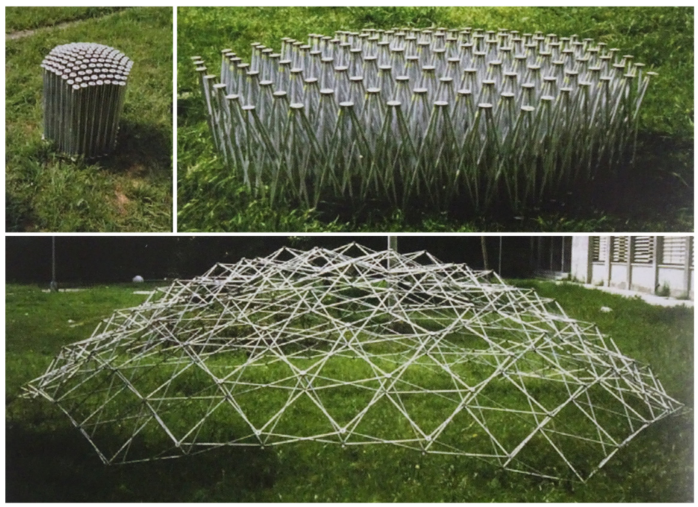

Figure 2.24 *Triangular tessellation model. (Escrig, 2012)*

- Trapezoidal tessellations can be produced from a spherical grid of meridians and parallels. The outcome is a deployable structure that has irregularities in bar lengths and at joint angles. Figure 2.25 reveals differences between photographs taken to the original scale model. The misfit can be presumably attributable to the utilised joint-type and their capacity to rotate.

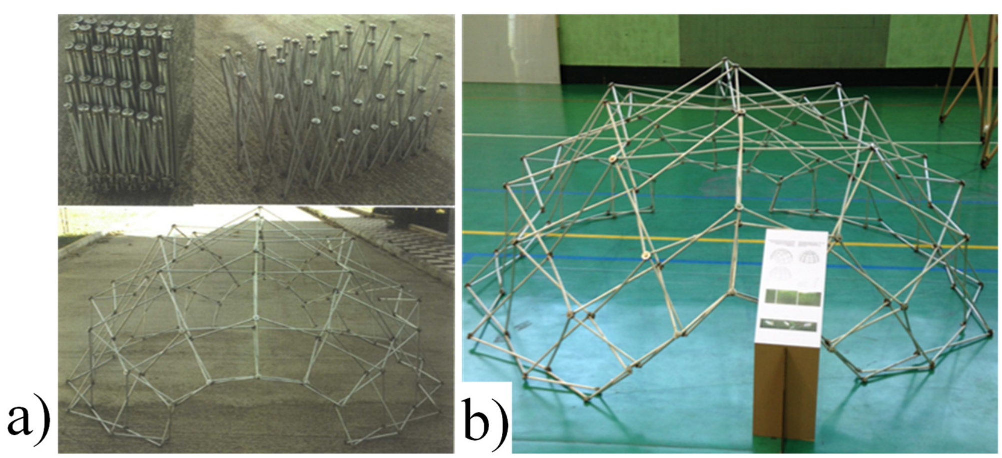

Figure 2.25 *Deployable Structure based on meridians and parallels: (a) (Escrig, 2012), (b) (Gómez Lizcano 2013) - unpublished personal library.*

Another example incorporates the former principles to a cylindrical vault of squares [Figure 2.26]. Even though, in theory, trapezoidal grids bring great stability to the structure without diagonals as long as the border is fixed (Escrig, 2012), there are no constructions on a larger scale. Besides, control over the lateral instabilities of the central arches during deployments might be needed.

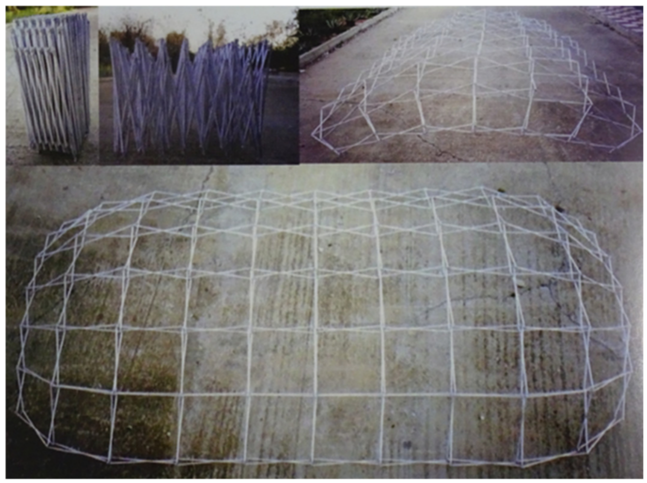

Figure 2.26 *Combination of cylindrical arches with spherical segments. (Escrig, 2012)*

- The deployable cover on Sao Paulo's Olympic swimming pool was built in 1994 and is the largest scissor structure built to date (Escrig, et al., 1996; 1996), (Sánchez, et al., 1996). It is made up of two spherical domes of 30m x 30m x 9m with identical polar units and joints with fixed pivots at 90°, as seen in Figure 2.27. Although the ideal angle positioning of scissors changes during movements, the reduced spherical portion of the structure helps to lower the exhibited snap-through effect.

In agreement with Pérez Valcárcel (2014), a single dismantling and reopening occurred in 1997 during the service period; later on, removal of the lateral enclosures in the summer was preferred, while the roofing membrane created a shadowed interior.

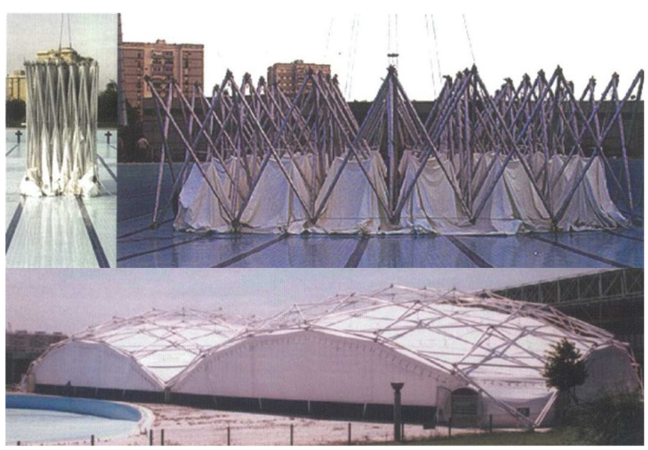

Figure 2.27 *Sao Paulo's Olympic swimming pool, Seville. (Escrig, 2012)*

2.3.5 Carlos Hernández

In the Massachusetts Institute of Technology [MIT], Carlos Hernández (1987) started working for his master's in architecture under the supervision of Waclaw Zalewski. Their collaboration continued at the Central University of Venezuela during the project *ESTRAN 1*, an ephemeral cover structure following an economy of and simplicity in construction offered by a cylindrical vault with a squared configuration that is triangulated and stabilised employing tensors (Hernández, 1988).

The initial prototype, shown in Figure 2.28, had technical specifications planned on-site to maximise ease of handling, transportation and storage. The aluminium frame weighed approximately 500kg plus 100kg of fabric; it had a starting packet of 1m x 1m x 4,20m and produced a deployed geometry of 14m of span, 8m width and 7m height, to cover a surface area of 112 sq.m.

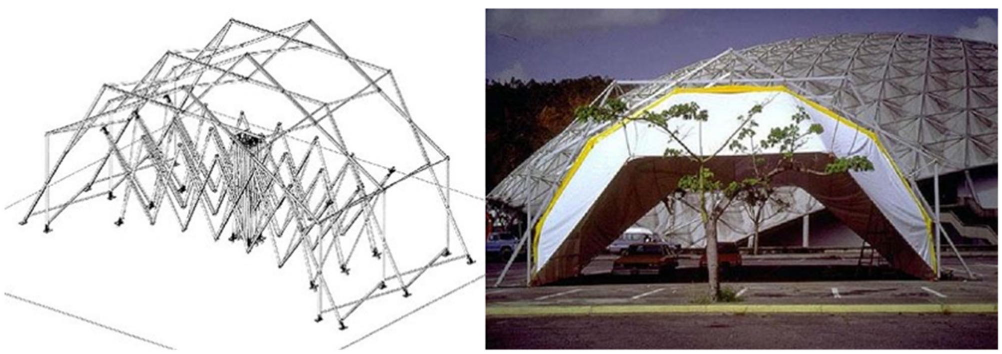

Figure 2.28 *ESTRAN 1: (a) Concept, (b) Prototype. (Fundación UCV - TECNIDEC S.A. - Grupo ESTRAN c.a., 2001 - 2004)*

An itinerant pavilion was built in 2005, having an anticlastic membrane that hung below two main arches. This variation resulted in a major wind resistance capacity and fewer connection points [Figure 2.29]. It covered a total area of 350 sq.m, utilising steel tubing instead of aluminium to reduce cost; nonetheless, the material replacement tripled the total weight to 1500kg (Hernández & Cebrian, 2010).

Figure 2.29 *Pavilion for itinerant exhibitions. Tara Tara, Edo. Falcon, Venezuela (2005). (Fundación UCV - TECNIDEC S.A. - Grupo ESTRAN c.a., 2001 - 2004)*

A final version, named *ESTRAN 1.1*, had improved technical details and was calculated to meet European building standards for wind speeds (100 km/h) and snow loads (up to 30 kg). The design aimed to evolve into a commercial product: it describes a turtle shell-like curvature on a quadrangular subdivision, an internal span of 16m in the main arches and 12.18m in the lower ones, a width of 12.41m and a maximum interior height of 8m. The transport dimensions are 1.4m x 0.8m x 4.9m, and the total surface area is 186 sq.m when deployed (Hernández, 1999).

Because of the synclastic geometry, the mechanism is not considered stress-free and controlled deformations occur. Figure 2.30 shows an artistic rendition of the design.

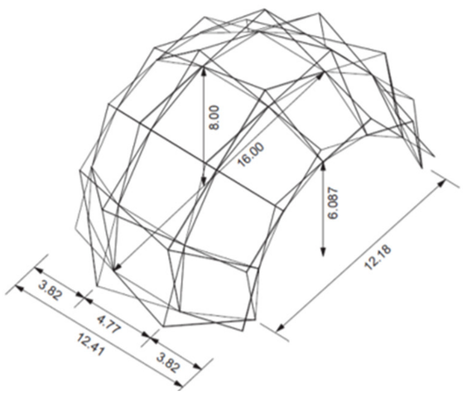

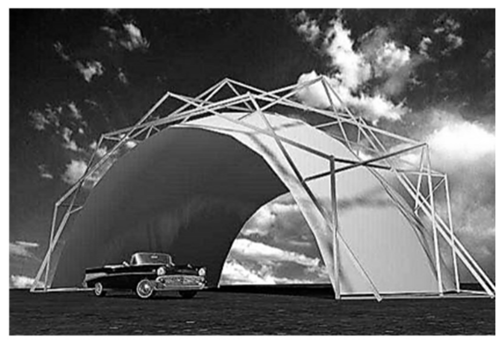

Figure 2.30 *ESTRAN 1.1. (Hernández, 1999)*

2.3.6 Anandasivam Krishnapilliai, Yechiel Rosenfeld, Robert Logcher and Charis Gantes

When Anandasivam Krishnapillai was a student of Architecture simultaneously with Aeronautics and Astronautics at MIT, representative bi-stable deployable structures were developed and then protected by patent (Krishnapillai, 1992). It consists of straight and stress-free scissors in the open and closed positions only, even if producing bending effects during intermediate stages by cause of geometric incompatibilities [Figure 2.31].

During movements, a limited flexible capacity of the members is required. In the final position, the construction becomes self-stabilised with no internal residual stresses and can withstand an applied load, thus generalising and improving Zeigler's work.

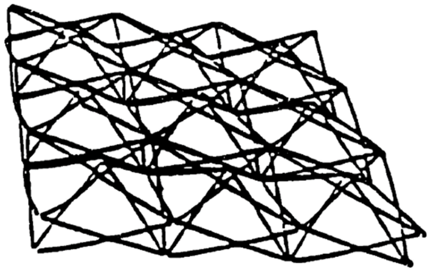

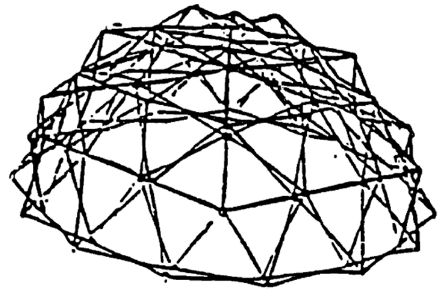

Figure 2.31 *Krishnapillai's flat and curved deployable structures. (Gantes, 1991)*

At the Civil Engineering Department of MIT, Yechiel Rosenfeld and Robert Logcher introduced the structural terminology of the "clicking" phenomenon occurring during bi-stable structures movement (Rosenfeld & Logcher, 1988), [Figure 2.32]. Charis Gantes worked on determining the specific designs for flat and curved deployable geometries and investigated the non-linear structural behaviour extensively for longer than a decade, exposing a necessary and complex design process that includes analytical and numerical attention to preserve the load capacity of the structure during its service. The main findings and a guideline to design deployable structures were published in Gantes (2001).

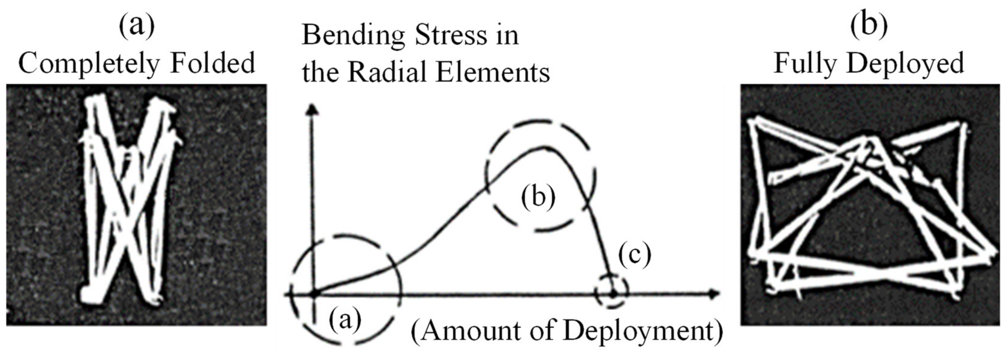

Figure 2.32 *Illustration of the "clicking" Phenomenon. (Rosenfeld & Logcher, 1988) [Digitally enhanced]*

Additionally, Gantes, et al. (2000) investigated models for a deployable Zeppelin cover and an emergency shelter [Figure 2.33]. Since a geometrical incompatibility exists to create a fluid shape based on bi-stable arches of truncated square pyramids, an optional methodology was used in both cases to adapt passive substructures (Kwan & Pellegrino, 1994). The proposal allows more design freedom, decreases the intensity of the snap-through, and stiffens the whole structure in the deployed configuration. However, constructability and serviceability difficulties need to be considered ahead of its implementation.

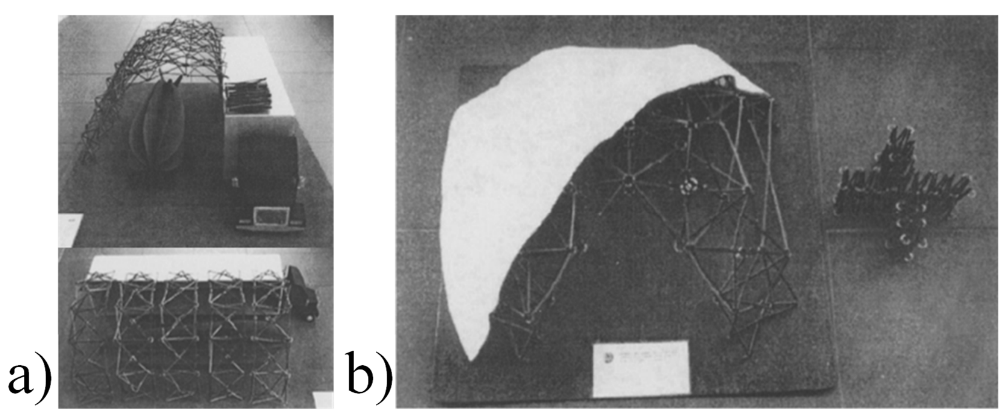

Figure 2.33 *(a) Deployable Zeppelin Cover, (b) Emergency Shelter. (Gantes, et al., 2000)*

2.3.7 Chuck Hoberman

During the 90s, a new range of concepts was presented to the public; one of them was invented by the North American Chuck Hoberman, who formulated the angulated scissors (Hoberman, 1990). The idea was initially used for a popular kinetic spherical toy and later produced multiple transformable objects. For instance, the principle behind polyhedrons changing their size but not the shape and geometry during movements, was transferred to the subdivision of a half hemisphere to obtain a dome [Figure 2.34].

a) 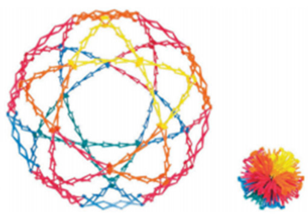 b) 

Figure 2.34 *(a) Hoberman Sphere Toy (1990), (b) Expandable Geodesic Dome (1991). (Hoberman Associates, Inc., 2012)*

Instead of portability, another option is to produce radial expansion and retraction of structures that remain fixed to a site (Hoberman, 1991). *The Iris Dome* (1994) is a loop assembly in which the system's centre deploys towards the perimeter of the main geometry; the border nearly maintains continuous dimensions during movements, and ground fixing detailing is needed. A structure model at the Museum of Modern Art in New York City, USA, is illustrated in Figure 2.35.

Figure 2.35 *The Iris Dome (1994). (Hoberman Associates, Inc., 2012)*

Through time, the versatility of angulated units has inspired many other researchers to explore the realisation of new geometries that are not directly compatible with polar and translational mechanisms. Hoberman has found further opportunities as well, especially in live entertainment and kinetic structures. Examples are suggested in Figure 2.36:

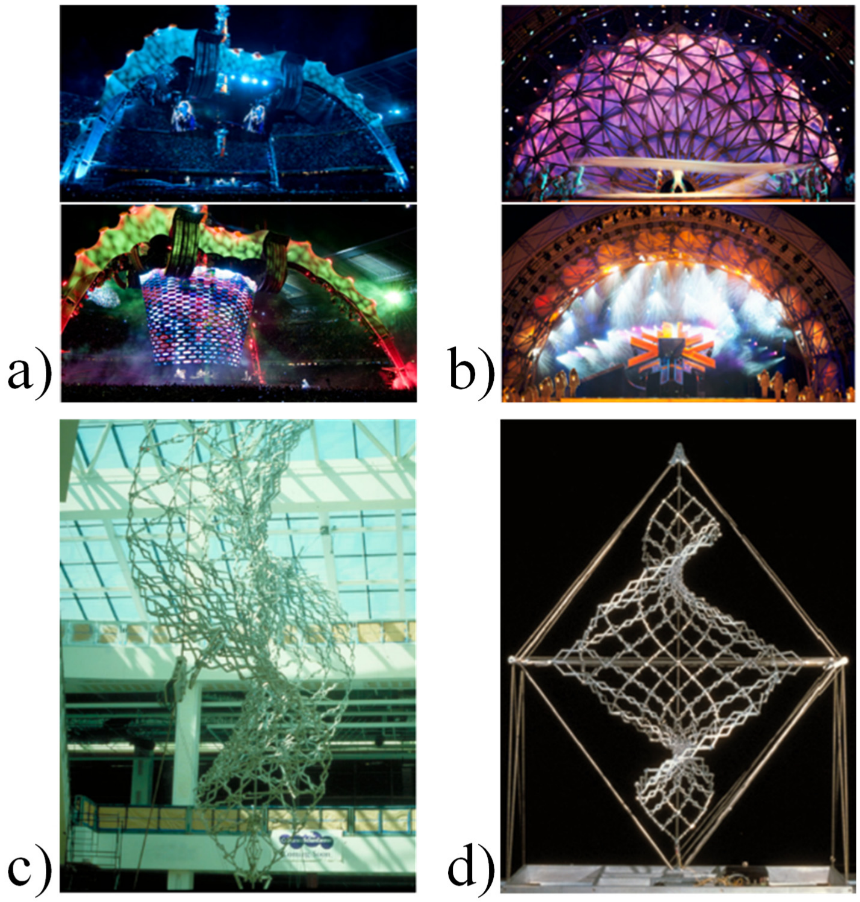

Figure 2.36 *(a) Expanding Video Screen (2009), (b) Olympic Arch (2012), (c) Expanding Hypar, (d) Expanding Helicoid (2007). (Hoberman Associates, Inc., 2012)*

2.3.8 Luis Sánchez-Cuenca Lopez

The Spaniard Luis Sánchez-Cuenca Lopez (1996a; 1996b; 1996c) extended the potential of translational scissors from a straight or inclined deployment to multiple curved possibilities with complete coherence during the expansion process.

Figure 2.37 (c) exemplifies the use of curved-translational scissors over an arbitrary arch; multiple bar lengths are needed to get this result.

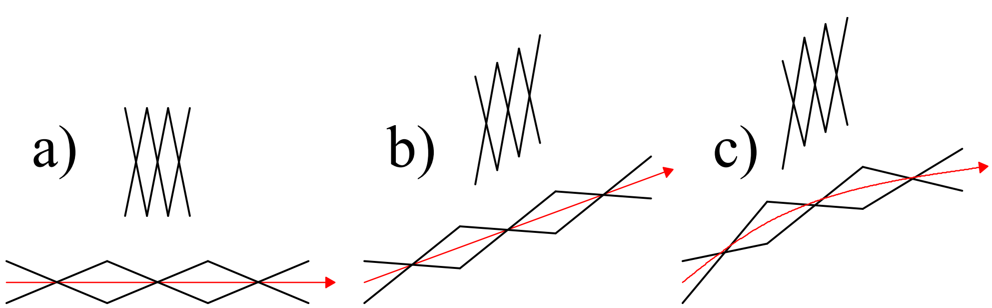

Figure 2.37 *Translational scissors extension lines:(a) Straight, (b) Inclined, (c) Curved.*

Once the desired extension lines in 2D are solved, the repetition along the Cartesian coordinate planes X and Y produces a family of scissor grids with a quadrangular base. His theories made the generation of simple translational models possible, or in other cases, surface combinations between clastic, synclastic or anticlastic geometries [Figure 2.38].

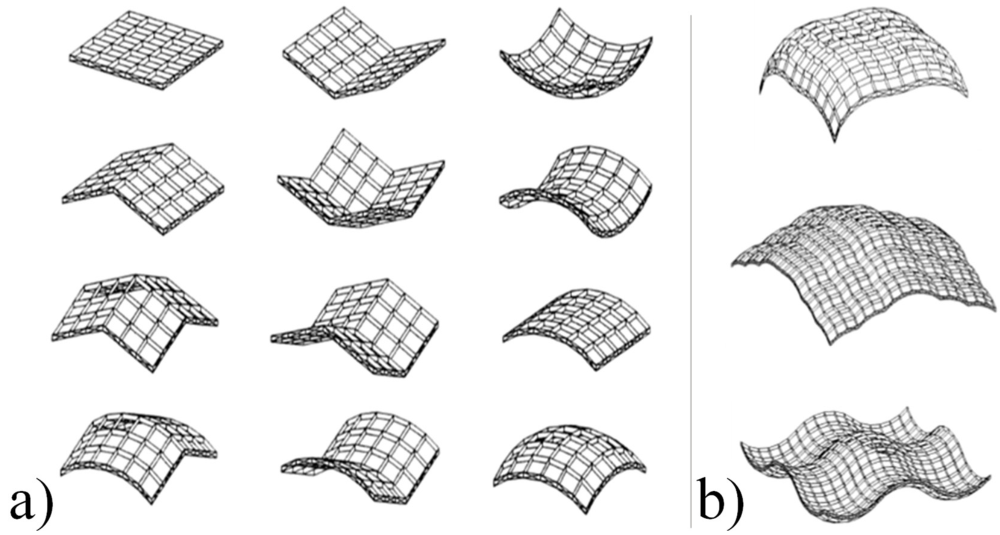

Figure 2.38 *(a) Basic expandable translational models, (b) Surface combination examples. (Sánchez-Cuenca, 1996a)*

Cables or additional bracing components are proposed methods to triangulate the in-plane stability, and locking devices are essential for rigidising the deployed structure. Figure 2.39 demonstrates a couple of full-scale examples of great interest that were built by the author.

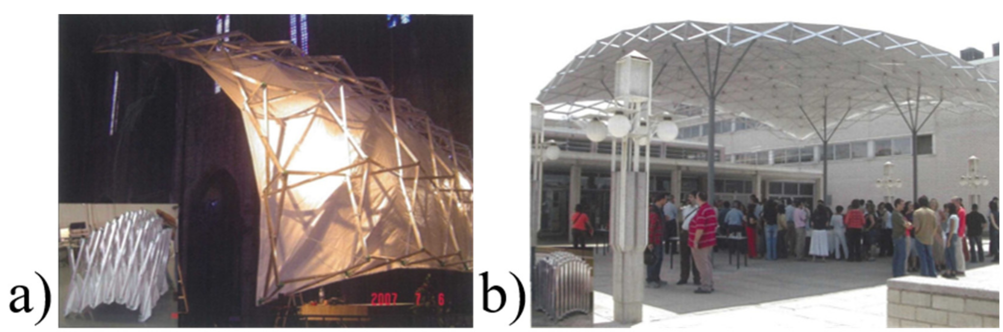

Figure 2.39 *(a) Acoustic structure in the Torroella de Montgrí Festival (2007), (b) Temporary roofing at the University of Girona (2007). (Escrig, 2012)*

2.3.9 Katsuhito Atake

The Japanese Architect Katsuhito Atake formulated a complementary constructive technique with polar units (Atake, 1998). It consists of ring-type groupings comprising three or more scissors and complete pin joints like a door hinge.

In regular polygons, only the triangular pyramid is stable during all the deployment phases; other solutions such as squared or pentagonal increase the degrees of freedom and produce a weaker structure. [Figure 2.40]

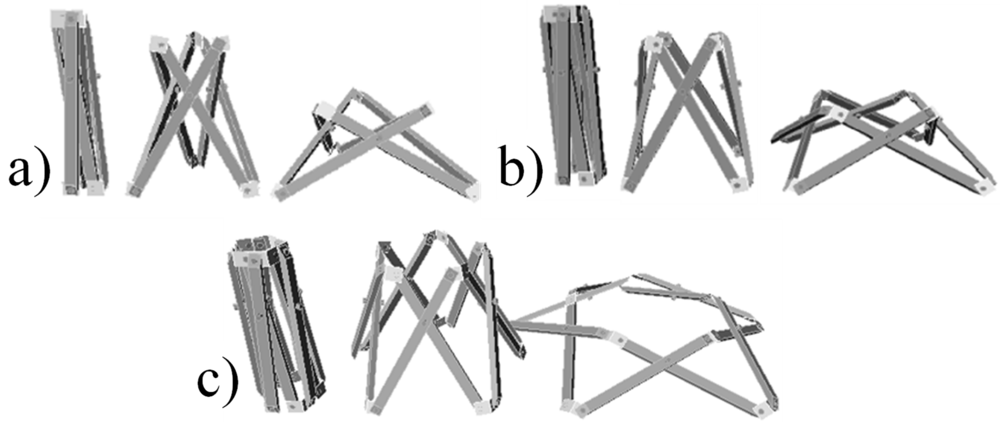

Figure 2.40 *(a)Triangular pyramid, (b) Squared pyramid, (c) Pentagonal pyramid. (Atake, 2000)*

By adopting sliced skew prisms comprising 4 or 6 scissors on the lateral faces, a sliced tetrahedron or a sliced octahedron is obtained, just as in Figure 2.41. More complex three-dimensional shapes can be obtained when grouping the prior modules, but tension elements like wires or membranes are needed to add stability and get adequate strength (Atake, 2000).

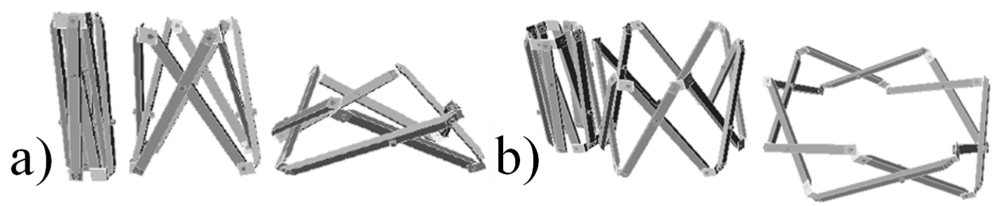

Figure 2.41 *(a) Sliced tetrahedron, (b) Sliced octahedron. (Atake, 2000)*

Despite the theoretical advantages of adding degrees of freedom to the joints for assuming the geometrical incompatibilities with this method, other challenges are added for the design and the installation process for medium to large-scale structures. Otherwise, the components must have enough elastic capacity during movements to resist deformations with an applied and controlled force.

Some experiences were built by the *Katsuhito Atake Institute Co., Ltd. Architects*, using a crane to suspend the structure during the installation:

- Figure 2.42 (a) is a double pyramidal geometry prototype testing in Yokkaichi-Japan, planned as a storehouse for a livestock waste disposal tank. It weighs 2ton, has a height of approximately 10m, and a surface area of 200m2.

•Figure 2.42 (b) corresponds to a private base dome project built in the Chita Peninsula – Japan; it has 9m in diameter, is 4.5m in height and 500 kg of weight.

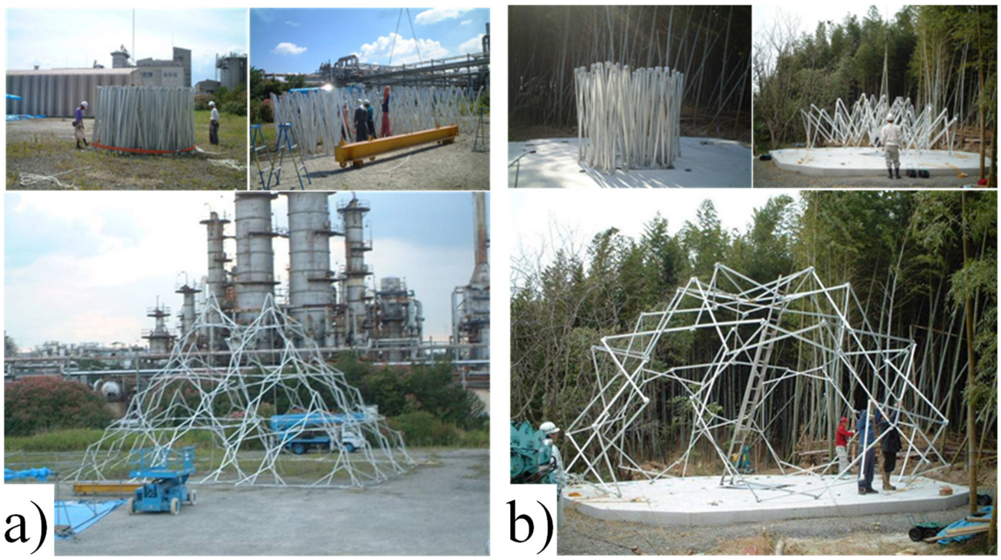

Figure 2.42 *(a) Double pyramidal geometry, 2004. (ATAKE INSTITUTE Co., Ltd., 2007a)*
(b) Semiregular polyhedron dome, 2003. (ATAKE INSTITUTE Co., Ltd., 2007b)

A structural analysis to build a cylindrical vault based on Atake's design was done recently by Hiroyuki Tagawa, et al. (2015). The functioning stability during & after the deployment process was evaluated for a design configuration with outer dimensions of approximately 7.2m in span and 3.9m in height. According to the published document, it is evident that arches of squared pyramids are weaker than arches with sliced tetrahedrons. For this reason, a diagonal stiffening with nylon ropes was used on each model after deployment to reduce twist or translational deformations significantly.

Figure 2.43 shows the deployment process with human power by eleven female students of the 2014 Architectural Design Class at the Mukogawa Women's University. Although it was planned to be deployed with the frame and membrane cover connected, difficulties arose due to unexpected friction and wind pressure; afterwards, it was manually post-tensioned to correctly fit the membrane to the vault entrance edges.

Figure 2.43 *Cylindrical vault, 2014. (Mukogawa Mowen's University, 2005-2014)*

2.3.10 Recent developments

Since these developments, an extensive list of additional authors has experimented with the problems associated with scissor structures, although many were published as a theory with no continuity.

To cite a recent representative patent, the Spanish architect Rodrigo José Ramos Jimenez (2015) has addressed the problem of angular instability on geometries with a quadrangular subdivision. The invention seeks to stabilise the structure without needing additional cables or bars once it is open by combining curved translational and polar scissors. Under these circumstances, the kinematic incompatibilities deform the main components in a controlled manner, and the structure may require flexible enclosure materials, which changes the amount of tension needed.

Two types of modules are identified in Figure 2.44: [i] oblique-triangular prisms with irregular bases towards the supports; and [ii] solids with trapezoidal sections, which are also truncated since the bases are not parallel. The experimental prototype has a covered area of 12m x 12m, a height between 5m and 6.5m and folded dimensions of 2m x 3m x 4m. With the aid of incorporated electric hoist systems, the structure is envisioned as a solution for rapid-assembly tents by the company *ArkiDes* (Singulark Arquitectura Y Estructuras Singulares Sl., 2014) since it can be made fully operational by at least two operators in less than 60 minutes.

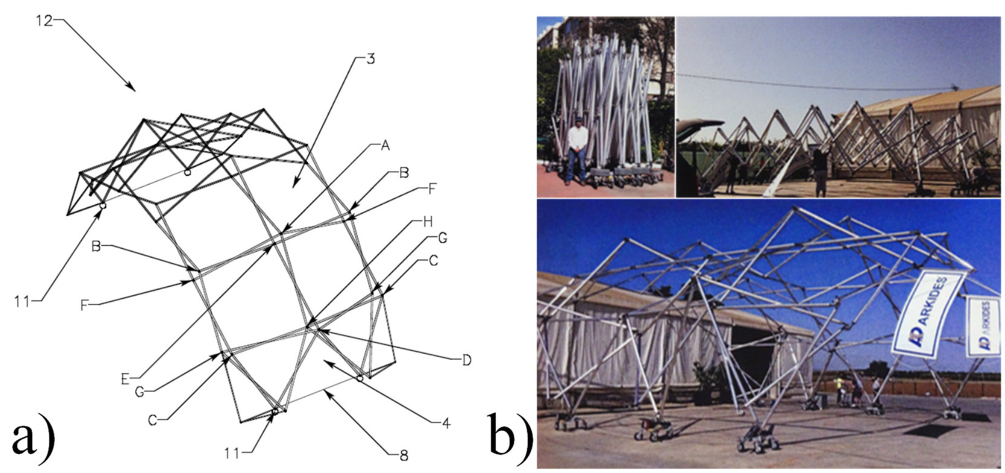

Figure 2.44 *(a) Basic geometry (Ramos Jiménez, 2015), (b) Prototype. (Ramos Jiménez, 2013)*

The *TRANSFORM research group* within the Architectural Engineering Department of Vrije Universiteit Brussel [VUB] has likewise given extensive contributions to scissor structures during recent years. Their work has focused on the classification, design methods, structural analysis, manufacturing, and generation of new digital design tools to reduce the related difficulties still unsolved.

The continuous interdisciplinary association of a team of entrepreneurs and researchers led by Niels De Temmerman and Tine Tysmans founded the Belgian start-up *Konligo* in 2018, promoting lightweight and transformable structures. An improved connector was developed and protected by patent (Koumar, et al., 2019), in addition to the WIPO [PCT] patent application of a foldable scissor module for doubly curved scissor grids (Roovers & De Temmerman, 2018).

•Figure 2.45 (a) illustrates *Fastival* [2017-2018], a product for outdoor events based on the principles of a cylindrical vault with a quadrangular mesh subdivision and diagonal cables for tensioning. Once deployed, it has dimensions of 7m x 3.5m x 3.5m [span, width, height] and 40cm x 60cm x 1.8m for transporting, weighing approximately 100kg. Structural specifications are designed to withstand wind loads of 100km/h and additional hanging loads of 150kg in total. It can be mounted by two to four persons in less than 10 minutes.

•Figure 2.45 (b) illustrates *Ondo* [2018], a product for exposition stands and interiors which is based on a pair of wave-like domes with a quadrangular mesh subdivision and diagonal cables for tensioning. Once it is deployed, each structure has dimensions of 6.6m x 6.6m x 6m [span, width, height] and 40cm x 60cm x 1.8m for transporting, with a weight of approximately 250kg. Structural specifications are designed to resist a maximum of 400kg equally distributed per module, while an attachment point can support a maximum of 10kg. Manual lift equipment is required when pulling up the structure.

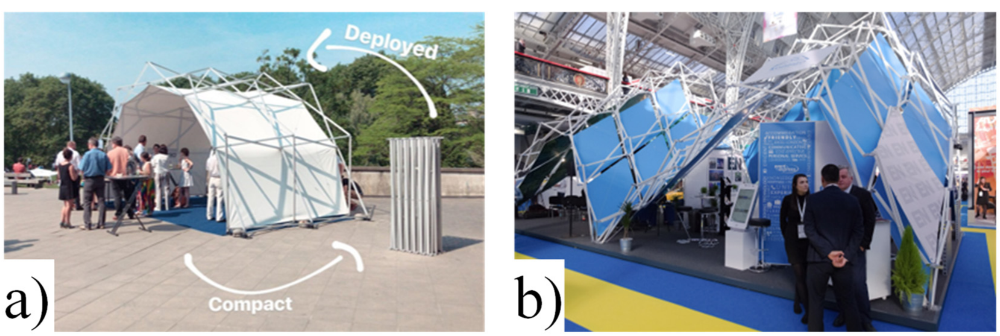

Figure 2.45 *(a) Fastival, (b) Ondo. (Konligo, 2019)*

2.4 Discussion on the historical overview

A synthesis of the main aspects of existing prototypes, products and patents is:

• Latest developments in umbrella-type structures have achieved dimensions and typologies that transcend traditional ones to architectural-engineering levels. Besides, there are other possibilities of creating mechanisms with a single degree of freedom different from classic pantographs, as in Calatrava (1993) and *Ten-Fold Engineering Limited* (2018). Current technologies mean an opportunity to develop new transportable and transformable architecture with differentiated aesthetics, meeting the constructive requirements of various scenarios and intense environmental conditions.

- Although it was not included in the prior listing, scissor collapsible canopy tents are top-rated worldwide due to their practicality. They are beneficial when needing an easy, compact, and rapidly erectable tent with light structural standards, although they also lack stability due to the slenderness of the telescopic legs and often require tensioning cables or counterweights. Early developments of this kind of scissor structure can be found in Carter (1986), Lynch (1987; 1988).

Figure 2.46 shows a configuration with similar characteristics to those known today.

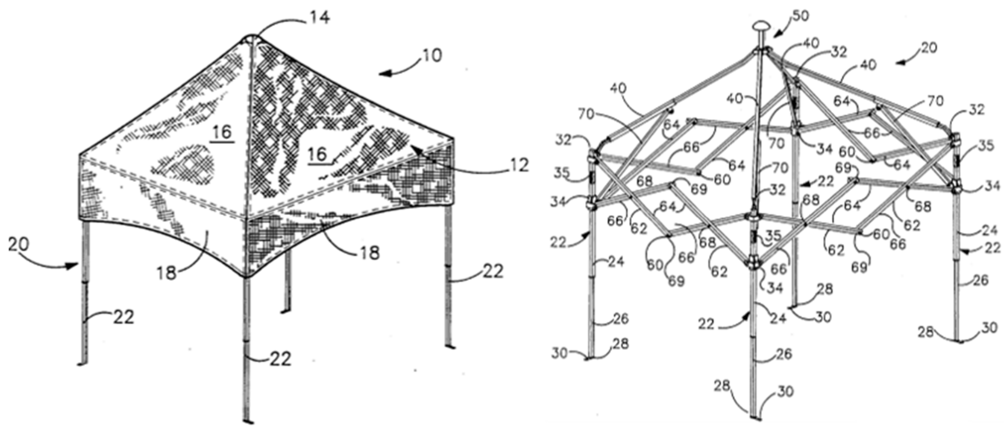

Figure 2.46 *Canopy structure and structural framework. (Lynch, 1988)*

For other kinds of deployable tents, even the simplest form of a cylindrical vault with a quadrangular mesh subdivision can represent constructive problems on large dimensions, since it also brings significant weight. In Hernandez (1999), Hernández & Cebrian (2010), the need for operators to balance the structure against lateral instabilities and the possibility of cables getting entangled in intermediate positions were reported. Besides, it is necessary to guarantee a proper tension in the deployed state, where gradual losses can be produced over time.

On small or medium scales like in *Konligo Fastival* this might not produce significant problems; however, recurrent usage can likewise cause permanent deformations on components. Under safety standards, adequate training and movement synchronisation are necessary to prevent risky personnel procedures. For instance, the normative UNE EN 13782 (Comité técnico AEN/CTN 305 Carpas y Estructuras Móviles, 2016) specifies safety requirements during design, calculation, installation, maintenance and operation of single or grouped temporary constructions with a surface area over 50m2. There is also great importance in controlling angular deformations during the folding process because gravity can cause sharp movements and overexertions.

• Stress-free structures simplify the design process as the linear structural response in the deployed configuration excludes the need for sophisticated analysis and make on-site manipulation effortless due to their mechanism behaviour. By contrast, a complex and time-consuming calculation is required in exchange for the self-stabilisation feature of self-locking and bi-stable solutions, as the structural feasibility has contradictory behaviours between the material flexibility during deployments and a balanced stiffness on the service life (Gantes, et al., 2000).

When planning and designing structures acting as a single bundle, other factors to bear in mind are:

1. Technical detailing is needed to reduce friction on moving parts and eliminate any sharp edges that may cause tearing of the covering fabric.
2. A maximum transport capacity of 2.5m in width and between 6-12m in length.
3. The military shelters *DRASH* and *BASE-X* restrict installations by human force to spans near 8-10m.
4. Structural deployments with a crane could be eased by hanging the covering membrane from the scissor's lower nodes.
5. The simplest way to work safely on manual locking is by using scaffolds. Riggers need to climb the structure when obstruction problems exist, implying material handling difficulties and timing increases for adjusting all the components.

For this thesis explorations, transportable tents will seek solutions on a large-scale above 10m, a stress-free behaviour, minimum operators, and setup time during manual locking. As in Escrig Pallarés & Sánchez Sánchez (2007a), these dimensions could justify an automatic diagonal rigidisation for assuring a controlled and homogenous interaction between parts. Besides, it is essential to satisfy the needs of use and reuse, for instance, in renting where the selection of cranes as suspension method causes the structure to be supported only from certain joints, generating cantilevers and increasing the possibility of unwanted lateral deformations.

2.5 Chapter summary

This chapter extended the essentials of deployable structures, by pointing out the relevancy of sliding-pantograph mechanisms and scissor technologies for transportable & transformable architecture through history. From the early 1960s to recent research, detailed literature revision has taken place, providing relevant authors' innovations. The explanation included advantages and disadvantages of geometry, manufacturing and installation methods, achieving the first objective of this thesis. After discussing the main aspects of existing prototypes, products & patents, the target in solving the structural and constructive problems of quadrangular expandable grids were identified, as it is strategic on large-scale transitory scenarios demanding frequent re-location or rapid installation.

3 KEY PRINCIPLES AND METHODOLOGY

3.1 Introduction

The purpose of this chapter is to discuss the indispensable theories to design, evaluate, manufacture and build 1:1 deployable structures using scissors & sliding mechanisms. It is concerned with the necessary procedures for the geometrical formulation, digital modelling, motion simulation, mockup testing, and structural performance following The European standards (Eurocodes).

Conflicting the three-dimensional ideals of triangular expandable grids, Chapter 2 documented implicit construction challenges that can occur on any non-flat surface. As quadrangular subdivisions can generate lateral distortions, a usual solution is to incorporate tensioners or add diagonal bars once the structure is deployed. In other cases, the covering material could bring a relative rigidity, but it tends to be unstable and difficult to manipulate during movements (Escrig, 2012, pp. 56,57).

Based on the problem represented in Figure 3.1, the case study exploration focuses on understanding the kinetic behaviour of representative flat, clastic, synclastic, and anticlastic patterns, for appraising the feasibility of adapting diagonal control through complementary stress-free mechanisms.

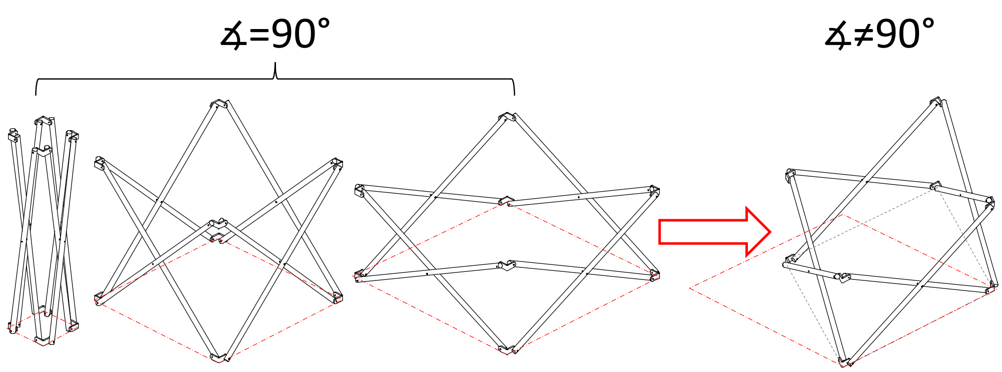

Figure 3.1 *A regular square prism deployment: the base turns into a rhombus.*

Subsequent reduced-models fabrication is adopted to transcend digital drawings theory and contrast the kinematical functionality; likewise, this process identifies prospective combinations for transportable & transformable applications in architecture, from the singular modules exposed. Lastly, preliminary structural analysis data is collected to define constructive parameters during the mechanism expansion or folding, the climate load approximations to full-scale uses, and the complementing locking devices to obtain proper functioning during service.

In agreement with Figure 3.2, a holistic and reciprocal method is necessary to obtain an overall spatial evaluation, validity, and reliability of the study by continuous feedback:

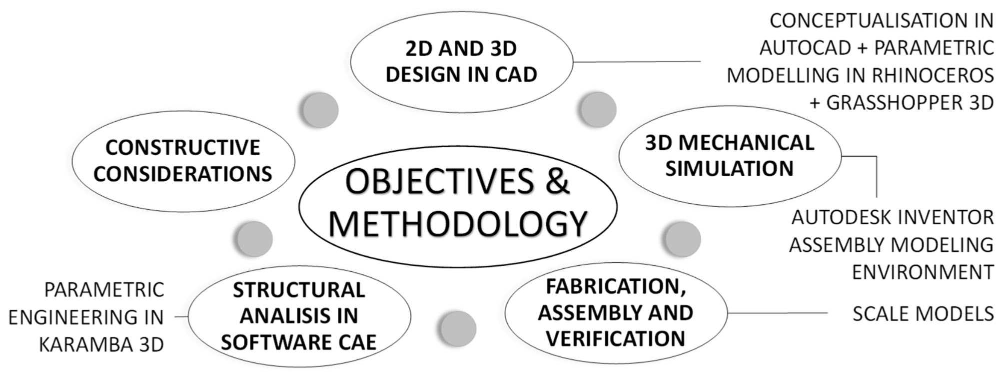

Figure 3.2 *Synthesis of research objectives and interconnected methodological procedures.*

3.2 Methods to design pantograph structures

3.2.1 Geometric expressions

Key concepts are worth mentioning following Abraham Tchako (2008), to examine the constitution of a deployable structure incorporating scissors & sliding mechanisms:

- DoF [*Degrees of Freedom]*: *Number of independent motions of a particular link or between the components interacting in a mechanism.*

- Mechanism: *A set of moving parts that work together to achieve a force transmission.*

- Kinematic chain: *An assemblage of links and joints «or linkages» providing a controlled motion. At least one element is grounded or attached to the frame.*

- Link: *A nominally rigid body or element that possesses a minimum of 2 nodes.*

- Node: *A singular attachment point between links through joints.*

- Joint: *A connection between two or more links at their nodes; it can be denoted as articulations in mechanisms.* The most familiar joints are indicated in Figure 3.3:

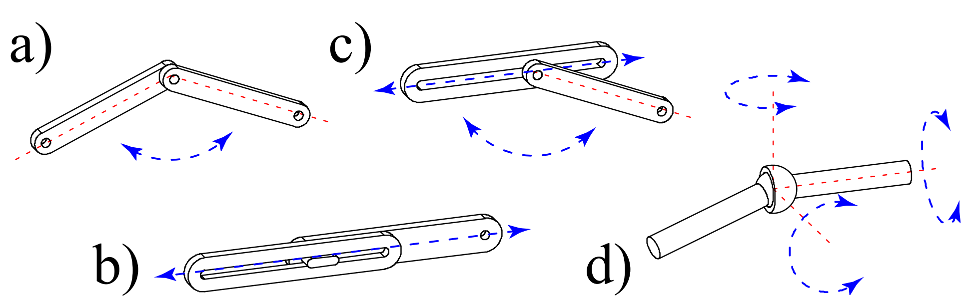

Figure 3.3 *Joint types: a) R-joint, b) P-joint, c) Half-joint, d) S-joint.*

• Revolute joint (R): *A joint that allows a rotary motion. Also called pin joint or hinged joint* [Figure 3.3a].

• Prismatic joint (P): *A joint that allows relative translational freedom or linear motion [slider]. Since a line is a continuous succession of points in space, both joined links possess a minimum of 2 nodes [Figure 3.3b].*

• Half-joint: *A combination between the revolute joint (R) and the prismatic joint (P). The roll-slide movement produces 2 DOF's* [Figure 3.3c].

• Spherical joint (S): *A joint with three independent rotational freedoms. In planar mechanisms, a multiple-joint is not used (J = 3)* [Figure 3.3d].

• Joint order: *The order corresponds to one number less than the total of links (L) joined. From the kinematic point of view, there exist an equivalency of (L-1) degrees of freedom.* Examples are shown in [Figure 3.4]:

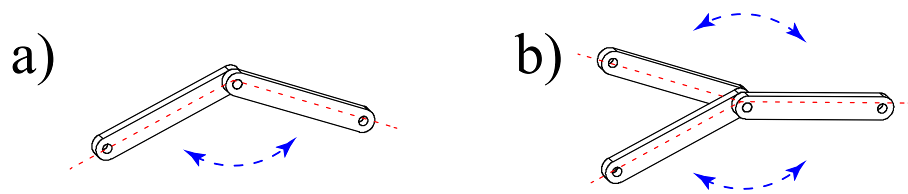

Figure 3.4 *a) First order R-joint [2 links = 1DOF], b) Second order R-joint [3 links = 2DOF].*

On a system of *n* rigid bodies moving in two dimensions, every free-standing link has 3 DoF of the Cartesian coordinates: two mutually perpendicular translations [x,y axes] and one rotation [z axis]. Therefore, joints can impose restrictions to reduce the number of independent displacements that the mechanism has.

The Grübler–Kutzbach equation can be utilised to calculate the degrees of freedom of a planar linkage:

$$\boldsymbol{M} = 3(\boldsymbol{L} - 1) - 2\boldsymbol{J_1} - \boldsymbol{J_2}$$

Where:
$\boldsymbol{M}$: degree of freedom or mobility of the mechanical system
$\boldsymbol{L}$: number of moving bodies [links] including the fixed body
$\boldsymbol{J_1}$: joints with 1DoF [R-joints, or P-joints]
$\boldsymbol{J_2}$: joints with 2DoF [half-joints]

Figure 3.5 references basic triangular exercises in 2D and synthesises the mobility results. It is noticeable that a truss structure has no mobility [Figure 3.5a], and variations of deformable triangles are achievable: a three-link mechanism with two revolute joints and a half-joint is represented in Figure 3.5b, while four links with three revolute joints and one prismatic or sliding joint are exposed in Figure 3.5c.

On pantograph structures, the last scenario can be understood as a telescopic frame that maintains a triangular pattern.

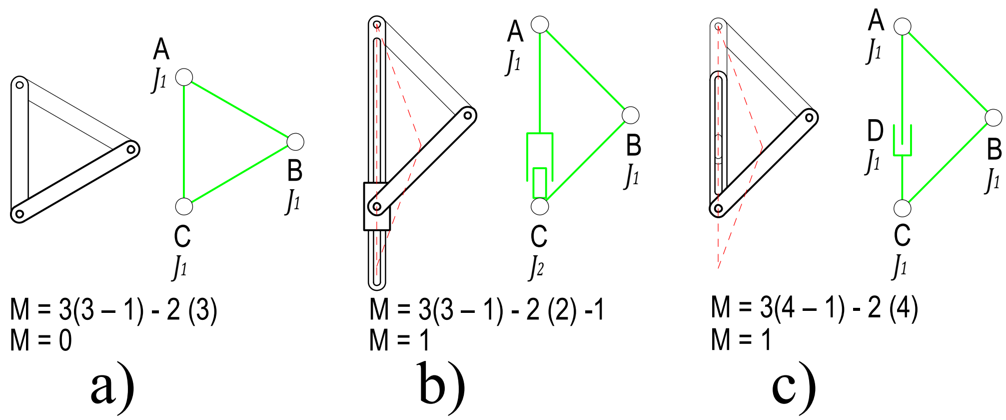

Figure 3.5: *Triangular configurations: (a) No mobility, (b and c) 1DOF.*

On the other hand, a four-bar linkage creates a 1Dof pattern [Figure 3.6a]; however, if the traditional deformable quadrilateral mechanism is connected to another, it generates a higher number of independent movements and thus, a random force transmission [Figure 3.6b]. Scissors can be created simply by prolonging the length of the links from a module to the next [Figure 3.6c]; as a result, each link obtains a minimum of 3 nodes and the system acquires intermediate hinges between bars pairs [e.g., the semi-lengths between the nodes $\overline{DC}$ + $\overline{CE}$ pertain to the same link].

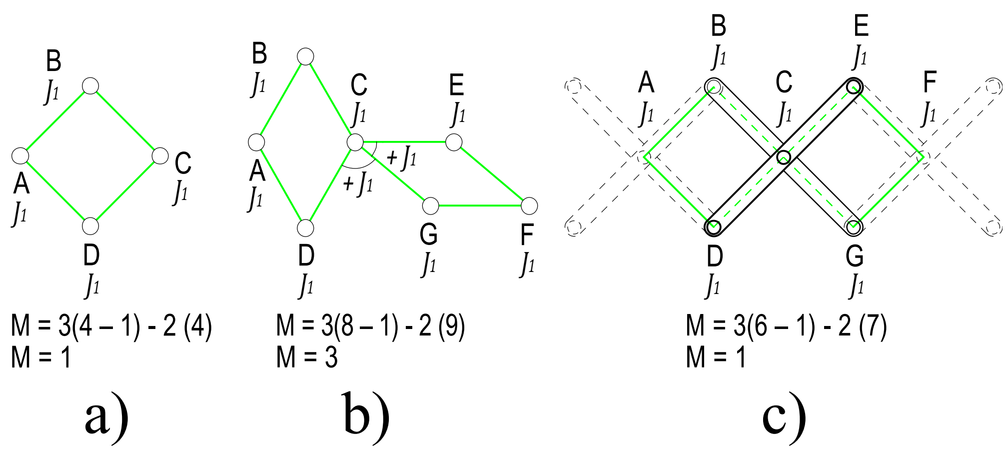

Figure 3.6: *Quadrangular configurations: (a) A four-bar linkage, (b) A linkage of articulated bars, (c) A scissors linkage.*

Taking by reference the geometrical analysis by Santiago Calatrava for his PhD thesis (1981; 1993), it is possible to project a two-dimensional mechanism on the π plane to get deployable rhomboidal modules. Therefore, a spatial abstraction of an umbrella can be evaluated, and an equivalent simplification of a deployable tent with a quadrangular base can be understood, since the schematic mechanism repeats in the x and y directions.

Despite the single mobility expressed in Figure 3.7, lateral instabilities can be inferred for these configurations on three dimensions:

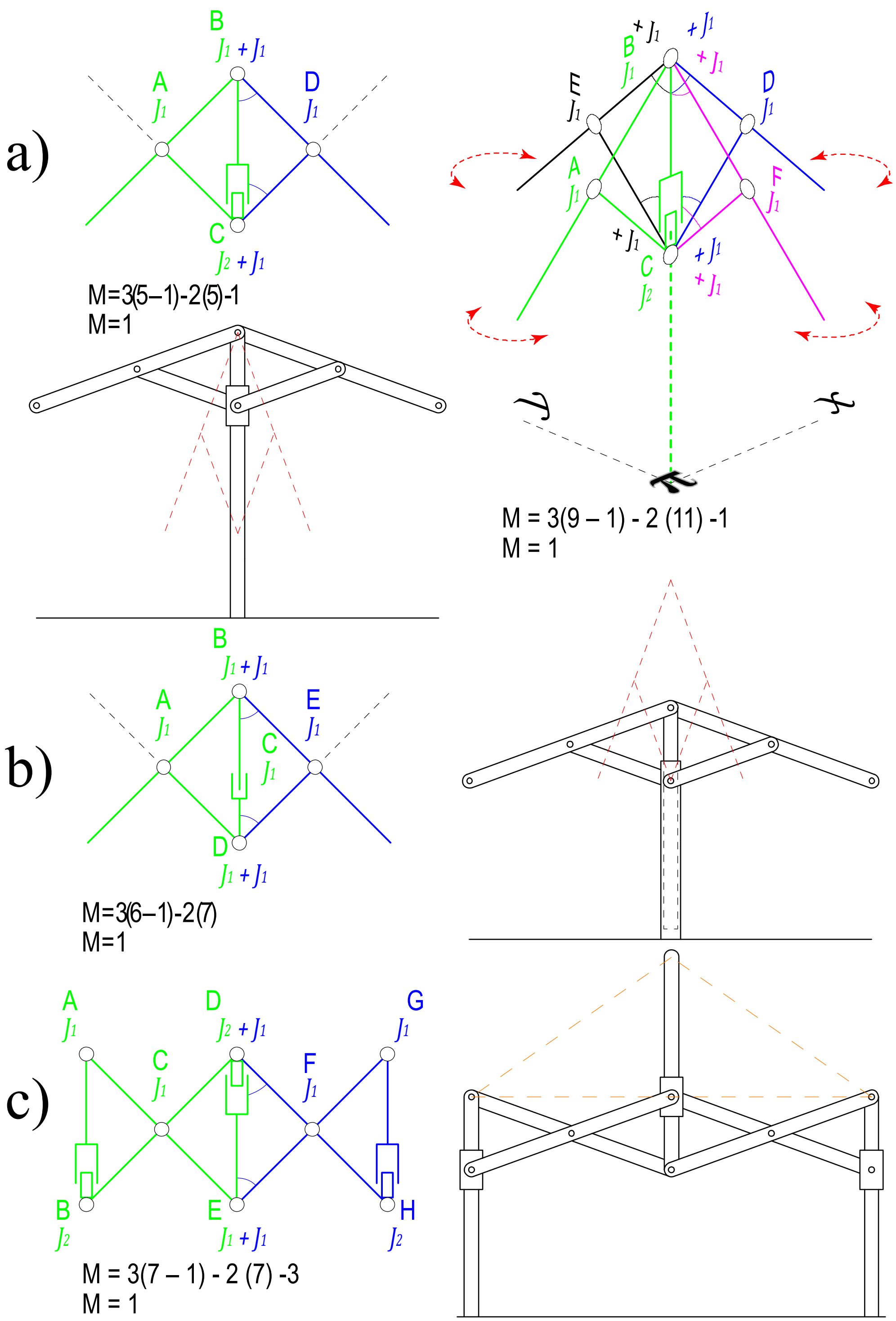

Figure 3.7: *Umbrella like shape: a) With a rigid mast, b) With a telescopic mast; c) Deployable tent representation.*

In brief, a system of links and joints could be classified according to their mobility:

- The system becomes a mechanism when M > 0.
- The system becomes an isostatic structure when M = 0.
- The system becomes a hyperstatic structure when M < 0.

However, occasionally the Grübler–Kutzbach equation results are incorrect on planar mechanisms. Kinematical paradoxes can occur, for instance on special geometries, by redundant linkages or due to size differences between links [Figure 3.8].

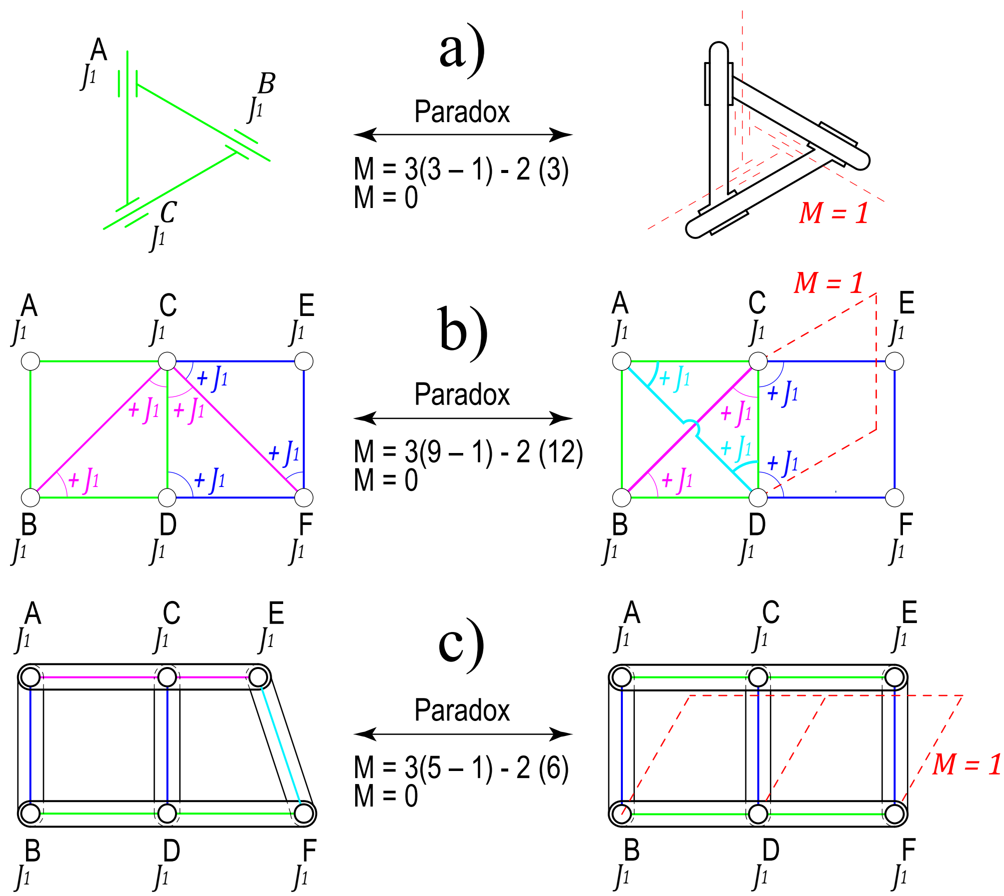

Figure 3.8: *Kinematical paradoxes: a) A slidable triangular bar system, b) Superfluous link on a mechanism, c) A parallel crank mechanism.*

An overconstrained mechanism might be obtained if a linkage has mobility M = 0 or less, but it still moves in practice. This geometrical particularity is typical on spatial scissor structures, despite the fact that the Grübler–Kutzbach mobility formula considers six possible independent movements for the joints [3 translations and 3 rotations in the x, y, z Coordinate Axis System]:

$$\boldsymbol{M = 6(L-1) - 5J_1 - 4J_2 - 3J_3 - 2J_4 - J_5}$$

Since the redundant constraint equations governing these mechanisms have many variables [e.g., it can be caused when joints are restricting the same degrees of freedom], a kinematic diagram or graph is necessary to decompose the chain complexity. Experts have proposed different methods, among which the most adopted is the screw theory (Zhao, et al., 2009; Nagaraj, et al., 2009; Han, et al., 2019).

During the case studies assessment, this thesis utilises substitute software applications to counterbalance the limitations on calculating mobility by a simplified equation: parametric design [Section 3.2.2] and mechanical simulations [Section 3.3]. Physical models performance is tested before a complementary structural analysis.

3.2.2 The ellipses theory in Grasshopper 3D

In agreement with Escrig (1984a)**,** the following equation should be used to obtain a fully compacted structure:

$$\boldsymbol{l_i + l'_i = k_{i+1} + k'_{i+1}}$$

In other words, when scissors are connected, the sum of the bars' semi-lengths on one side should be equal to the adjoining units. This method can be used when connecting any scissor-type, as shown in Figure 3.9:

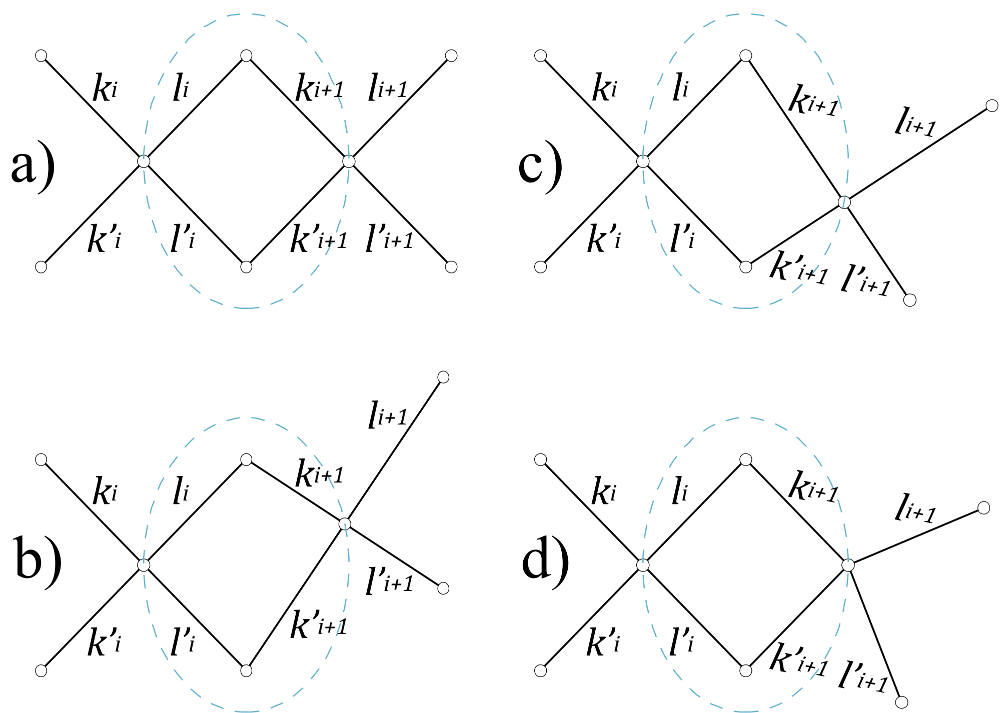

Figure 3.9 *Representation of Escrig's deployability condition: (a) Plane translational units, (b) Plane translational units + curved translational units, (c) Plane translational units + polar units, (d) Plane translational units + angulated units.*

The ellipses method was first introduced by Luis Sánchez-Cuenca Lopez (1996a; 1996b; 1996c), and later De Temmerman (2007, pp. 39-86) adopted a step-by-step procedure for the consecution of scissor linkages through computer modelling, and the automation in Cabri Geometry II: a software created by Marie Laborde y Franck Bellemain in 2000, for the interactive learning of mathematics and sciences. These variables are fundamental for defining a simplified three-dimensional parametric scenario, in which the mechanism and the ellipses transformation are synchronously emulated; consequently, I chose to learn the design environment of Rhinoceros® version 5 SR9 64-bit and the plug-in Grasshopper™ version 0.90076.

Rhinoceros was originally created by Robert McNeel & Associates in 1980 as a complement of AutoCAD [Autodesk]; it is based on the NURBS mathematical model, and nowadays it is the market-leading industrial design CAD software. Grasshopper is an intuitive graphical algorithm editor created by David Rutten at Robert McNeel & Associates in 2007; it allows to control geometric modelling on three dimensions without precise programming knowledge, simply by dragging and connecting components onto a canvas. The robust and versatile interface has been widely accepted by a community of professionals across various fields, including architecture, engineering, and product design, among others. Beginners can be target users, as the logic for manipulating the elements in visual programming is executed graphically instead of textually.

Understanding the ellipses principles on scissors and sliding mechanisms followed by a geometric construction sequence is a convenient way to assess the thesis goals on a first level, instead of an algorithm with specialised mathematics, expressions & conditionals, or by scripting and code. The correct conception of a single ellipse is sufficient to govern and control varied deployable structures, as it was previously shown in Figure 3.9; therefore, a customised base file can be created to support many other realisations during the exploration. Summarised explanations to obtain an ellipse matching a scissor-type mechanism are indicated in Figure 3.10 to Figure 3.13:

- Conceive an imaginary plane translational scissor between the nodes $\overline{AC}$, $\overline{CE}$ and $\overline{BC}$, $\overline{CD}$.

- The first parameter is to create a circumference with a centre in E, and radius (r_1):

$$\boldsymbol{r_1 = \frac{\overline{CE} + \overline{CD}}{2}}\textit{; since for a plane translational scissor } \overline{CE} = \overline{CD}\textit{, then, } \boldsymbol{r_1 = \overline{CE}}$$

- The movement is controlled by the rotation (α) of the bar $\overline{AC}$, $\overline{CE}$, taking by reference node E. The bar $\overline{BC}$, $\overline{CD}$ is simply mirrored about the node C, that is always intersecting the circumference during displacements.

• To create the ellipse geometry in Grasshopper, it is necessary to define the focal points at the nodes D, E, and the centre [origin O] located at the imaginary mid-point of the line segment $\overline{DE}$. Subsequently, the semi-major axis corresponds to the radius distance r_1, and the semi-minor axis is equal to $\overline{OC}$.

• A second parameter to get curved translational units or polar units requires creating a circumference with a centre in E and radius (r_2), that is always intersecting the ellipse during displacements:

$$\boldsymbol{r_2 = \overline{EF}}$$

• To create angulated units, the bars semi-lengths $\overline{FG}$ and $\overline{FH}$ are obtained about a kink angle (ω). For all cases, double-sized ellipses could be used to project contiguous scissors along a specific curvature.

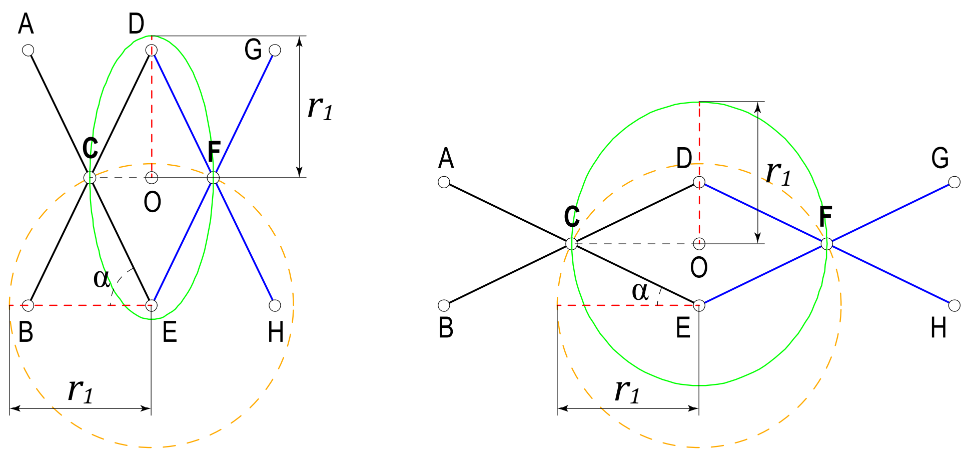

Figure 3.10 *The ellipses method using plane translational units.*

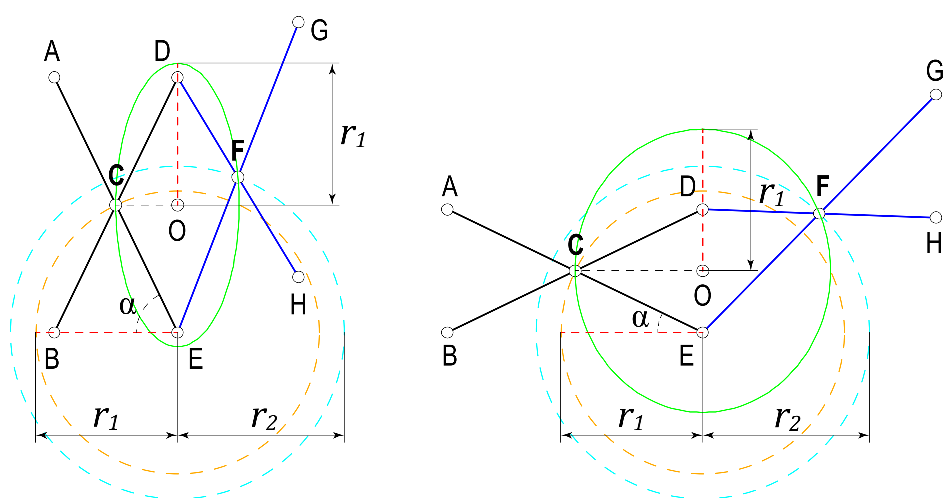

Figure 3.11 *The ellipses method using plane translational units + curved translational units.*

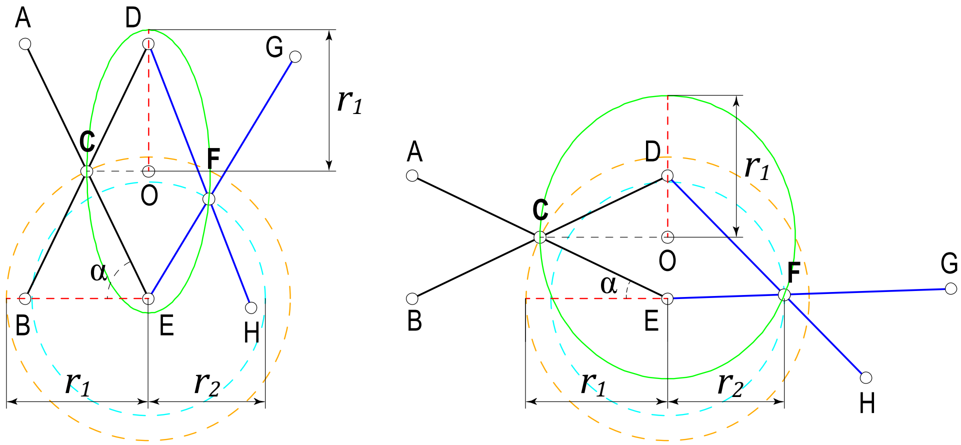

Figure 3.12 *The ellipses method using plane translational units + polar units.*

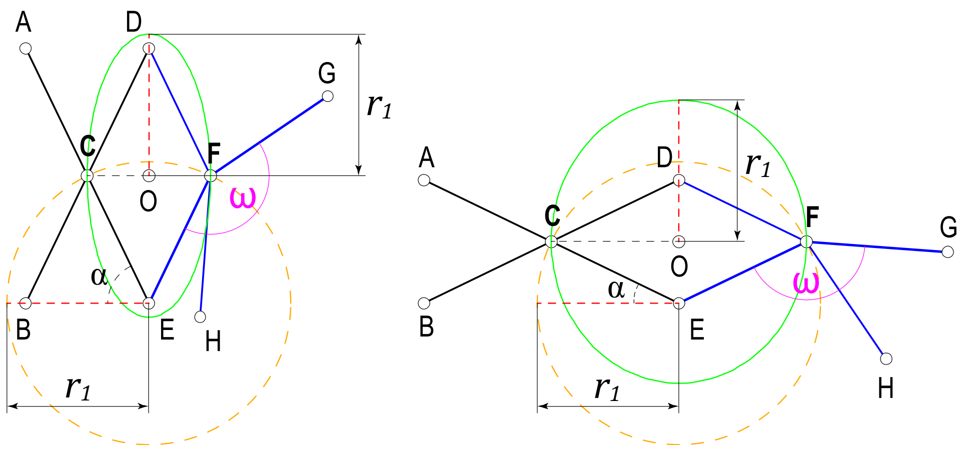

Figure 3.13 *The ellipses method using plane translational units + angulated units.*

From the defined parameters, a sequence of transformed replicas controls diverse geometrical arrangements and its kinematics simplification (e.g., using the move, rotate 3D, orient components). For this reason, a real-time deployment visualisation of the model facilitates a primary decision-making source during the case studies conceptualisation.

Figure 3.14 suggests prismatic modules that are theoretical "unrolled abstractions" of planar linkages, thus keeping simultaneous and unique parametric movement control. However, structural stability is not granted for every case since other aspects need to be aforethought, such as the joint types and the eventual out-of-plane beams buckling when external forces are applied.

A triangular prism is rigid in all directions, but a quadrangular prism is intrinsically conditioning the angular deformations by the Unit X / Unit Y vectors, or the XZ, YZ face planes of the parametric file. Likewise, in the conversion from 2D to 3D, it is notable that the ellipses can be turned into ellipsoids.

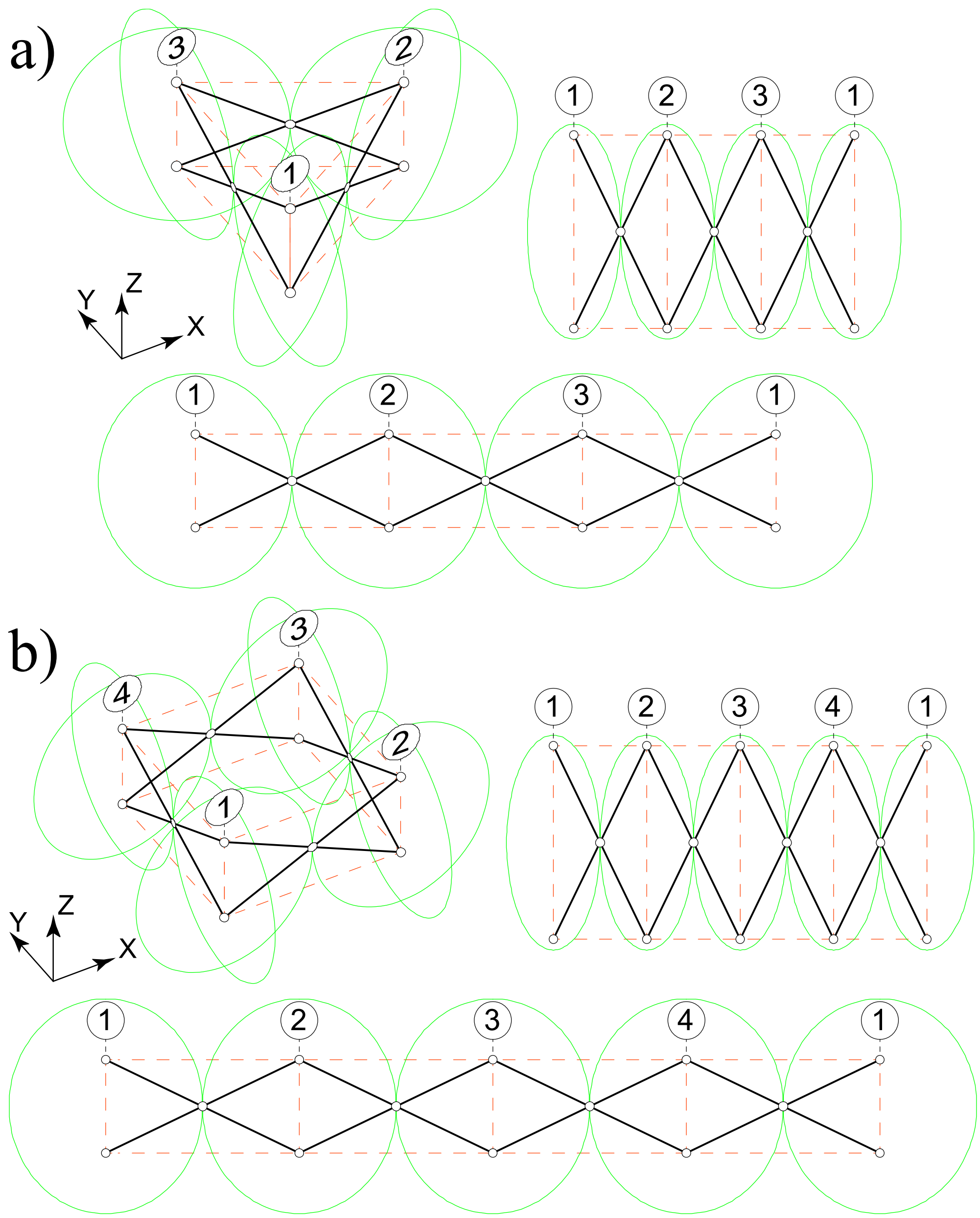

Figure 3.14 *Standard configurations: a) Regular triangular prism, b) Regular square prism.*

The previous elementary examples can be progressively modified and combined to configure more complex geometries, instantaneously evaluate variables such as the joints' eccentricities, the linear or angular dimensioning, and determine the fabric compatibility matching the structure deployment [Figure 3.15].

A further inspection could be performed through the interactive plug-in for physics and constraint solver Kangaroo3d (Piker, 2013); however, this is not included in the current thesis.

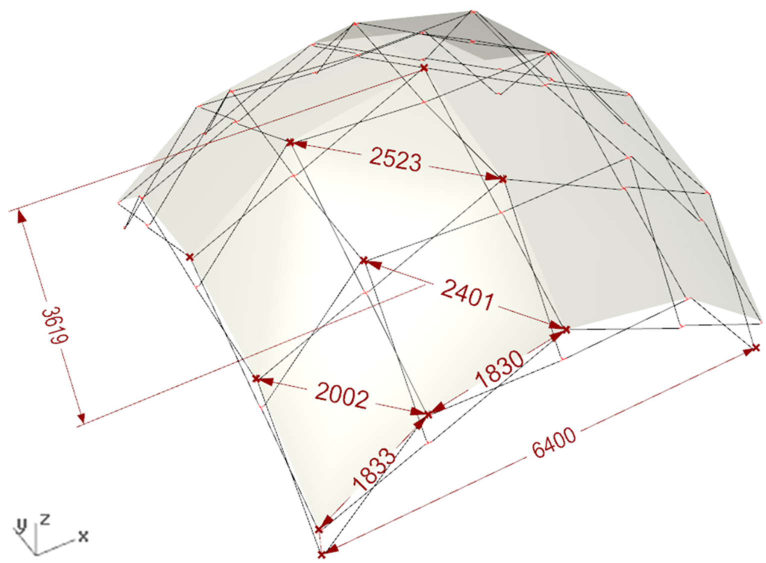

Figure 3.15 *Inspection of the membrane compatibility for an arbitrary synclastic structure.*

3.3 Movement simulation in Autodesk Inventor

Autodesk Inventor is a software for the parametric modelling of solids created in 1999, as the competitor of existing specialised design, fabrication, and engineering packages: CATIA [1977], Pro/ENGINEER [1991], SolidWorks [1995], and Solid Edge [1996]. Extensive and complex mechanical assemblies can be tested from adjustable part creations, allowing users to produce and enhance new products. Functionality is not limited to the interface since AutoCAD *.dwg or other cad software ACIS *.sat files can be imported/exported as sketches, easing the data processing for this research.

Whereas it is feasible to obtain static [or dynamic] structural analysis in Autodesk Inventor, the timing and computational requirements are significantly lower in the parametric design environment of Rhinoceros® + Grasshopper™ + the structural analysis tool provided by the plug-in Karamba3D [Section 3.5]. On the other hand, detailed engineering is essential to prevent excessive local deformations on the scissor's bars, optimise the joint dimensions and the material capacities; nonetheless, it is considered beyond the scope.

Three-dimensional mechanical simulations complementing the case studies are the central focus through the platform, bearing in mind that it is not directly possible to cause deformations on the components assemblage. Therefore, stress-free deployable structures using scissors and sliding mechanisms are evaluated.

In the model information tab, the degrees of mobility [dom] indicate the possible movement types of the entire mechanism. This value is calculated by the sum of all the degrees of freedom minus the constraints, and each kinematic chain is examined for whether it is closed (Autodesk Inc, 2021), [Figure 3.16]:

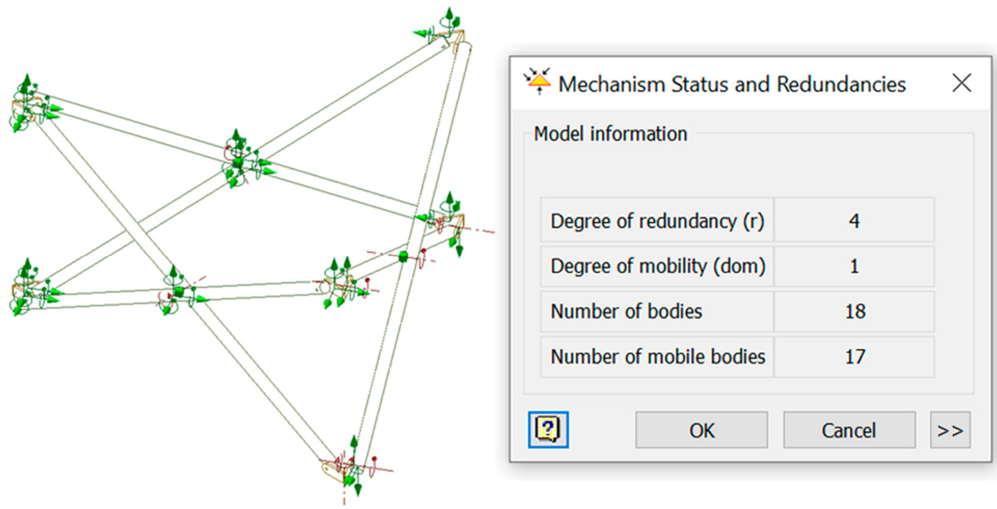

Figure 3.16 *Example of a mechanism status and redundancies dialogue box.*

Inductive kinematic testing was performed on equivalent triangular prisms from the prior art; the modelling and assembly conditions are the same, despite contrasting scissor typologies [i.e., the number of parts, and rotary vertex joints acting as door-hinges]. The result validates a single degree of movement for all cases. Still, rotary vertex joints are only required by Figure 3.17b in practice, since the basic triangle forming the oblique prism produces angular differences during transformations:

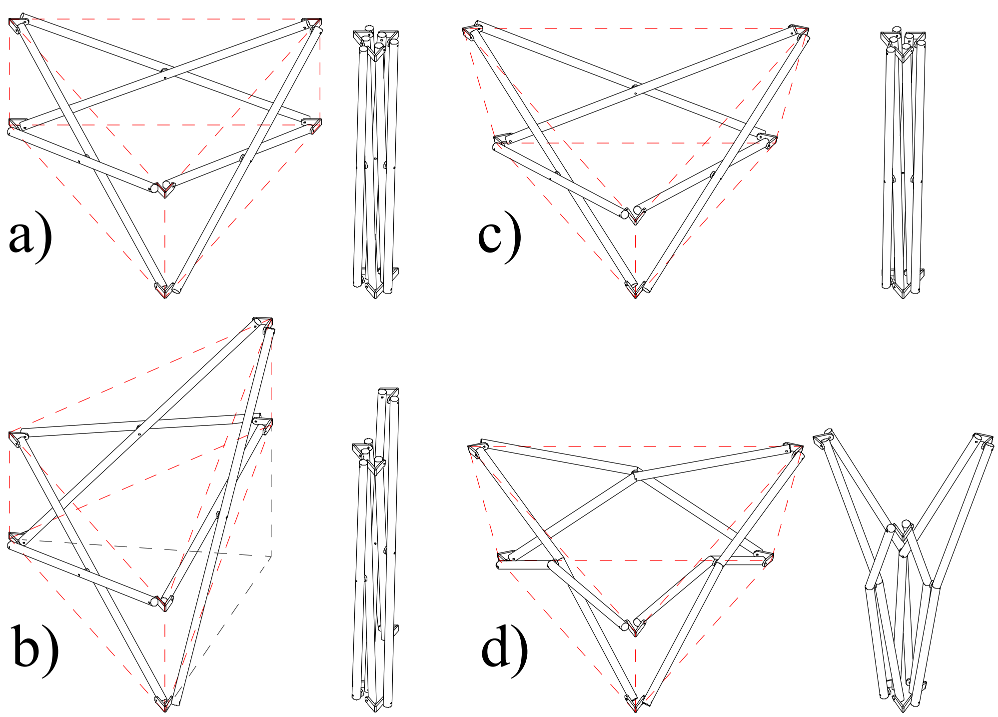

Figure 3.17 *Triangular prism variations: a) Right prism using plane translational units, b) Oblique prism using plane and curved translational units, c) Truncated prism using polar units, d) Truncated prism using angulated units.*

3.4 Fabrication on scale models

3.4.1 Additive Manufacturing

In consideration of the joints importance on scissors and sliding mechanisms, testing and validating processes in this thesis employ additive manufacturing techniques [AM], also known as three-dimensional printing [3DP or 3D printing], in combination with light industrial tools.

Digital modelling & fabrication recourses may comprise subtractive manufacturing [machining] and other technologies to produce physical objects; however, the selected method is the most popular and cost-effective route to explore and validate concepts on plastic scale models. Besides, the applicability of AM has reached experimental developments in ceramic, concrete, and metals, meaning future opportunities for the construction sector (Buchanan & Gardner, 2019).

In recent years, high-resolution 3D printers have become more affordable, user-friendly, and reliable. Established technologies to print plastics for production parts or custom manufacturing incorporates stereolithography [SLA] and selective laser sintering [SLS]; nonetheless, fused deposition modelling [FDM] is chosen for simple prototyping when demands are lower than industrial levels.

Models were printed in the most used plastics: ABS and PLA, although the latter was preferred. An original Prusa i3 mk2 with 1.75mm filament and 0,4 extruder nozzle was calibrated to create a 40-60% triangle pattern infill, depending on the required strength, shape variations, and parts functionality.

3.4.2 Other materials, tools & accessories

For the scale models in Section 5.2, the primary prism dimensioning of each case study follows the equation depicted in Section 3.2.2:

$$\boldsymbol{l_i + l'_i = k_{i+1} + k'_{i+1}}$$

$\boldsymbol{l_i + l'_i}$ = 50 cm
$\boldsymbol{k_{i+1} + k'_{i+1}}$ = 50 cm

Scissor beams are made of aluminium 6063-T5 round tubes Ø12.7mm, zinc-plated machine screws: pan head M3X5mm to M3X35mm, M3 nuts, and washers. During the repetitive manual fabrication procedure, a mini drill press with variable speed is adapted to get a low-tech controlled motion on the x-axis, by using an aluminium t-slot extrusion 45X45mm rail linked to the machine bench, and 3D printed brackets to calibrate the distances between each perforation [Figure 3.18]. Parts are sized by a 1/4-inch to 1-1/8-inch tubing cutter with a ratchet handle and assembled using a cordless electric screwdriver.

Ordinary material is chosen for testing the covering membrane compatibility to the structure; however, a lightweight waterproof fabric [e.g., PVC / Polyester / Nylon / Acrylic / HDPE / other] is more suitable for final prototypes. Eyelet punch pliers and 4 mm eyelets are optional reinforcement tools to protect the fabric from tearing when exposed to stress.

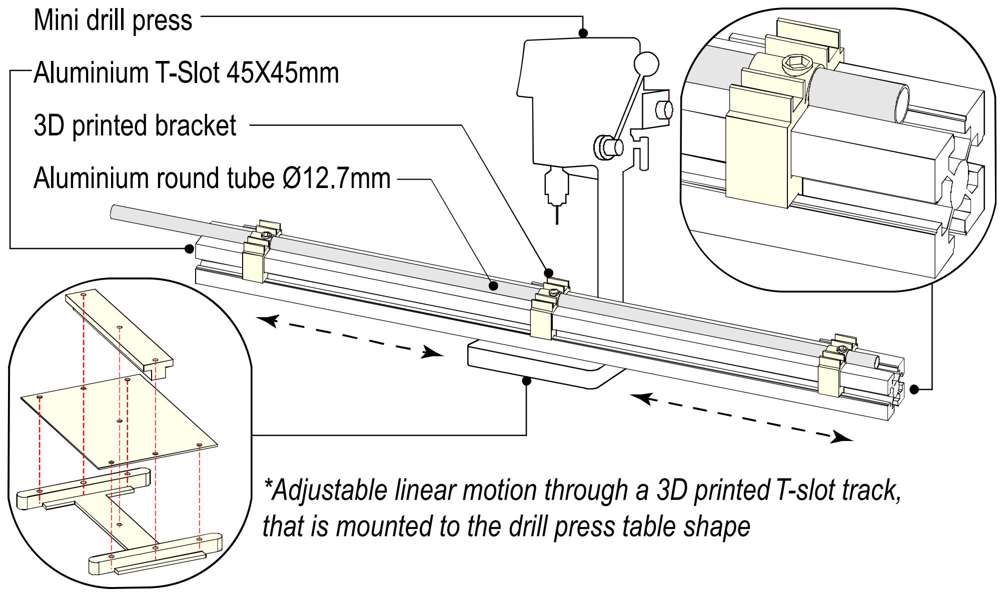

Figure 3.18 *Linear motion on a mini drill press.*

3.5 Preliminary structural analysis

3.5.1 Structural assessment in Karamba 3D

Karamba is a Finite Element Analysis FEA software released to the public in 2010 by Clemens Preisinger, in collaboration with Bollinger und Grohmann ZT GmbH. The parametric environment integrated on Rhinoceros® + Grasshopper™ allows architects and engineers to assess the data flow between geometrical or structural variables, with an immediate response to any input change [i.e., truss, beam, and shell elements]. For this reason, behaviour predictions of statical models under external loads can be assessed during early design (Preisinger, 2013).

This thesis phase follows the methodological modelling concepts for the parametric analysis of deployable scissor structures in Karamba (Alegria Mira, et al., 2012); (Alegria Mira, 2014, pp. 45-47). The connectivity between geometric components from the line model conversion to a beam model, material properties, cross-sections, support conditions, and loads are further explained in Chapter 6 for the assessment of theoretical tents. The data collected is performed in Karamba version 1.2.2 – build 161020 (Preisinger, 2016); and the workflow can be likewise generalised to umbrellas incorporating pantograph-sliding mechanisms.

Ideally, the ellipses method can produce arbitrary curvatures from conic sections to define architectural enclosures beyond the traditional mono-pitch or dual-pitch roofs, circular cylindric vaults and hemispherical domes [Figure 3.19]; thus, the geometry outlines are established by a combination of case studies.

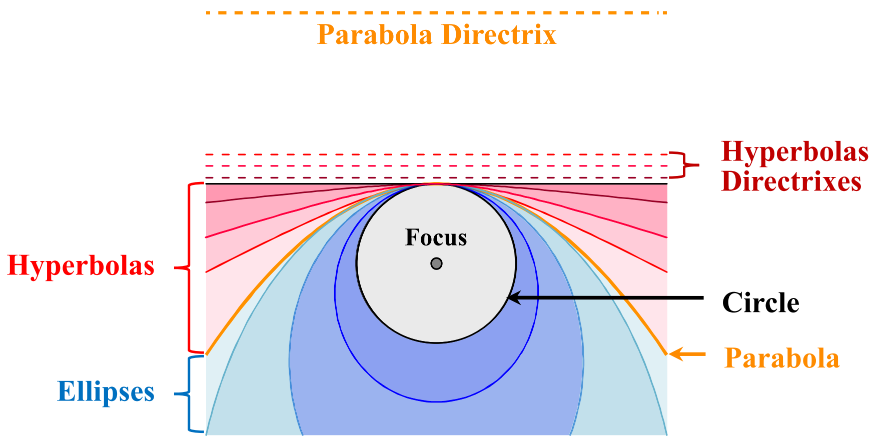

Figure 3.19 *Conics.*

Modelling simplifications are accepted for the targeted conceptual analysis: beams are assumed as the main load-bearing members for this study, whereas comparison to alternative stabilisation methods by cables is performed; for the covering fabric, a mesh geometry is only active to calculate its weight and the wind or snow load areas of incidence, despite that the material may also produce a structural contribution. Since joints and hinges are created employing zero-length springs, the geometry is controlled by 3 translational stiffnesses *Ctx, Cty, Ctz* [kN/m] and 3 rotational stiffnesses *Crx, Cry, Crz* [kNm/rad]; therefore, there exists a constructive parameter in the model, but further research is needed for structure in these one-dimensional elements.

Being design done within the elastic range, under given loads Karamba assumes the maximum stress in a cross-section lying below the yield stress of the material (fy), and the ModelView-component displays utilisation of cross-section as the ratio of actual stress and yield stress; hence, values below 100% are effective indicators in the ranges of compression and tension.

Although detailed engineering is not covered, the structural kinetical evolution is inspected for a deployed geometry under service loads and between intermediate positionings under self-weight only, to visualise critical conditions that may affect the design, planning and installation on site. For instance, the procedure of raising or lowering the structure from the terrain level produces differential gravity forces to a hanged package from a tower or a crane; this may well determine the feasibility of production, construction, and operation, as the material capacities could be exceeded at any moment by a concentration of force.

3.5.2 Eurocode climate loads

The basis of calculation of wind velocity and wind velocity pressure are formulated in the same sequence of the European Standard EN 1991-1-4, Section 4 (Technical Committee CEN/TC250, Structural Eurocode, 2005):

$\boldsymbol{v_b = c_{dir} \cdot c_{season} \cdot v_{b,0}}$		
Symbols	**Definitions**	**Value**
c_{dir}	directional factor [*Recommended value: 1*]	1
c_{season}	seasonal factor [*Recommended value: 1*]	1
$v_{b,0}$	fundamental value of the wind velocity	26 m/s
v_b	basic wind velocity	26 m/s

$\boldsymbol{v_m(z) = c_r(z) \cdot c_o(z) \cdot v_b}$		
Symbols	**Definitions**	**Value**
$c_r(z)$	roughness factor	0.960
$c_o(z)$	orography factor [*Recommended value: 1*]	1
v_b	basic wind velocity	26 m/s
$v_m(z)$	mean wind velocity	24.977 m/s

$\boldsymbol{c_r(z) = k_r \cdot ln\left(\frac{z}{z_0}\right) \quad for \quad z_{min} \leq z \leq z_{max}}$		
Symbols	**Definitions**	**Value**
k_r	terrain factor	0.19
z	height above the ground	7.85m
z_0	roughness length [*Terrain Category II*], terrain category parameter to evaluate.	0.05m
$c_r(z)$	roughness factor	0.960

$\boldsymbol{k_r = 0.19 \cdot \left(\frac{z_0}{z_{0,II}}\right)^{0.07}}$		
Symbols	**Definitions**	**Value**
z_0	roughness length [*Terrain Category II*], terrain category parameter to evaluate.	0.05m
$z_{0,II}$	roughness length [*Terrain Category II*], standard given by the formula.	0.05m
k_r	terrain factor	0.19

$\boldsymbol{\sigma_v = k_r \cdot v_b \cdot k_l}$		
Symbols	**Definitions**	**Value**
k_r	terrain factor	0.19
v_b	basic wind velocity	26 m/s
k_l	turbulence factor [*Recommended value: 1*]	1
σ_v	standard deviation of the turbulence	4.94 m/s

$\boldsymbol{l_v(z) = \dfrac{\sigma_v}{v_m(z)} = \dfrac{k_l}{c_o(z) \cdot ln(z/z_0)} \quad for \quad z_{min} \leq z \leq z_{max}}$		
Symbols	**Definitions**	**Value**
σ_v	standard deviation of the turbulence	4.94 m/s
$v_m(z)$	mean wind velocity	24.977 m/s
$l_v(z)$	turbulence intensity	0.197

$\boldsymbol{q_p(z) = [1 + 7 \cdot l_v(z)] \cdot \dfrac{1}{2} \cdot \rho \cdot v_m^2(z) = c_e(z) \cdot q_b}$		
Symbols	**Definitions**	**Value**
$l_v(z)$	turbulence intensity	0.197
ρ	air density	1.25 kg/m3
$v_m(z)$	mean wind velocity	24.977 m/s
$v_m^2(z)$	(mean wind velocity)^2	623.893 (m/s)^2
$q_p(z)$	peak velocity pressure	0.929 kN/m2

$\boldsymbol{c_e(z) = \dfrac{q_p(z)}{q_b}}$		
Symbols	**Definitions**	**Value**
$q_p(z)$	peak velocity pressure	0.929 kN/m2
q_b	basic velocity pressure	0.422 kN/m2
$c_e(z)$	exposure factor	2.200

$\boldsymbol{q_b = \dfrac{1}{2} \cdot \rho \cdot v_b^2}$		
Symbols	**Definitions**	**Value**
ρ	air density	1.25 kg/m3
v_b	basic wind velocity	26 m/s
v_b^2	(basic wind velocity)^2	676 (m/s)^2
q_b	basic velocity pressure	0.422 kN/m2

From the case studies exploration, a synclastic deployable tent with a distinctive aspect to the typical semi-cylindrical vault is structurally assessed by comparable stabilisation methods. Since there is a lack of consensus on international building codes to calculate wind loads on varied curved roofs, other authors have proposed specific wind-tunnel research to design catenary vaults (Bradley, et al., 2016). Besides, the source for the Eurocode 1-1-4 vaulted roofs [Section 7.2.8: Figure 7.11] is unknown, unreliable, and outdated (Cook, 2007, pp. 44-45). This explains why the Building Research Establishment recommends new external pressure coefficients [Cpe,10] for the National Annex to British Standard (Technical Subcommittee B/525/1, Actions (loadings) and basis of design, 2010).

Notwithstanding these limitations, it is selected a generalised implementation of the Eurocodes values for vaulted roofs with a rectangular base, due to the wider countries acceptance. Chapter 6.3.1 describes the main curvature from different scissor types: plane translational, polar, and curved translational; although the characteristics do not precisely match the definition of a circular cylindrical roof. In line with Figure 3.20, it can be understood as a simplified parabola approximation supported on walls D and E; therefore, zones A, B, C are interpolated from an f/d value of 0.32 and h/d value of 0.334.

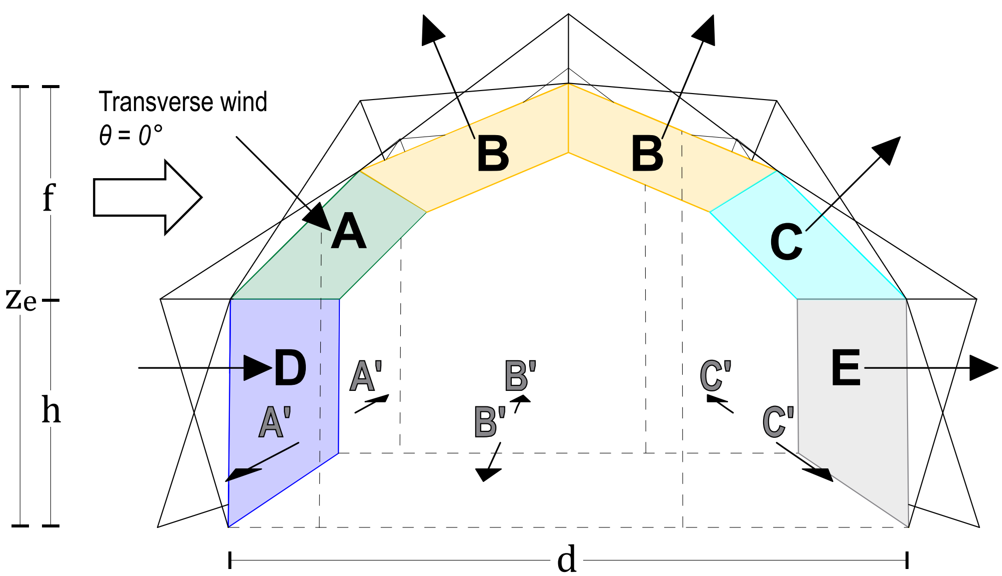

***Figure 3.20** External pressure assessment for transverse winds.*

<u>Notes:</u> 1) Roofs and walls should be divided into zones.

2) Reference height (z_e) = 7.85m, (f) = 3.84m, (h) = 4.01m, span (d) = 12m, transversal length 8.02m.

3) A', B', C' are vertical-side walls projections, as the structure is calculated as a closed design.

To evaluate the longitudinal wind external pressure coefficients, a complementary procedure is included. Although the British Standard BS 6399-2 (Technical Subcommittee B/525/1, Actions [loadings] and basis of design, 1997) was superseded by Eurocode 1 series, this method approximates different curvatures using the pitch angle for each plane face, as occurs in mansard roofs and other multi-pitch roofs. In Figure 3.21, the vertical walls A', B', D, E are deduced from Eurocode 1-1-4: Table 7.1, and the recommended values G, H, I by interpolation of (EC) Table 7.4b.

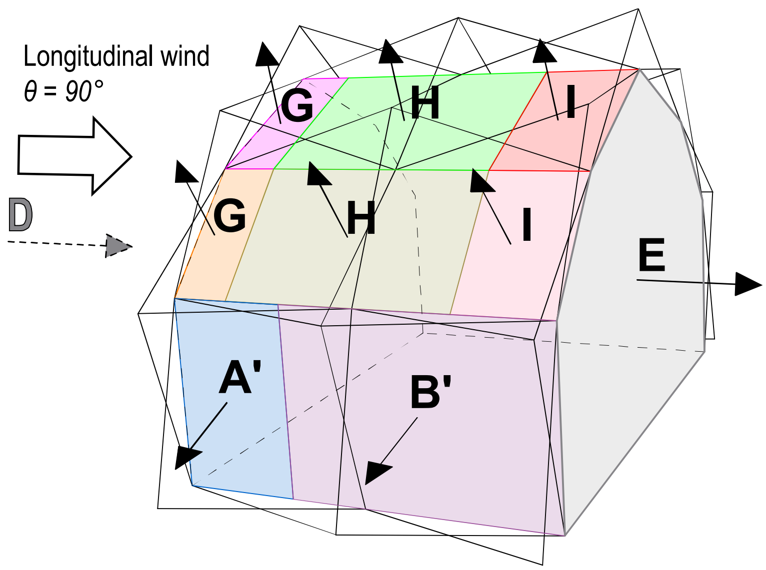

***Figure 3.21** External pressure assessment for longitudinal winds.*
<u>**Notes:**</u> **1)** Roofs and walls should be divided into zones.
2) Zone F is simplified within G since it belongs to a small local area.

On the other hand, Eurocode 1-1-4: Section 5 stipulates the procedure to calculate wind actions on external and internal surfaces. Values for $c_{pe,10}$ are used to design the load-bearing structure, and each area is referenced in Karamba by subdividing a mesh geometry that computes loads to the scissor joints. Internal pressure coefficient $\boldsymbol{c_{pi}}$ is governed by a closed geometry, and the value is taken as the most onerous of +0.2 and -0.3.

$$\boldsymbol{w_e = q_p(z_e) \cdot c_{pe}}$$
$$\boldsymbol{w_i = q_p(z_i) \cdot c_{pi}}$$
$$\boldsymbol{w = w_e - w_i}$$

Symbols	**Definitions**
q_p	peak velocity pressure
(z_e)	reference height for the external pressure
(z_i)	reference height for the internal pressure
c_{pe}	pressure coefficient for the external surfaces
c_{pi}	pressure coefficient for the internal surfaces
w_e	wind pressure acting on the external surfaces
w_i	wind pressure acting on the internal surfaces
w	total wind pressure acting on the structure

Figure 3.22 summarises a datasheet of the wind pressures for vertical walls and the vaulted roof simplification.

	Vertical walls				
	A'	B'	C'	D	E
$c_{pe,10}$	-1.2	-0.8	-0.5	0.753	-0.408
c_{pi}	0.2	0.2	0.2	-0.3	0.2
w_e	-1.116	-0.744	-0.465	0.700	-0.379
w_i	0.186	0.186	0.186	-0.279	0.186
w	-1.302	-0.930	-0.651	0.979	-0.565

	Vaulted roof								
	Wind direction θ = 0°			Wind direction θ = 90°					
				Pitch angle α = 22.78°			Pitch angle α = 45		
	A	B	C	G	H	I	G	H	I
$c_{pe,10}$	0.402	-1.02	-0.4	-1.352	-0.704	-0.5	-1.4	-0.9	-0.5
c_{pi}	-0.3	0.2	0.2	0.2	0.2	0.2	0.2	0.2	0.2
w_e	0.374	-0.948	-0.372	-1.257	-0.655	-0.465	-1.302	-0.837	-0.465
w_i	-0.279	0.186	0.186	0.186	0.186	0.186	0.186	0.186	0.186
w	0.653	-1.134	-0.558	-1.443	-0.841	-0.651	-1.488	-1.023	-0.651

Figure 3.22 *Values for the wind pressures per zone [kN/m2].*

Complementary snow loads are assessed according to the European Standard EN 1991-1-3 (Technical Committee CEN/TC250, Structural Eurocodes, 2003).

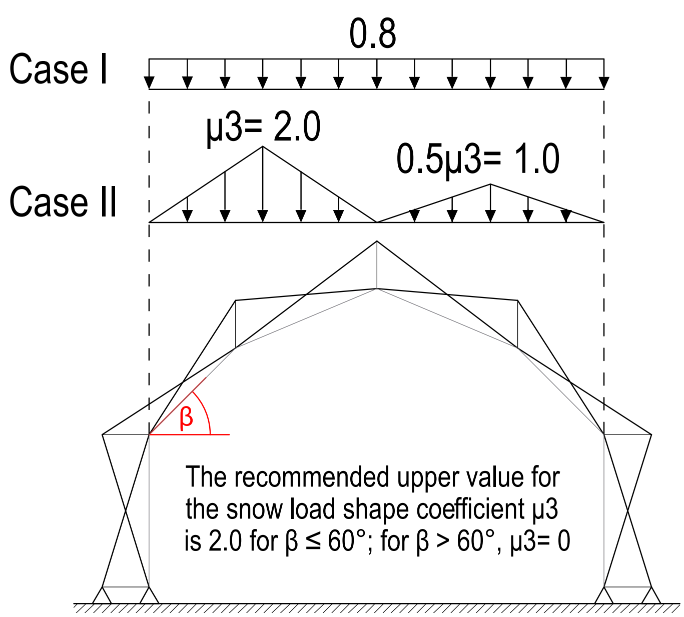

Figure 3.23 *Snow load shape coefficients for cylindrical roofs.*

Notes: **1)** Case I: Undrifted load arrangement, Case II: Drifted load arrangement.
2) The characteristic value of snow load is 0.50 kN/m²

3.5.3 Passive cables and tensioned locking devices

As means of lateral stabilisation, case studies mainly target to incorporate crossed bars mechanisms. Later, a traditional crossed cable-stiffening comparison is performed in the finite element model, assuming a perfectly levelled terrain to get proper tension in the maximum deployed position; otherwise, this may cause the need for manual adjustments in real scenarios.

For the preliminary static load simulations, beam cross-sections can be selected using Karamba standard library, however, an aluminium alloy 6061 T6 and yield strength 24.5kN/cm2 is created to improve the structural capacity. Also, a Pfeifer PG cable is chosen from the product catalogue (PFEIFER Holding GmbH & Co. KG, 2015): Spiral Strand DIN EN 12385, GALFAN-coated, useful in lightweight architecture, bridges, façades, or truss systems demanding a high-performance functionality by small cross-sections.

Among other possibilities, Figure 3.24 illustrates the selected cross-bracing cable distribution between scissors. An equivalent configuration was proposed by Lara Alegria Mira PhD (2014, p. 76); (Alegria Mira, et al., 2014), for the experimental setting and testing of a 1:1 prototype.

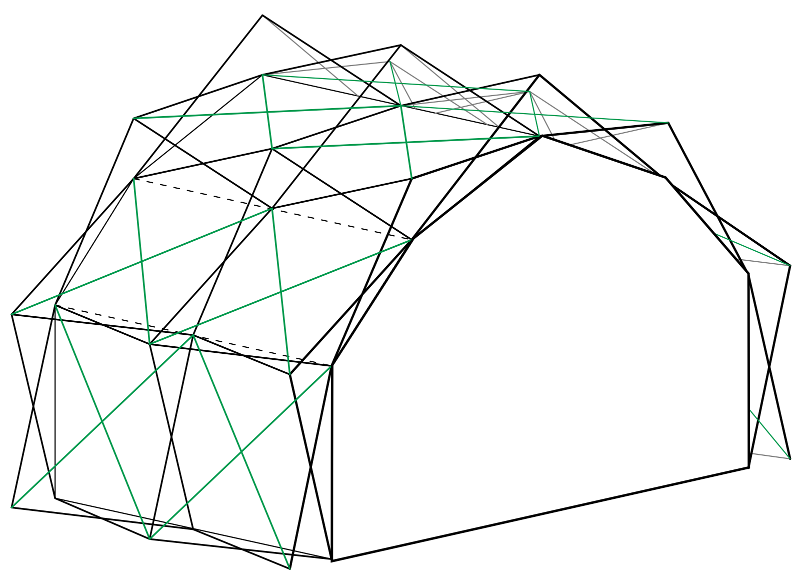

Figure 3.24 *Passive cables configuration [green lines].*

Since stress-free scissors are required to guarantee proper functioning during service, manual locking is standard on small-medium scales. Additional adjustments on larger scales are also possible if a trained operator works in heights [riggers] or incorporates specialised tools [like scaffolds]. This thesis seeks to minimise the associated risks, facilitate regular usage, and provide an enhanced structural capacity.

A deflection limit serviceability constraint of **δ < L/100** is considered sufficient by experts on emergency shelters from Médecins Sans Frontières (Koumar, et al., 2014).

Although the prior criteria apply in certain temporary constructions, the Eurocode standards indicate a conservative maximum deflection limited to the structure span divided by 250 [**δ < L/250**]. Accordingly, a related examination is performed through tensioned locking devices, targeting sufficient strength and stability on large scale structures (Kokawa, 1995; 1996; 1997; De Temmerman, 2007); for instance, Figure 3.25 conceptualises a zigzagging active cable, guided by pulley systems among scissors.

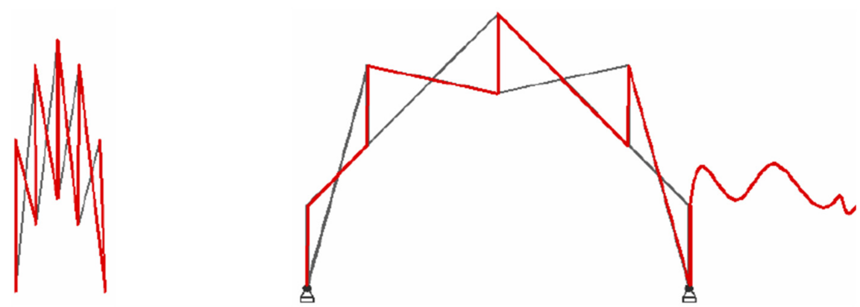

Figure 3.25 *An active cable [marked in red] connects upper and lower scissor nodes; after deployment, it is locked to stiffen the structure. (De Temmerman, 2007, p. 154)*

As the preliminary structural inspection of this thesis is not projected to be applied to a final design, no additional levels of safety are defined in the FE model. Therefore, each compared scenario can be further optimised to specific needs and verified by a structural engineer to fulfil the building codes.

3.6 Thesis editing

The common usage and versatility of Microsoft Office is the standard thesis editing set of applications: Word is the central text processor for the entire organizing and the bibliography citations, supported by spreadsheets in Excel, and image gallery classified in PowerPoint. Adobe Illustrator and Adobe Photoshop software's are selected for the digital improvement of vector graphics [points, lines, curves] and raster graphics [pixel images, photographs].

3.7 Chapter summary

This chapter provided the main procedures for obtaining an overall spatial evaluation, validity and reliability of the study, thus accomplishing the thesis second objective. Cutting edge digital modelling, analysis and fabrication methods are employed, as the reasoning behind the limitations of deployable structures using scissors & sliding mechanisms require a mixture of qualitative and quantitative research:

First, key variables were identified to conceptualise 1DOF geometries, equations, and conditions for the early design phases. Next, preliminary draftings in AutoCAD or Rhinoceros 3D, the parametric environment of the plug-in Grasshopper 3D, and the mechanical simulation of Autodesk Inventor assist in virtually recreating the case studies kinematics, since the most significant advantage of having these computer tools is to evaluate different configurations and its modifications instantaneously. Then, the functionality of the proposals against physical to-scale models is eased by 3D printing techniques for the joints, and light industrial tools for the additional system components. Finally, a simplified structural prediction in Karamba3D follows the European Standards for permanent constructions, even if the exploration is targeted for temporary and mobile architectural applications. During the real-time data collection phase, tensioned locking devices are considered to control the proper climate load deflection limits.

4 THEORETICAL CASE STUDIES

4.1 *Introduction*

The purpose of this chapter is to formulate automatic diagonal rigidisation methods for quadrangular expandable grids from the prior art, by ensuring synchronised and controlled parts interaction with 1DOF. Kinematic mechanism design is vital to satisfy the needs of use and reuse, since size and shape alterations during deployment/folding may produce components deformations or collapse by an intense force concentration; besides, the structural system gains strength at the operational state via manual locking.

Case studies exploration correspond to prisms, following the geometric principles of deformable quadrilaterals. Figure 4.2 indicates supporting definitions for the conceptual understanding:

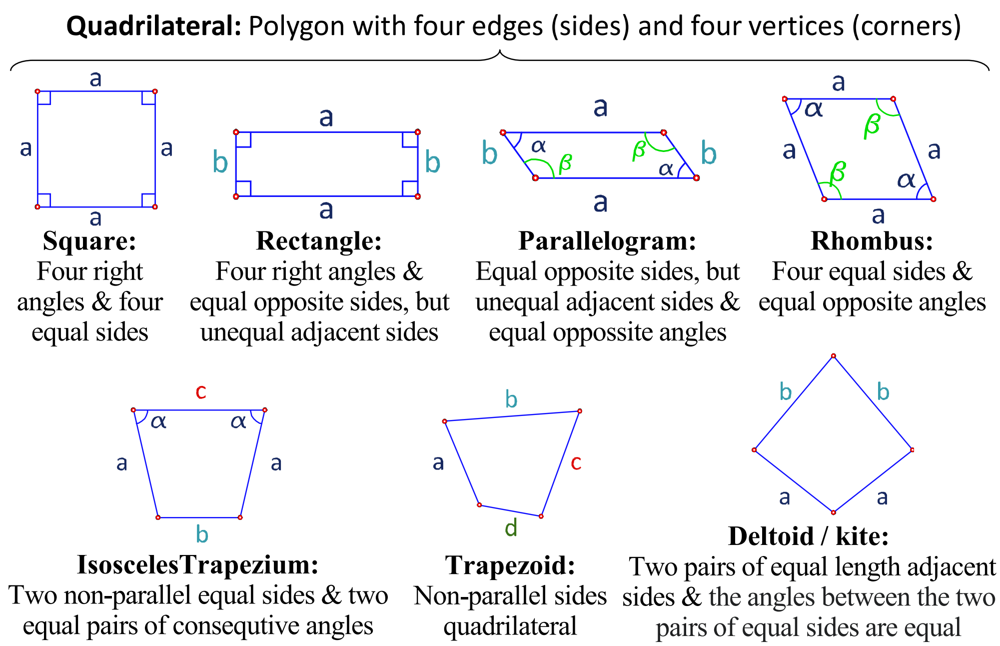

Figure 4.1 *Classification of quadrilaterals.*

4.2 *Overview of case study 1 to 8*

4.2.1 Case Study 1

In Escrig, et al. (1995, p. 484), the possibility to stabilise the angular deformation of a deployable regular square prism formed through stress-free plane translational scissors was evidenced, by incorporating a new set of irregular plane-translational scissors on the diagonals [Figure 4.2]. This theory was only examined in two dimensions, for being too complex in their opinion. However, a diagonal bracing with induced snap-through behaviour can be commonly found in self-locking and bi-stable structures, to achieve an instantaneous operational balance at the open conformation [Figure 4.3].

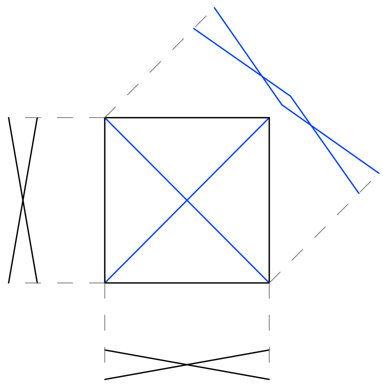

Figure 4.2 *Representation of a stress-free regular square prism.*

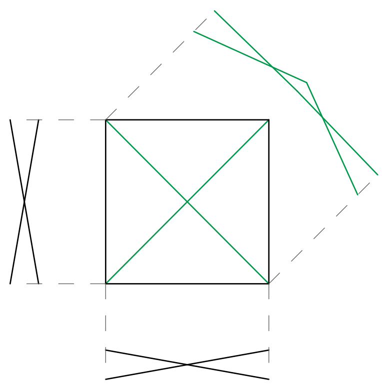

Figure 4.3 *Representation of a bi-stable regular square prism: controlled deformations occur during movements due to geometrical incompatibilities.*

Although Escrig selected the simplicity of stabilisation with cables for this example, assembly imperfections can affect the fragility vs resistance material capacities; therefore, the structure might be prone to failures during installation or dismantling, unlike ideal conditions. Current advances and accessibility on digital fabrication technologies make further explorations of the diagonal scissors outline worthwhile, especially as the constructions reliability is necessary for certification processes.

The resulting conformation can be hereinafter denoted as a 'stress-free regular square prism with double diagonalisation'. To allow a spatial rotation about a specific node, the joint solution provided by Escrig & Sánchez (2007b) was examined on the upper and lower centrally located connectors, while keeping displaced rotational axes on all the prism vertexes [Figure 4.4(a)]. After concluding the process of 3D design, parts assembly, and movement simulation, intersections between bars were detected before the desired folded position, affecting the compactness for transportation [Figure 4.4(b)]:

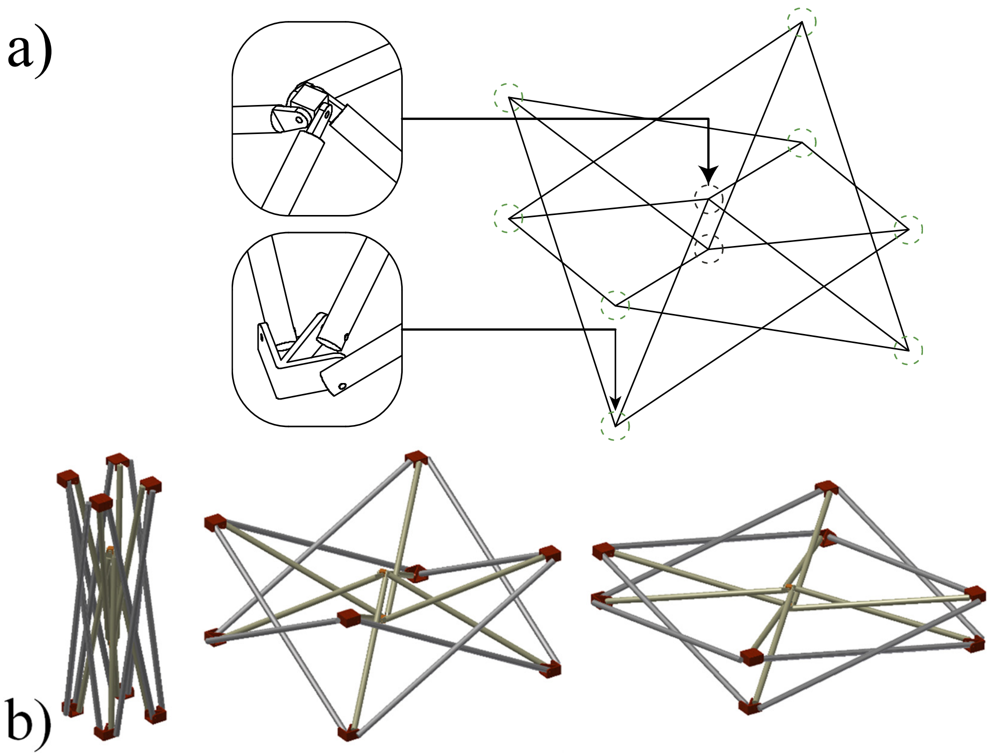

Figure 4.4 *First approach to obtain a stress-free regular square prism with double diagonalisation: (a) Design parameters, (b) Movement simulation.*

A preferred solution can be obtained according to Figure 4.5, starting with the desired eccentricity for the prism vertex joints «values [a] & [b] are equal», and subsequently by shifting the internal scissors of the module from its original position, along its 45° diagonal axes to obtain the values [d] & [e]. A direct representation was created by software, but it can also be mathematically indicated by the Pythagorean Theorem.

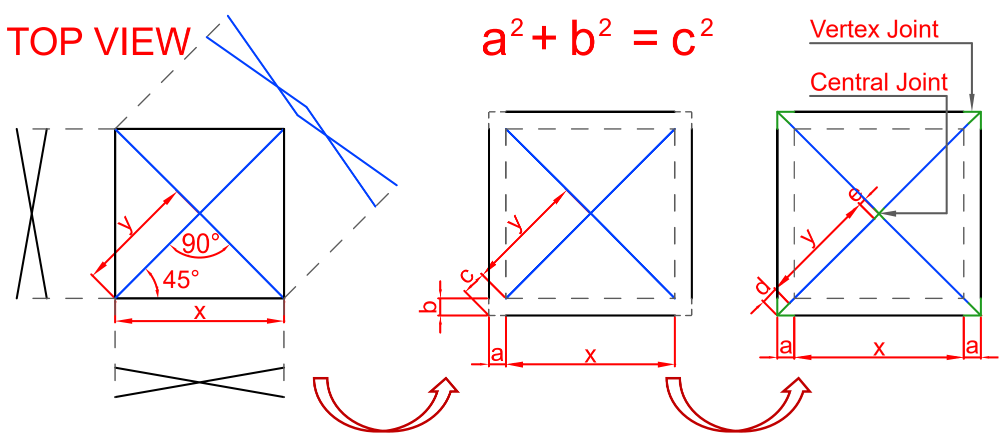

Figure 4.5 *Sequence to get a central joint with displaced rotational axes.*

Notes: **1)** The values [x] & [y] are not used in the equation, as the mechanism opening position is not an essential factor.

2) The shifting magnitude of the diagonal scissors can be chosen according to the designer's needs.

Figure 4.6(a) demonstrates the proposal's components design and movement feasibility, taking into account the minimum necessary variables on all the joint eccentricities and the beam cross-section.

A flat disposition is not necessarily beneficial for a roof. In some cases, just a slight inclination of the structure or the textile is enough under rainy weather, but in some other scenarios like a storm or snow, the slope requirements could be higher than 20 degrees. With this premise, a slidable element could be included between the centrally located joints, elevating the membrane's height to generate a pyramidal geometry. This additional condition can be appreciated in Figure 4.6(b).

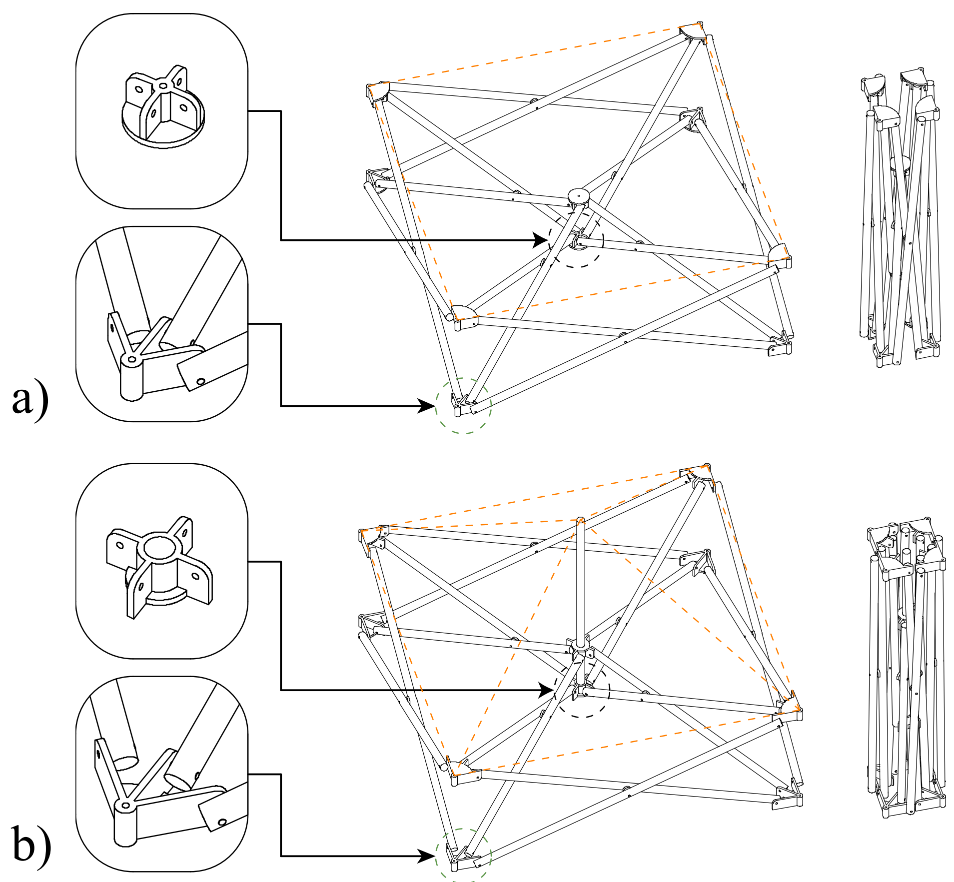

Figure 4.6 *Preferred solution on a stress-free regular square prism with double diagonalisation: (a) Minimum eccentricity at joints, (b) Adjustments to insert a slidable object.*

A non-conventional arrangement is possible by supporting the diagonal scissors not in the original prism vertexes, but along the bars located in the contouring faces. The procedure to obtain this modification embodies a regular rectangular prism that intersects the main module and, to keep it compatible with movements, the scissor semi-lengths **[a = b = c = d]** should be equal, therefore **[a + b = c + d]**.

As it was used in the final confirmation of Figure 4.7, a pair of coplanar scissors can be further rotated to produce a centrally located joint that maintains 90°. Nonetheless, the joints located within the lengths of the external bars are no longer at 45° when connecting the diagonal scissors.

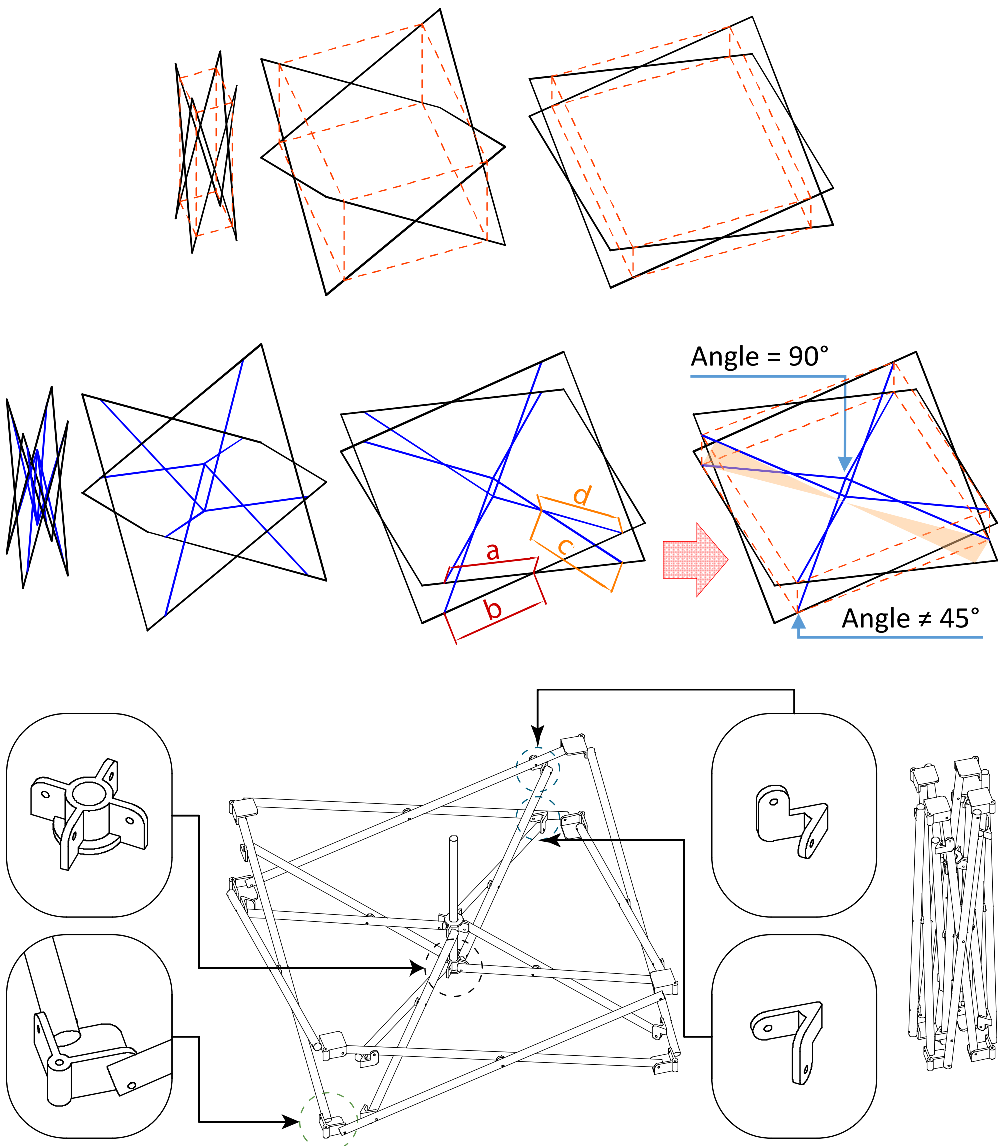

Figure 4.7 *Sequence to get a modified regular square prism using four internal scissors.*

The grouping outline in Figure 4.8(a) establishes a stable flat surface in all directions and is known in the literature as a four-way grid structure formed with isosceles grid cells (De Temmerman, 2007, p. 76). Suppose double scissors on a single diagonal are used, as in Figure 4.8(b); in that case, multiple positions will be allowed according to the grid's subdivision, and it is recommended to match up as many rods around a single joint as possible.

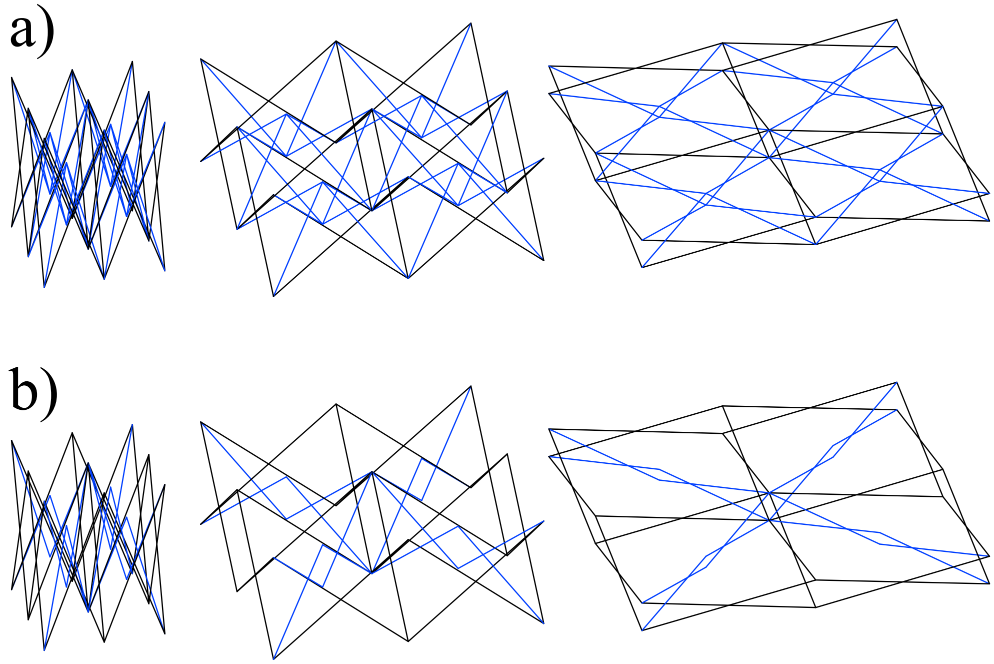

Figure 4.8 *Regular square prism grouping examples: a) Double diagonal, b) Single diagonal.*

Each module partition suggests different scenarios that can be brought into the discussion: unlike Figure 4.9(a) standard triangulation, a couple of scissors need to be sequentially connected on the same plane in Figure 4.9(b). According to De Temmerman (2007, p. 137), the effect of integrating double units creates a quadrangular pattern; therefore, non-triangulation of the grid can lead to in-plane instability.

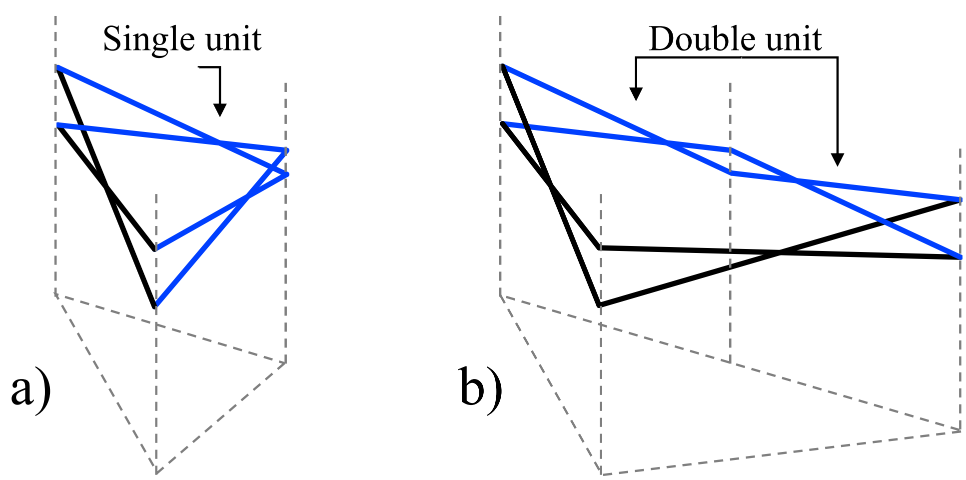

Figure 4.9 *Diagonalisation scenarios: (a) Three scissor units, (b) Four scissor units.*

Figure 4.10 utilises the Grübler–Kutzbach equation for comparing an analogous schematic four-bar linkage, as the starting point for the inspection:

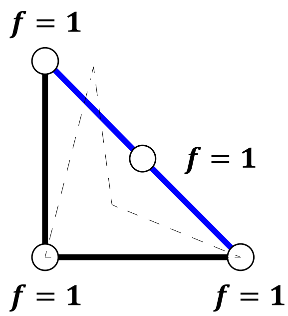

$$\boldsymbol{M} = 3(\boldsymbol{E} - 1) - 2\boldsymbol{\Sigma}\,\boldsymbol{J}_{1i}.\,\boldsymbol{i}$$
$$\boldsymbol{M} = 3(\boldsymbol{4} - 1) - 2[\boldsymbol{4}]$$
$$\boldsymbol{M} = 9 - 8$$
$$\boldsymbol{M} = 1$$

Figure 4.10 *Planar linkage using four moving bodies and four joints with 1DoF.*

In general terms, the prior mechanism in 2D behaves with a non-wanted degree of freedom. However, knowing the methodological limitations for directly evaluating this type of three-dimensional deployable structure by a simplified equation, a different approach can be obtained when using an Autodesk Inventor movement simulation environment. On such assemblies, the double scissor units behave more like a truss connection, in which the pin joint can restrict lateral movements; hence, the module retains a triangular base.

Figure 4.11 explains the modelling and assembly parameters during real-time testing using the software. At this stage, an extra rotational degree of freedom was allocated on each vertex connection to verify the module stability. This interpretation should also be estimated from the buckling perspective, since the scissor beams could suffer deflections; additional outcomes from scale models are commented in Chapter 5.

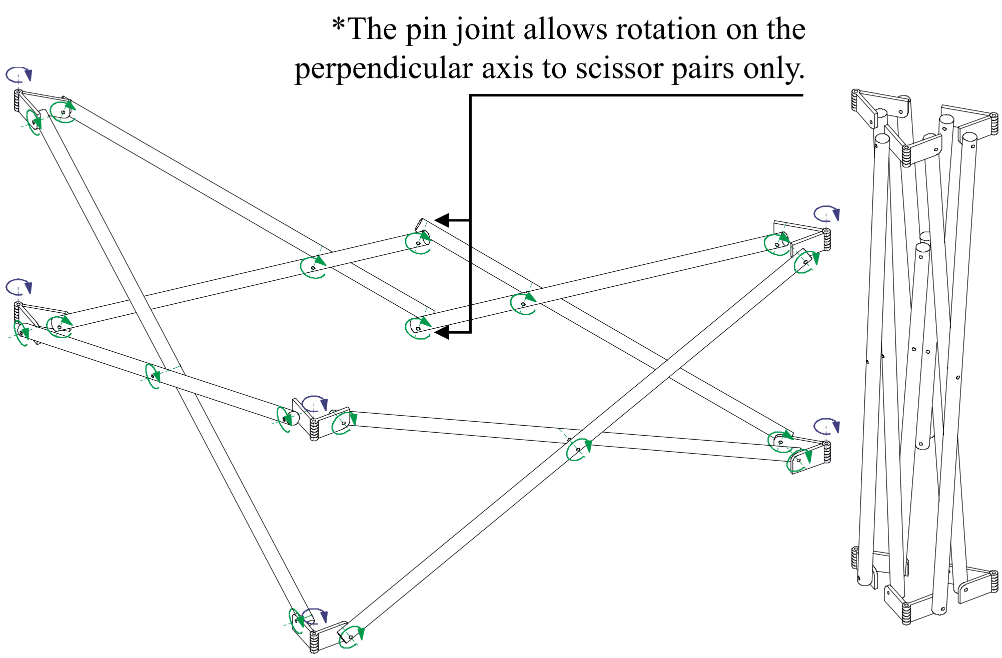

Figure 4.11 *Three-dimensional linkage using four scissor units.*

4.2.2 Case Study 2

The acquired experience from the first case study demonstrated the possibility of reducing the geometry while maintaining 1 DOF. As it is exemplified in Figure 4.12, the design process of shortening the length of some of the scissor's elements and eliminating the need for redundant connections produces novel irregular shapes.

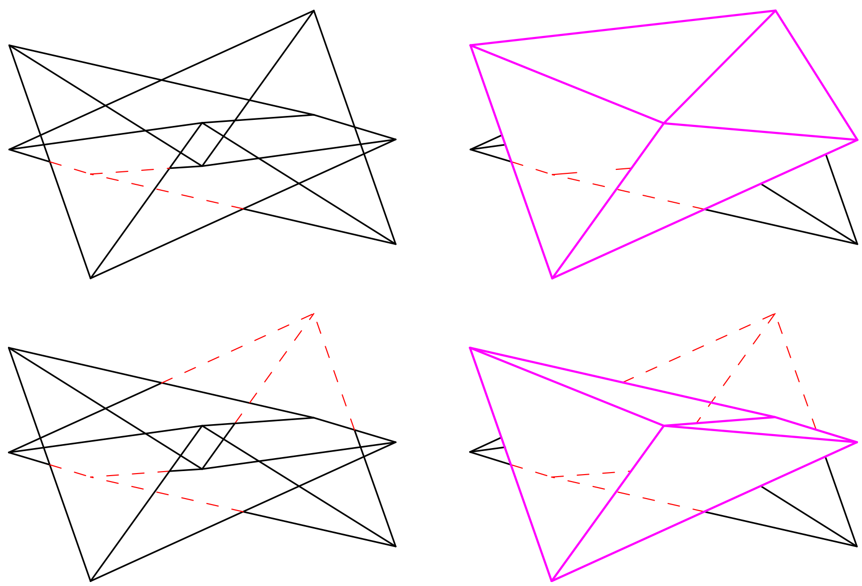

Figure 4.12 *Sequence to get modules with irregular shapes.*

A three-dimensional approximation was motion-simulated after transforming the module to the minimum predictable mechanism, as shown in Figure 4.13. To visualise the in-plane stability, hypothetical extra rotational degrees of freedom were considered on each joint, maximising the effect of the possible deformations.

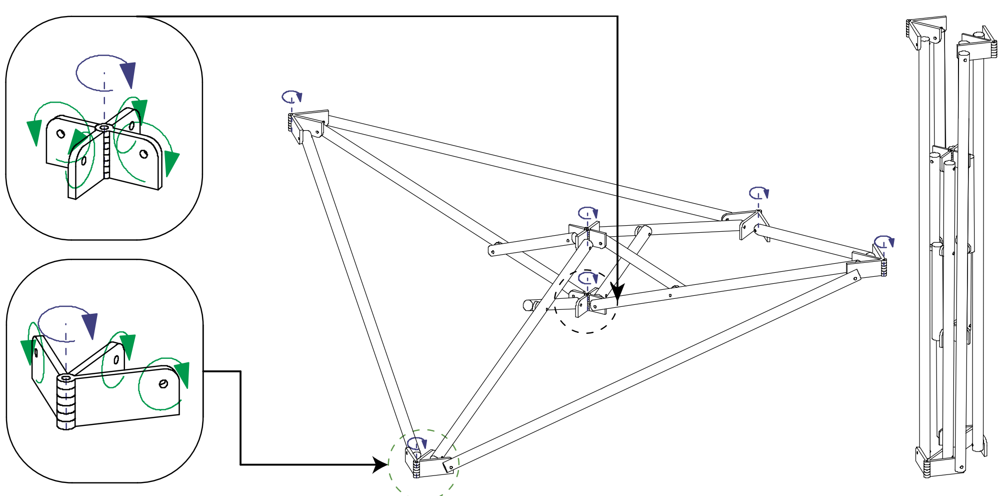

Figure 4.13 *Three-dimensional representation of a model with irregular shapes, using extra rotational degrees of freedom at joints.*

In real fabrication circumstances, the connections can maintain fixed pivots at 90° and 45°, respectively; Figure 4.14 utilises reinforced joints on the perimeter for balancing the load distribution on each pivot.

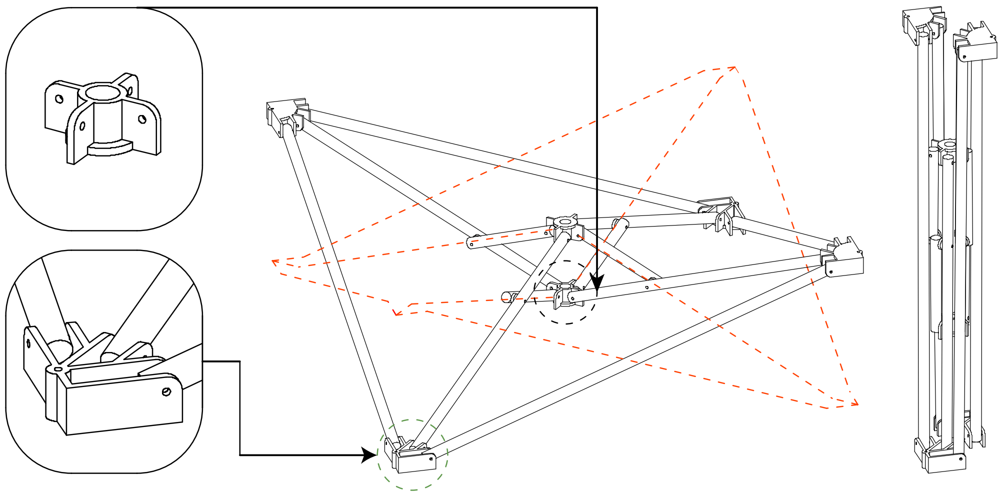

Figure 4.14 *Model with irregular shapes, using joints with fixed pivots at 90° and 45°.*

From a structural point of view, the previous resulting geometry complements the proposal from Santiago Calatrava (1981; 1993) [Figure 4.15], as an analogy to the cube principles of deployability. Considering that the mechanism should behave as a load-bearing structure, pantographs could bring significant rigidity while keeping a stable motion.

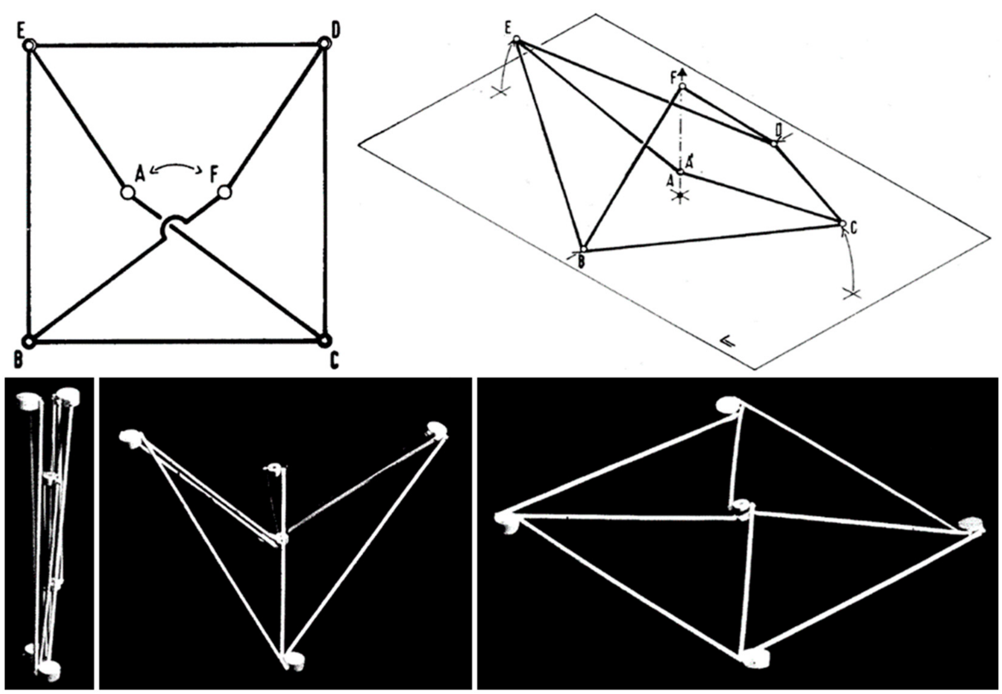

Figure 4.15 *Deployability of a square-base model. (Calatrava Valls, 1981), [Digitally modified]*

An unstable structure is obtained when analysing a virtual model based on Calatrava's example, utilising joints with additional rotational degrees of freedom. Joints with fixed pivots at 90° and 45° produces theoretical stability while retaining the nodes $\overline{AF}$ perpendicularly aligned to the base during movements. Differences can be appreciated in Figure 4.16(a) and Figure 4.16(b); still, the scale model in Chapter 5 evidences a weak mechanism for the second set-up.

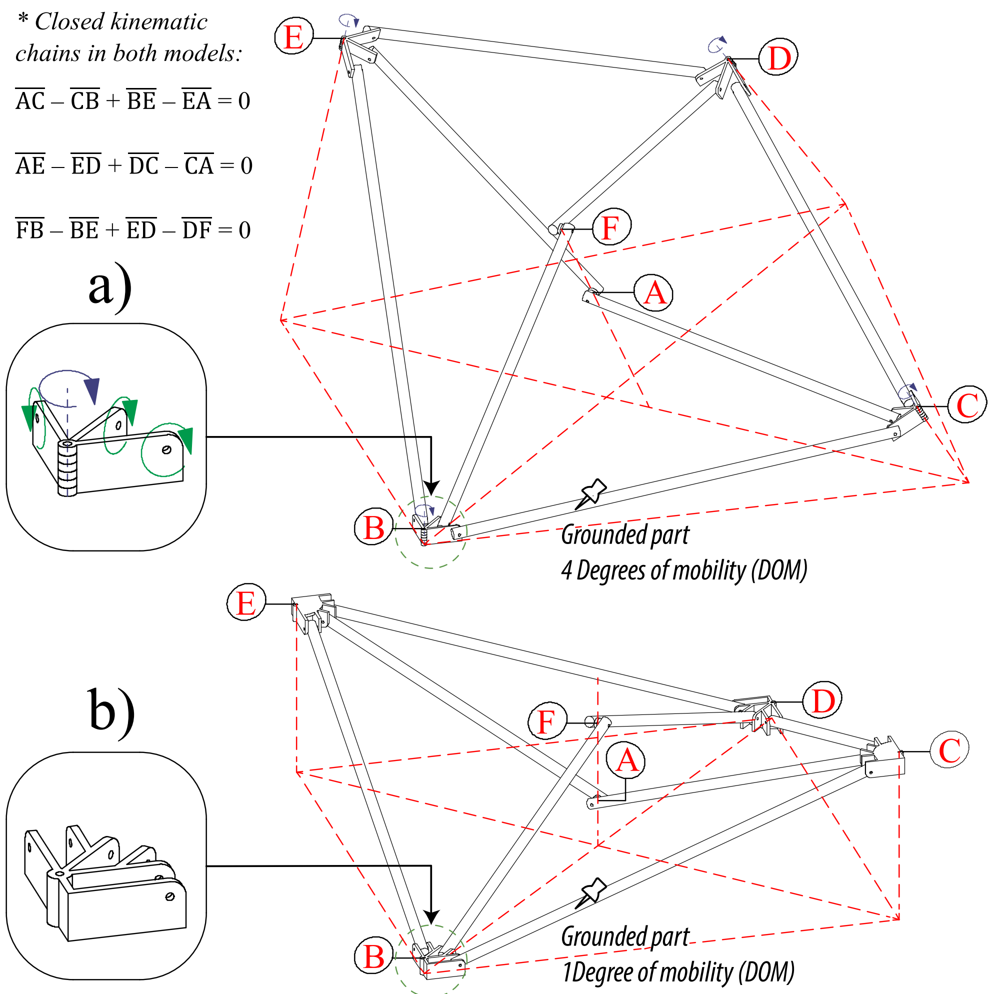

Figure 4.16 *Movement simulation based on Calatrava's example: (a) Unstable, (b) Theoretical stability.*

On the other hand, some groupings can be obtained from the outcomes of this particular case: By using 4 modules, the original scheme can be decomposed, for instance, to create an umbrella shape on which the central support of a mast controls the vertical stability and transmits the loads to the base, while the structural ribs should effectively absorb wind loads and keep proper membrane tensioning [Figure 4.17]. In the same way, if the initial proportions are taken as a reference, a simpler approach with a smaller number of parts can be achieved, although with a covered surface area that is 50% smaller in the expanded position [Figure 4.18].

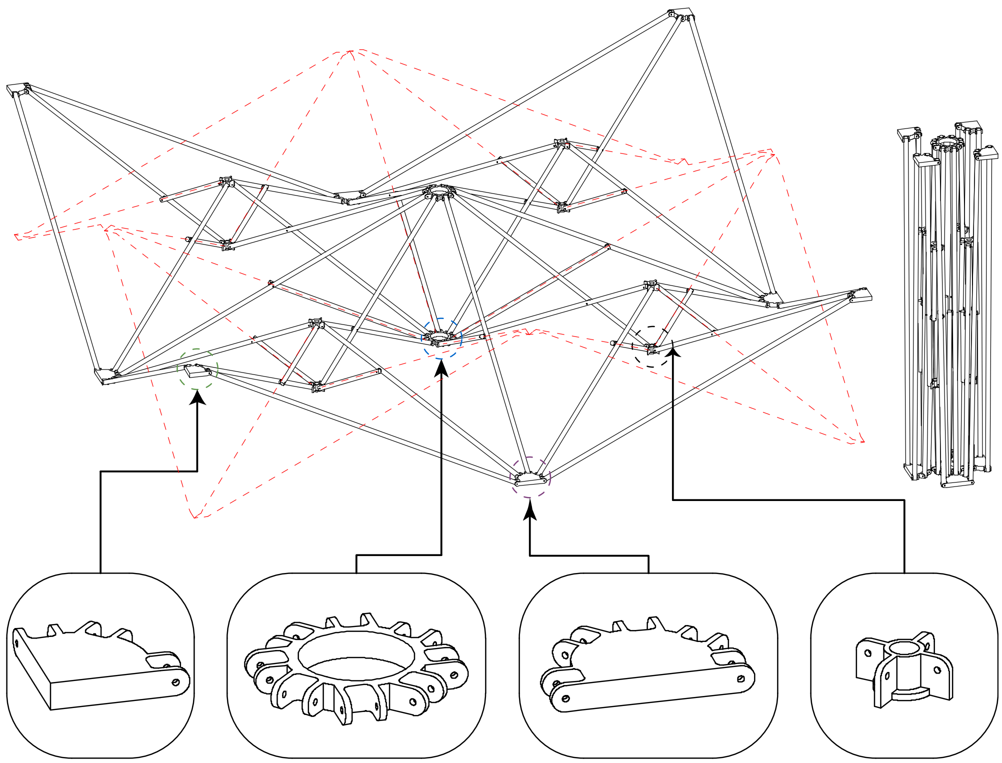

Figure 4.17 *An umbrella grouping possibility from modules with irregular shapes.*

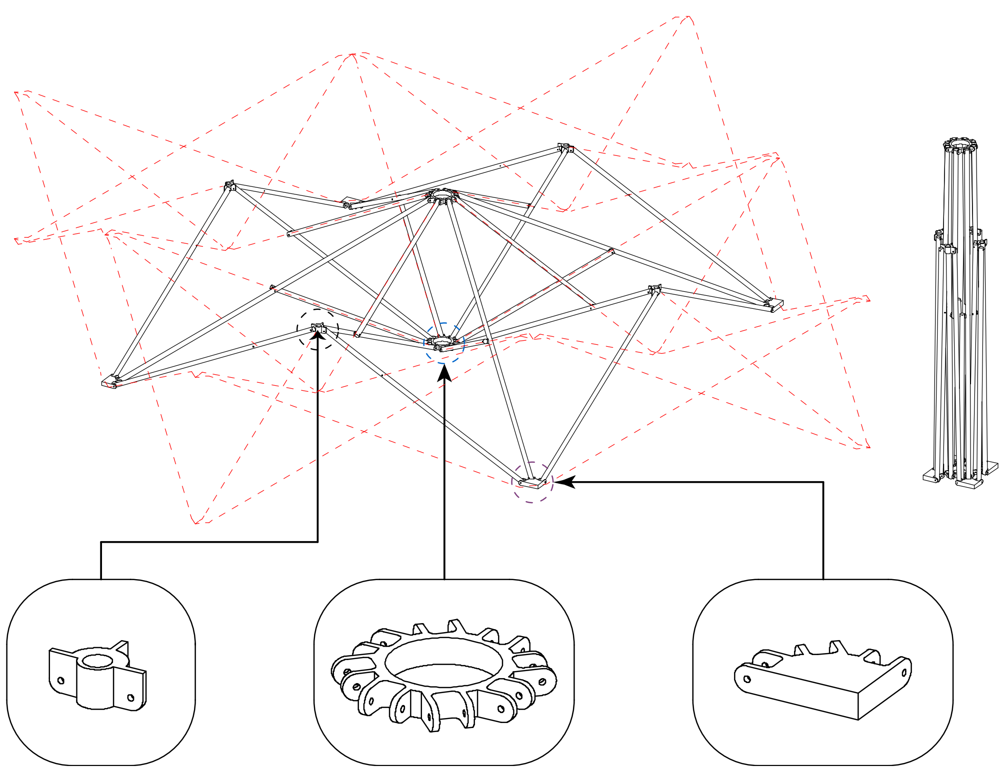

Figure 4.18 *A simplified umbrella grouping possibility from modules with irregular shapes.*

Figure 4.19 contains samples that can be useful for tents supported through vertical legs on the perimeter. In agreement with the obtained results, the minimum roofing inclination is about 10°, which is adequate to evacuate rainwater. Scenarios with snow loads need complementary systems to raise the membrane and should be studied in greater detail.

The upper or lower positioning of the fabric also generates optional forms that can be optimised to create cutting patterns by 3D faces or hyperbolic paraboloids.

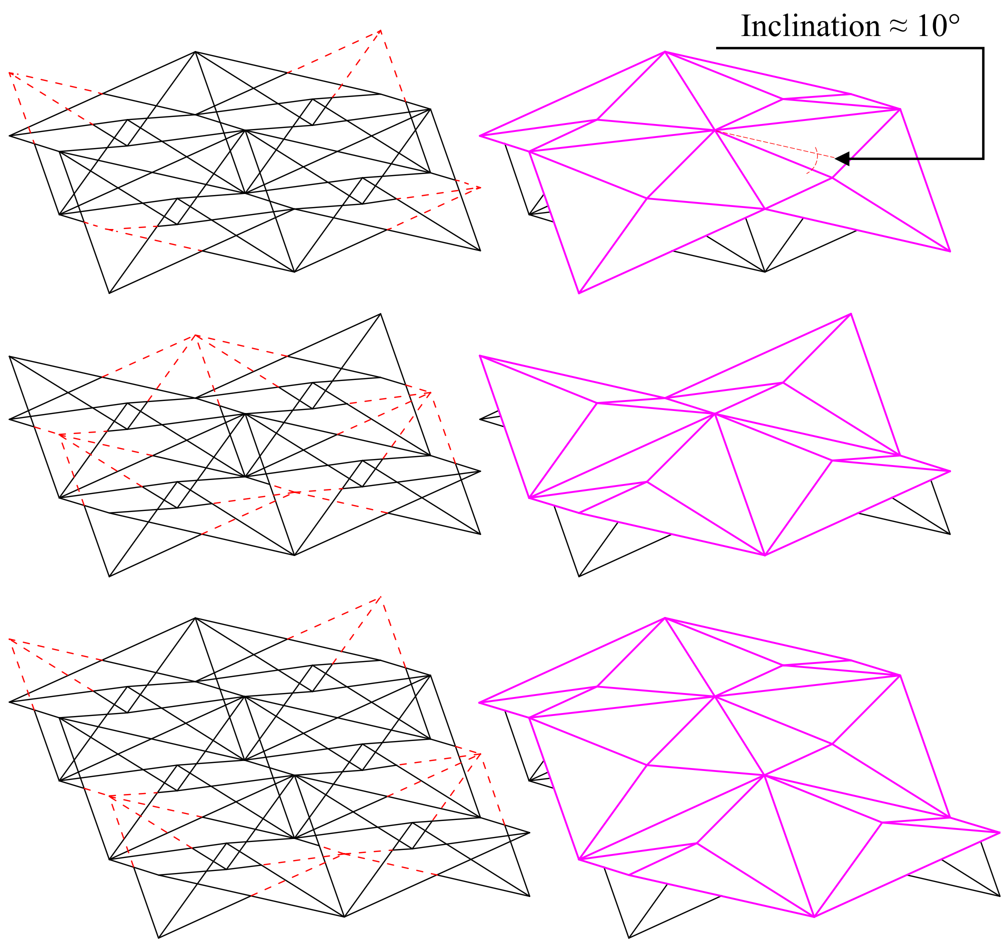

Figure 4.19 *Tent-like grouping possibilities from modules with irregular shapes.*

4.2.3 Case Study 3

Continuing with the exploration, an oblique rectangular prism that inclines in a single direction was considered. As it can be seen from Figure 4.20, the typical conformation has a pair of plane translational scissors between the axes 1-4 & 2-3, in addition to a couple of curved translational scissors between the axes 1-2 & 3-4. Later, a possibility to insert irregular curved-translational scissors for stabilisation was identified.

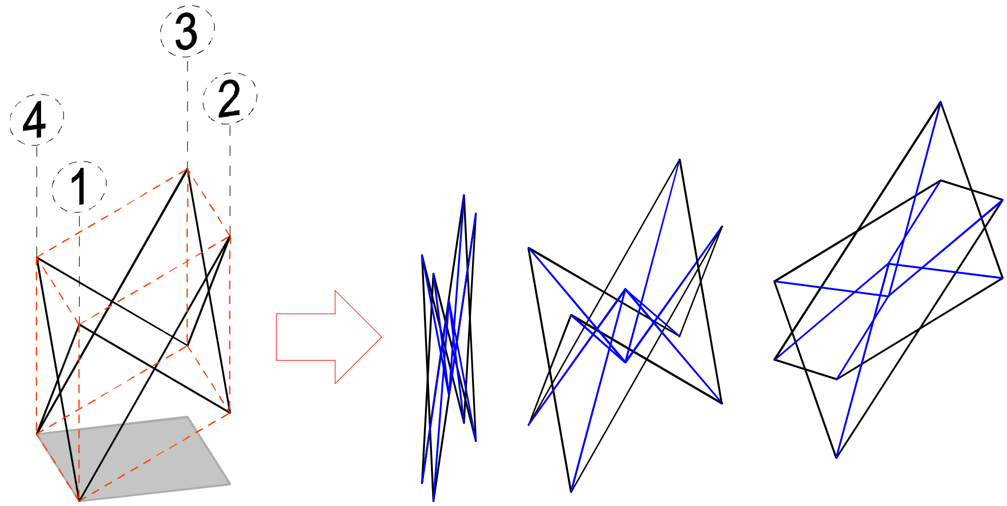

Figure 4.20 *Stabilisation scheme of an oblique rectangular prism.*

A detailed inspection revealed the necessity of allowing joints with added rotational degrees of freedom, as the condition for connecting the diagonal scissors and getting stress-free compatibility.

A first attempt on solving the three-dimensional geometry was made by displacing the internal scissors of the module from its original position along its diagonal axes, just as it was explained when using modelling software or the Pythagorean Theorem in case study 1. Figure 4.21 indicates how all the vertex joints and the centrally located joints were dimensioned, and the assembly to evaluate the movement simulation.

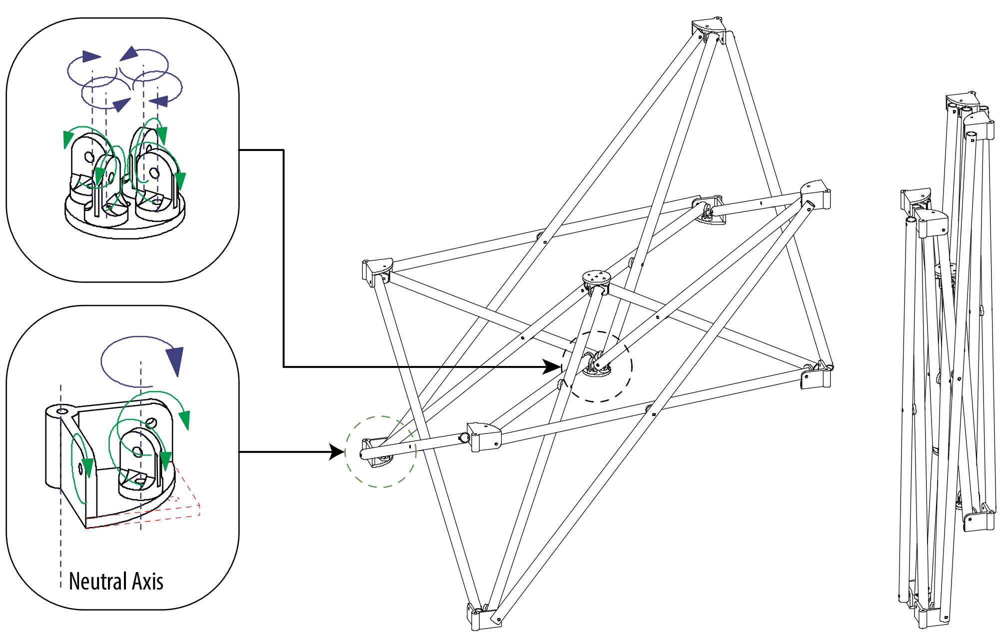

Figure 4.21 *First approach of a stress-free oblique rectangular prism with double diagonalisation.*

In the second attempt shown in Figure 4.22, each of the joints was augmented with a rotary pivot plus an additional eccentricity to reduce interferences when the mechanism is folded.

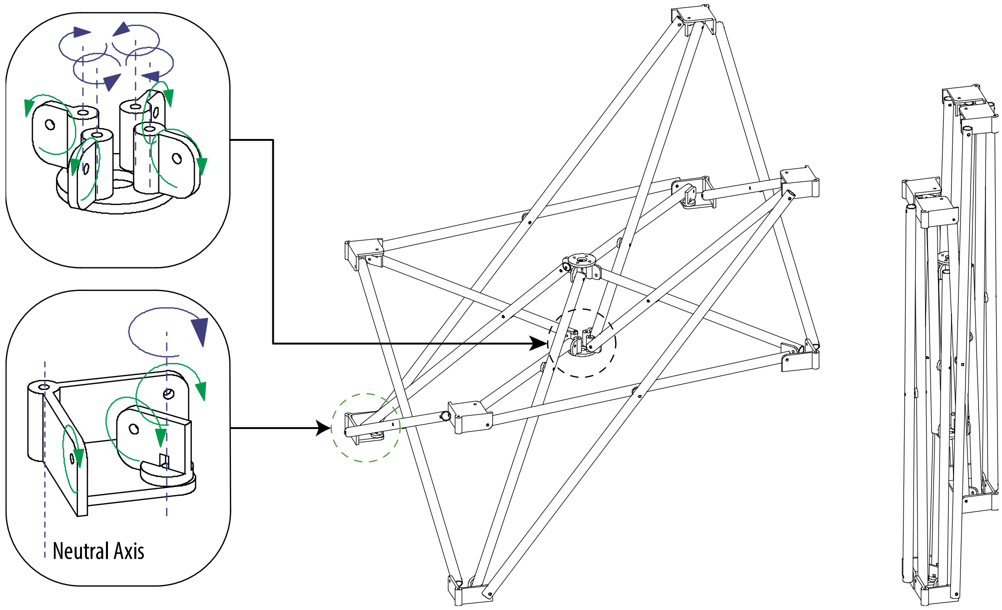

Figure 4.22 *Second approach of a stress-free oblique rectangular prism with double diagonalisation.*

Despite the stability gained by 4 diagonal scissors on the prior couple of attempts, a contrasting triangular instability can be demonstrated in Figure 4.23, since the central joints have an undesired turning capacity.

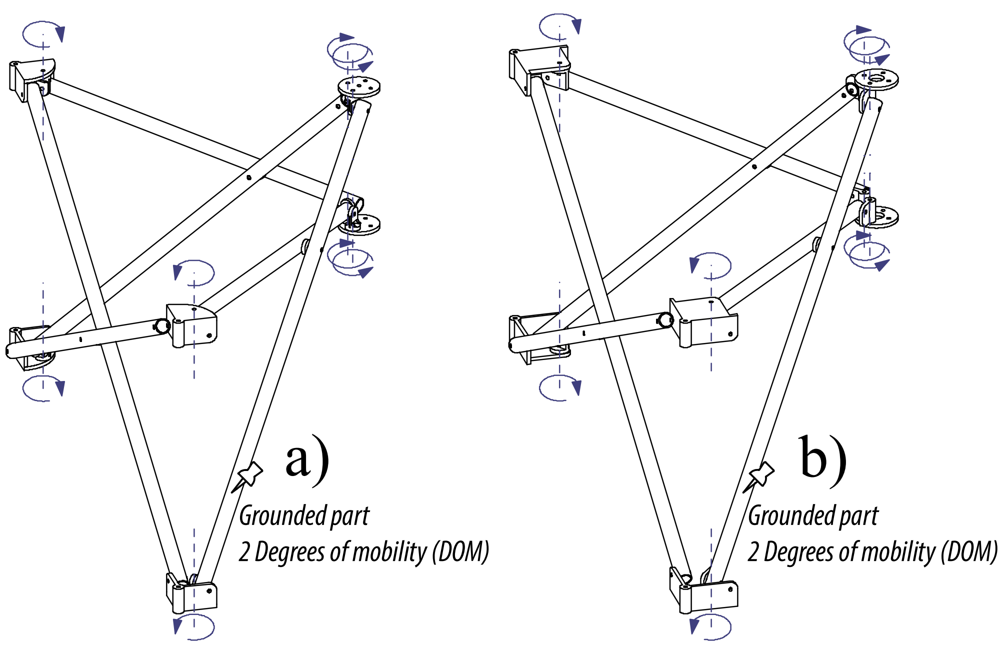

Figure 4.23 *(a) Model based on the first approach, (b) Model based on the second approach.*

A practical modification was originated for the vertex joints by strictly maintaining the location of the original rotary pivot, and then displacing the internal scissors along its diagonal axes. In this manner, all connectors have a rotary pivot plus an additional eccentricity, and central joints behave like a door hinge with fixed coplanar arms. According to Figure 4.24, the mechanism preserves a single degree of movement even on the simplest triangulation form.

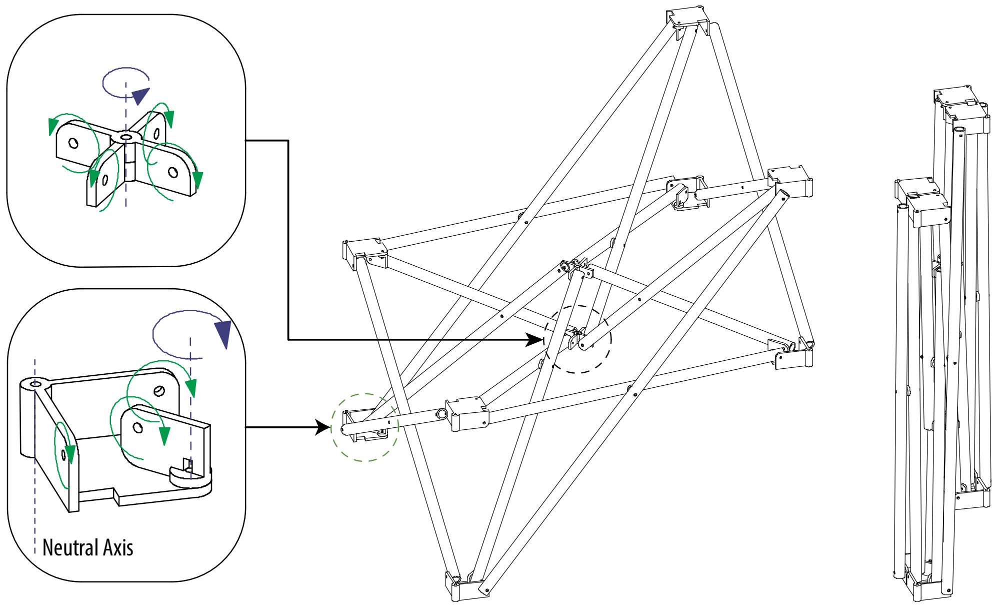

Figure 4.24 *Adjusted solution of a stress-free oblique rectangular prism with double diagonalisation.*

Figure 4.25 establishes a possible stabilisation by connecting only a pair of irregular curved-translational scissors in diagonal.

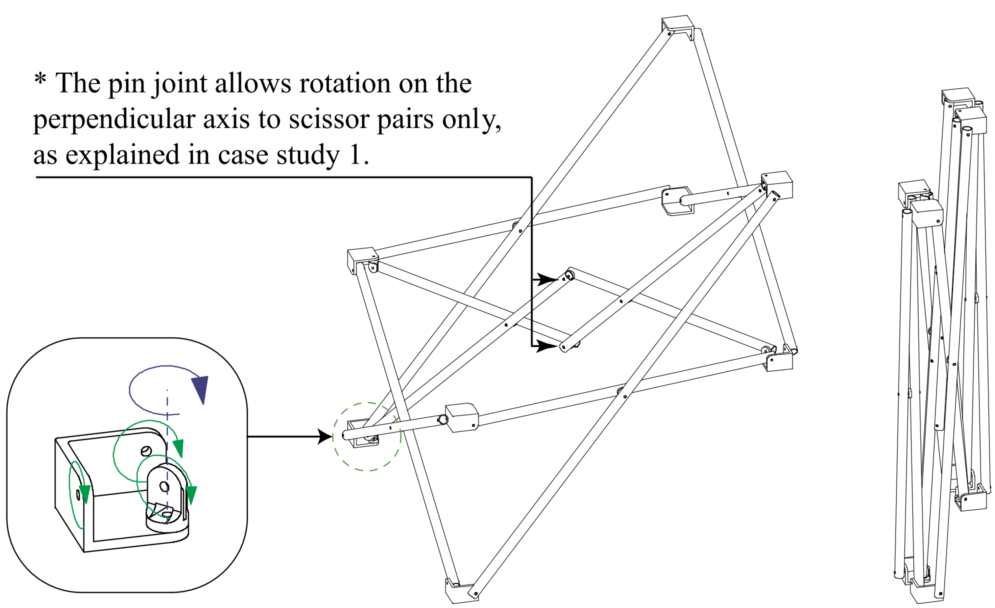

Figure 4.25 *A stress-free oblique rectangular prism with a single diagonalisation.*

By maintaining constant bar-lengths between modules, the repetition of case study 3 can produce an inclined deployment [e.g., a gabled roof]; otherwise, a single curvature geometry is obtained when varying the proportions of the adjacent module [e.g., a cylindrical vault]. Figure 4.26 indicates rigidisation alternatives utilising an extra rotational degree of freedom at the joints, which facilitates the mechanism adaptation to any of these conditions.

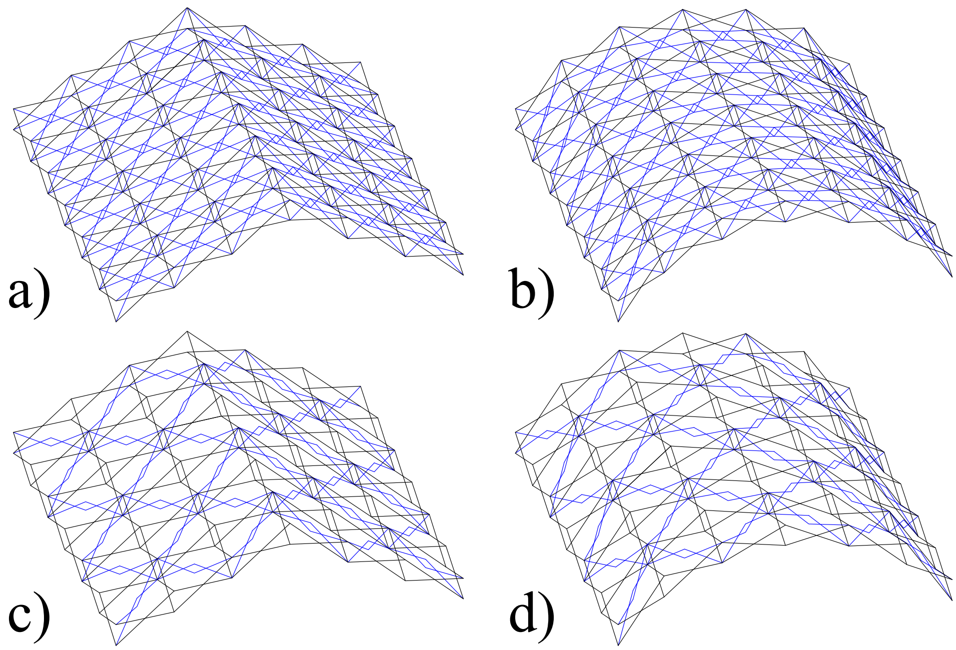

Figure 4.26 *Oblique rectangular prism grouping examples: (a) Gabled roof with double diagonals, (b) Cylindrical vault with double diagonals, (c) Gabled roof with single diagonals, (d) Cylindrical vault with single diagonals.*

In contrast to previous indications, one more possibility was focused on eliminating the requirement for additional degrees of freedom at the joints. To obtain a stress-free triangulation with this procedure, a modification incorporates an imaginary regular rectangular prism that is not directly supported in the original oblique rectangular prism vertexes, but intersecting the longest bars of the curved-translational scissors.

As visualised in Figure 4.27, diverse angulated connections are produced to link a new set of irregular plane-translational scissors. As stated in analogous analysis, a predictable degree of movement is maintained since the stabilisation occurs through fixed joints. The mechanism is well-matched if the values **[a = b = c = d]** are true and the sum of the scissors semi-lengths is equal **[a + b = c + d]**.

It should be noted that the number of joint types can be increased depending on the inclination of the adjacent module. Besides, it is possible to simplify the geometry to a single diagonalisation with a pair of contiguous plane-translational scissors.

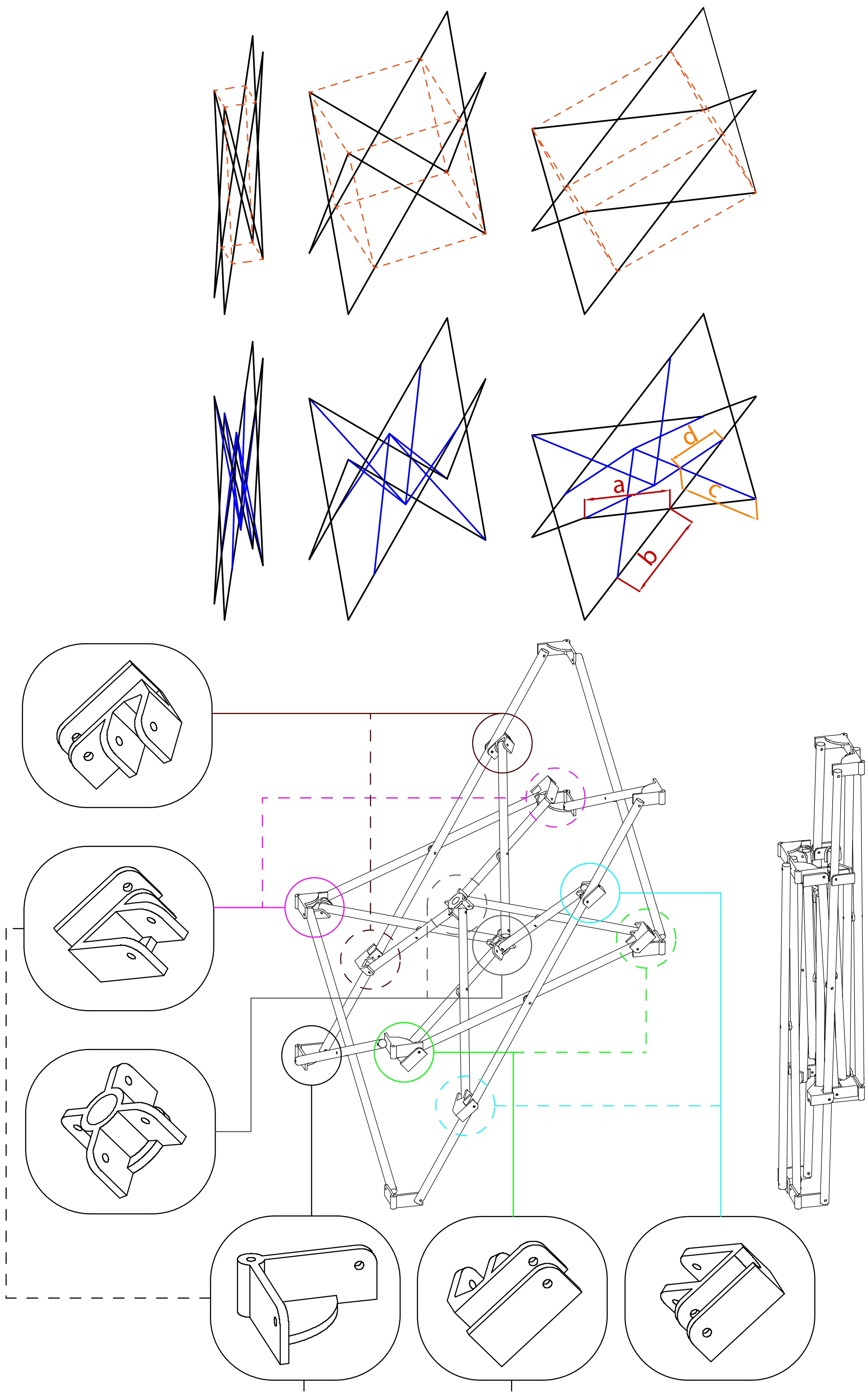

Figure 4.27 *Sequence to get a modified oblique quadrangular prism using diagonal connectors with fixed pivots.*

4.2.4 Case Study 4

Matching single curvature possibilities, Figure 4.28 synthesises a trapezoidal cross-section prism [or simply trapezoidal prism depending on the orientation] through a couple of plane-translational scissors between the axes 1-4 & 2-3, and two more polar scissors between the axes 1-2 & 3-4. Bent planes between the diagonal axes 1-3 & 2-4 create geometrical incompatibilities; for this reason, some prior solutions have utilised cables or flexible bars for configuring the diagonal scissors, which are kept twisted during the whole movement and thus reducing the load-bearing capacity.

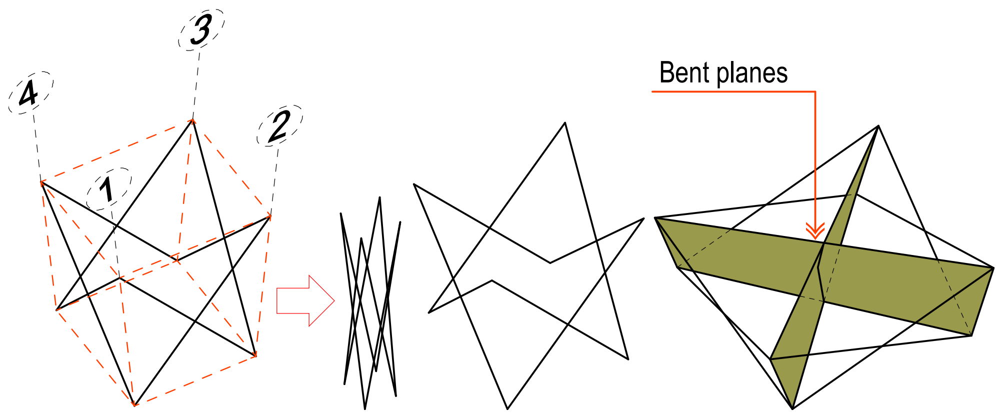

Figure 4.28 *A trapezoidal cross-section prism utilised in the prior art.*

Figure 4.29 shows an imaginary linking of a regular rectangular prism; in this way, four irregular plane-translational scissors can be incorporated to triangulate the module, and the proposed equation compatibility is accomplished **[a = b = c = d]**.

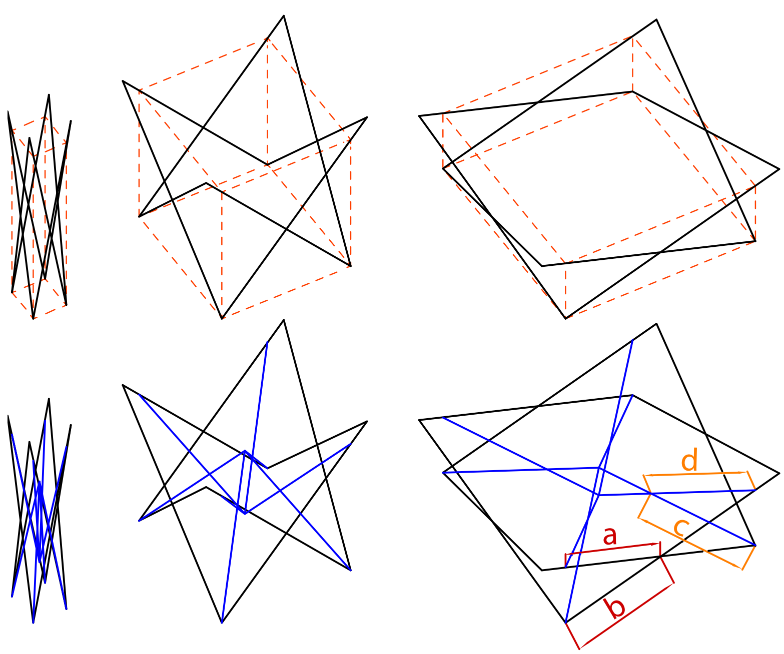

Figure 4.29 *Sequence to get a stress-free trapezoidal cross-section prism with double diagonalisation.*

To keep a stress-free mechanism, the lower vertexes of the trapezoidal prism require a new set of joints with an independent movement capacity, in addition to a new set of upper joints intersecting the polar scissors within the bar-lengths. Optional joint types are possible according to the compared configurations in Figure 4.30.

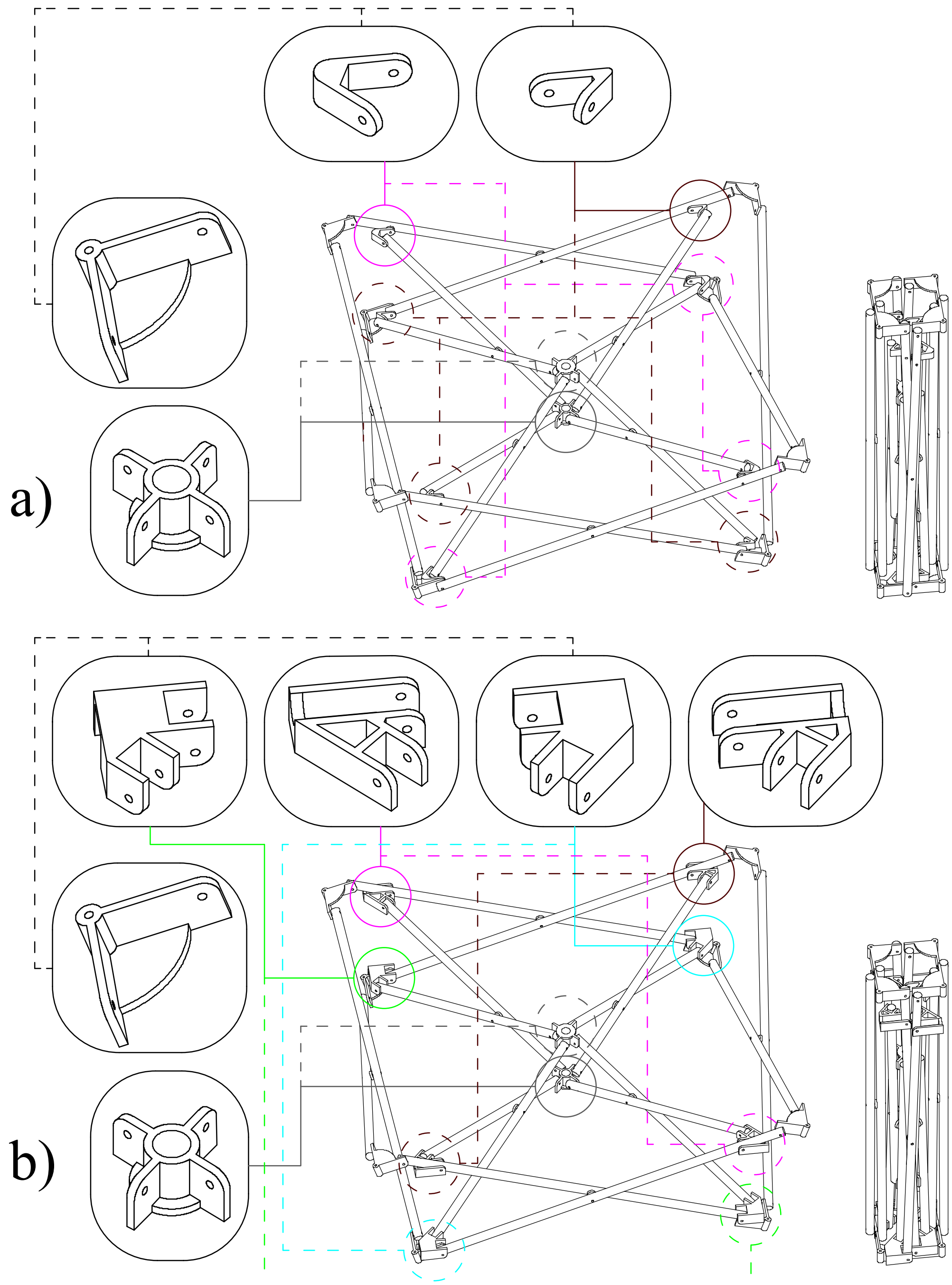

Figure 4.30 *A stress-free trapezoidal cross-section prism with double diagonalisation: (a) Standard joints, (b) Reinforced joints.*

The mechanism could retain stability and reduce the number of moving parts by simplifying the diagonals to a pair of contiguous plane-translational scissors. An abstract sketching of the independent movement between the diagonal connectors and the main prism vertexes is shown in Figure 4.31:

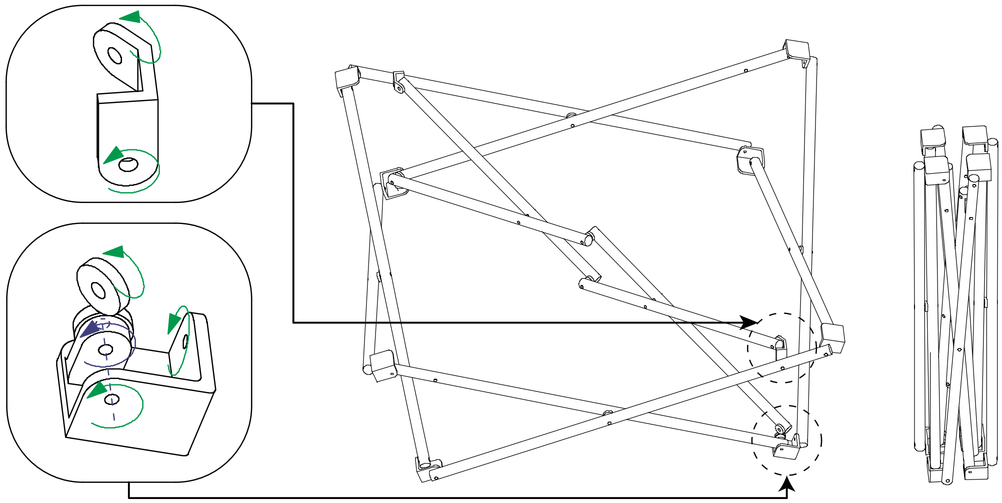

Figure 4.31 *A stress-free trapezoidal cross-section prism with a single diagonalisation.*

As it was mentioned before, groupings of trapezoidal cross-section prisms might produce an inclined deployment [e.g., a gabled roof] or a single curvature [e.g., a cylindrical vault], in addition to the patterns in case study 3. The different joint types are determined by the polar scissors eccentricity, while the desired geometry and its dimensions vary upon the module orientation [Figure 4.32].

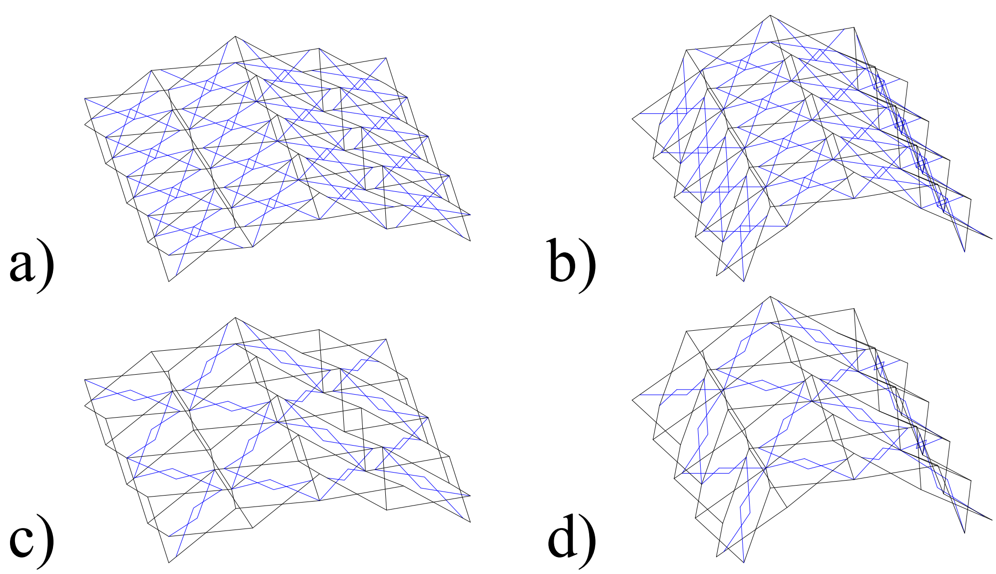

Figure 4.32 *Trapezoidal cross-section prism grouping examples: (a) Gabled roof with double diagonals, (b) Cylindrical vault with double diagonals, (c) Gabled roof with single diagonals, (d) Cylindrical vault with single diagonals.*

4.2.5 Case Study 5

An oblique rhombic prism is obtained by joining identical curved translational scissors between the axes 1-2, 2-3, 3-4, 4-1. Symmetrical upper and lower vertex joint elevations are maintained on the axes 2 and 4, enabling a single consistent diagonal bracing during deployment. This is not the case when attempting to directly connect diagonal scissors between axes 1-3, as the module produces irregular extensions in dimension and inclination.

Optional outlines are indicated in Figure 4.33. The same diagonal scissors set is kept, but with an upward or downward orientation; furthermore, Figure 4.34 displays the mechanical assembly and compatibility of the system by standard 90°/45° joints.

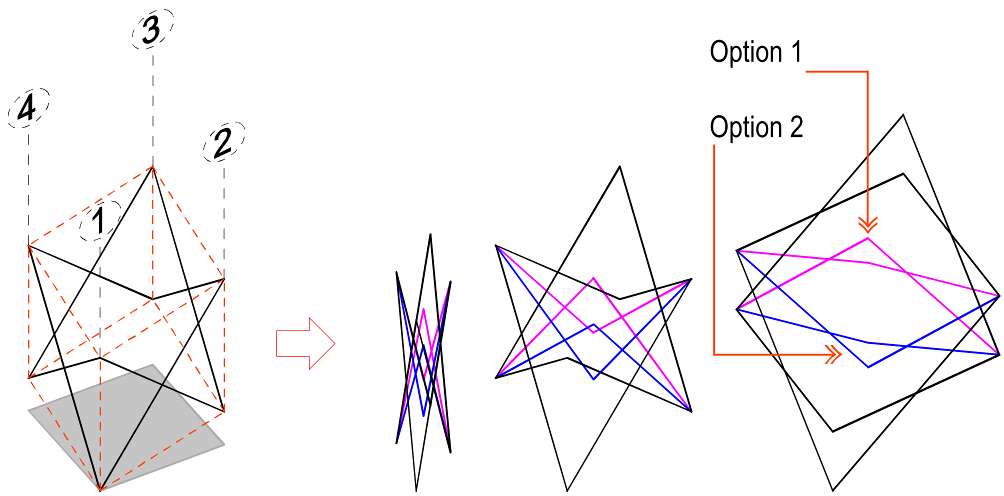

Figure 4.33 *Stabilisation scheme of an oblique rhombic prism.*

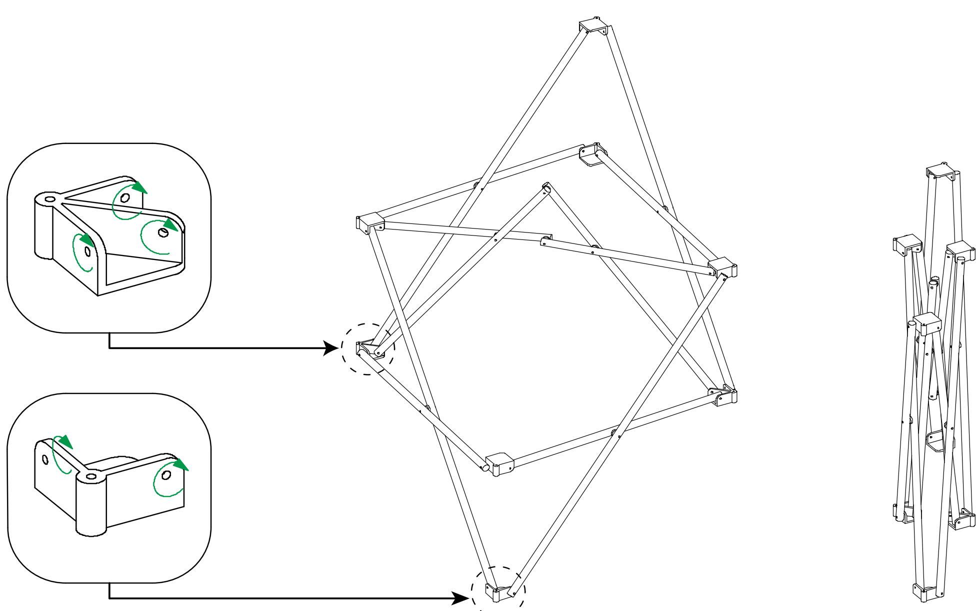

Figure 4.34 *A stress-free oblique rhombic prism with single diagonalisation and 90°/45° joints.*

From prior art grouping possibilities, synclastic and anticlastic appearances are obtained by a unique prism repetition. In Figure 4.35, a singular compatible diagonal is incorporated into the original quadrangular conformation.

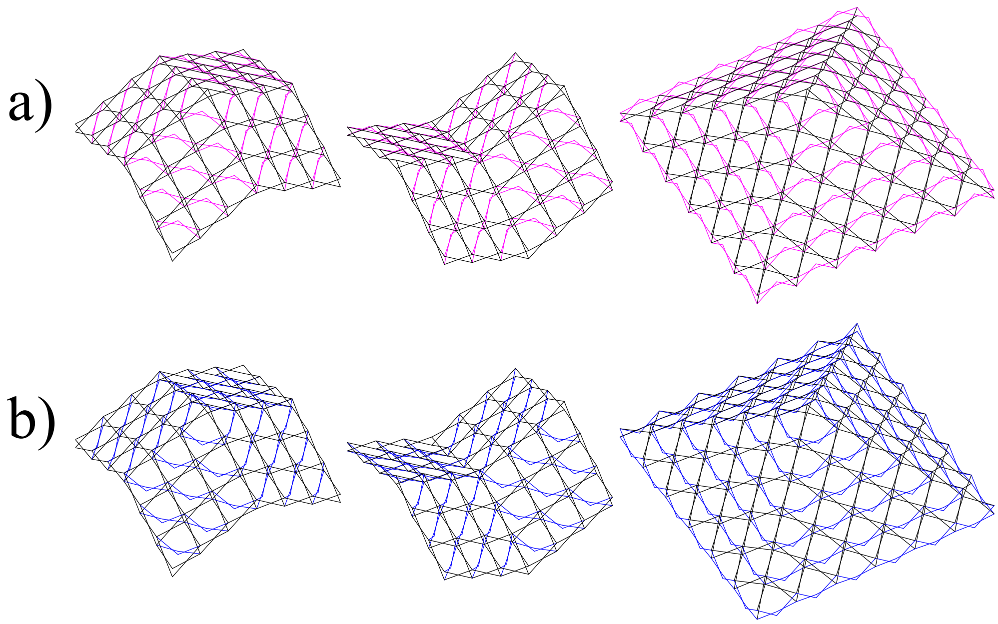

Figure 4.35 *Oblique rhombic prism grouping examples: a) upwards diagonal scissors [Option 1], b) downwards diagonal scissors [Option 2].*

By contrast, oblique rhombic prisms can be progressively adapted to produce an equivalent lateral stabilisation over some double curvatures having an expandable quadrangular grid projection. As formulated by Luis Sánchez Cuenca (1996a; 1996b; 1996c), the procedure to obtain these geometries consists of combining translational arches about the global perpendicular axes X and Y; therefore, the orientation of the diagonal scissors varies depending on the final arrangement.

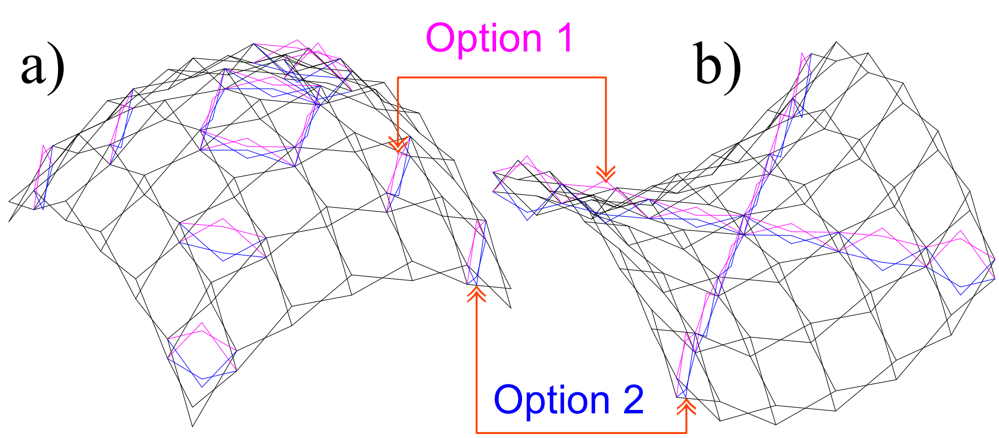

Figure 4.36 *Surfaces from generic translational arches and the possible lateral stabilisation using diagonal scissors: a) Synclastic, b) Anticlastic.*

Note: Option 1: upwards diagonal scissors, Option 2: downwards diagonal scissors.

4.2.6 Case Study 6

In correlation with double curvature geometries, an oblique rhomboidal prism can be obtained by grouping two identical curve translational scissors between the axes 1-2 & 3-4, and a new set of curved translational scissors with a different length between the axes 2-3 & 4-1 [i.e., a rhomboid is a parallelogram with unequal adjacent sides].

As the original prism has irregular conditions between the cross-planes 1-3 & 2-4, dissimilar inclinations are produced between the contouring faces. The real magnitude interconnectivity abstraction and the ellipses method reveals multiple possibilities to find approximate stress-free diagonal scissors; for this reason, a direct mechanical assembly and movement simulation was not implemented in software. Knowing that a slight mismatch can produce a vast snap-through effect, an iterative procedure by trial and error was performed instead, before the scale model test.

The following equations should be executed to get a fully compacted structure: [a+b=c+d]; [c'+d'=e'+f'] and [e+f=g+h], [Figure 4.37].

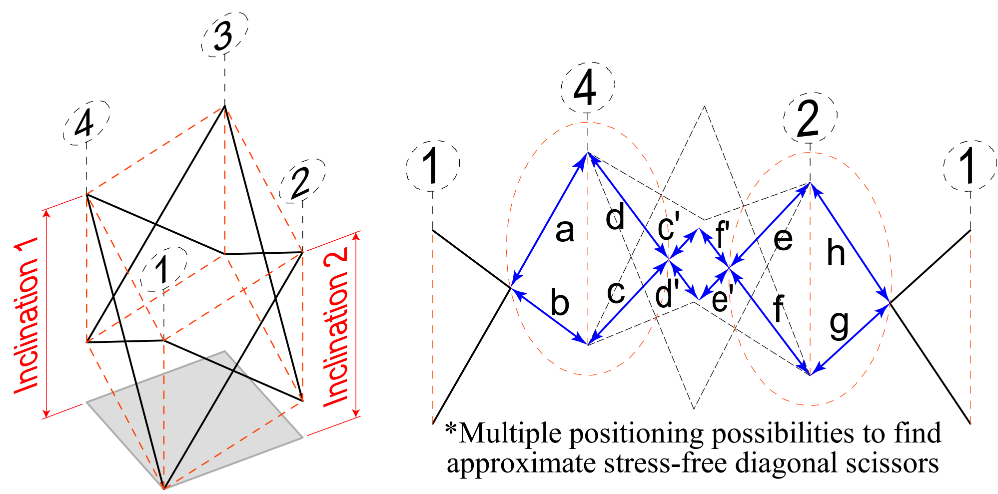

Figure 4.37 *Stabilisation scheme of an oblique rhomboidal prism.*

Figure 4.38 illustrates complementary combinations of case study 5 and 6:

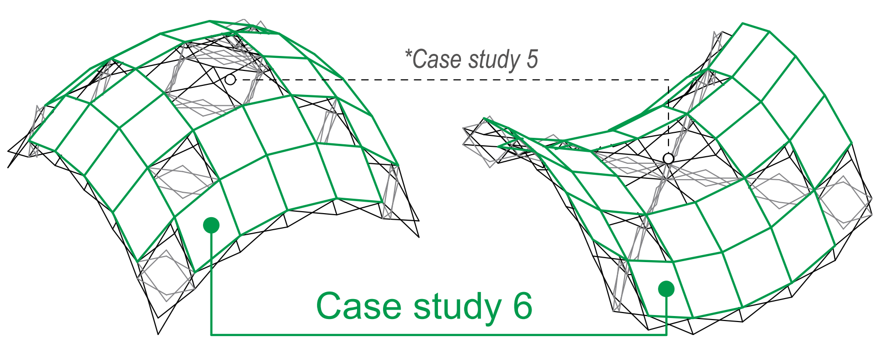

Figure 4.38 *Oblique rhomboidal prism grouping examples: a) Synclastic, b) Anticlastic.*
Note: Only highlighted modules in Green colour.

4.2.7 Case Study 7

A square pyramid frustum incorporating equal length bars and intermediate hinge eccentricities facing the same direction is presented in Figure 4.39. As polar scissors can produce kinematical incompatibilities, the snap-through behaviour may be avoided by adopting additional degrees of freedom on each vertex joint [acting as ordinary door hinges] (Atake, 2000). However, this only applies to triangular patterns, as stated in prior chapters; otherwise, the lateral instability effect increases. The basic representation of diagonal axes 1-3 & 2-4 is symmetrical, and a stabilisation with stress-free scissors may be approximated by the ellipses method [Figure 4.39].

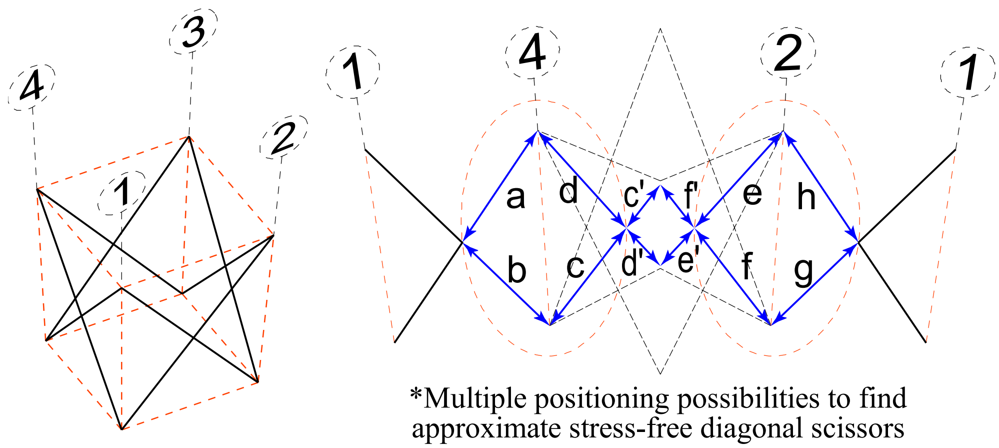

Figure 4.39 *Stabilisation scheme of a square pyramid frustum.*

Although this scheme can be optimised in parametric environments, the effectiveness of reducing geometry deformations is contrasted by the mobility constraints imposed by the scissor-types. As vertex joints can turn during movements, added spatial inconsistencies and complexities to the exploration were noticed; therefore, an extensive trial and error process was necessary before the scale model fabrication. Contrary to other case studies, limited grouping variants are envisaged unless other rhombus pyramid frustums are analysed in dept. An example is in Figure 4.40, as the analogue route to obtain a spherical geometry from polar units and equal length bars (Morales, et al., 1996). However, the study continuity is beyond the scope of this thesis.

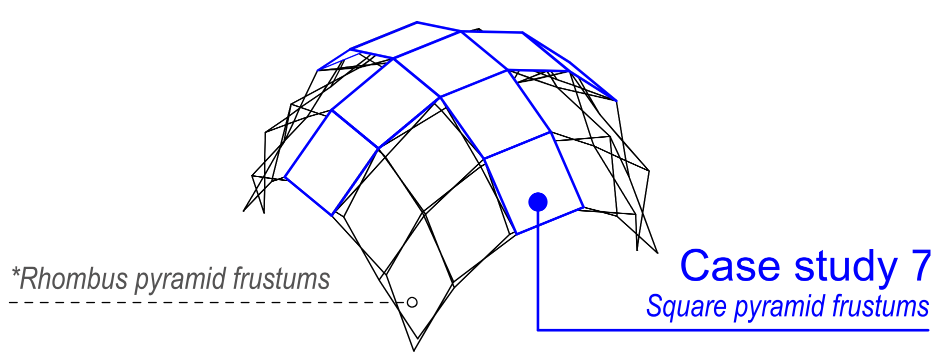

Figure 4.40 *Truncated pyramids groupings example.*

4.2.8 Case Study 8

One more exploration is based on a skew type of prism with four identical polar scissors and different orientations between adjacent contouring faces, thus obtaining a sliced tetrahedron. More complicated foldable structure combinations would be created from the ideals in the literature review, as this geometry is considered "an almost stable solution" by Katsuhito Atake (2000).

In Figure 4.41, non-compatible bent planes between the axes 1-3 & 4-2 can be noticed; to prevent twisted bars during movements and improve the structural performance, a stabilised stress-free diagonalisation idea was initially projected by introducing an imaginary regular square prism that is not directly supported in the main prism vertexes, but intersecting the polar scissors within its bar lengths. Although the abstraction of show feasible results on a wireframe model, the three-dimensional version had major inconsistencies when determining the connectors by a simplified mechanism. For this study, the potential fabrication and testing are restricted, as joint conditions become the weakest elements in the system.

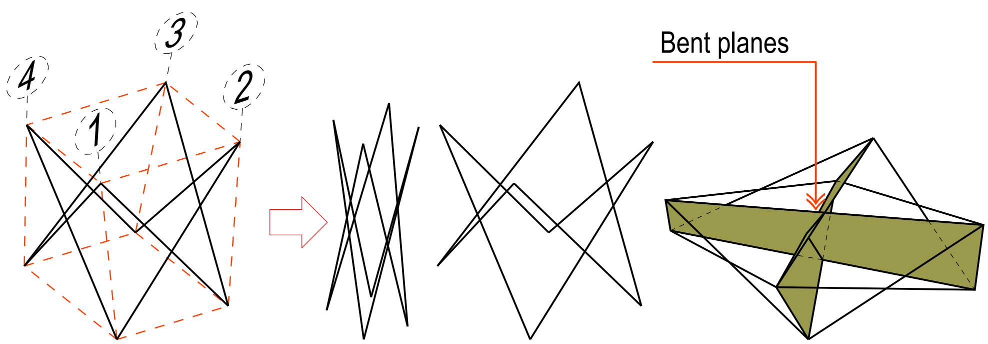

Figure 4.41 *A sliced tetrahedron utilised in the prior art.*

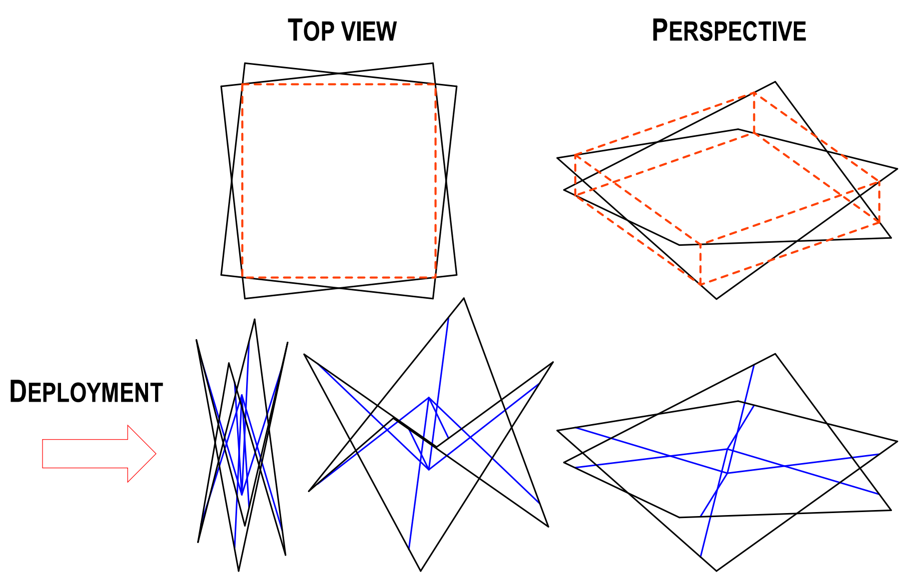

Figure 4.42 *Scheme of a sliced tetrahedron with double diagonalisation.*

4.3 Discussion on case studies

The ongoing work provided alternative automatic solutions for triangulating expandable quadrangular grids, seeking to control representative stress-free constructions at a large scale, minimising the risk of deformations during movements, and foreseeing the correct distribution of loads.

Although case study 1 configures an elementary pattern based on the prior art, its understanding had a great significance for conceptualising more complex models and is essential for defining geometrical combinations. Fundamentals for the three-dimensional design and the joint requirements were evaluated from a mechanical perspective, to propose matching alterations and module simplifications.

• Case study 2 produces optional irregular shapes. Stress-free mechanism scenarios were studied, but equivalent concepts may apply to configurations with controlled deformations.

• Case studies 3 and 4 are stress-free modules, with an innovative manner to solve the angular distortion problems of former homologous quadrangular prisms. The design evolution was accompanied by the conceptual movement requirements and definition of varied joint types.

• A single diagonal was directly found to be compatible with scissors in case study 5.

• Indications by the ellipses theory methodology could reduce the snap-through behaviour, and approximate stress-free diagonal scissors for the case studies 6 and 7. Iterations were achieved manually by trial and error, although in further explorations it could be automated through the add-on Galapagos, a generic platform embedded in Grasshopper for the application of evolutionary algorithms on problem-solving.

• Spatial deviations added major complexities to solve the abstract rigidisation of case study 8, limiting further explorations during this study.

The connectivity amongst scissor types can configure variable conic curves, if the ellipses method is consistent with design criteria (Sánchez-Cuenca, 1996a). Figure 4.43 exemplifies arches utilising curved-translational units and a stabilised quadrangular base, in contrast to existent triangulated scissor grids by Roovers & De Temmerman (2014b). From this linkage repetition, simple curvature geometries could be obtained directly.

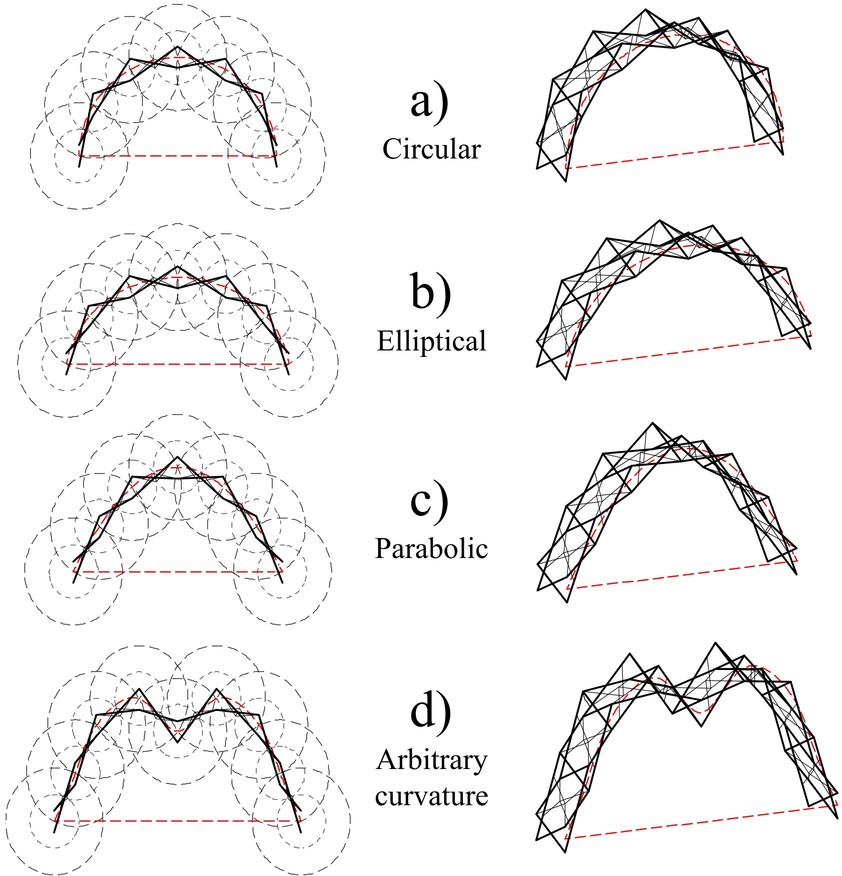

Figure 4.43 *Diagonalised arches by curved-translational units*

It is also feasible to get a structural frame rigidisation of single and double-curved geometries, combining arches from case studies 1, 3 and 4[1]. In Figure 4.44, the non-diagonalised spaces correspond to modules at case studies 5 and 6; therefore, they are less likely to be required. However, positioning restrictions exist for the membrane compatibility in any double curvature structure produced by translational scissors. This condition is considered in chapter 5.3.4.

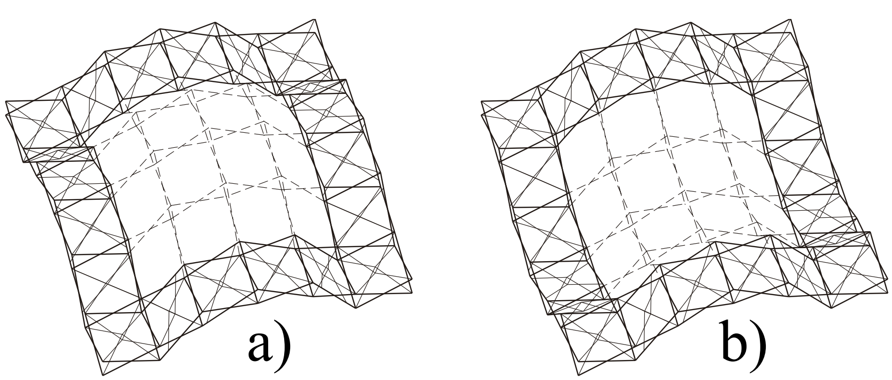

Figure 4.44 *Diagonalised geometries by curved-translational arches: a) Synclastic, b) Anticlastic.*

Note[1]: Theoretically, curved translational deployments can be obtained by altering the orientation of equal polar scissor pairs [e.g., a polar scissor is rotated 180° in respect to the coplanar-adjoining pair].

4.4 Chapter summary

This chapter categorised eight expandable prisms associated with existing quadrangular grids, to study the feasibility of self-regulating the lateral instabilities. The assessment was initially provided in virtual models from the morphological and kinematical point of view, indicating the proposals evolution, opportunities, limitations and grouping examples. Single and double diagonal mechanisms were tested according to the modules' complexity, and it was identified an essential dependence of different joint types for granting a steady performance with one degree of freedom.

It was fulfilled the objective of examining the functionality of the proposals via 2D & 3D modelling, parametric design, and mechanical simulations. The following research stages include physical testing on reduced models and preliminary structural analysis.

5 SCALE MODELS FABRICATION & POTENTIAL OUTCOMES

5.1 Introduction

The purpose of this chapter is to bring into practice the case studies proposals, as literature review authors often suggested that merely theoretical approaches should not be taken as conclusive. For example, owing to the great complexity derived from deployable structural systems, the double curvature models I recreated in the past through curved-translational scissors require exceptional efforts to reach the open position, even if the design has a stress-free behaviour, and despite the spans between supports are less than 3 meters [Figure 5.1 & Figure 5.2].

Figure 5.1 *A synclastic surface using curved-translational scissors. (Gómez Lizcano, 2012).*

Figure 5.2 *A synclastic surface using curved-translational scissors and telescopic legs. [Personal library -unpublished work, 2014].*

Therefore, the proposed mechanisms' perceptions of manufacturing, assembly, and physical motion are reviewed at a reduced scale. Since ABS/PLA materials are used on the 3D printed joints, a contrasting high stiffness of the aluminium beams cross-section facilitates the identification of possible mismatches, such as stability, fragility, smoothness or friction. Likewise, the structural compactness and the covering fabric suitability with the rest of the components contribute during refining the study by continuous feedback. Afterwards, a recapitulation of the potential grouping outcomes for transportable and transformable applications is indicated.

5.2 Manufacturing

5.2.1 Case Study 1

The evolution of case study 1 among its different variants showed an adequate structural response, confirming prior mechanical simulations predictions. As the first fabricated attempt, lateral instability differences were immediately noticed on a partial assembly without diagonals, contrasting each triangulated modification of the module.

Although all printing calibrations are equivalent in quality, some joint types tend to resist more stresses; this is just a relative perception since to make a fair comparison, non-standard shapes, dimensions, and divergent printing layer orientations should be considered. On the other hand, diagonal connectors at 45° could be problematic to manipulate with a screwdriver if the joint eccentricities are too short.

As it could be inferred, the covering fabric has full compatibility with movements due to the simplicity of planar geometries. The lateral sides gradually increase their dimensions when the mechanism deploys, allowing as much tensioning as desired until a final, locked position. Scenarios are presented in Figure 5.3 to Figure 5.7:

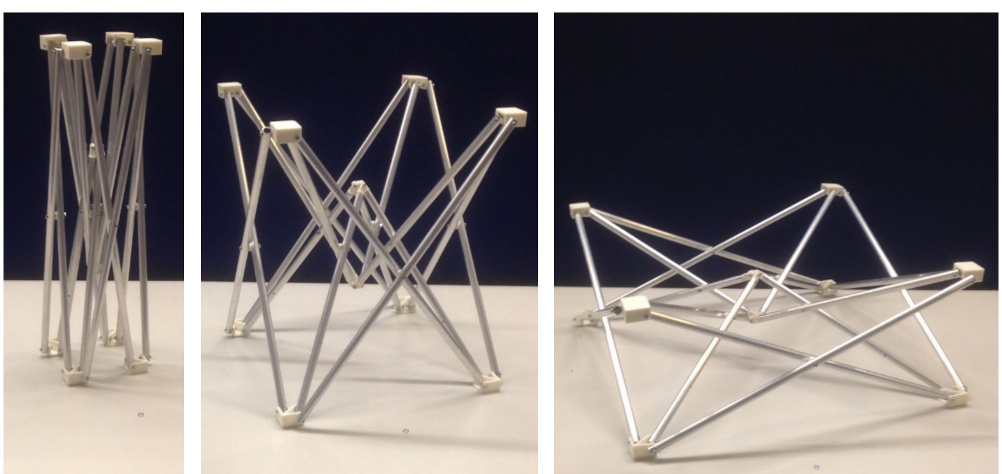

Figure 5.3 *Manufactured sample of the first approach to obtain a stress-free regular square prism with double diagonalisation.*

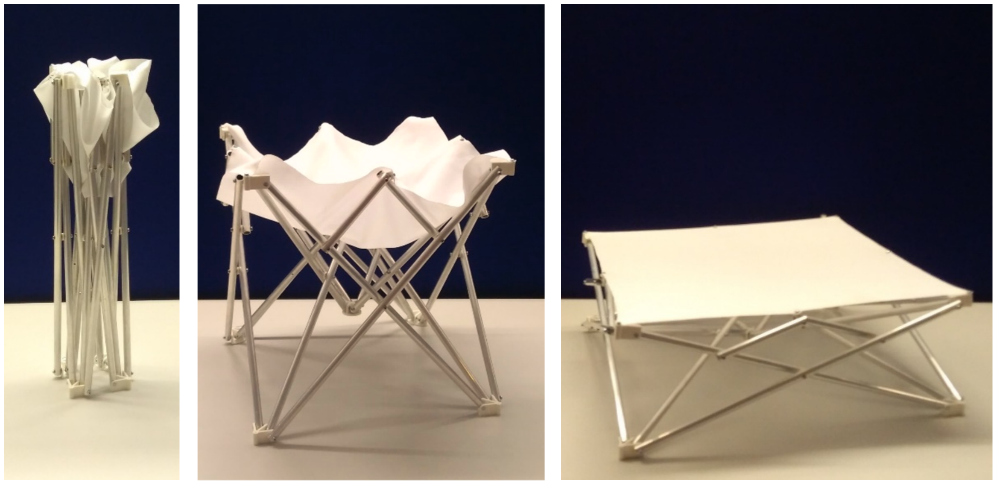

Figure 5.4 *Manufactured sample of the preferred solution to obtain a stress-free regular square prism with double diagonalisation, and a minimum eccentricity at joints.*

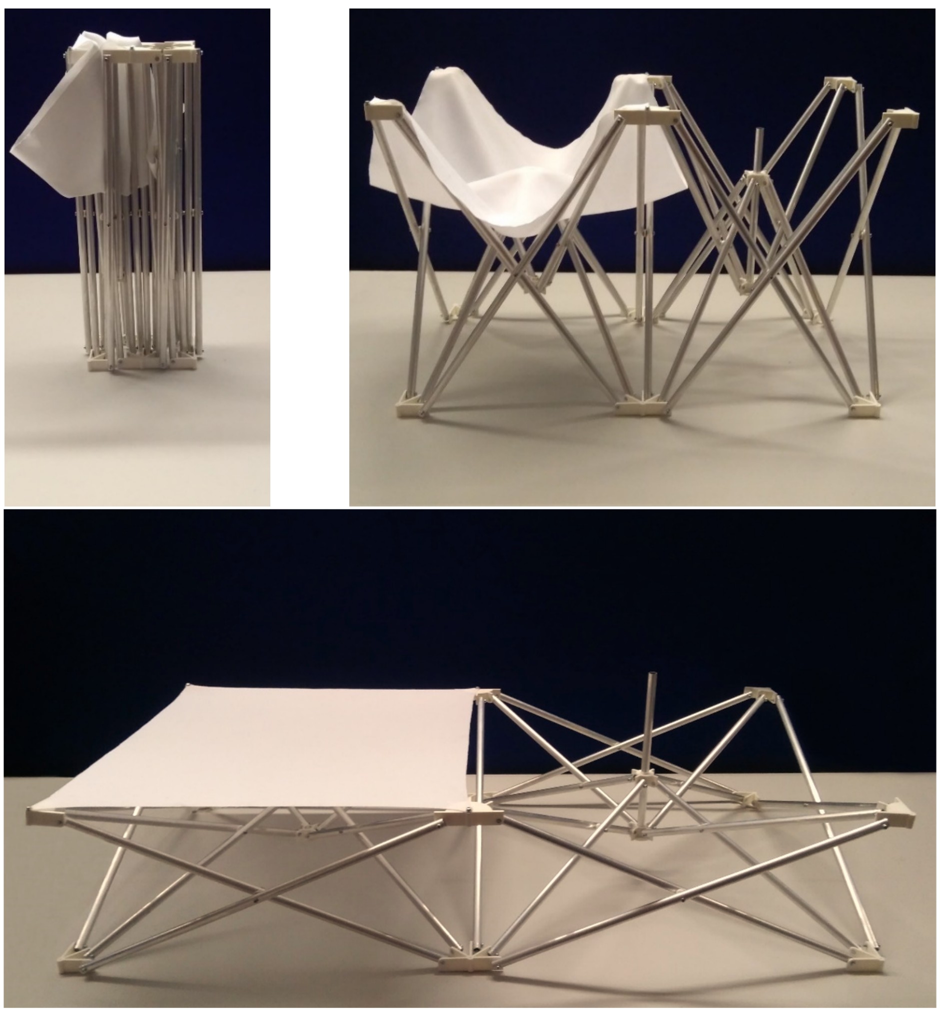

Figure 5.5 *Manufactured sample of the preferred solution to obtain a stress-free regular square prism with double diagonalisation, and a contrasting adjustment to insert a slidable object.*

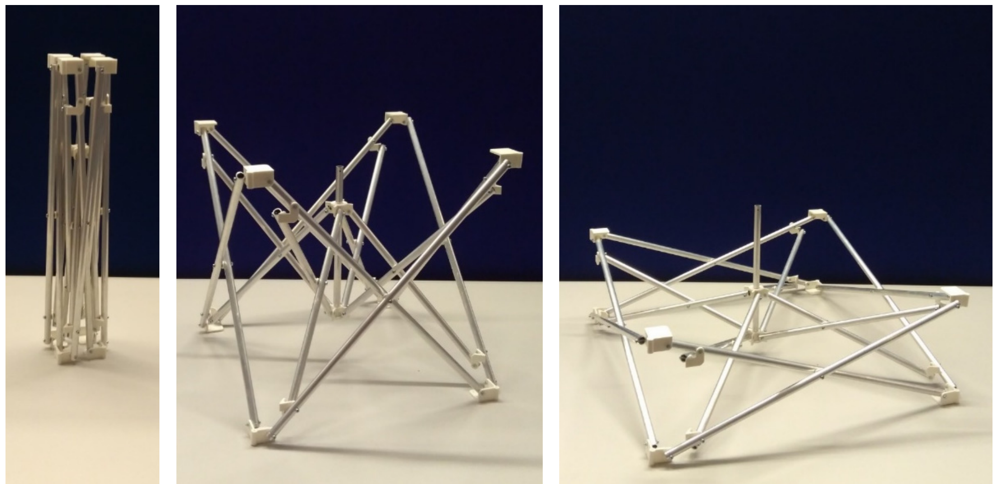

Figure 5.6 *Manufactured sample of a modified regular square prism using four internal scissors.*

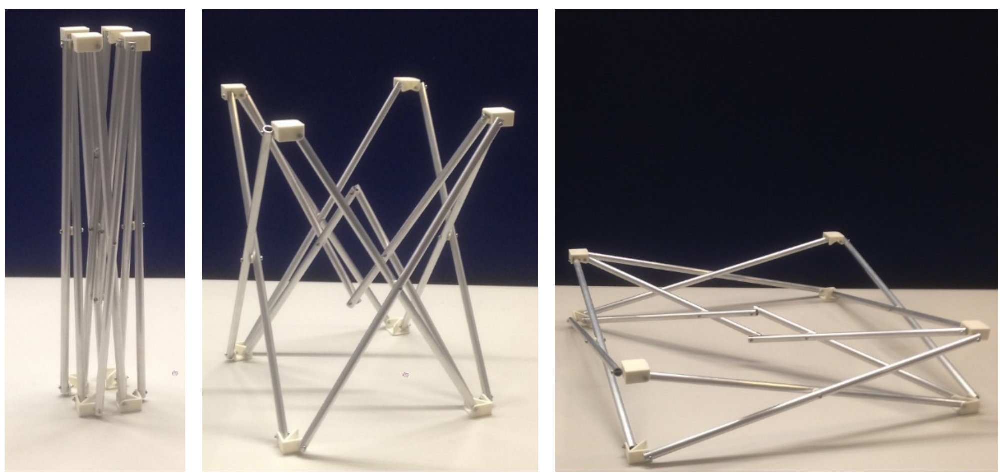

Figure 5.7 *Manufactured sample of a stress-free regular square prism with single diagonalisation.*

5.2.2 Case Study 2

A representative minimum predictable module with irregular shapes served as the fundamental testing to support the studied novel concepts. Initially, Figure 5.8 recreates the expressed structure by Santiago Calatrava (1981; 1993) on a scale model; and unlike the perfect constraint conditions imposed by the joints in the mechanical simulation of Section 4.2.2 [Figure 4.16b], a weak structure was obtained by joints with fixed pivots at 90° and 45°. This result can be attributed to the material capacities or minor mismatches during manufacturing, creating a vast effect on the mobility of the mechanism.

Instead, Figure 5.9 and Figure 5.10 verify a single degree of freedom when employing the proposed rigidisation by pantographs, demonstrating the potential for full-scale buildings subjected to external loads. Robust joints with double support on each end of the bars may well be considered, as an additional misalignment-controlling factor.

Figure 5.8 *Manufactured sample of Calatrava's square-base model.*

Figure 5.9 *Manufactured sample of a module with irregular shapes.*

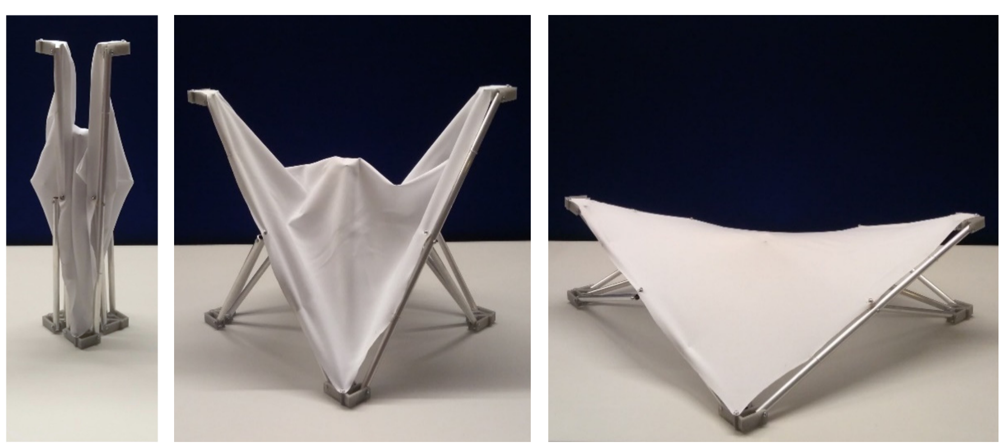

Figure 5.10 *Manufactured sample of a module with irregular shapes, integrating a covering fabric.*

An aleatory positioning and dimensioning of complementary pantographs [semi-scissors] can produce added incompatibilities and deformations. The design exercise of mutating case study 1 was shown to be adequate to obtain a stable stress-free structure in case study 2.

5.2.3 Case Study 3

The continuous analysis between conceptual designs and mechanical simulations expressed in Section 4.2.3 matches the scale-models progression in Figure 5.11 to Figure 5.14.

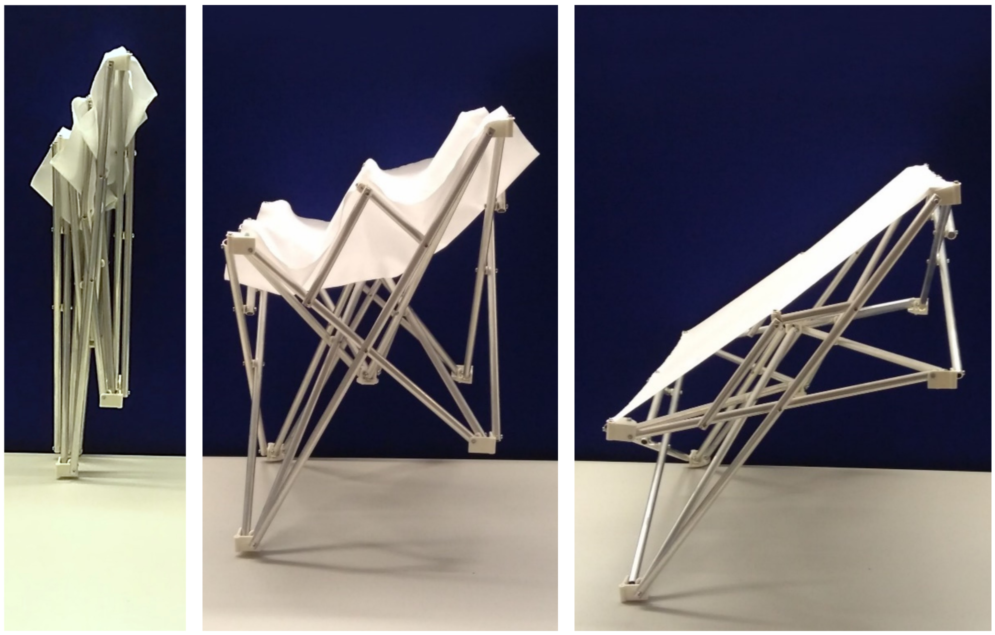

Figure 5.11 *Manufactured sample of the first approach to get a stress-free oblique rectangular prism with double diagonalisation.*

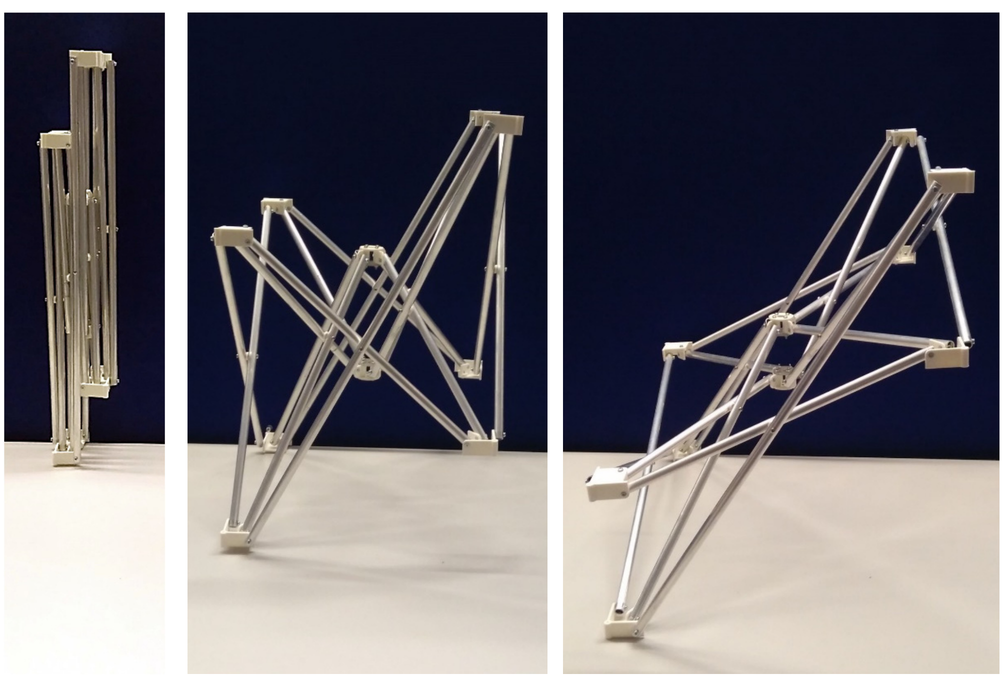

Figure 5.12 *Manufactured sample of the second approach to get a stress-free oblique rectangular prism with double diagonalisation.*

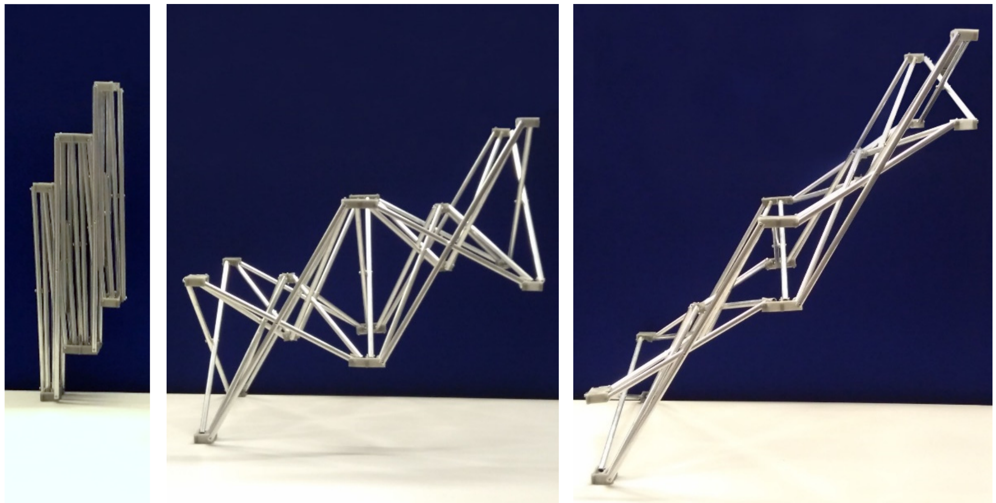

Figure 5.13 *Manufactured sample of the adjusted solution on a stress-free oblique rectangular prism with double diagonalisation.*

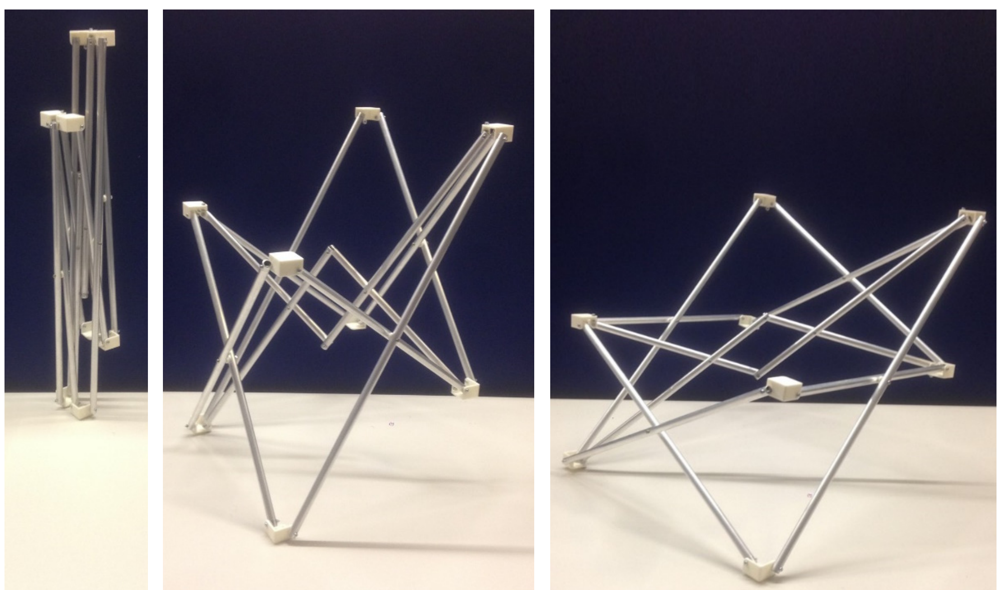

Figure 5.14 *Manufactured sample of a stress-free oblique rectangular prism with a single diagonalisation.*

On the other hand, a scenario in which flexible material is exposed to the elements was theorised, instead of the projected rotary joints on the diagonal scissors. The diagonals angular variation during movements was measured to estimate the resulting deformation, and real-time data from a parametric design was collected. As an example, using the same proportions from Figure 5.13, the produced information for the diagonal scissors connected in the vertex joints is between 44.2° in the initial position and 35.7° in the final one; hence the difference is 8.5°, or more, depending on the desired inclination and thickness for the deployed configuration. In addition to this, the oscillations in the centrally located joints were up to 17°.

Depending on the opening degree, and due to the PLA material, it is noticeable that deformations are absorbed by the joints, which are then prone to break. In Figure 5.15, the 3D printed vertex joints' flexibility was tested using a fixed diagonal pivot at 45°, and a hinge-type form was used for the centrally located joints.

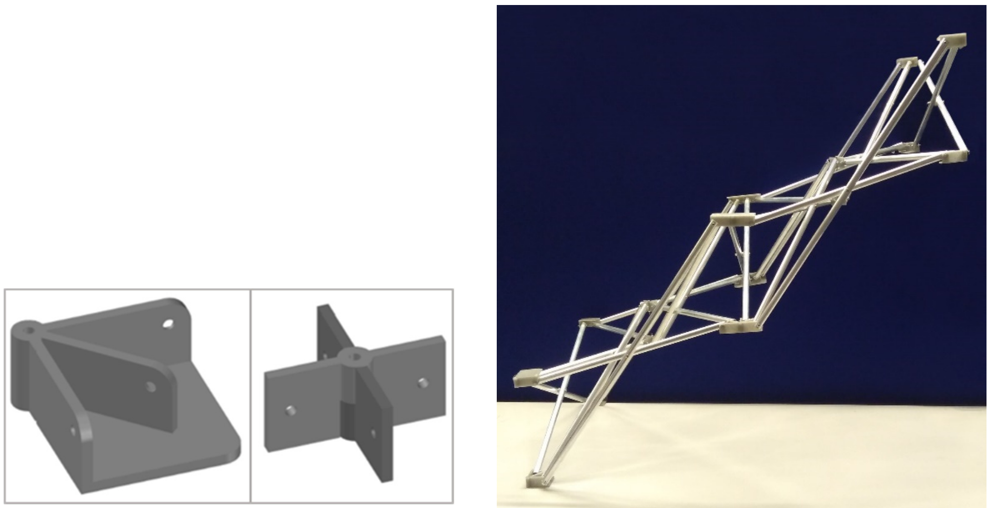

Figure 5.15 *Manufactured sample of a snap-through behaviour oblique rectangular prism with double diagonalisation.*

Unlike in Figure 4.27, a trial model of a modified oblique quadrangular prism using fixed pivots diagonal connectors was produced in Figure 5.16; some of the diagonal bars were shortened, and the additional joints within the length of the lateral scissors were suppressed. Although the mechanical simulation in software has appropriate mobility, the scale model reveals a lack of rigidity at the vertex joints when a force is applied. Double pivotal support of the joints increases security against the lever effect, counterbalance the eccentricity, controls probable assembly maladjustments, material flexibility, and irregular fabrication tolerances.

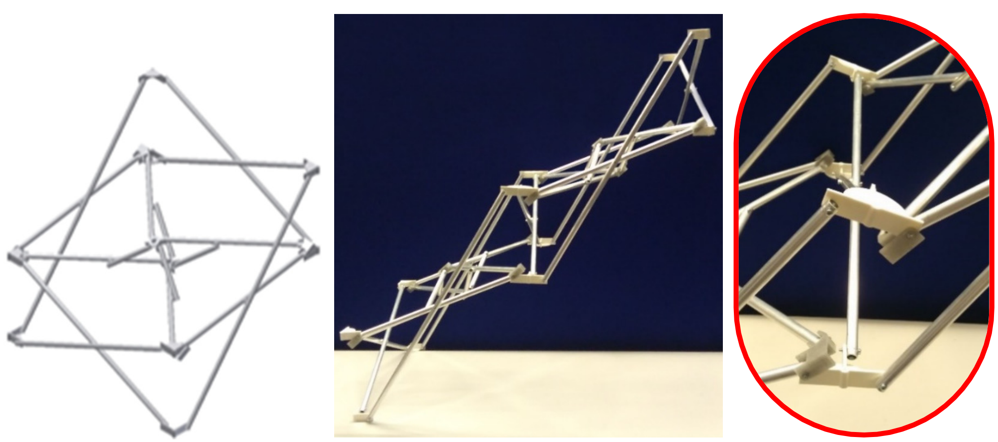

Figure 5.16 *Manufactured sample of a modified stress-free oblique rectangular prism with double diagonalisation.*

5.2.4 Case Study 4

As in prior case studies, the original theories and joint types understanding evolved through decision-making experiences on scale-models; single and double alternatives of diagonalisation were verified, and the complementary textile was attached to perceive the compatibility [Figure 5.17 & Figure 5.18].

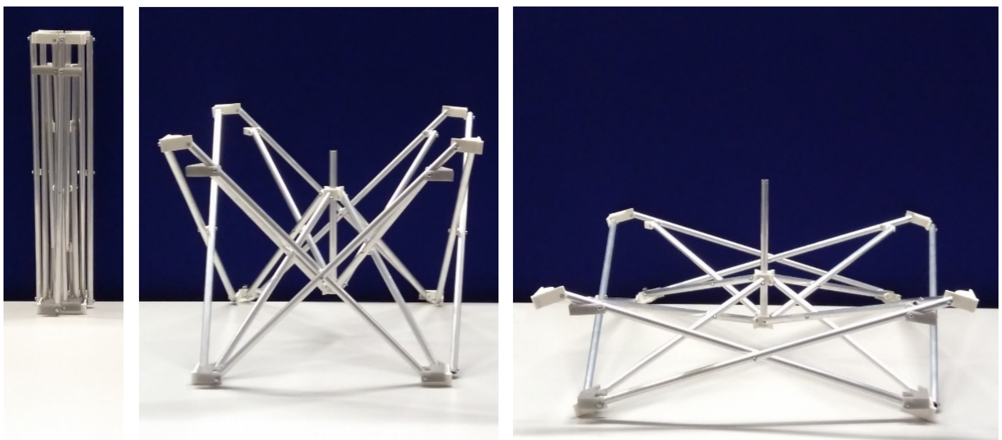

Figure 5.17 *Manufactured sample of a stress-free trapezoidal cross-section prism with double diagonalisation.*

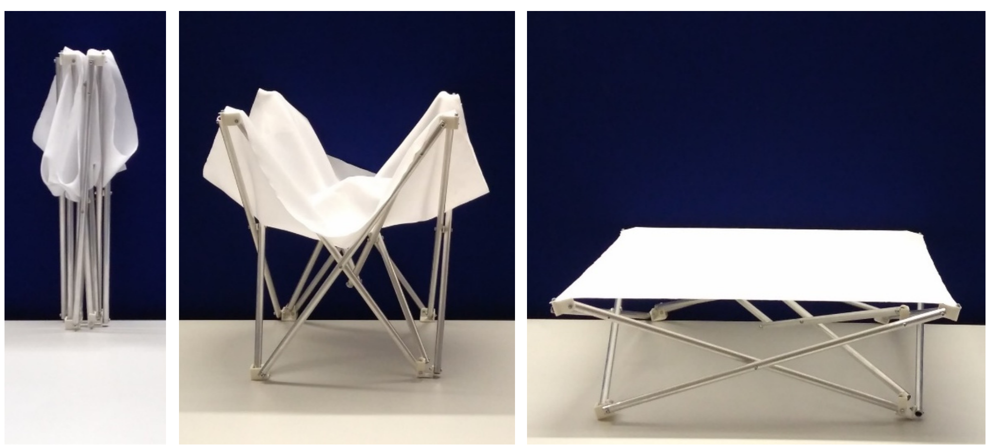

.

Figure 5.18 *Manufactured sample of a stress-free trapezoidal cross-section prism with a single diagonalisation and the membrane attached.*

5.2.5 Case Study 5

As no major complexities were found by fixed diagonal connectors at 90°/45°, the mechanical assembly and fabrication were evaluated straightforward in Figure 5.19. The structure solely can be raised to any theoretical level without restrictions, but once the fabric is added, the maximum compatible position occurs when the shortest bar of each of the curved-translational scissors is in parallel alignment to the ground. This condition should be considered in the design, as the shortest prism diagonal loses its length, so the membrane's tension will be lower.

Another aspect to highlight in the event of reaching the maximum deployed position is the need to fit the membrane to the diagonal scissors elevation. This aspect should be considered when defining the cutting patterns; besides, softening all possible sharp edges is required for avoiding blockages or ripping.

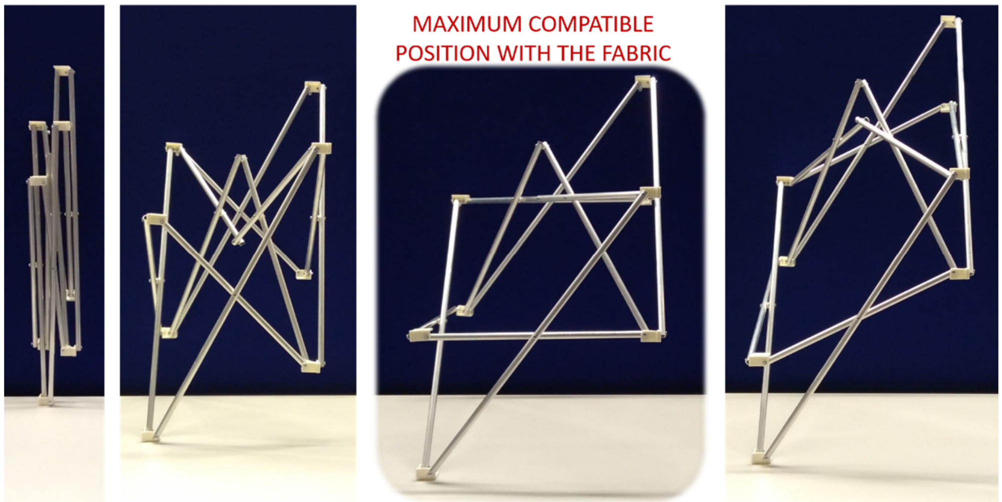

Figure 5.19 *Manufactured sample of a stress-free oblique rhombic prism with single diagonalisation and 90°/45° joints.*

5.2.6 Case Study 6

After the iterative trial and error process to approximate stress-free behaviour on the congruent diagonal scissors, a need for allowing rotary joints was detected [Figure 5.20]. Although the structure can be effectively perceived as kinematically stable and no evident friction exists, the membrane compatibility needs to be assessed.

Figure 5.20 *Manufactured sample of an approximated stress-free oblique rhomboidal prism with single diagonalisation and rotary joints.*

5.2.7 Case Study 7

Geometrical incongruences were detected during the iterative process to approximate stress-free diagonals. An intuitive and analytical work was necessary to get the partially successful results of Figure 5.21; however, the model tends to be unstable nearing the compact position only, as there is a need for additional degrees of freedom. By contrast, stability is increased after half-deployment, and the structure is perceived as effectively stabilised.

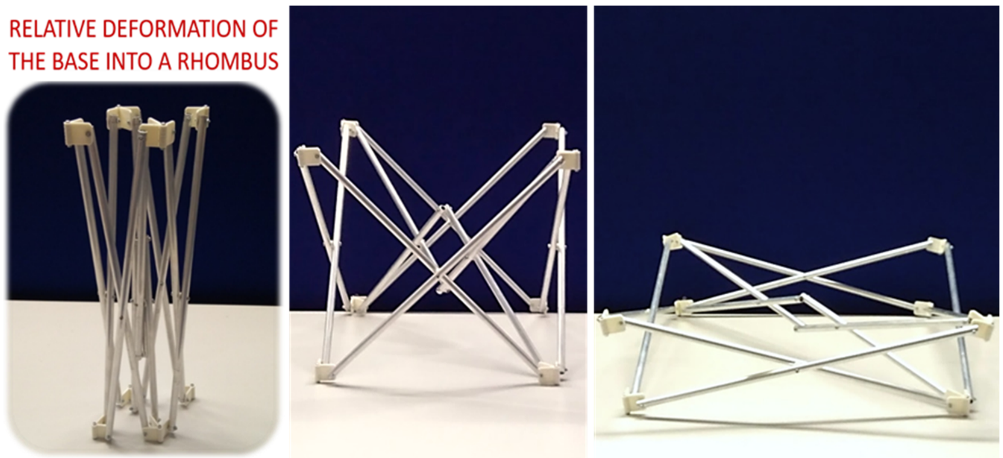

Figure 5.21 *Manufactured sample of an approximated stress-free square pyramid frustum prism with single diagonalisation and vertex joints with additional degrees of freedom.*

On the other hand, preliminary 3D printings were made to perceive and analyse the required joints' characteristics [Figure 5.22]. As in the conceptual wireframe model, each connector eccentricity is a sub-mechanism that can rotate about the original prism vertex node. The PLA material and the reduced torque pressure applied to the central bolt [the screw and the nut] creates reduced friction in the scale model, but in the case of generating a synclastic geometry by polar scissors, exhaustive and detailed digital fabrication processes would increase the complexity, if compared to optional case study methods.

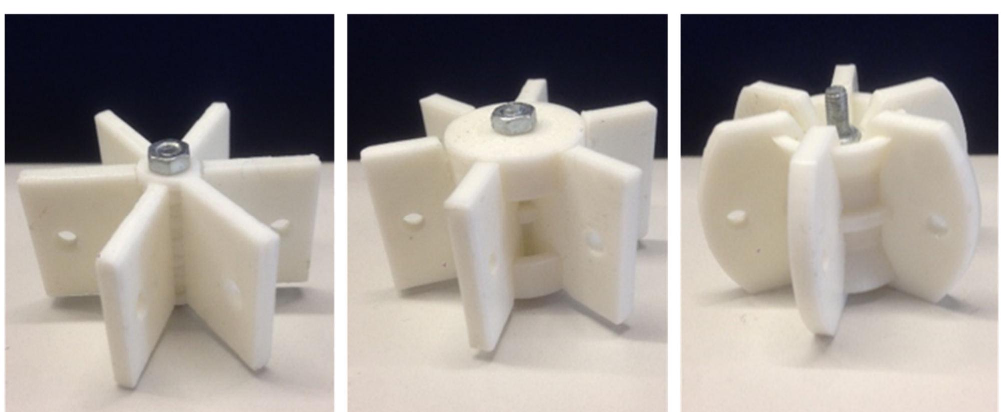

Figure 5.22 *Joint explorations joints with additional degrees of freedom.*

5.2.8 Case Study 8

A standard sliced tetrahedron replica revealed movement instabilities on a reduced model [Figure 5.23]. Nonetheless, the suggested stabilisation produced major spatial inconsistencies and did not continue during this study, as was stated in Section 4.2.8.

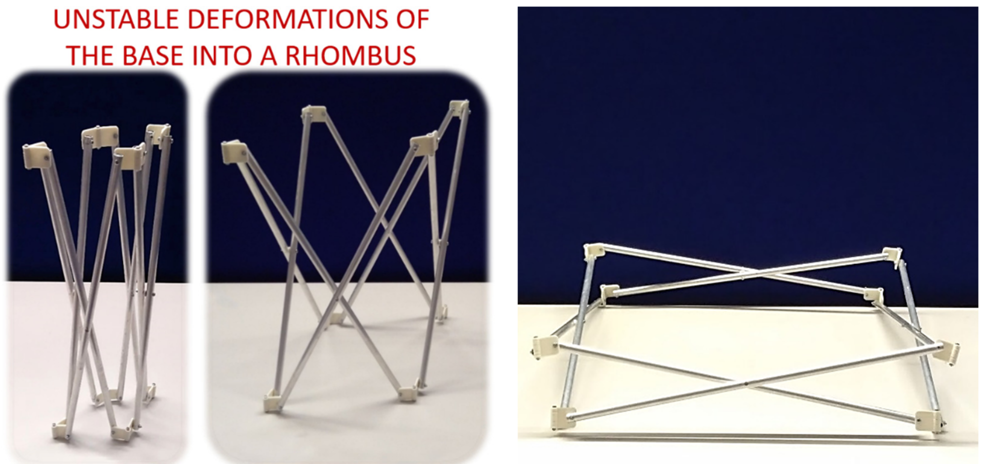

Figure 5.23 *Manufactured sample of a sliced tetrahedron from the prior art.*

5.3 Potential outcomes & image collection

5.3.1 Flat shapes

A common scissor structure for architectural uses nowadays is a collapsible canopy [pop-up tent] raising a slidable central mast to shape a pyramidal roof (Carter, 1986), (Lynch, 1987; 1988). On larger scales, a practical variant for creating protective shelters or similar relocatable constructions might be, for instance, a deployable roof standing on containers (Ma, et al., 2010).

Scaffolds could be employed as rapid demountable supporting systems [Figure 5.24]. By human force only, these on-site, pre-assembled sets of parts serve to elevate a roof from the ground level, once the deployable structure is locked. Thus, the covering membrane can be effectively and securely prestressed by operators at a lower position; the versatility of the combined constructive methods produce optional roof heights, pitch angles, shape variations, and the possibility of incorporating wheeled platforms, counterweights or anchors.

Although fundamentals for case study 1 were initially provided by Escrig et al. (1995), the three-dimensional inspections in this study estimate favourable conditions for greater installation frequencies, as the mechanical performance during deployment improves the geometrical inconsistencies non-triangulated patterns. The magnitude of the towers and the integration of the scissors could be perceived as a stable unit [e.g., a gantry construction]. However, detailed engineering is required to validate this.

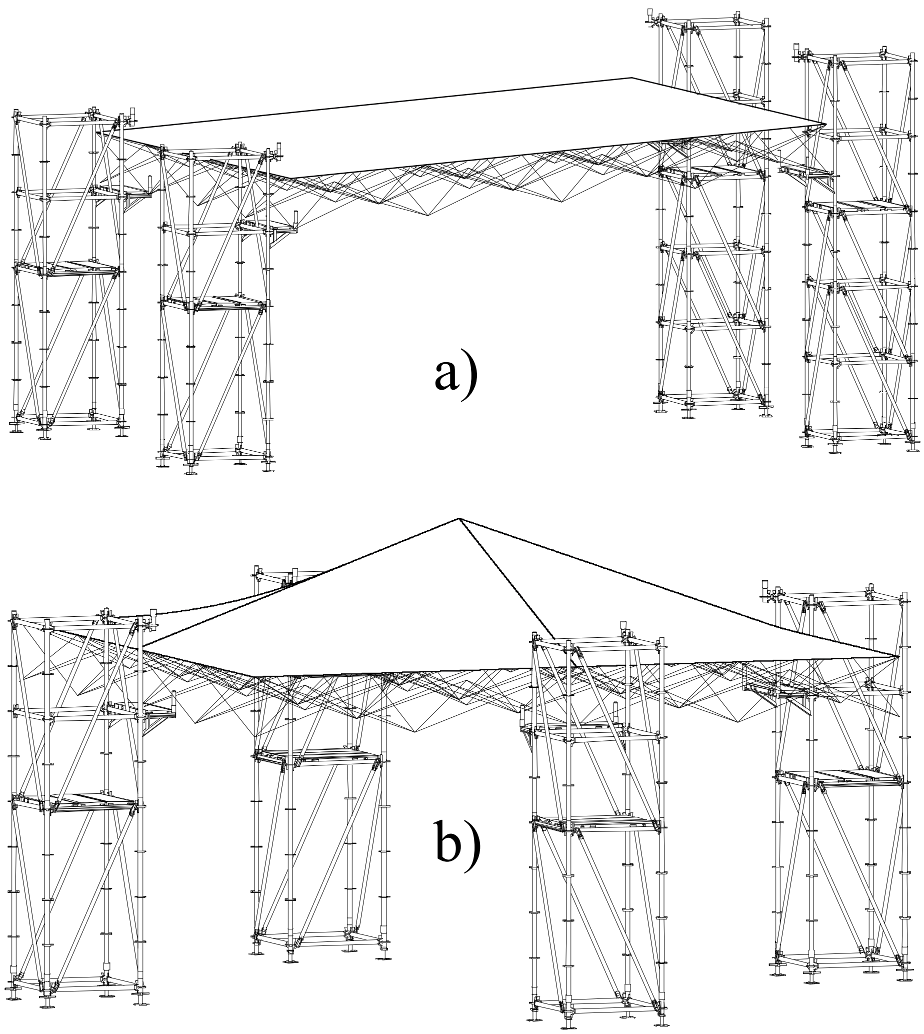

Figure 5.24 *Geometries from case study 1: a) Unlevelled flat roof supported on scaffolds, b) Pyramidal tensioned roof supported on scaffolds.*

5.3.2 Irregular shapes

Taking by reference the self-supported umbrella bar concept (J. Meissl GmbH, 2019), a rigidised Hypar installation sequence by at least 2 persons is depicted in Figure 5.25. The proposal is envisaged to be effective from a geometrical perspective; the dynamic response of wind and the bending forces on the mast base require further calculations.

On the other hand, a Hypar tent could be raised from a basic truck-mounted crane [Figure 5.26]. To prevent slender and laterally unstable slidable columns on large scales, a minimum roof thickness ratio of 1/3 the total height is chosen; the reduced number of combined modules compared to analogous deployable tent proposals could benefit the structural performance once it is fully locked. After designing by software, a scale model and the covering fabric were tested [Figure 5.27]; variations of case study 2 may well be projected for more demanding structures.

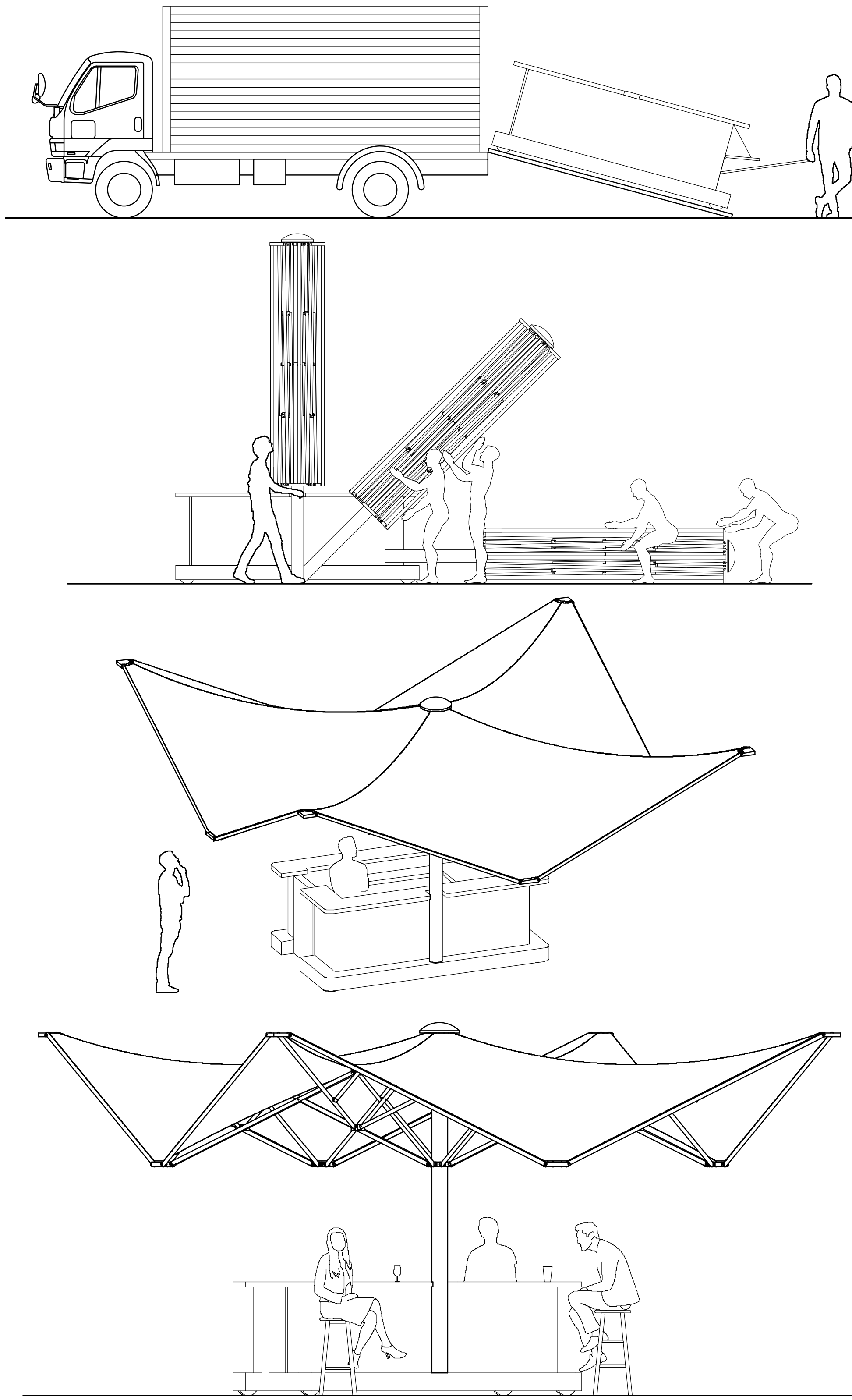

Figure 5.25 *A transportable Hypar umbrella-bar.*

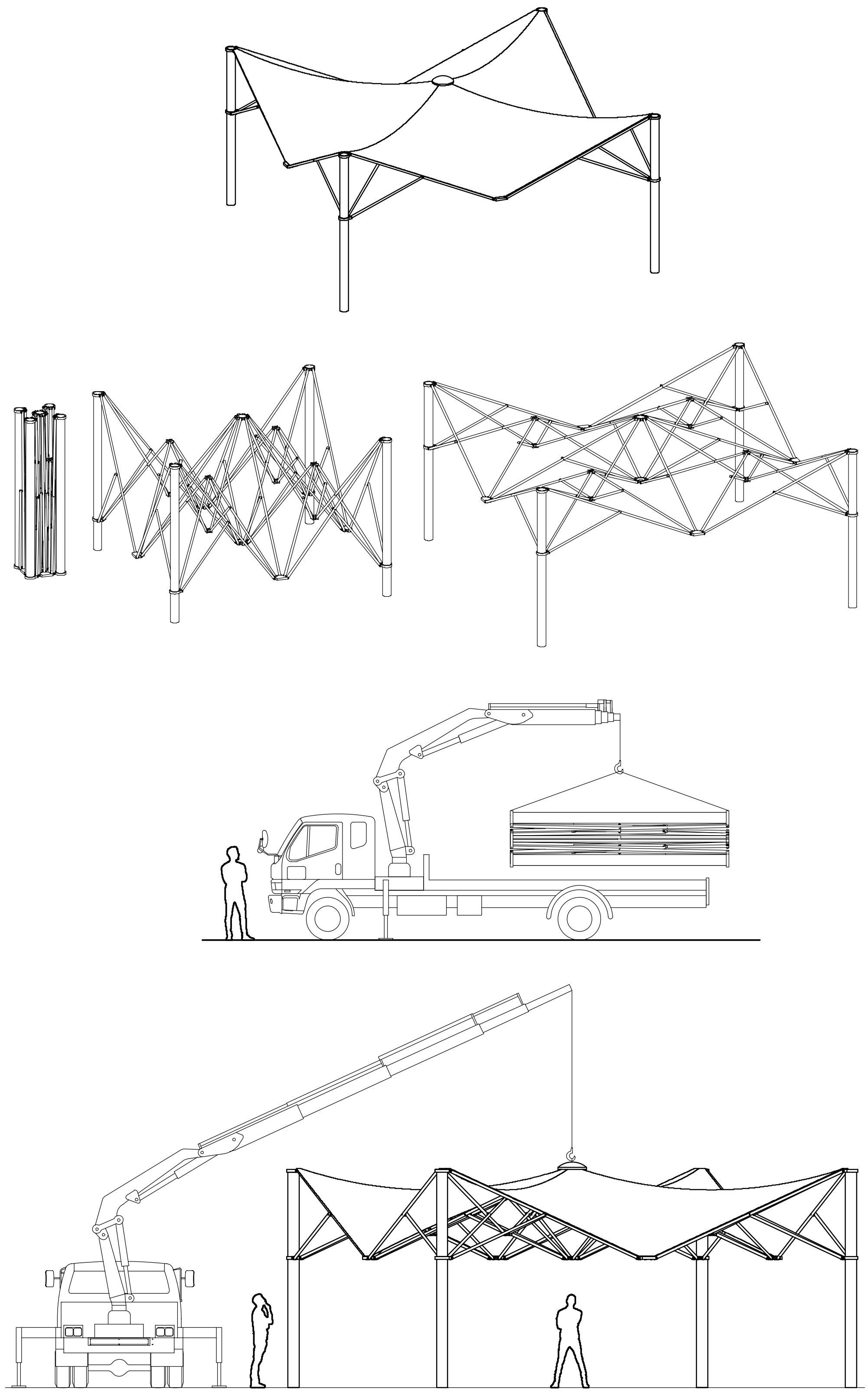

Figure 5.26 *A deployable Hypar tent.*

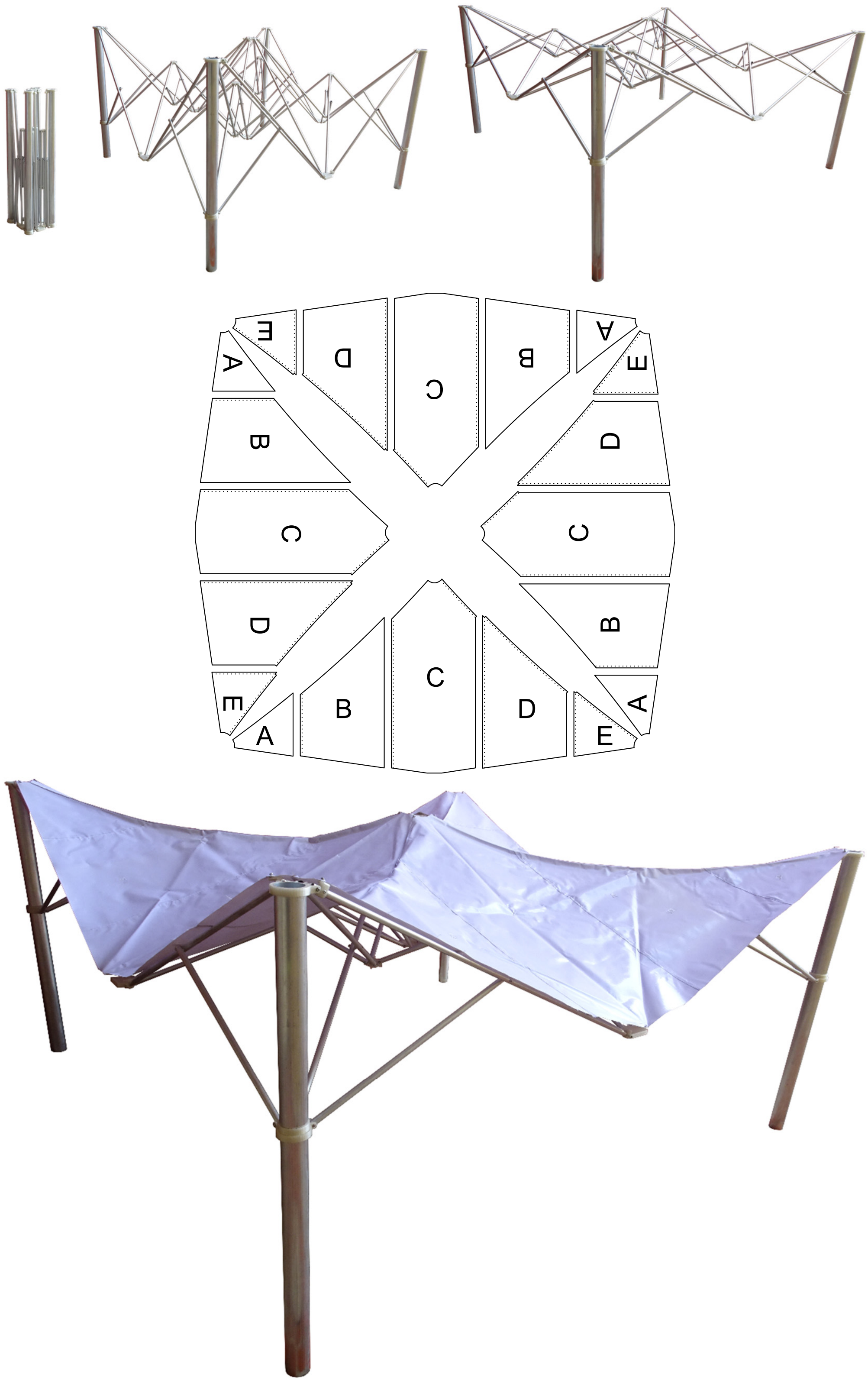

Figure 5.27 *A deployable Hypar tent scale model and cutting patterns for the fabric.*

5.3.3 Single curvature shapes

As stated in prior chapters, the generic prism repetition from case studies 3 and 4 create curved-translational or polar deployments; accordingly, starting from quadrangular prisms, stress-free diagonalised arched structures are potential outcomes. In architecture, these geometries can shape roofs mounted on existing constructions or behave as self-standing vaults. [Figure 5.28].

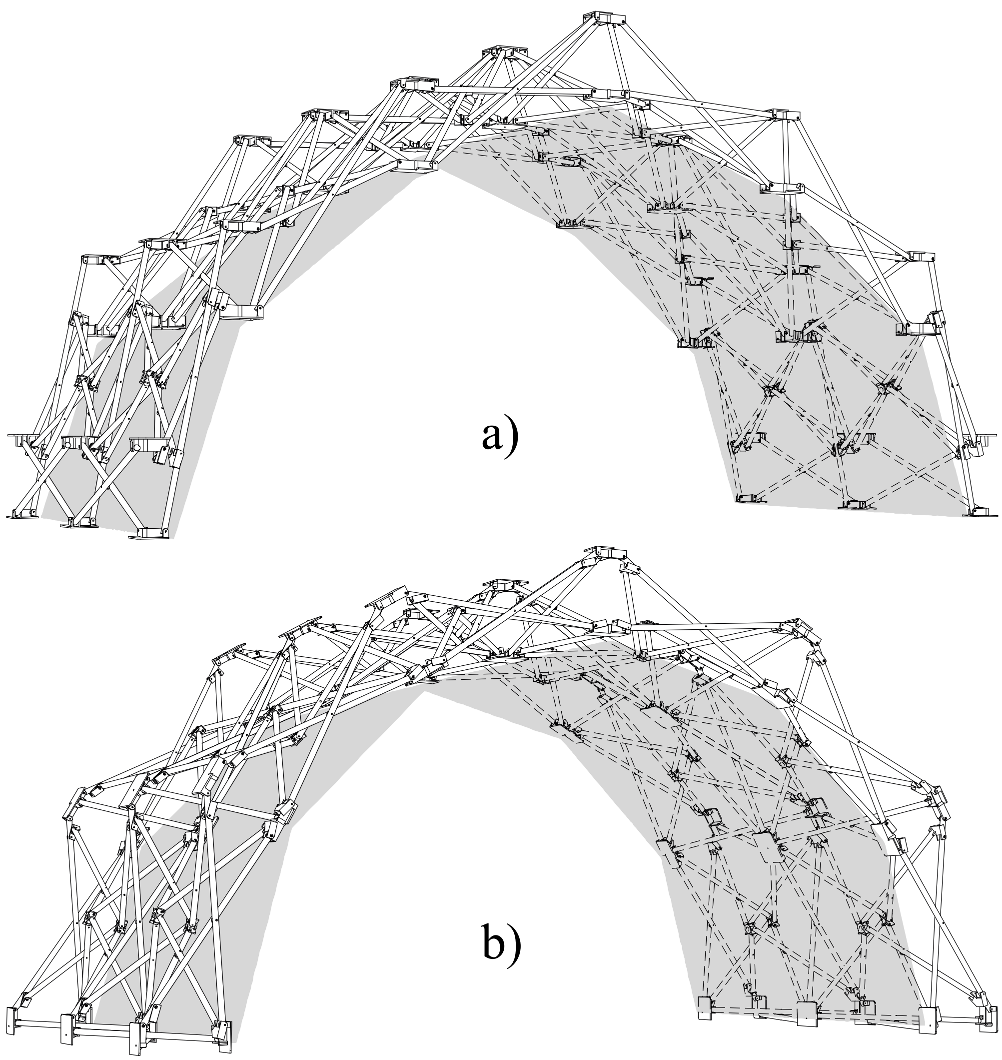

Figure 5.28 *Deployable single curvature tents: a) from case study 3, b) from case study 4.*

Thus, case studies 1, 3, and 4 are likely to be combined [Figure 5.29]. A scale model was fabricated in Figure 5.30, and despite the larger number of parts, an equivalent simplification of case study 4 can be obtained by a four-bar mechanism in pyramid [Figure 5.31]. In the last case, the joint maintains a stress-free condition, and a rectification of the turning effect between differential movements was explored; therefore, case studies 1 and 3 are also likely to be reduced if needed.

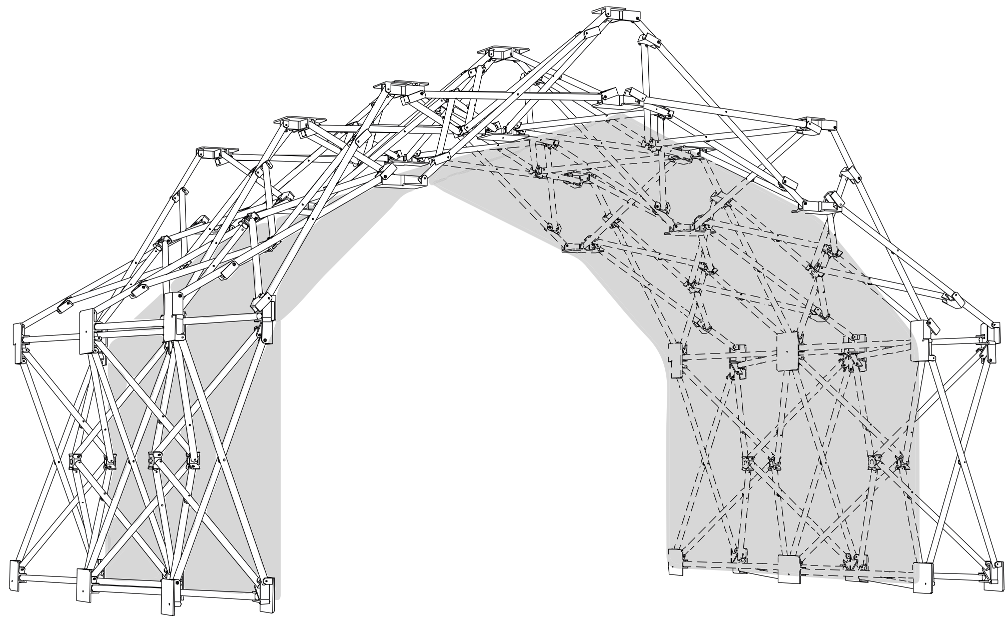

Figure 5.29 *A deployable single curvature tent from case study 1, 3 and 4.*

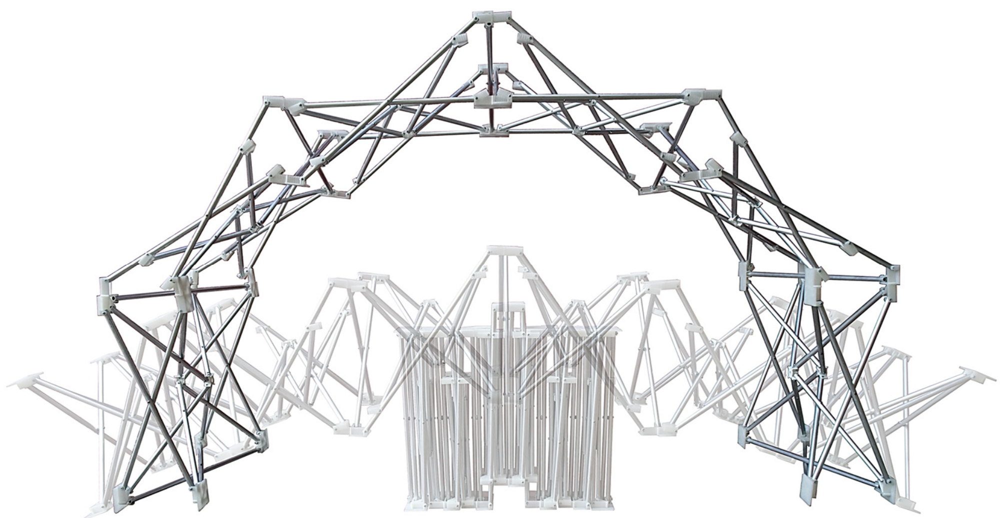

Figure 5.30 *Scale model of a deployable single curvature tent from case study 1, 3 and 4.*

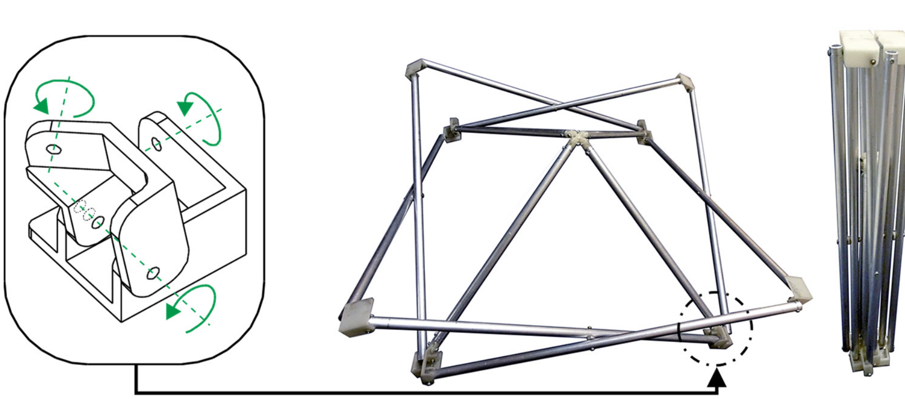

Figure 5.31 *Scale model of a simplified case study 4.*

5.3.4 Double curvature shapes

Experiments by Sanchez-Cuenca (1996c) highlighted the incompatibility problem for a dome requiring a flexible fabric: during roof deployments, the quadrangular modules nearing ground supports have lengthy diagonal extensions to the final position. To test this conclusion, all the relevant dimensions of a simplified geometry were measured by a parametric design.

Considering a curved-translational scissors arch in two-dimensions, it was identified that compatibility could be controlled, if the deployed position of each scissor does not exceed an imaginary parallel position between the ground and the shortest bar. At this exact position, the membrane suffers a maximum diagonal extension [Figure 5.32]; if exceeded, the tension is gradually lost.

A replica of this exercise could be followed to get an anticlastic shape, since the same type of elements producing the arches are connected, only with a different orientation. There are limitations for getting the maximum desired final inclination in both cases; thus, optional methods would require a membrane post-installation.

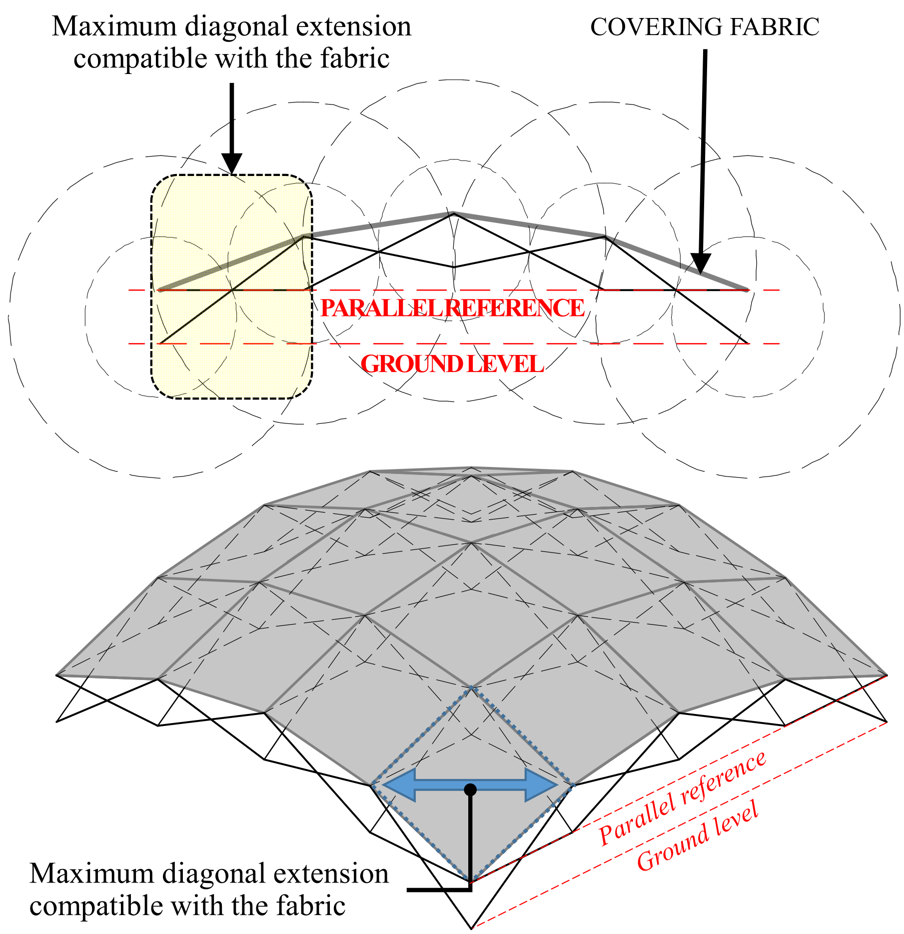

Figure 5.32 *Covering fabric compatibility example.*

As the covering fabric compatibility is not granted to all double curvature inclinations in the same way, reduced geometries could be compensated by scaffolds [Figure 5.33], and laterally rigidised by a structural frame of perimetral arches, as in Chapter 4.3.

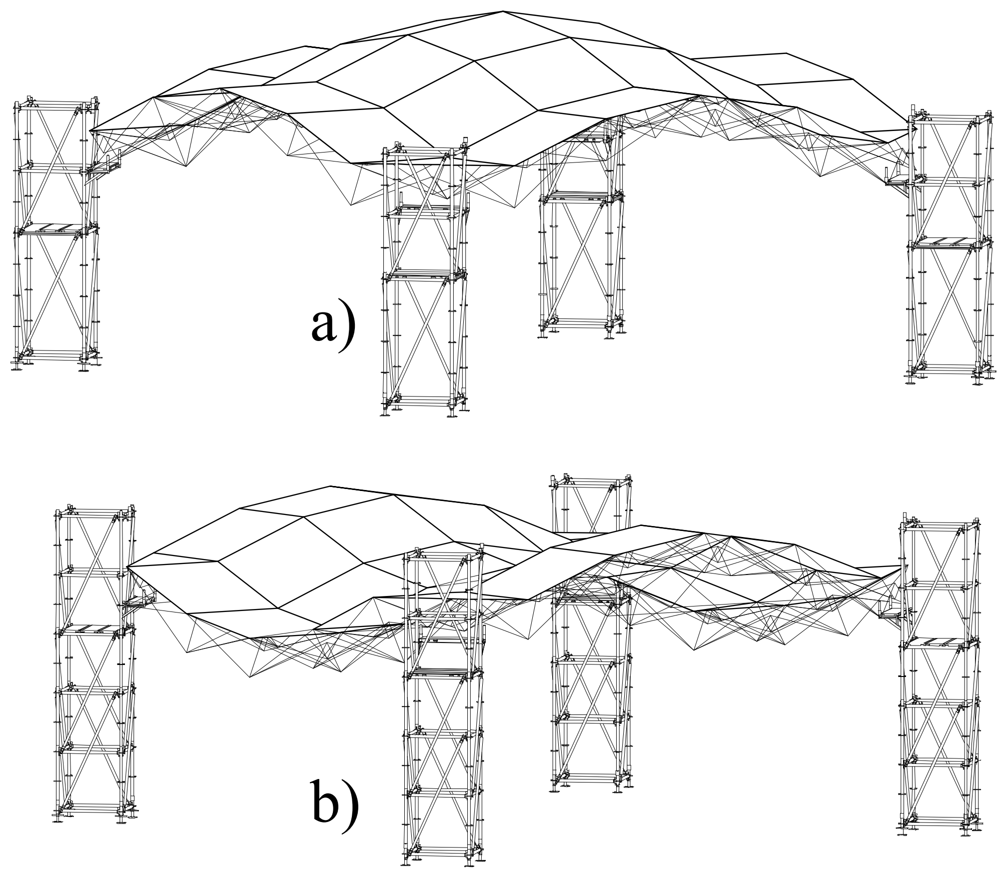

Figure 5.33 *Compatible roofs by reduced geometries: a) Synclastic roof supported on scaffolds, b) Anticlastic roof supported on scaffolds.*

5.4 Discussion on constructive considerations

Potential constructions are often determined by the maximum transport platform width [2.5m], and external equipment can replace material handling when human access is not possible due to structural scale. Typical deployable structures have been installed by a crane or scaffolds, although mechanical devices might offer alternative solutions: e.g., motorised actuators, hydraulic systems, cable pulley systems, among others.

As represented in Figure 5.34, specialised equipment available for raising loads could be a practical solution for a relatively low-cost installation, and carrying the compact geometry for its storage. Accordingly, proposals need to estimate the manipulation procedure by operators, the safety instructions, maximum heights and load capacities.

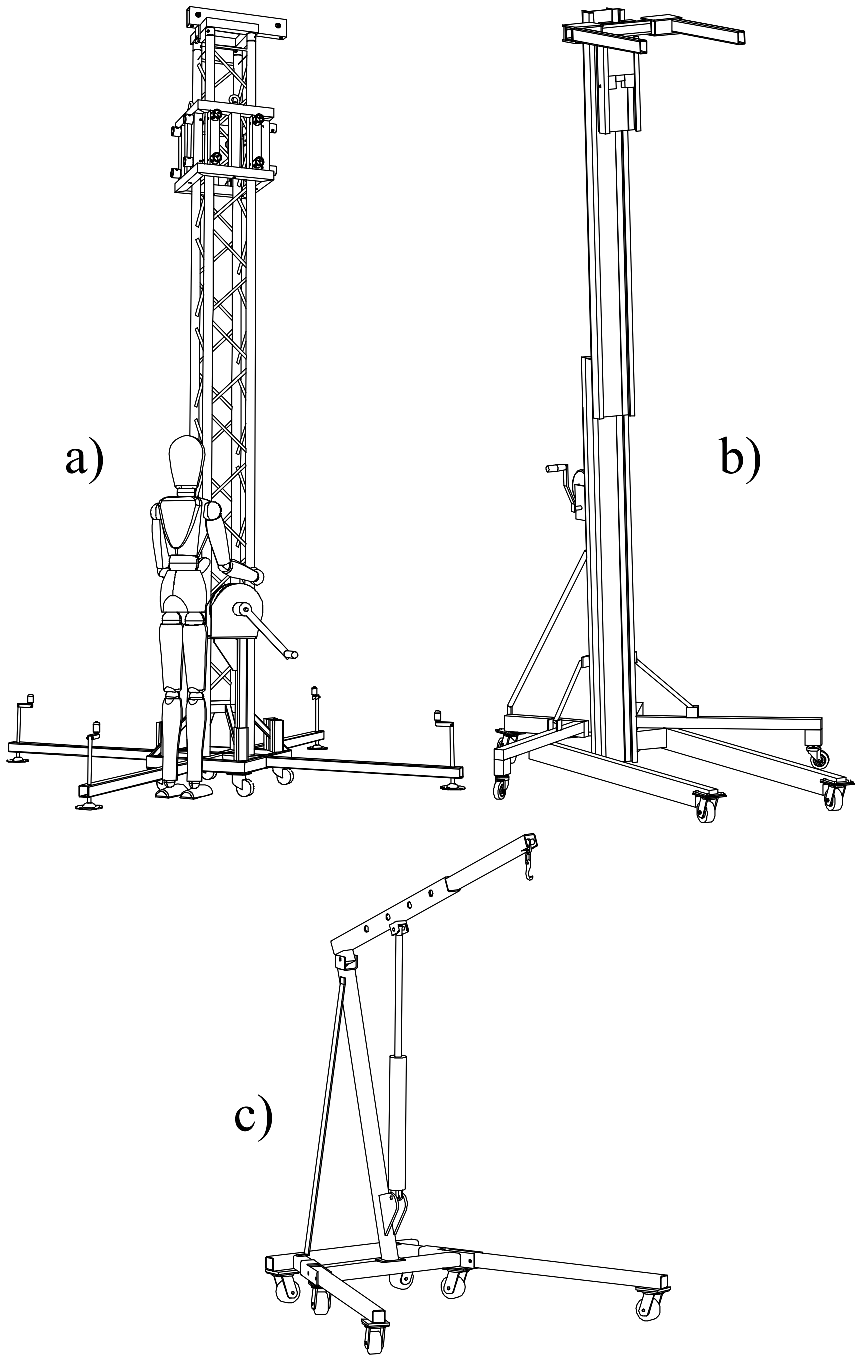

Figure 5.34 *Optional equipment for raising loads: a) Truss system, b) Material hoist / material lift, c) Small foldable hydraulic lift.*

An important aspect to highlight in agreement with Hernández & Cebrian (2010, p. 48) is the required available area, and the crane capacities associated with the boom length, more so than lifting capacities. Knuckle, telescopic, and foldable cranes are preferred due to the structural expansion and the hanging volumetry equilibrium from at least the central point. A free-obstacle frontal position of 6m is the recommended minimum.

The varied number of components can benefit from the latest technological advances for higher production efficiencies; then, human labour can focus on preassembly and planning. Useful manufacturing methods for deployable structures are, among others:

- Customised beam cross-sections.
- Autofeed bandsaws [automatic bandsaw].
- Four-axis tube plasma/fiber laser cutters [metal sheets, square and round tubes].
- Milling, router, laser, plasma cutting tables.
- CNC Hydraulic press [sheet metal].
- Mould casting [e.g., lost PLA], extrusion moulding for the joints.
- Automated linear actuators [multi-drill press].
- Hand-held fiber-laser welding machine, or the traditional MIG, TIG technologies.
- Laser engraving/metal carving for coding different part references.
- Heat welding for polyester fabric.

5.5 Chapter summary

This chapter reviewed the scale models analogous to prior explorations through software CAD/CAE, providing actual data on manufacturing, assembly, aesthetics, and motion perceptions. Representative flat, clastic, synclastic, & anticlastic surfaces were proposed as 1:1 scale potential outcomes; besides, a discussion on the construction process and a list of the latest manufacturing methods were included, thus attaining the fourth objective of the thesis.

In the first instance, substantial lateral deformations appeared on the main quadrangular base modules. After triangulating the geometries by scissors, a stress-free movement and adequate force transmission were obtained in most cases due to the manufacturing precision using 3D printing & low-cost industrial tools. It is notorious that the arising attributes from these explorations would produce relative lower compactness, increase in material consumption and weight, compared to analogous systems stabilised with cables or post-installed bars. However, simplifications allowed creating a four-bar pyramidal mechanism or the effectiveness of a single diagonalisation using scissors.

On the other hand, the covering membrane could be theoretically designed on top or below the structure. Incorporating it before deployment or after depends on the specific kinetic compatibility, logistics and fabrication detailing to avoid damages or ripping.

6 PRELIMINARY STRESS ANALYSIS

6.1 Introduction

The purpose of this chapter is to provide an insight into the structural properties of kinetic architecture using scissors & sliding mechanisms. The methodology studied by Lara Alegria Mira for her PhD dissertation is followed at the beginning (Alegria Mira, 2014, pp. 45-47) for comparing stress analysis predictions to a scale model load testing. Full-scale conceptual designs are assessed during deployment according to usual installation procedures, and afterwards considering the Eurocodes for prioritising identical climate load conditions to permanent and static structures.

6.2 Experimental testing calibration and validation

6.2.1 Parametric finite element model [FEM]

For experimental testing, the preliminary FE model is a three-dimensional scissor structure with 0.5m bar lengths, matching the magnitudes of a scale model. Lateral stabilisation is not considered at this stage; two main scissor-typologies exist in the main curvature: plane-translational scissors towards the terrain and four polar scissors on top. In the open conformation, fully locked supports are set [Figure 6.1].

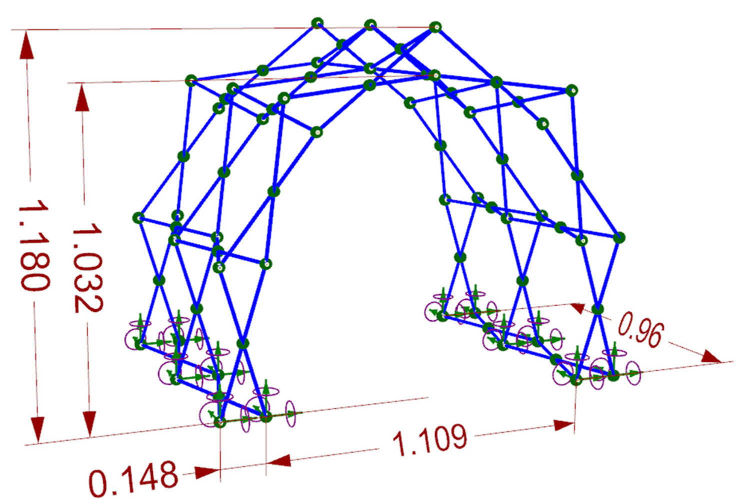

***Figure 6.1** Initial design variables.*
Notes: Dimensions in meters; beams are represented in Blue and connections by Green circles.

The geometry parameters are created in Grasshopper, then converted into a beam model employing the "Index to Beam" component, and zero-length springs on all hinges/joints to obtain Karamba calculations. Nodal identification is eased by setting a variable joint eccentricity.

Springs help to define the stiffness relationship between two nodes belonging to an independent scissor beam, but keep equal cartesian coordinates to simulate the correct motion. While each node has six degrees of freedom, six spring-constants define the connection by the "Cross Sections" multi-component: 3 translational C_{tx}, C_{ty}, C_{tz} [kN/m] and 3 rotational C_{rx}, C_{ry}, C_{rz} [kNm/rad]. At first, infinitely stiff spring-constants with a high value of 10^{12} kN/m or kNm/rad are utilised for creating the vertex joints.

The "Beam-Joints" component then modifies the definitions by adding new hinges at the endpoints of the beams to allow the scissor mechanism, whereas the spring hinges control the rotational capacity of a bolt about the intermediate connector of each scissor. Instead of scripting tools, all parts were created one by one to verify the correct assembly; simultaneously, it was decided, according to the local coordinate system, that all beams on the y-axes should correspond to the orientation of the hinges. In Figure 6.2, this is obtained through the "Orientate Beam" component, and it enables the release of the spring rotational local axis C_{ry} exclusively [C_{ry} is set to zero].

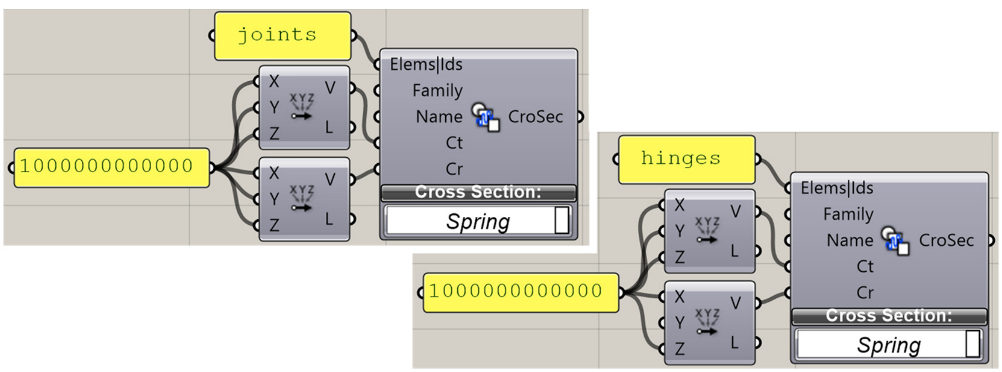

Figure 6.2 *Definition of zero-length springs on joints and hinges.*

Beams are created matching the scale models and the local provider specifications [Figure 6.3]:

- Circular hollow cross-section: 1.27cm diameter and 0.107cm wall thickness.

- Aluminium 6063 T5 material: 6900kN/cm^2 Young's Modulus [E], 2700kN/cm^2 Shear modulus [G], 27kN/m3 Specific weight [gamma], 0.0000234 Coefficient of thermal expansion *(1/C°)* [alphaT], 11.2kN/cm^2 Yield strength [fy].

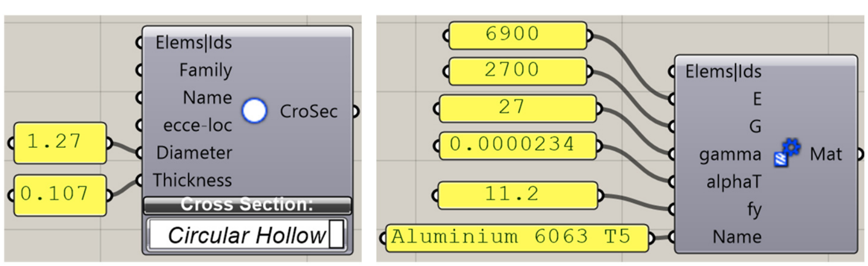

Figure 6.3 *Cross-sections and material properties.*

The resulting total mass of the structure is ≈ 3.37kg, obtained from the linked scissors but not the joints. Two main load situations are evaluated: under gravity and a point load of 0.178kN, considering the second-order theory [Th.II] via the AnalyzeThII-component. It is based on small displacements and computes axial forces through the element's geometric stiffness matrix: for beams, compressive forces decrease the element stiffness, and tensile forces increase its bending stiffness (Preisinger, 2016).

Model performance under symmetric load conditions is calculated in Figure 6.4 and Figure 6.5.

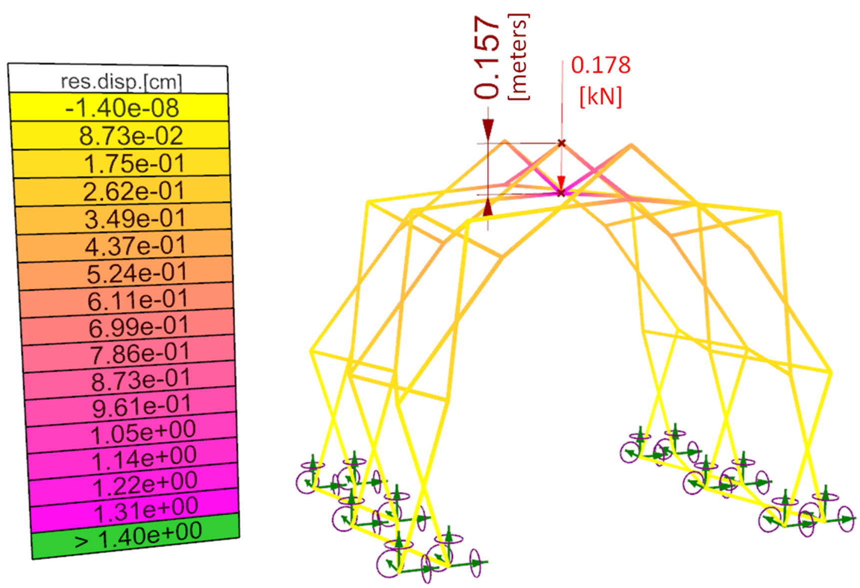

Figure 6.4 *FE model deflections under symmetric loading.*
Note: The colour range indicates Yellow for low displacements and Magenta for high displacements.

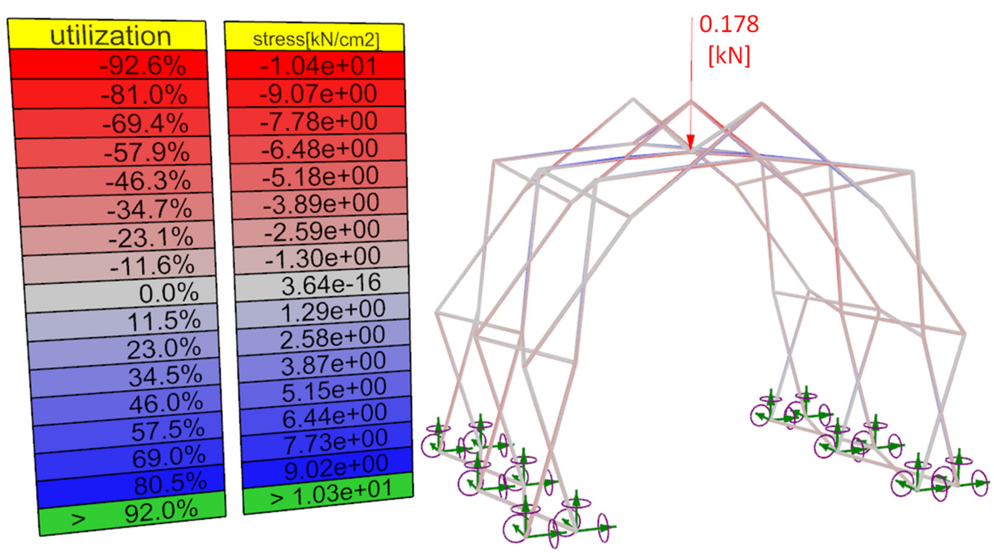

Figure 6.5 *FE model utilisation and stresses under symmetric loading.*
Note: The colour range indicates Red for compression and Blue for tension.

On the other hand, asymmetric load conditions are calculated according to Figure 6.6 and Figure 6.7:

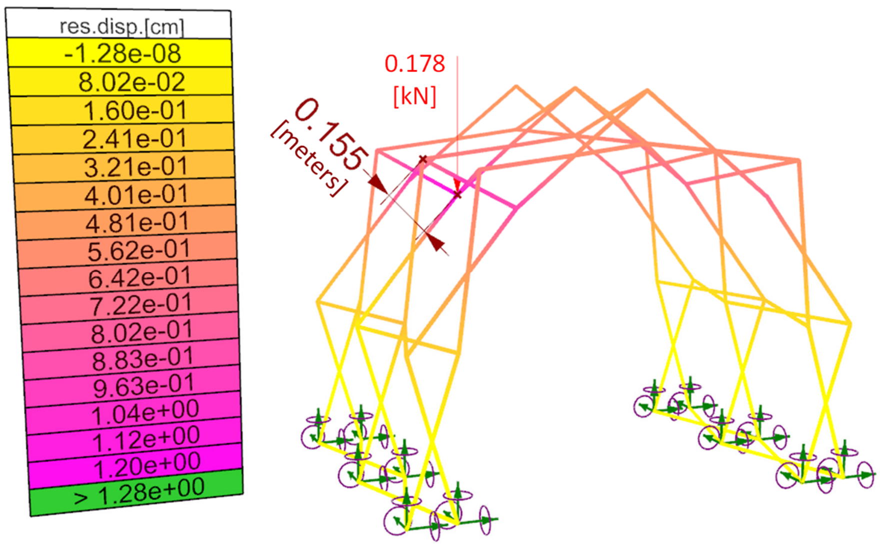

Figure 6.6 *FE model deflections under asymmetric loading.*
<u>Note:</u> The colour range indicates Yellow for low displacements and Magenta for high displacements.

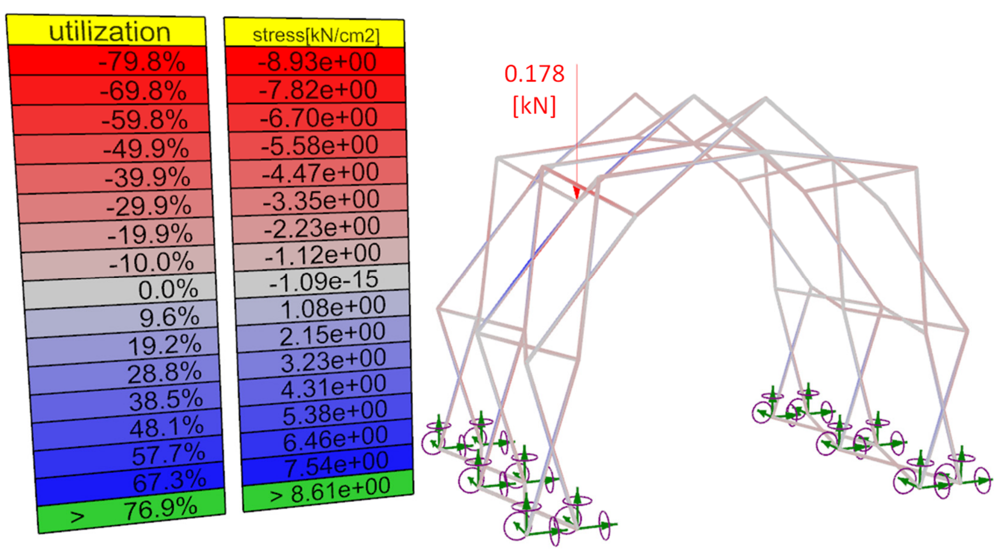

Figure 6.7 *FE model utilisation and stresses under asymmetric loading.*
<u>Note</u>: The colour range indicates Red for compression and Blue for tension.

6.2.2 Scale model conditions and results

In contrast to the FE model, the experimental scale model requires connectors with actual geometry and dimensions. The main arch beams are linked through pin-joints at the end nodes; however, it was decided to add sufficient joint-eccentricity for the transversal scissors only. Since an infill of 40% in a triangular pattern on the PLA printing parameters was employed, the mass calculation is negligible from the total.

Figure 6.8 incorporates supplementary beams below the structure to lock the main curvature extension; hence, the structure cannot suffer longitudinal displacements or rotations at the supports under the designated loads. To recreate the fixed-joint foundations and site preparation on real scenarios, anchors or counterweights should be analysed.

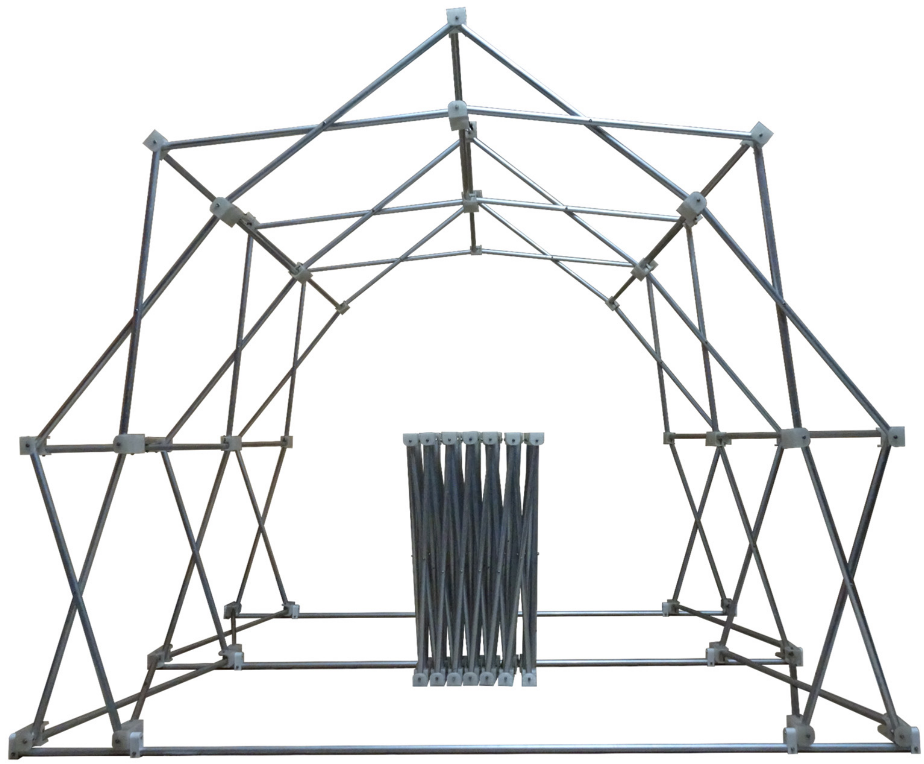

Figure 6.8 *Experimental scale model matching the FE initial design variables.*

Eight units of 5lb cast-iron disks are the point loads for testing [0.178kN or 40lbs], as specified in Figure 6.9. Although a high material utilisation was projected for the symmetric load, the feasibility of withstanding the elastic limits' stresses avoided plastic deformations or collapsing.

On the other hand, the data collected in Figure 6.10 are satisfactory. A small percentual difference between models can be attributed to the non-zero dimensions of the joint nodes in the scale model, the relative flexibility of the plastic material, and fabrication or assembly imperfections owed to joint stiffnesses variations over the whole structure, when compared to the theoretical conditions of the FE model.

The finite element model predictions can be improved if the representative value of the spring hinges stiffnesses is further calibrated to 1-1 prototypes under self-weight only. This can be measured using Digital Image Correlation and Tracking [DIC], as demonstrated by Alegria Mira, et al. (2014).

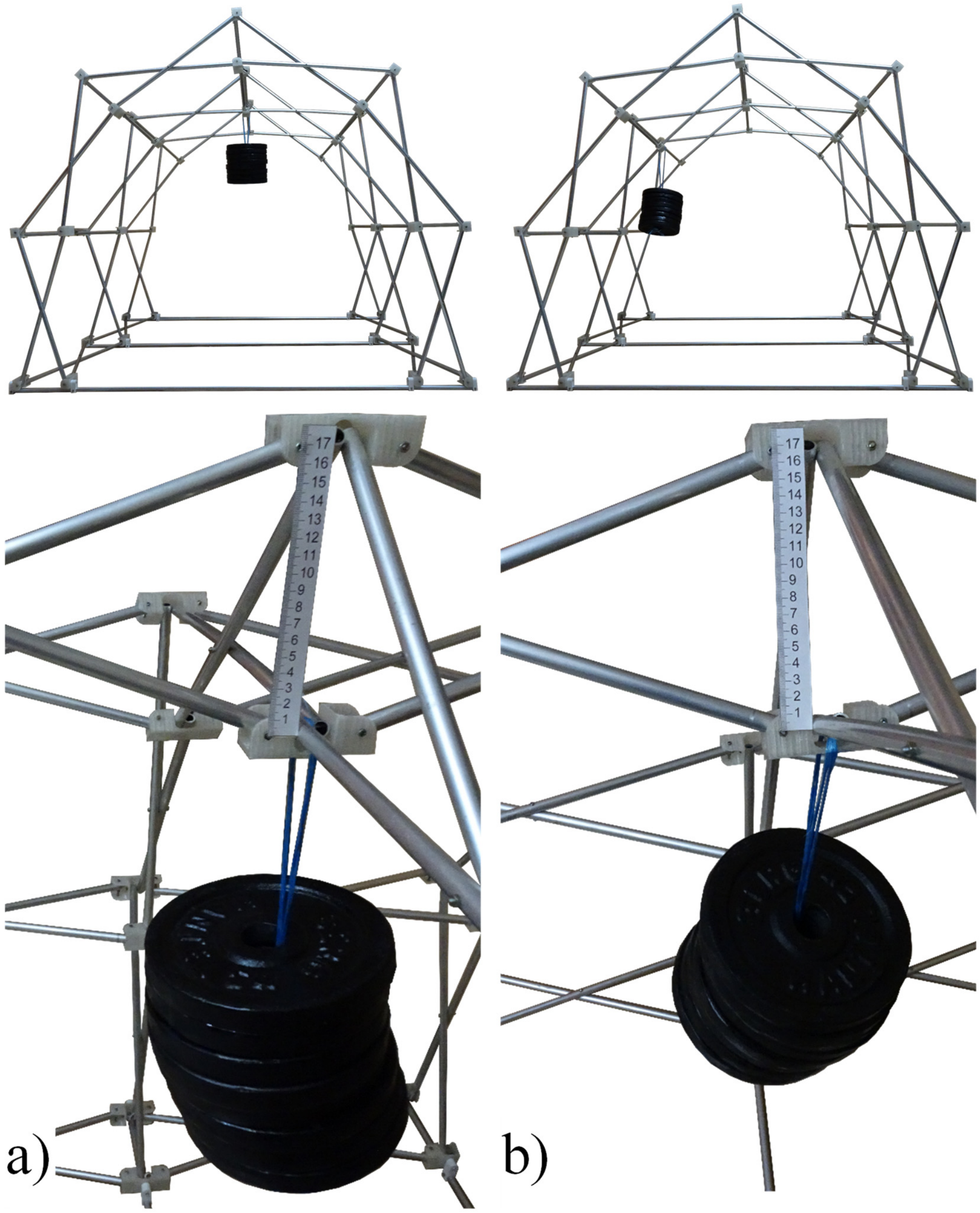

Figure 6.9 *Experimental scale model load deflections: (a) symmetric, (b) asymmetric.*

	FE deflection [m]	*Experimental deflection [m]*	*Difference [%]*
0.178 kN Symmetric	0.157	0.168	7.01
0.178 kN Asymmetric	0.155	0.167	7.74

Figure 6.10 *Comparison of FE and experimental maximum deflections.*

6.3 Conceptual design combining case studies 1, 3 and 4

6.3.1 Geometry definition

The prior structural predictions with Karamba 3D provided sufficient confidence to analyse complementary parameters on a larger model. Multiple scissor types and bar lengths are ordered in Figure 6.11, which references the approximated design dimensions in the open configuration.

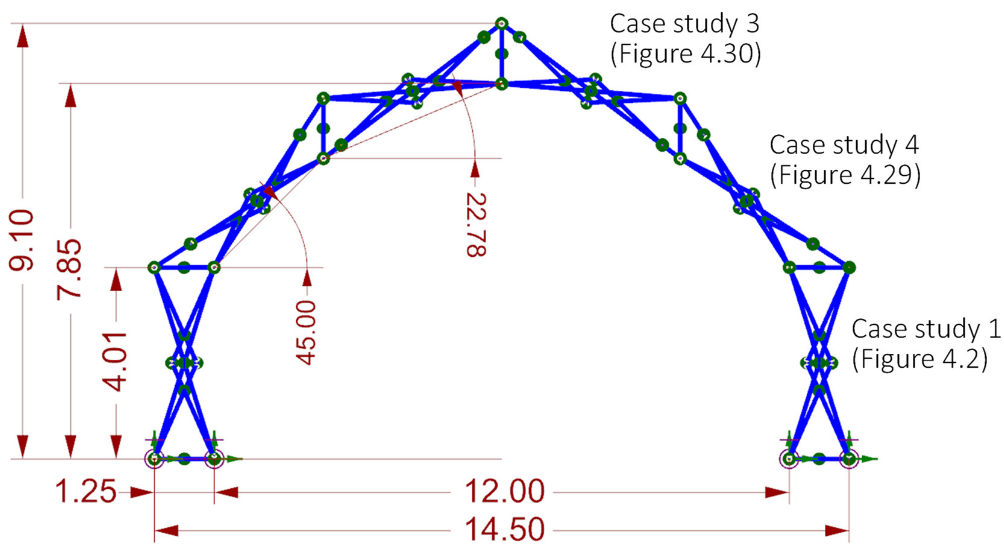

Figure 6.11 *Synclastic structure combining case studies 1, 3 and 4.*

<u>Notes:</u> 1) Dimensions in meters; beams are represented in Blue and connections by Green circles.
2) The projected span value corresponds to 14.5 meters and the transversal length 8.02 meters.

The combination of regular polar or curved-translational scissors produce arches with superior intermediate expansion phases to the operational span; this factor can directly influence the construction planning, not only because of the necessary surface area. The transformable procedure has great importance, since the geometrical and structural attributes could produce higher stresses than the wind load requirements once the construction is fully installed and locked. Likewise, the geometry can adopt incompatible positioning during movement, compromising the correct load distribution and increasing the failure risks (Hernández, 1999, p. 32).

In line with this study goals, stress-free structures have the advantage of simplifying parametric FE check-ups on different movement positions. Under self-weight, alternative installation procedures can be compared, and for the erected geometry, multiple load estimations according to the Eurocodes. The following examples compare diagonal stabilisation by scissors or passive cables, and estimates active cables as a tensioned-locking device resource. Although the data will not converge to a final design, the pre-dimensioning sets a structural equivalency and serves to identify critical conditions that might be prone to future optimisation processes.

Main elements are created as follows [Figure 6.12 and Figure 6.13]:

• Circular hollow beams cross-section: 13.97cm diameter, 0.23cm wall thickness, and aluminium 6061-T6: 6900kN/cm2 Young's Modulus [E], 2700kN/cm2 Shear modulus [G], 27kN/m3 Specific weight [gamma], 0.0000234 Coefficient of thermal expansion (1/C°) [alphaT], 24.5kN/cm2 Yield strength [fy].

• 0.015kN vertical point loads are set on each joint as a representative weight value.

	FE model with diagonal scissors	**FE model with diagonal cables**	***Difference [%]***
	Units		
Beams	160	64	*250.0*
Joints	114	42	*271.4*

Figure 6.12 *Quantification of beams and joints.*

• A preinstalled membrane of 600g/m^2 is considered for the roof and the sidewalls; however, its structural interference is omitted. The weight is obtained by a Mesh Load at the open configuration and calculated as hanging points to the lower joints of the scissors. The collected data is manually transcribed as Point Loads for the mobility inspection instead of a mesh geometry, to avoid possible inaccuracies due to variability on dimensions [i.e., the mesh simplification does not have physical properties to produce sagging on the covering membrane].

• A traditional diagonalisation is evaluated through Passive Cables to compare the case studies configuration. A **Pfeifer PG20** Spiral Strand DIN EN 12385, GALFAN-coated is chosen (PFEIFER Holding GmbH & Co. KG, 2015). In Karamba, a circular hollow cross-section: 1.41cm diameter, 0.705cm wall thickness approximates an initial rigid rod, and later the bending stiffness is deactivated by the Modify Element component, thus turning beams into truss elements [i.e., in trusses only axial forces are transferred]. Material properties were customised as follows: 16000kN/cm2 Young's Modulus [E], 6666.6kN/cm2 Shear modulus [G], 78.5kN/m3 Specific weight [gamma], 0.000012 Coefficient of thermal expansion (1/C°) [alphaT], 69.807kN/cm2 Yield strength [fy]. The last value was standardised from a limit tension of 109kN, the resulting normal force and the utilisation factor under determined loads of the FE model.

• Tension locking devices are evaluated as Active Cables & pulleys, to provide supplementary positioning control. The continuous conceptual cable is simplified as discrete fragments, connecting upper and lower scissor nodes in the FE model. A **Pfeifer PG25** was created by an equivalent procedure to passive cables, but it integrates a circular hollow cross-section: 1.7cm diameter, 0.85cm wall thickness and a 69.61kN/cm2 Yield strength [fy]. This value was calibrated from a limit tension of 158kN, the resulting normal force and the utilisation factor under determined loads.

	FE model with diagonal scissors	FE model with diagonal cables	*Difference [%]*
	Mass [kg]		
Beams	1441.2	720.5	*200.0*
Joints	174.4	64.2	*271.4*
Roofing membrane & sidewalls	198.8	198.8	*N/A*
Passive cables [Diagonal stabilisation]	N/A	167.6	*N/A*
Mass Subtotal [kg]	***1814.4***	***1151.2***	***157.6***
*Active cables *[Tensioned locking devices]*	*153.9*	*153.9*	*N/A*
MASS TOTAL [kg]	***1968.3***	***1305.1***	***150.8***

Figure 6.13 *FE model mass indicators.*

An examination of diverse tensioned locking device outlines in Karamba resulted in enhanced structural performances under the given load cases. The best combination was tested on a scale model [Figure 6.14], and although a continuous cable could be installed at each main arch, pulleys are prevented from getting stocked by dividing the forces.

During the deployment analysis by the second-order theory component, the upper limit of displacement increments from one iteration to the next was set to 1 [“RTol”]. At the open configuration, the Tension/Compression Eliminator component was added to prevent incorrect cable conditions.

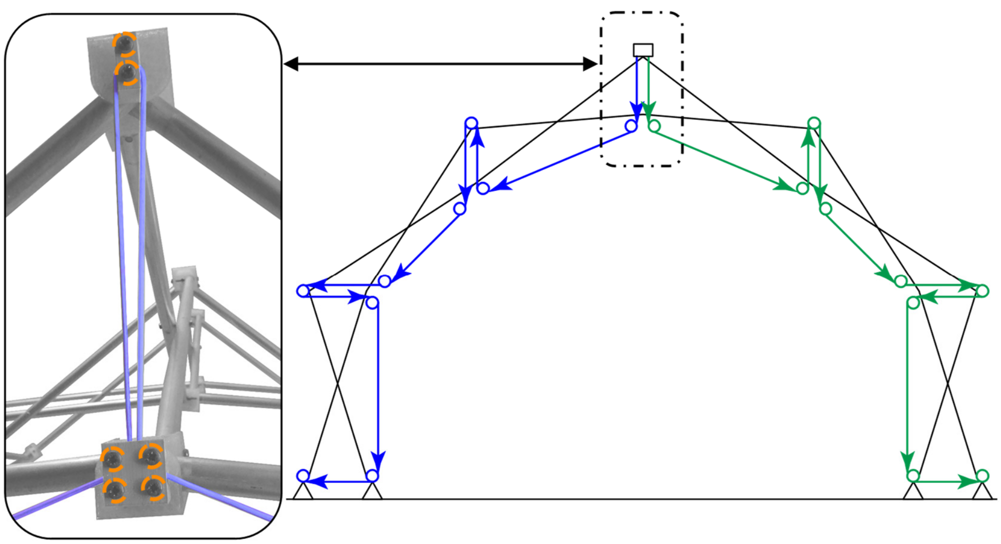

Figure 6.14 *Tension locking devices outline.*

6.3.2 Deployment at the ground level

As the starting point, six-wheeled platforms are defined in the model to indicate a hypothetical movement scenario under self-weight. Since the conceptual evaluation occurs by abstracting a sequence of fixed steps, no translations exist on the supports; however, rotations are allowed to establish the relative motion between linked scissors to the platform.

In the conversion from folded to open, it could be observed that the structure has a progressive surface expansion with a low height throughout the first half of the deployment. Afterwards, there is a contrasting transition in which the arch starts to rise verticality, and whereas the length has permanent dimensional increases, the span is reduced. This means that the wheeled platforms can be pulled outwards at the beginning, but nearing the maximum expansion at midway deployment, the structure is highly cantilevered and therefore critical stresses are obtained, as shown in Figure 6.15.

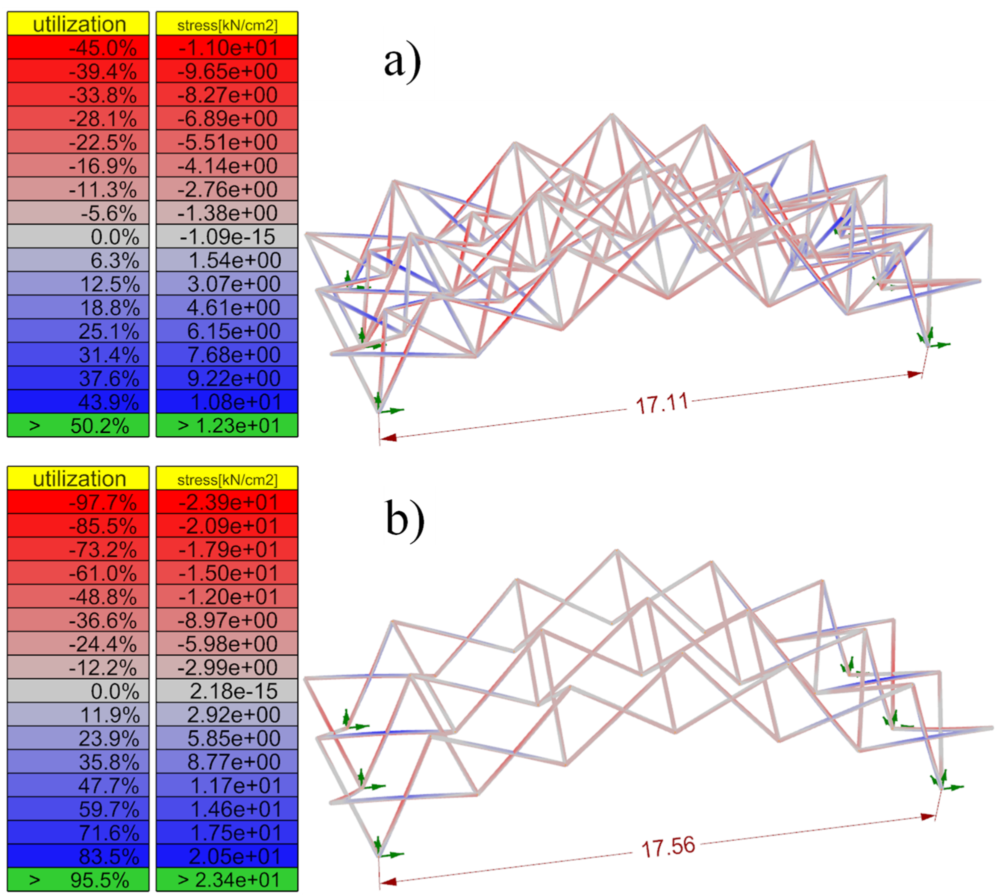

Figure 6.15 *Deployment at the ground level: (a) FE model with diagonal scissors, (b) FE model with diagonal cables [not shown].*

<u>Notes:</u> 1) The colour range indicates Red for compression and Blue for tension.
2) The models incorporate point loads [weights] for the membrane and cables.

Figure 6.16 summarises the FE model results, which are based on the second-order theory calculations [AnalyzeThII-component]; by contrast, it is worth remarking that first-order theory calculations [AnalyzeThI-component] produce lower deflections, utilisations and stresses, as the influence of axial forces is neglected (Preisinger, 2016).

This aspect is especially important for assessing the mechanism installation from the ground level; for instance, in the comparison proposed by Alegria Mira, et al. (2014) the experimental data produced larger vertical deflections than FE predictions during critical deployment phases. Besides, as terrain irregularities and climatic conditions could affect the structural exposure during movements, they should be considered part of future investigations to preserve the correct functioning.

	FE model with diagonal scissors	**FE model with diagonal cables**	***Difference [%]***
Critical positioning under self-weight [m]	17.11	17.56	*N/A*
Deflection [m]	0.42	0.759	*-0.447*
Utilisation [%]	50.2	95.5	*-0.474*

Figure 6.16 *Comparing FE model results for deployment at the ground level.*

Combining case studies 1,3,4 into the current arrangement produces a parabolic arch in which the final height is greater and the span less than a circumference arch. Modules in contact to the ground need to rotate 90° from the compact to the unfolded state, in a similar manner to the scale model on section 6.2.2. An update incorporated 3D printed accessories to reduce friction and manually activate the second half of the deployment by cables and pulleys.

Bearing in mind that the scale model material has sufficient strength to resist the tension of the pulleys, different scissors and nodal positions were tested. The adopted results are illustrated in Figure 6.17:

• The first half of deployment simply requires pulling out the compacted geometry, by applying minor efforts. [Figure 6.17a].

• Before the maximum critical expansion, a pulley is placed at the outer node of one of the arch sides for activating the necessary force that begins the elevation [Figure 6.17b].

• Instead of concentrating the stresses on a single point and right after the prior step, a new horizontal tied cable can significantly ease the task, by retracting the arch span and increasing the height [Figure 6.17c]. In the final position, the structure is ready to be locked.

Similar procedures have been proposed by Carlos Hernández (1999) and Rodrigo Ramos (2013); for this study, force distribution mainly implies the capacity of the scissors linked to the wheeled platforms. Other low-cost options by manual lifts can be used if the maximum height and weight capacities are appropriate, or by vertically pulling the structure from a mobile scaffold tower, which can later be used for manual locking.

a)

b)

c)

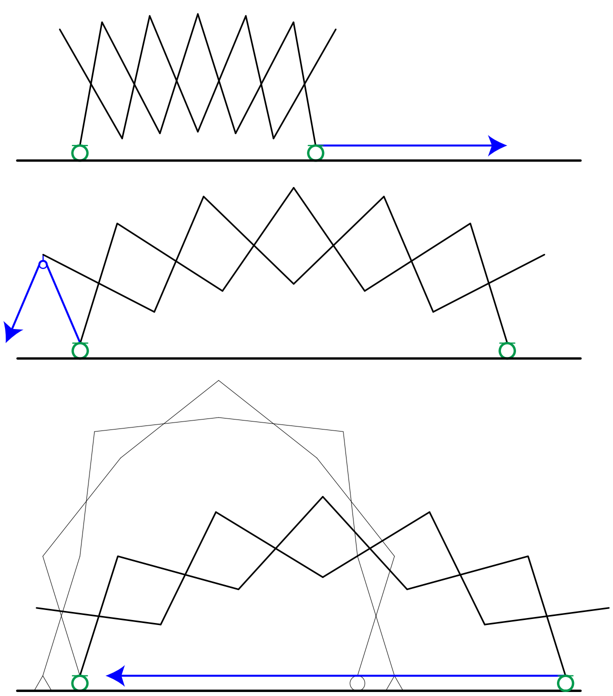

Figure 6.17 *Manual pulleys procedure based on the scale model described in section 6.2.2.*

The total mass of steel designed structures can be 3 times greater if compared to those made of aluminium. For this reason, additional complexities and stresses will occur during the deployment and reversibility processes at the ground level.

6.3.3 Deployment utilising a crane

To assist the decision-making process, representative prior art experiences of large deployable structures employing a crane are indicated:

• According to the project *ESTRAN 1* publications, the installation preserves the structure hanged throughout the transformation by a connecting hook at the top of the central arch, and a workman is required to keep the central arch alignment, as the method to prevent lateral instabilities is solely by tensioned cables in the final position (Hernández, 1999; Hernández & Cebrian, 2010). The procedure can be carried out with a crane and five operators in a few minutes (Hernández, 2014). However, even for these situations, the resulting stress on the scissors might be higher than wind loads once the structure is in service (Hernández, 2013).

• On the Sao Paulo's Olympic swimming pool, the conceptual process to hang the structure was from the lower scissor nodes, in this way, the mechanism tends to open by gravity, and forces are used to overcome the existing incompatibilities. Due to the project magnitudes and the cantilevers nearing the final position, four connectors were not acceptable; instead, eight hanging points were required (Pérez Valcárcel, 2014).

A brief test in the scale model from section 6.1.2 corroborated that a single hanging point at the top of the central arch creates a smooth deployment. However, since concentrating the structure cantilevered efforts may not be adequate, it iwas decided to test four hanging supports in the FE model for comparing purposes.

Taking by reference the third central part of the arched geometry of section 6.3.1, a group of four lower nodes can be interconnected to a crane by structural wire ropes having the same dimensions. By fixing the supports' translation capacity, different hypothetical deployment steps were evaluated; the most critical positioning for each case is depicted in Figure 6.18:

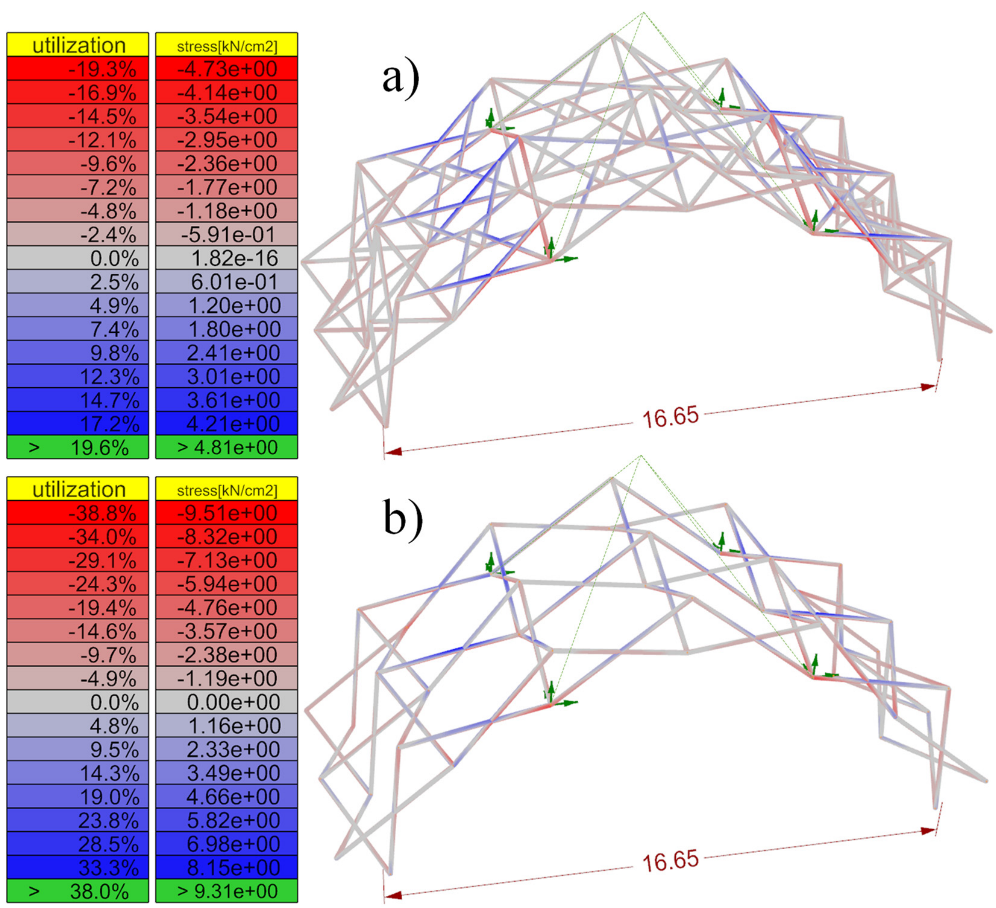

Figure 6.18 *First conceptual evaluation on hanged structures deployment: (a) FE model with diagonal scissors, (b) FE model with diagonal cables [not shown].*

Notes: 1) The colour range indicates Red for compression and Blue for tension.
2) The models incorporate point loads [weights] for the membrane and cables.

Figure 6.19 shows an equivalent possibility, but selects the adjoining group of four upper nodes. In contrast to the prior result, the FE model with diagonal scissors produces less favourable positions. Nonetheless, all hanged scenarios exhibit a better structural response to deployment than those at the ground level.

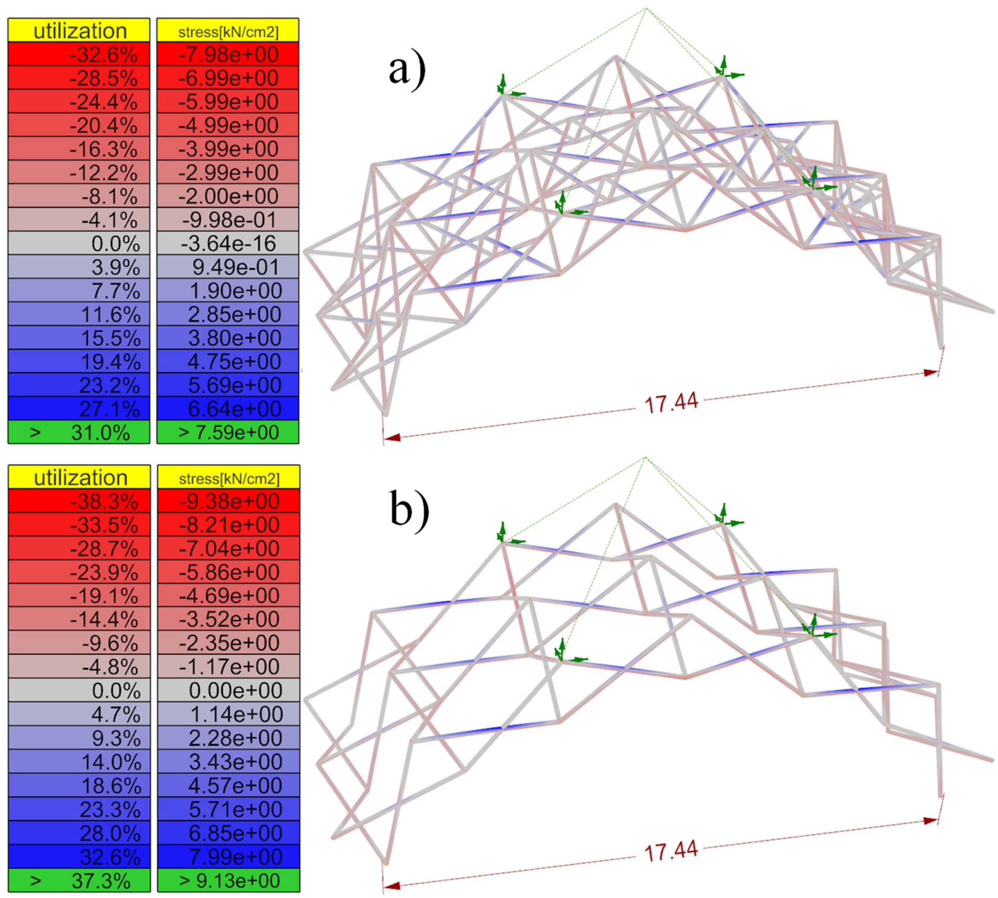

***Figure 6.19** Second conceptual evaluation on hanged structure deployment: (a) FE model with diagonal scissors, (b) FE model with diagonal cables [not shown].*

Notes: 1) The colour range indicates Red for compression and Blue for tension.
2) The models incorporate point loads [weights] for the membrane and cables.

The ease of mobility in the scale model was also tested by recreating both projected possibilities. The design criteria can determine the lower or upper membrane position and the best installation procedure:

- The four lower connection points require a minimum impulse in the opposite direction of the compacted form, to allow gravity to act on deploying the structure. During the process of pulling back the geometry, there would be no need for a crane, but in this circumstance, the system will gradually fall to the ground level and rest in the most critical position, indicated in Figure 6.15. If the hanging points are maintained instead, the structure can be retracted employing cables and only lowered at the end.

- The four upper connection points tend to contract the structure, and there is a need to pull the geometry outwards by connecting additional cables to the external-upper nodes between arches. Since the frame is hanged, the required force could be managed from the ground; nevertheless, the installation technique requires control. If the hanging points and an elevated crane positioning are maintained during dismantling, the force of gravity can be used to close the structure safely.

6.3.4 Estimations at the open configuration

Although this study does not consider specific counterweight or anchoring calculations, determining the correct manner to secure the structure to the ground is a crucial factor. An ideal condition would be to properly remove all rotational and translational degrees of freedom from the supports.

With the aim of reducing installation time and labour complexity, the membrane has been incorporated at all geometry phases. The FE model with diagonal passive cables is created for conceptual evaluation purposes, maintaining the nodal distances at the deployed position, but not pretension. Supplementary active cables and pulley systems are estimated to be properly locked from the ground, eased by an axial strain of -1mm/m [prestress] to improve the structural performance of the main arches.

Results from different load cases evidenced the most critical conditions by combined transverse winds and snow: drifted arrangement. Comparative models with diagonal scissors and cables are depicted in Figure 6.20 and Figure 6.21. Correspondingly, an overall evaluation is summarised by the charts in Figure 6.22 and Figure 6.23.

Suppose the structures are fixed to the ground, and only lateral stabilisation methods are considered; in that case, unfavourable deflections, excessive stress and eventually, the scissors beams might be exposed beyond their capacities under the designated loads. These are imposed variables by the design criteria, the scale, the severe climatic conditions creating internal/external pressures, in addition to vertical loads; however, the initial data collection is a practical manner of predicting each case's structural performance tendencies.

As the parametric modelling allows for improving these results, a first option would be changing the material properties from the software library. Instead, tensioned-locking devices assessed the second-selected option, bearing in mind that opposed to permanent structures, the significant number of moving parts in stress-free scissors are often required to be manually locked to prevent shifting out of position.

Drastic improvements fulfilling the Eurocodes required deformation limit of $\delta < L/250$ were obtained for both cases.

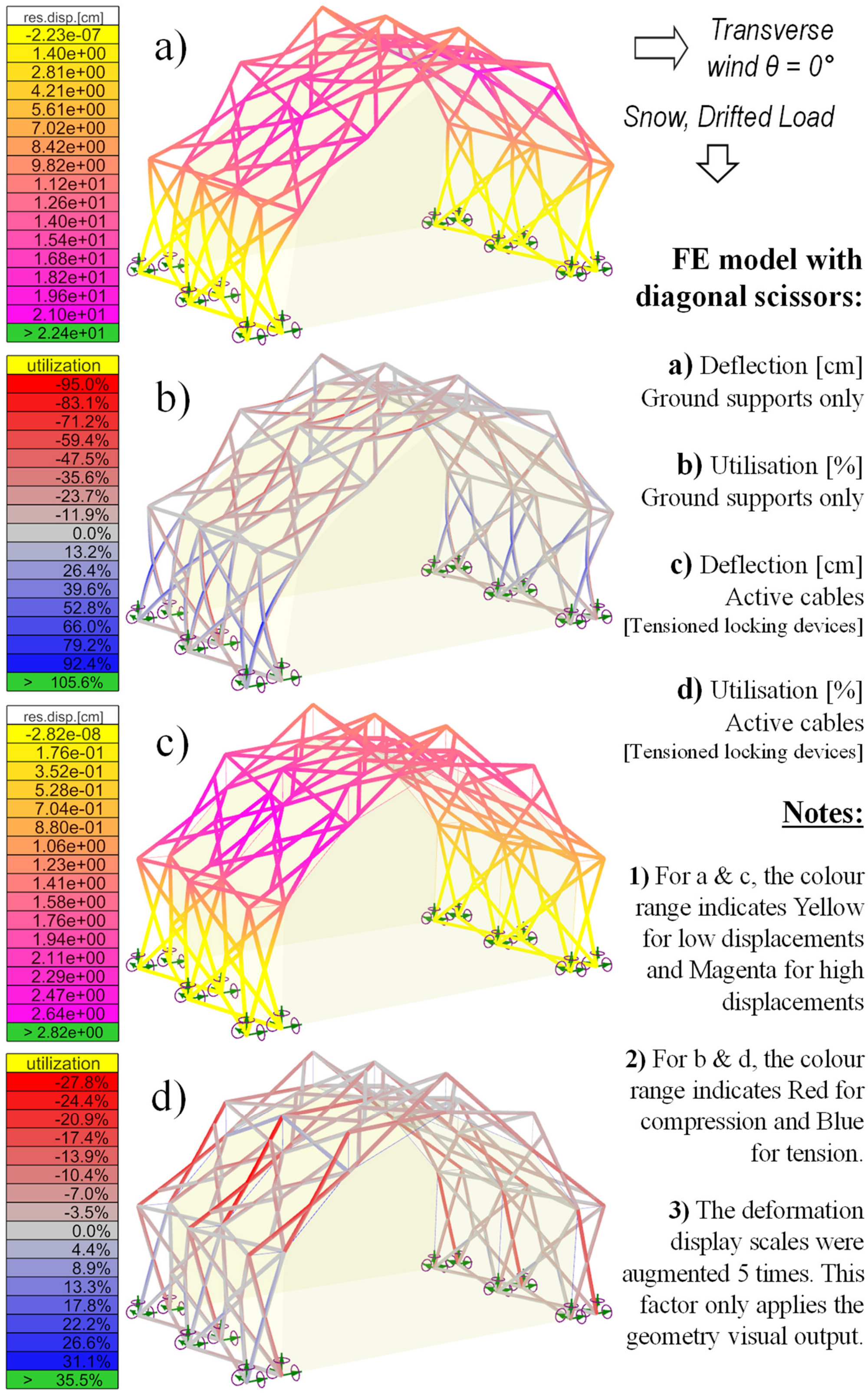

Figure 6.20 *Critical estimations at the open configuration: FE model with diagonal scissors.*

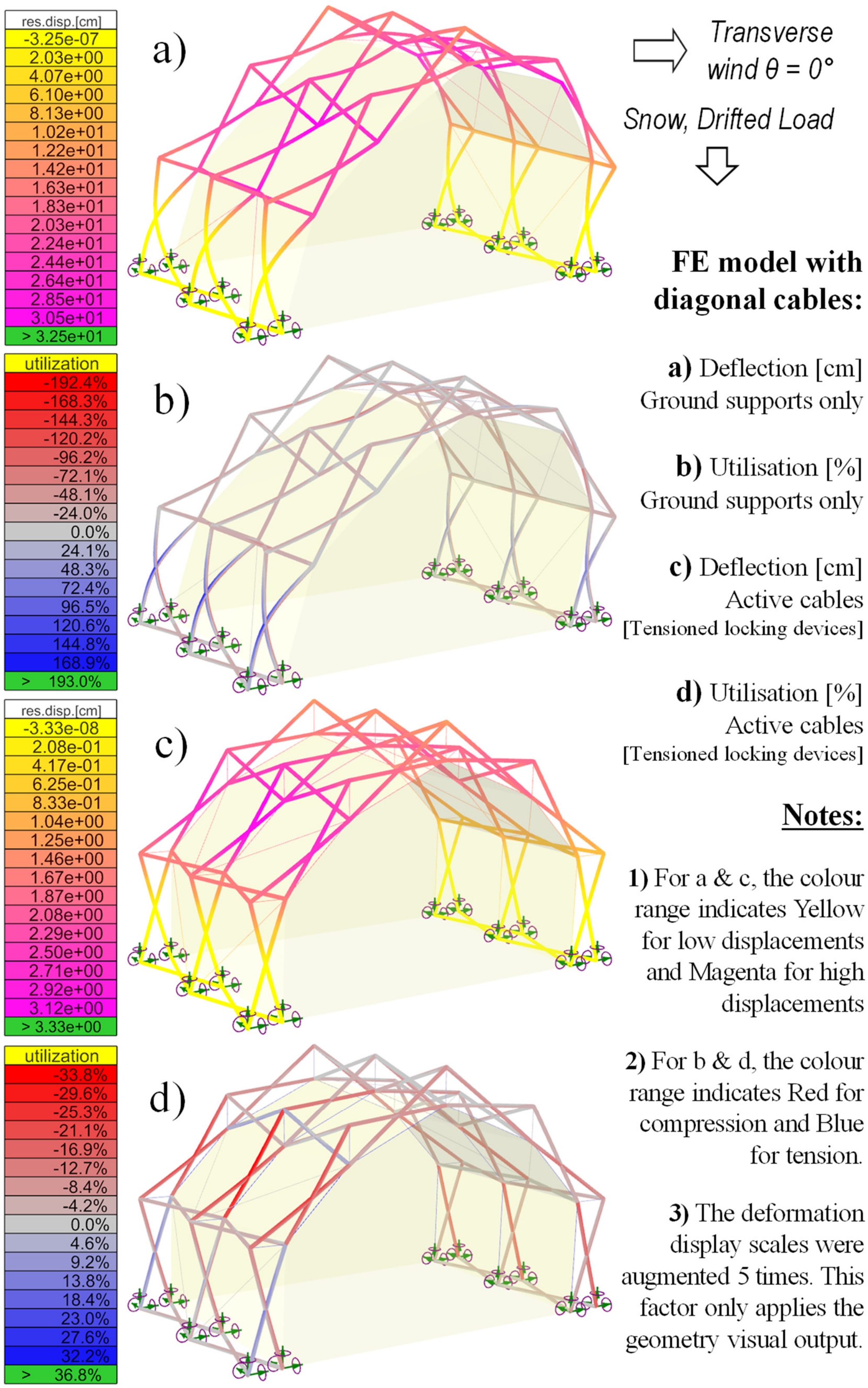

Figure 6.21 *Critical estimations at the open configuration: FE model with diagonal cables.*

Diagonals with scissors	*Deflection [m]*	*Resulting deflection value:* $x = \frac{span_{12[m]}}{deflection_{[m]}}$	*Total Utilisation [%]*	*Cable Utilisation [%]*
Transverse wind				
Ground supports only	0.199	60.3	-92.9 104.1	N/A
& active cables [Initial axial strain **-1** mm/m]	0.028	422.2	-26.0 40.3	**40.3**
Transverse wind + Snow, drifted load arrangement				
Ground supports only	0.224	53.6	-95.0 105.6	N/A
& active cables [Initial axial strain **-1** mm/m]	0.028	425.5	-27.8 35.5	**35.5**
Snow, undrifted load arrangement				
Ground supports only	0.077	156.7	-44.0 37.7	N/A
& active cables [Initial axial strain **-1** mm/m]	0.005	2660.8	-12.3 20.4	**20.4**
Snow, drifted load arrangement				
Ground supports only	0.144	83.3	-81.1 71.9	N/A
& active cables [Initial axial strain **-1** mm/m]	0.009	1369.9	-15.8 19.7	**19.7**
Longitudinal wind				
Ground supports only	0.075	160.9	-62.1 71.5	N/A
& active cables [Initial axial strain **-1** mm/m]	0.010	1181.1	-15.3 27.4	**27.4**
Longitudinal wind + Snow, drifted load arrangement				
Ground supports only	0.121	99.4	-90.9 77.4	N/A
& active cables [Initial axial strain **-1** mm/m]	0.015	786.4	-21.8 26.2	**26.2**

Figure 6.22 *Summarised evaluation: FE model with diagonal scissors and a lower membrane.*

Notes: 1) The coloured numbering indicates Red for compression and Blue for tension.
2) Active cables can be incorporated as a tensioned-locking device resource.

Diagonals with passive cables	*Deflection [m]*	*Resulting deflection value:* $x = \frac{span_{12[m]}}{deflection_{[m]}}$	*Total Utilisation [%]*	*Cable Utilisation [%]*
Transverse wind				
Ground supports only	0.287	41.7	-188.6 200.8	**41.5**
& active cables [Initial axial strain **-1** mm/m]	0.034	352.7	-31.9 43.7	**43.7**
Transverse wind + Snow, drifted load arrangement				
Ground supports only	0.325	36.9	-192.4 193.0	**26.1**
& active cables [Initial axial strain **-1** mm/m]	0.033	363.6	-33.8 36.8	**36.8**
Snow, undrifted load arrangement				
Ground supports only	0.130	92.3	-82.6 78.7	**6.6**
& active cables [Initial axial strain **-1** mm/m]	0.005	2434.1	-12.2 20.9	**20.9**
Snow, drifted load arrangement				
Ground supports only	0.251	47.7	-177.4 171.7	**15.6**
& active cables [Initial axial strain **-1** mm/m]	0.009	1321.6	-15.8 19.2	**19.2**
Longitudinal wind				
Ground supports only	0.088	136.2	-61.8 48.6	**38.2**
& active cables [Initial axial strain **-1** mm/m]	0.023	511.3	-23.8 31.3	**31.3**
Longitudinal wind + Snow, drifted load arrangement				
Ground supports only	0.266	45.0	-157.1 115.9	**58.1**
& active cables [Initial axial strain **-1** mm/m]	0.028	426.7	-29.8 31.9	**31.9**

Figure 6.23 *Summarised evaluation: FE model with diagonal cables and lower membrane.*

Notes: **1)** The coloured numbering indicates Red for compression and Blue for tension.
2) Active cables can be incorporated as a tensioned-locking device resource.

6.4 Discussion on conceptual designs

Introductory stress analysis for deployable tent structures showed the importance of securing the mechanism to become an effective load-bearing structure. In agreement with the installation overview, single curvature geometries with a quadrangular base benefit particularly from lateral stabilisation methods against longitudinal winds, but also throughout the typical kinetic phases of expansion or dismantling, since on large scales uncontrolled deformations can cause permanent damage.

Suitable strength and stability are added by counteracting other directions at the open configuration. Active cables and pulley systems throughout the lower arch nodes, plus the upper and lower scissor node connections were suggested for locking the vertical snow and transverse wind actions, thus significantly increasing the structural capacities on the weakest geometry spanning direction.

As the FE models incorporate one-dimensional hinges and joints through zero-length springs, imperfections are not accurately calculated. In Alegria Mira, et al. (2014) the correlation to an experimental prototype was specified, with the influence of the joint stiffness for the correct assessment of deployable scissor arches commented on specifically; however, determinants cannot be generalised, as the possible components maladjustments, manufacturing tolerances and joints eccentricities depend on each project. Besides, the three-dimensionality, local deformations and friction related to the connectors certainly affect the structural performance, needing detailed inspection by future research.

Associated generalities of compactness, number of units, and weight are susceptible to modifications and optimisation processes by integrated design criteria. It would be advisable to detail the effectiveness of the different joint types from Chapters 4 and 5; the best results from the scale models were preliminarily obtained by double support at the beams pivoting sides, maintaining proper positioning of the bolts, and preventing probable maladjustments.

The study reflects a moderate weight increase of the non-triangulated tent model, as there is a need for calculating passive and active cables. On the other hand, the case studies rigidised-model can be enhanced while reducing the number of components, selecting the most suitable cross-sections and simplifying to a single diagonal or four-bars pyramidal mechanism.

In some cases, the structural out-of-positioning could be controlled by evaluating the lateral walls; a simplification could be preliminarily accomplished by cables in different directions, although this would not affect the projected material or the weight of the membrane. Another option would be to perform movement predictions by the parametric environment of Rhinoceros + Grasshopper + Kangaroo physics.

Respectively, predictions from irregular shapes based on case study 2 can follow the enounced parametric modelling & analysis methodology. As a conceptual preamble, Figure 6.24 depicts fixed-supported structures dimensioning; from the material library an aluminium EN AW-6061 t4 is chosen, rectangular beams cross-sections [7.62cm x 2.54cm x 0.14cm], and square mast/columns cross-sections [10cm x 10cm x 0.5cm].

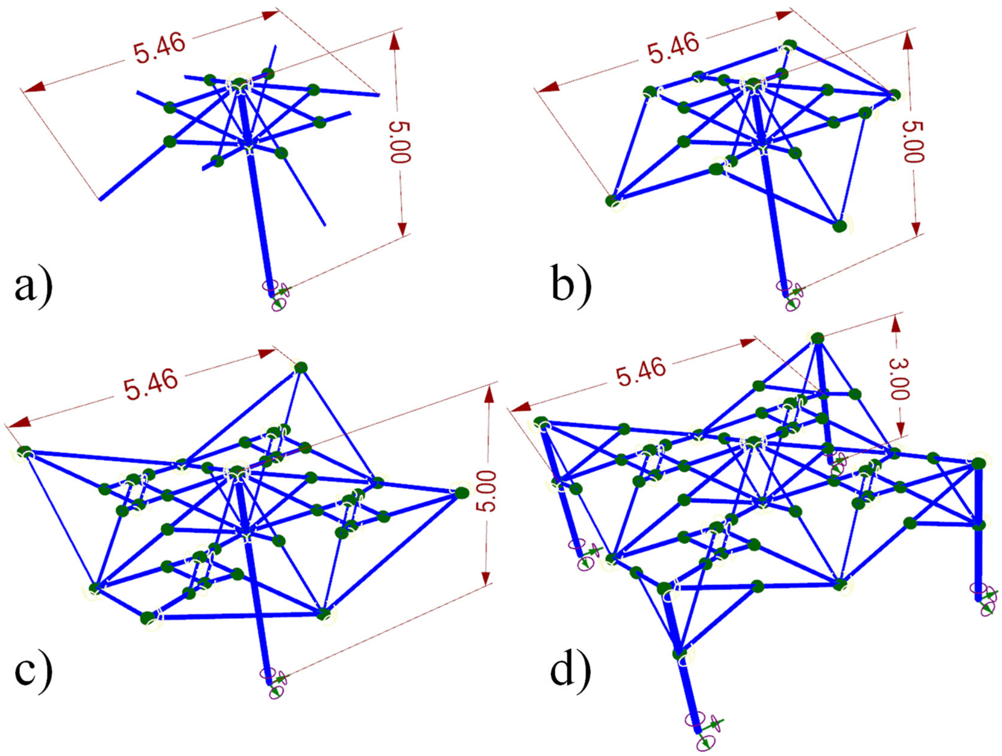

Figure 6.24 *FE model from case study 2 – initial design variables: a) non-rigidised Hypar umbrella, b) rigidised Hypar umbrella and simplified shape, c) rigidised Hypar umbrella and standard shape, d) rigidised Hypar tent and standard shape.*

A single lateral load of 0.45kN is set to register the pilot performance tendencies:

In line with the thesis hypothesis, the prior-art non-rigidised Hypar umbrella is the only model presenting a contrasting failure [Figure 6.25a]; for other rigidised Hypars, the contouring frame distributes stresses and diminishes deflections. In Figure 6.25b & Figure 6.25c, partial to moderate movement at the mast is noticeable; despite this, a torsional effect alters the outcomes and produces significant global distortions. To minimise this issue, specific design variables, such as the mast type, total height, materials, and cross-sections, should be evaluated according to load requirements.

By integrating the covering membrane, the airflow would create a dynamic behaviour beyond the considerations of this study. Additional calculations by wind tunnel tests, mast reactions, and foundations are needed to validate the effectiveness; this would promote potential applications on grander scales, as in the homologous contemporary samples from the literature review.

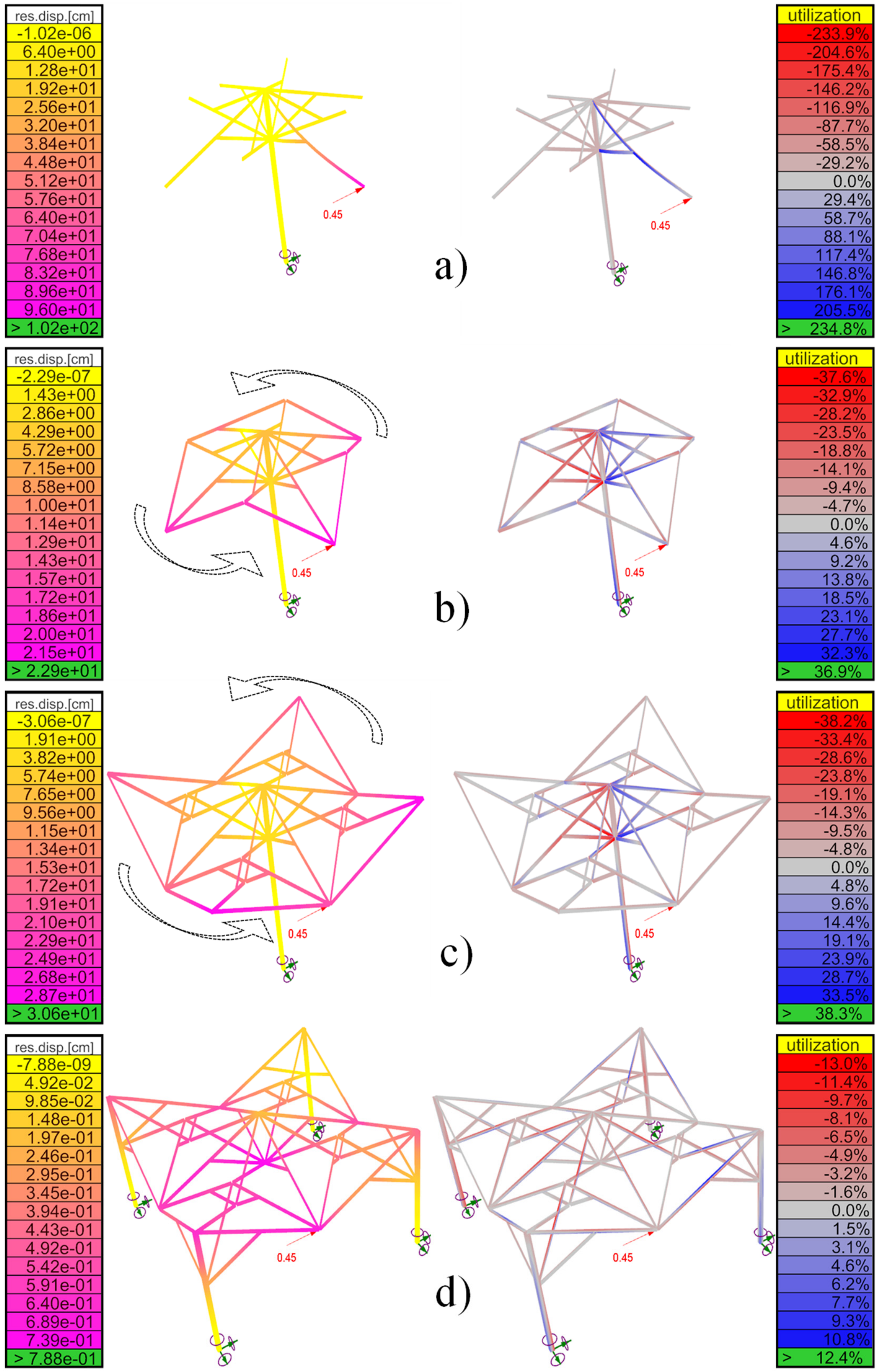

Figure 6.25 *FE models from case study 2 – deflections and utilisation: a) non-rigidised Hypar umbrella, b) rigidised Hypar umbrella and simplified shape, c) rigidised Hypar umbrella and standard shape, d) rigidised Hypar tent and standard shape.*

6.5 Chapter summary

This chapter appraised structural prerequisites derived from prospective deployable applications in architecture, evincing the components material capacities on virtual and physical models. Transportable & transformable proposals requiring transitory processes were conceptually studied, aiming to control moving out of position during the kinetic phase and when subjected to severe weather conditions.

For comparing purposes, a theoretic large-span tent having lateral stabilisation through scissors & passive cables was inspected during the mounting or dismantling process, relating a differentiated force transmission: from the ground level with human power and an elevated position with a crane. Even if theoretically the mechanism has one degree of freedom, anchored or counterweighted supports are not enough to acquire optimal strength at the operational state. Following the European building standards, a conservative deflection limit of the span divided by 250 is desirable [$\boldsymbol{\delta < L/250}$]; therefore, it was effectively suggested an enhanced outline of active cables guided by pulleys [tensioned locking devices] throughout the scissors upper and lower joints.

Additionally, a brief inspection over irregular shapes demonstrated the practicality of rigidised Hypar umbrellas or tents from case study 2. It was successfully reached the thesis closing objective of carrying out preliminary analysis methods by specialised structural engineering software; still, future detailed engineering is necessary to refine, optimise and preserve the systems integrity before implementation.

7 CONCLUSIONS

The present work sought to contribute to the evolving knowledge of *deployable structures using scissors and sliding mechanisms* by developing new ways to stabilise the angular distortions of classic quadrangular expandable grids, control deflection limits, and enhance the structural performance of large-span kinetic architecture.

Due to the system complexity, aim and objectives were brought to completion through explorative & experimental procedures, supported by recent digital modelling and fabrication technologies. Conceptual designs were assertively undertaken, prioritising virtual environments and scale models, testing the intrinsic mechanical components, the material capacities, and the constructive determinants.

By using the proposed methodology, potential outcomes were evaluated at early stages in terms of the mutual relationship between the geometry, the kinematics and the structural response:

(I) In light of the existing literature, several mechanisms were first re-created for gaining expertise in the field to a deeper level and identifying gaps in knowledge.

(II) In the parametric design environment of Rhinoceros® + Grasshopper™, it is a merit of this thesis to have simplified the geometrical logic of the ellipses theory to allow the kinetic mechanism, instead of an algorithm with specialised mathematics, complex expressions & conditionals, or by scripting and code.

(III) The size and shape alterations were effectively assessed through real-time motion simulation in Autodesk Inventor, granting elements three-dimensional definition, stress-free behaviour and a single degree of movement.

(IV) Physical testing provided a better understanding of strengths and weaknesses between case studies. The successful incorporation of 3D printing and low tech tools eased the rapid modification to enhance final proposals. Arduino-based technologies may help automate the fabrication procedure at a low cost, such as creating belt-driven or rack-and-pinion linear actuators.

(V) The limitations of mobile and temporary applications were structurally estimated in Karamba3D. A tunnel-like scissor structure ratified the ideals of strengthening the geometry through diagonal mechanisms and at the open state through added active cables & pulley systems [tensioned locking devices]. The exploration brought major serviceability against severe weather conditions following the Eurocodes, optimising the installation time and reducing the risk of working at heights. The workflow can likewise be generalised to umbrellas incorporating pantograph-sliding mechanisms.

7.1 Contributions

The primary outcomes relating to this study aims and objectives are derived from inspecting and understanding different pre-existing configurations, for obtaining the innovative alternatives in the case studies 2, 3 and 4:

- After the conceptual process of decomposing a stress-free flat deployable square from the prior art, case study 2 generates a novel 1DOF three-dimensional solution combining scissors, sliding-pantograph mechanisms, and single hinged bars. Potential constructions for transportable tents or transformable umbrellas integrating consistent double-curvature covering membrane [e.g., 3D faces or Hypars] could be defined by detailed engineering. Under the classification given by Hanaor and Levy (2001), it is a hybrid between Pantographic and Bars Double Layer Grids DLG [Figure 7.1].

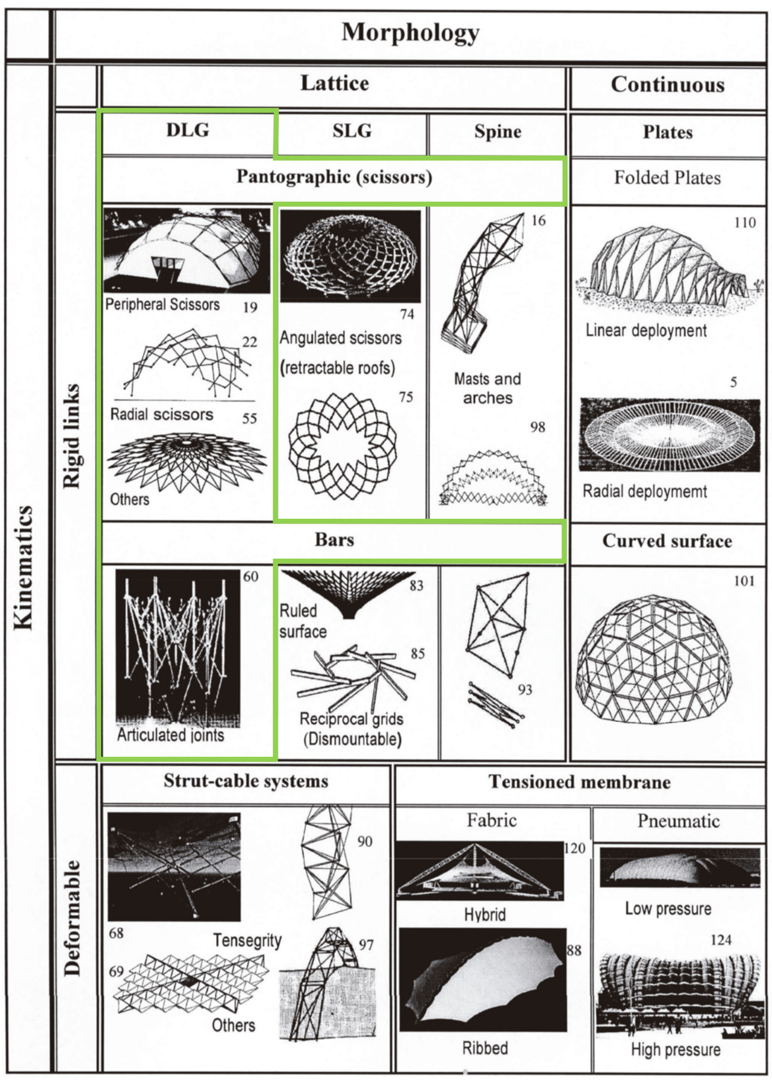

***Figure 7.1** Deployable structures classification chart. (Hanaor & Levy, 2001)*

• Complementing the prior art of an oblique quadrangular prism, and the prior art of a trapezoidal prism, case studies 3 and 4 achieved stress-free mechanical triangulations thru non-conventionally connected scissors. In agreement with the classification of singly curved scissor grids given by Roovers & De Temmerman (2014b), an updated module category might be indicated for each of the analogous configurations having a quadrangular base [Figure 7.2].

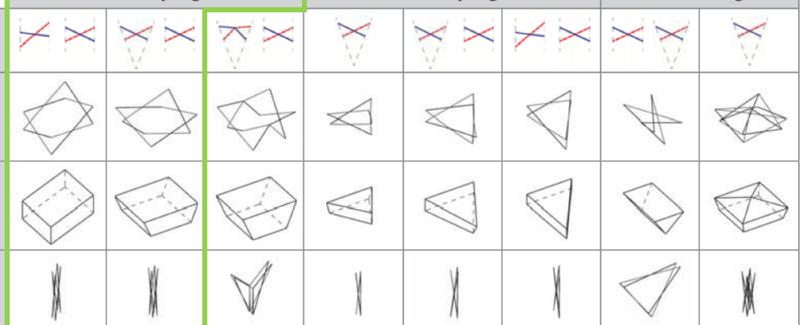

	Quadrangulated double-layer grid			Triangulated double-layer grid			Parallel linkage of linear scissor grids	
Scissor unit type(s)								
Basic module in deployed position								
Polyhedron described by basic module in deployed position								
Basic module in fully folded position								
Non-circular curvature	x	x	x		x	x		x
Deployment	foldable	foldable	foldable	incom-patible	incom-patible	foldable*	foldable*	snap-through
Needs external bracing	x	x	x					
Compactness ***	+	++	-	++	++	+	--	+
Single rod length		x		x	x			
Single joint hub	x	x	x	x	x	x**		

* Foldable if the angles between the scissor-unit planes in the grid are allowed to vary: special joint hubs required.
** Joint hub has to allow angular distortions of which the magnitude varies along the grid, thus it depends on the joint design.
*** Compactness in the stowed position, given as a scale from most compact (++) to least compact (--).

Figure 7.2 *Classification of singly curved scissor grids. (Roovers & De Temmerman, 2014b)*

On the other hand, to allow a matching mechanical and geometrical variability with the case studies 3 and 4, a stress-free flat deployable square from prior art was examined in case study 1. Consistent with the existing groupings, the membrane compatibility is corroborated for all single curvatures and is possible for reduced synclastic & anticlastic double curvatures; likewise, the rigidised perimetral frames are adequate, employing the explored arches.

Through the ellipses theory method in combination with geometrical parameters, the motion conceptualisation of deployable structures based on stress-free scissors and sliding mechanisms was simplified. Simulations by three-dimensional part assemblages proved to be an effective route to understand the evolution of the proposals, and the scale-models were fundamental for selecting potential outcomes in architecture or obtaining feedback for supplementary improvements during the study timeline. Lastly, by incorporating tensioned locking devices to the preliminary structural assessment, a remarkable positioning control for the estimated scenarios occurred; this partial result serves as the decision-making source for future detailed engineering of transportable and transformable developments.

7.2 Lessons learned

At first, a non-conventional design criteria focused on the structural morphology of scissors and sliding mechanisms was associated with the constitutive key concepts, and the motion evaluation in two-dimensions by the Grübler–Kutzbach equation. The applicability of the kinematics was analysed by virtual models, to determine the volumetry coincidence to equivalent physical scale models, the selected additive manufacturing process settings and the material selection.

The ideation phase followed an empirical workflow to define the geometry construction by a simple parametric logic sequence in Rhinoceros®+Grasshopper™. During the learning curve on the software utilisation, a time-consuming manual step by step method was performed, although with effective results on the early examination of the proposals. As in some case studies a snap-through behaviour was inherent to the geometry, alternative indications by the ellipses theory methodology can approximate stress-free diagonal scissors.

Mechanical simulations in Autodesk Inventor and 3D printing made conceptualisation of the required joints by free form possible; later, the complexity and deviations from theory to practice between models was appreciable, as in some cases imperfections can produce unwanted instabilities, slight movement tolerances and misalignments. Models with double support joints evidenced better results, and testing the needed torque on bolts-nuts [pivots] is recommended.

Beyond previous conditions, a complementary qualitative and quantitative assessment through parametric finite element models in Karamba was required, to preliminarily assess the proposal's constructability, in agreement to hypothetical climatic conditions and the Eurocodes. Despite that detailing the components of a full-scale prototype has not been implemented, partial results were contrasted to a scale model, for a preliminary calibration of the finite element model, and for the recreation of the installation procedure from the ground or a hanged position. Moreover, the feasibility of introducing cables and pulley systems was tested, to rigidise the main arches against vertical and transverse loads.

Despite the evolution of deployable structures during recent decades, evident unsolved complexities exist. Actual technologies would eventually resolve the remaining inconsistencies by major precision, without this representing a displacement of human activity by robots, as there are automated and semi-automated needs during fabrication, assembly, transportation, installation and dismantling.

Circular economy concepts are intrinsic to these models, as the building is relocatable, reusable and recyclable. In some other cases, although the global dependence on plastic is problematic, the new environmental challenges of 3D printers makes managing waste by collecting, shredding, melting and recovering filament possible.

7.3 Limitations of the study

Even if this work incrementally improved the case studies and demonstrated its competitive attributes, it was appreciated the complexity and deviations from theory to practice in models. The proposed structures' real-life applicability requires more profound analysis through full-scale prototyping and experimental testing. Accepted limitations to establish this research were: additional time for detailed engineering, fabrication labour, specialised machinery, materials lack of spaces, among other factors.

It was shown that it is possible to continue updating the construction sector with advanced technological innovations based on 1DOF deployable structures. Among the most successful scenarios, the exploration contributed to envisage planar, clastic, synclastic and anticlastic geometries. However, it was noticed that a greater number of interconnected components would create joint hypermobility [loose joints], friction issues between moving parts, and eventually differentiated torque on the bolts-nuts. These were very specialised and technically focussed aspects to be considered by this study.

7.4 Areas for future research

In addition to the enounced aspects that may require further attention [e.g., optimisation of components through detailed engineering, supplementary wind tunnel simulations, 1:1 prototyping, mounting procedures, physical testing, anchors/counterweights, compactness], the result of this thesis had a great impact on the novel outcomes from the case study 2, and agrees with this reasoning:

"*Overconstrained mechanisms give a kinematic advantage over regular mechanisms in the sense that their mobility is only given within specific geometric bounds. This means that unexpected degrees of freedom due to slight material deformations are less common in them, making them more reliable, particularly for 1DoF mechanisms. This is also the reason why the most successful deployable structures are based on overconstrained mechanisms, giving them more controllability on the kinematic level"* (Bouten, 2015, p. 84)

Even if the case study 2 outcomes emerged by a quadrangular module of case study 1, equivalent geometrical variants on polygonal patterns and pantograph reinforcement are estimated as achievable [e.g., hexagonal; octagonal; as the complement of former studies by Calatrava (1981)]. In Figure 7.3, complementary hexagonal modules are depicted; alternative research might calculate stress-free mechanisms or reduced snap-trough structures by the ellipses methodology employed in case study 6 & 7 [Figure 4.37 & Figure 4.39].

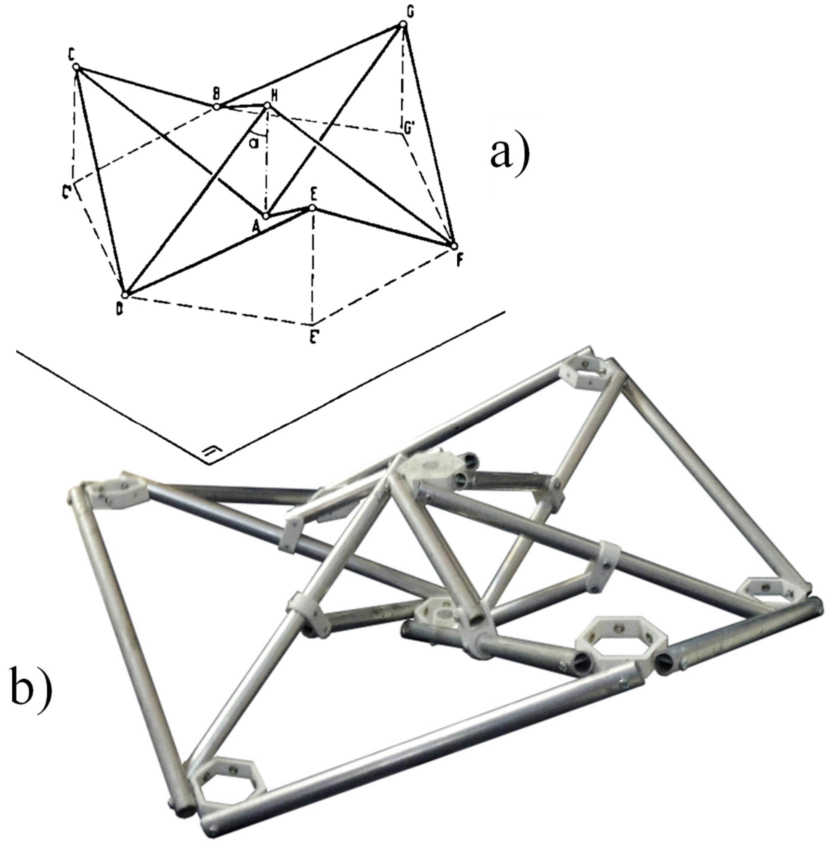

Figure 7.3 *Deployability of a hexagonal-base model: a) Calatrava Valls concept (1981), b) Rigidised scale model proposal.*

REFERENCES

Alegria Mira, L., 2014. Parametric structural assessment of deployable scissor systems. Optimising the Universal Scissor Component, PhD thesis, Vrije Universiteit Brussel, Brussels.

Alegria Mira, L., De Temmerman, N. & Preisinger, C., 2012. Structural optmisation of deployable scissor structures using new computational methods. *WIT Transactions on The Built Environment,* Issue 124, pp. 469-480.

Alegria Mira, L., Thrall, A. P. & De Temmerman, N., 2014. Deployable scissor arch for transitional shelters. *Automation in Construction,* Volume 43, pp. 123-131.

ATAKE INSTITUTE Co., Ltd., 2007a. *Katsuhito ATAKE INSTITUTE Co., Ltd. ARCHITECTS.* [Online]
Available at: http://www.atake-i.com/yokkaichi.htm
[Accessed 09 07 2019].

ATAKE INSTITUTE Co., Ltd., 2007b. *Katsuhito ATAKE INSTITUTE Co., Ltd. ARCHITECTS.* [Online]
Available at: http://www.atake-i.com/dejavu.htm
[Accessed 09 07 2019].

Atake, K., 1998. *Framework structure.* United States, Patent No. 5,761,871.

Atake, K., 2000. ATAKE's structure - new variations of the scissors technique. *WIT Transactions on The Built Environment,* Volume 47, pp. 143-154.

Autodesk Inc, 2021. *Inventor Support and Learning - Mechanism Status and Redundancies Reference.* [Online]
Available at: https://knowledge.autodesk.com/support/inventor/learn
[Accessed 01 01 2021].

Becher, K., 1977. *Large shelter umbrella.* United States, Patent No. 4,000,750.

Bouchard, P.-A., 2004. *Mobile Shelter Comprising an Umbrella-Like Collapsible Marquee.* WIPO (PCT), Patent No. 2,004,029,388.

Bouten, S., 2015. Transformable Structures and Their Architectural Application, M.Sc. thesis, Universiteit Gent, Department of Structural Engineering.

Bradley, R. A., Gohnert, M., Goliger, A. M. & Mistry, Y., 2016. Wind loading on catenary vault structures. *Journal of the South African Institution of Civil Engineering,* 58(4), p. 29–47.

Buchanan, C. & Gardner, L., 2019. Metal 3D printing in construction: a review of methods, research, applications, opportunities and challenges. *Engineering Structures,* Issue 180, p. 332-348.

Calatrava Valls, S., 1981. Zur Faltbarkeit von Fachwerken, PhD thesis, ETH Zurich, Zürich.

Calatrava, S., 1993. Sobre la plegabilidad de entramados. In: F. Escrig, ed. *Arquitectura transformable.* Sevilla: Escuela Técnica Superior de Arquitectura de Sevilla (E.T.S.A.S.), pp. 35-93.

Calvo López, J. & Sanz Alarcón, J. P., 2011. ARQUITECTURA PLEGABLE PARA UNA DÉCADA PRODIGIOSA. La obra de Emilio Pérez Piñero y la arquitectura de los años sesenta. *EGA Expresión Gráfica Arquitectónica,* Issue 17, pp. 114-127.

Carter, M. C., 1986. *Quick erection collapsible shelter.* United States, Patent No. 4,607,656.

Comité técnico AEN/CTN 305 Carpas y Estructuras Móviles, 2016. *UNE-EN 13782:2016 Temporary structure - Tents - Safety,* Madrid: AENOR Asociación Española de Normalización y Certificación.

Cook, N., 2007. *Designers' Guide to EN 1991-1-4 Eurocode 1: Actions on structures, general actions part 1–4. Wind actions..* Haig Gulvanessian ed. London: Thomas Telford Publishing.

De Temmerman, N., 2007. Design and Analysis of Deployable Bar Structures for Mobile Architectural Applications, PhD thesis, Vrije Universiteit Brussel, Brussels.

Elmokadem, A., Ekram, M., Waseef, A. & Nashaat, B., 2018. Kinetic Architecture: Concepts, History and Applications. *International Journal of Science and Research (IJSR),* 7(4), pp. 750-758.

Escrig Pallarés, F., 1984a. Estructuras espaciales de barras desplegables. *Informes de la Construcción,* 36(365), pp. 36-46.

Escrig Pallarés, F., 1984b. *Sistema modular para la construccion de estructuras espaciales desplegables de barras.* Spain, Patent No. 532,117.

Escrig Pallarés, F., 1993. Geometrías de las estructuras desplegables de aspas. In: F. Escrig, ed. *Arquitectura Transformable.* Sevilla: Escula Técnica Superior de Arquitectura de Sevilla (E.T.S.A.S.), pp. 95-124.

Escrig Pallarés, F. & Sánchez Sánchez, J., 2007a. *Arco desplegable de grandes dimensiones.* Spain, Patent No. 2,268,963.

Escrig Pallares, F. & Sánchez Sánchez, J., 2007b. *Nudo articulado espacial para mecanismos plegables de aspas.* Spain, Patent No. ES2,286,921.

Escrig, F., 2012. *Modular, ligero, transformable. Un paseo por la arquitectura ligera móvil.* Sevilla: Universidad de Sevilla, Secretariado de Publicaciones.

Escrig, F. & P. Valcarcel , J., 1986. Great size umbrellas solved with expandable bar structures. In: M. B. &. M. D. Bono, ed. *Proceedings of the First International Conference on Lightweight Structures in Architecture, LSA 86.* Sydney: Unisearch Limited, University of New South Wales, pp. 676-681.

Escrig, F., Pérez Valcárcel, J. & Sánchez, J., 1996. Deployable cover on a swimming pool in Seville. *Journal of the International Association for Shell and Spatial Structures: IASS,* 37(1), pp. 39-70.

Escrig, F., Valcárcel, J. P. & Sánchez, J., 1995. Deployable structures squared in plan: Design and construction. In: *Int. Conference on Spatial Structures: Heritage, present and future IASS.* Milán: International Association for Shell and Spatial Structures IASS, pp. 483-492.

Escrig, F., Valcárcel, J. P. & Sánchez, J., 1996. La cubierta desplegable de la piscina de San Pablo, de Sevilla. *Hormigón y acero,* Issue 199, pp. 85-114.

Fenci, G. E. & Currie, N. G., 2017. Deployable structures classification: A review. *International Journal of Space Structures,* 32(2), p. 112–130.

Fundación UCV - TECNIDEC S.A. - Grupo ESTRAN c.a., 2001 - 2004. *Grupo ESTRAN c. a. - Estructuras Transformables.* [Online]
Available at: http://www.grupoestran.com/portafolio/est_transformables/
[Accessed 26 10 2019].

Gantes, C., 1991. A Design Methodology for Deployable Structures , PhD thesis, Massachusetts Institute of Technology, Massachusetts.

Gantes, C., 2001. *Deployable Structures: Analysis and Design.* 2 ed. Southampton: WIT Press.

Gantes, C. J., 2011. Section 10.3: Deployable Structures. In: I. Mungan & J. F. Abel, eds. *Fifty Years of Progress for Shell and Spatial Structures, In celebration of the 50th Anniversary Jubilee of the IASS (1959-2009).* Madrid: International Association for Shell and Spatial Structures (IASS), pp. 373-390.

Gantes, C. J., Connor, J. J., Logcher, R. D. & Rosenfeld, Y., 1989. Structural analysis and design of deployable structures. *Computers & Structures,* 32(3/4), pp. 661-669.

Gantes, C. J., Tsouknaki, , D. N. & Kyritsas, S. C., 2000. Combining active and passive sub-structures insnap-through type deployable structures. In: S. Pellegrino & S. D. Guest, eds. *IUTAM·IASS Symposium on Deployable Structures: Theory and Applications.* Cambridge: Kluwer Academic Publishers, pp. 107-116.

Gendriesch, J., Schubert, J. & Prang, A., 2004. *Umbrella for protection from sun or rain has cloth mounted above radial arms whose angle is individually adjustable with respect to horizontal.* Germany, Patent No. 20,305,166.

Gómez Lizcano, D. E., 2012. Estructuras Móviles de Doble Curvatura con un Grado de Libertad, Master's thesis, Universidad Nacional de Colombia, Bogotá.

Gómez Lizcano, D. E., 2013. An expandable pendentive dome and polyhedral mechanisms using angulated scissors with sliding elements. In: F. Escrig & J. Sánchez, eds. *New Proposals for Transformable Architecture, Engineering and Design. In the Honor of Emilio Pérez Piñero.* Seville: STARBOOKS Structural Architecture, pp. 53-58.

Hanaor, A. & Levy, R., 2001. Evaluation of Deployable Structures for Space Enclosures. *International Journal of Space Structures,* 16(4), pp. 211-229.

Han, B. et al., 2019. Kinematic Characteristics and Dynamics Analysis of an Overconstrained Scissors Double-Hoop Truss Deployable Antenna Mechanism Based on Screw Theory. *IEEE Access,* Volume 7, pp. 140755-140768.

Haug, E., de Kermel, P. & Gélenne, P., 2003. Numerical Simulations for Wind Load Design of Large Umbrellas. In: M. Mollaert, ed. *Tensinet Symposium: Designing tensile architecture.* Brussels, Belgium.: Vrije Universiteit Brussel (VUB), pp. 108-117.

Hernandez Merchan, C. H., 1987. Deployable Structures, M.Sc. thesis, Massachusetts Institute of Technology, Massachusetts.

Hernández, C. H., 1988. ESTRUCTURAS TRANSFORMABLES ESTRAN 1. Estructura de barra transformable de figuración cuadrada. *TECNOLOGÍA Y CONSTRUCCIÓN,* 4(1), pp. 103-118.

Hernández, C. H., 1999. DESARROLLO DE ESTRUCTURAS TRANSFORMABLES: ESTRAN 1. *TECNOLOGÍA Y CONSTRUCCIÓN,* 15(1), pp. 7-36.

Hernández, C. H., 2013. *Estructuras transformables la experiencia del IDEC. SABER UCV.* [Online]
Available at: http://saber.ucv.ve/handle/123456789/3782

Hernández, C. H., 2014. Evolución de las tensoestructuras en Venezuela. *Revista entre rayas,* Tensoestructuras IV(106), pp. 38-55.

Hernández, C. H. & Cebrian, R., 2010. Bóvedas transformables: mejoras y desarrollos. *TECNOLOGIA Y CONSTRUCCION,* 26(III), pp. 45-55.

Hoberman Associates, Inc., 2012. *Hoberman Associates - Company profile and selected works: 1990 - 2012.* [Online]
Available at: http://www.hoberman.com/HobermanPortfolio.pdf
[Accessed 25 10 2019].

Hoberman, C., 1990. *Reversibly expandable doubly-curved truss structure.* United States, Patent No. 4,942,700.

Hoberman, C., 1991. *Radial Expansion/Retraction Truss Structures.* United States, Patent No. 5,024,031.

J. Meissl GmbH, 2019. *J. Meissl GmbH - Umbrella bar and weather protection concepts.* [Online]
Available at: https://www.meissl.com/en/umbrellabars
[Accessed 26 10 2019].

Kokawa, T., 1995. A trial of expandable arch. In: G. C. Giuliani, ed. *Proceedings of the IASS International Symposium. Spatial Structures: Heritage, Present and Future..* Milano, Italia: IASS International Association for Shell and Spatial Structures, pp. 501-510.

Kokawa, T., 1996. Scissors Arch with Zigzag-Cable Through Pulley-Joint. In: I. A. f. S. a. S. Structures., I. A. f. B. a. S. Engineering. & U. S. F. f. Bauwesen, eds. *Proceedings of CONCEPTUAL DESIGN OF STRUCTURE.* Stuttgart: Institut für Konstruktion und Entwurf II, pp. 868-875.

Kokawa, T., 1997. Cable Scissors Arch - Marionettic Structure. In: J. C. B. L. W. a. P. O. Chilton, ed. *Structural Morphology Towards the New Millennium, IASS International Colloquium.* Nottingham, UK: School of Architecture, University of Nottingham, pp. 107-114.

Konligo, 2019. *Konligo - Create, unfold, fascinate..* [Online]
Available at: https://www.konligo.com/
[Accessed 26 10 2019].

Koumar, A., De Temmerman, N., Tysmans, T. & Baudouin, H., 2019. *IMPROVED CONNECTION ELEMENT FOR TENT BEAMS.* EUROPEAN PATENT APPLICATION, Patent No. 3,553,258 A1.

Koumar, A. et al., 2014. Multi-criteria optimisation of a barrel vault structure for emergency relief. In: R. a. P. R. Brasil, ed. *Proceedings of the IASS-SLTE 2014 Symposium "Shells, Membranes and Spatial Structures: Footprints".* Brasilia, Brazil: International Association for Shell and Spatial Structures IASS.

Krishnapillai, A., 1992. *Deployable structures.* United States, Patent No. 5,167,100.

Kwan, A. & Pellegrino, S., 1994. A New Concept for Large Deployable Space Frames. *lnternationai,* 9(3), pp. 153-162.

Lynch, J. P., 1987. *Collapsible canopy structure.* United States, Patent No. 4,641,676.

Lynch, J. P., 1988. *Collapsible canopy with telescoping roof support structure.* United States, Patent No. 4,779,635.

Ma, C., Liew, J. R. & Vu, K., 2010. Multi-functional deployable protective shelters. *Journal of the International Association for Shell and Spatial Structures,* 51(166), pp. 271-279.

Michalski, A., Gawenat, B., Gelenne, P. & Haug, E., 2015. Computational wind engineering of large umbrella structures. *Journal of Wind Engineering and Industrial Aerodynamics,* Issue 144, pp. 96-107.

Michalski, A., Haug, E. & Bletzinger, K.-U., 2007. On the application of the Fluid- Structure Interaction Simulation for the design of umbrella structures. In: E. Oñate & B. Kröplin, eds. *International Conference on Textile Composites and Inflatable Structures STRUCTURAL MEMBARNES 2007.* Barcelona: CIMNE_ International Centre for Numerical Methods in Engineering.

Michalski, A. et al., 2011. alidation of the computational fluid–structure interaction simulation at real-scale tests of a flexible 29 m umbrella in natural wind flow. *Journal of Wind Engineering and Industrial Aerodynamics,* Issue 99, pp. 44-413.

Morales, J., Sánchez, J. & Escrig, F., 1996. Geometry of deployable-structures generated by computer aided design. In: F. Escrig & C. A. Brebbia, eds. *Mobile and rapidly assembled structures II: Second International Conference on Mobile and Rapidly Assembled Structures, MARAS 96.* Southampton: Computational Mechanics Publications Ltd., pp. 253-258.

Mukogawa Mowen's University, 2005-2014. *Mukogawa Women's University Department of Architecture.* [Online]
Available at: http://arch.mukogawa-u.ac.jp/education/education2014/ArchitecturalDesignStudio_14M02_III.html
[Accessed 09 07 2019].

Nagaraj, B., Pandiyan, R. & Ghosal, A., 2009. Kinematics of pantograph masts. *Mechanism and Machine Theory,* 44(4), p. 822–834.

Otto, F., 1972. *Wandelbare Dächer / Convertible Roofs.* IL5 ed. Stuttgart: Institute for Lightweight Structures (IL), University of Stuttgart.

Otto, F. & Rasch, B., 1995. *Finding Form - Towards an Architecture of the Minimal.* Sabine Schanz ed. Stuttgard: Edition Axel Menges.

Peake, G. H., 1966. *Collapsible hyperbolic paraboloid umbrella.* United States, Patent No. 3,252,469.

Pellegrino, S. & Guest, S. D., 2000. *IUTAM-IASS Symposium on Deployable Structures: Theory and Application.* Southampton: Kluwer Academic Publishers.

Pérez Belda, E. A., 2013. The structures of Emilio Pérez Piñero. Evolution and types. In: F. Escrig & J. Sánchez, eds. *New Proposals for Transformable Architecture, Engineering and Design. In the Honor of Emilio Pérez Piñero.* Seville: STARBOOKS Structural Architecture, pp. 31-39.

Pérez Piñero, E., 1961. *Estructura reticular esterea plegable.* Spain, Patent No. 266,801.

Pérez Valcárcel, J., 2014. Félix Escrig y las estructuras desplegables. *Dijous a l'ACE: Associació de Consultors d'Estructures,* 49(3-18).

PFEIFER Holding GmbH & Co. KG, 2015. *PFEIFER-Zugglieder / PFEIFER-Tension Members.* [Online]
Available at: https://www.pfeifer.info/out/assets/PFEIFER_TENSION-MEMBERS_BROCHURE_EN.PDF
[Accessed 01 12 2020].

Piker, D., 2013. Kangaroo: Form Finding with Computational Physics. *Architectural Design,* 83(2), pp. 136-137.

Preisinger, C., 2013. Linking Structure and Parametric Geometry. *Architectural Design,* 83(2), pp. 110-113.

Preisinger, C., 2016. *PARAMETRIC STRUCTURAL MODELING: Karamba User Manual for Version 1.2.2.* [Online]
Available at: https://www.food4rhino.com/app/karamba3d

Prusmack, A. J., 2007. *Articulating hub assembly.* United States, Patent No. 2007/0084493 A1.

Puertas del Rio, L., 1991. Space frames for deployable domes. *Bulletin of International Association for Shell Sstructures IASS,* 32(2), pp. 107-113..

Ramos Jiménez, R., 2013. New geometry deployabe structure of X-Frame. In: F. Escrig & J. Sánchez, eds. *New Proposals for Transformable Architecture, Engineering and Design. In the Honor of Emilio Pérez Piñero.* Seville: STARBOOKS Structural Architecture, pp. 89-92.

Ramos Jiménez, R. J., 2015. *Cubierta desplegable de aspas.* Spain, Patent No. 2,523,425.

Rasch, B., 1989. *Protection umbrella with at least one protecting element.* WIPO (PCT), Patent No. 1,989,000,225.

Rasch, B., 2010. *Collapsible screen with tensioning device.* Europe, Patent No. 2,153,742.

Rasch, B. & Bradatsch, J., 1995. *Sunshade, particularly for stationary installation.* United States, Patent No. 5,441,068.

Rasch, B. & Bradatsch, J., 2007. *Roof-like screen.* Europe, Patent No. 1,820,416.

Robus Shelters Inc., 2019. *ROBUS SYSTEM.* [Online]
Available at: https://robusinc.com/
[Accessed 08 11 2019].

Rodriguez, C. & Chilton, J. C., 2004. Transformable and Transportable Architecture with Scissor Structures. In: F. Klassen & R. Kronenburg, eds. *Transportable Environments 3: Proceedings of the 3rd International Conference on Portable Architecture and Design.* Toronto: Ryerson University, pp. 87-93.

Rodriguez, C. & Chilton, J. C., 2006. Transformable and Transportable Architecture with Scissor Structures. In: R. Kronenburg & F. Klassen, eds. *Transportable Environments 3: Theory, context, design and technology.* Abingdon and New York: Taylor & Francis, pp. 145-157.

Roovers, K. & De Temmerman, N., 2014b. A classification of singly curved deployable scissor grids. In: R. Brasil & R. Pauletti, eds. *Proceedings of the IASS-SLTE 2014 Symposium "Shells, Membranes and Spatial Structures: Footprints".* Brasilia: International Association for Shell and Spatial Structures (IASS).

Roovers, K. & De Temmerman, N., 2014b. The design of a foldable triangulated scissor grid for single-curvature surfaces. In: N. De Temmerman & C. A. Brebbia, eds. *4th International Conference on Mobile, Adaptable and Rapidly Assembled Structures (MARAS2014).* Ostend: WIT Press, pp. 195-206.

Roovers, K. & De Temmerman, N., 2018. *A foldable scissor module for doubly curved scissor grids.* WIPO [PCT], Patent No. 2,018,167,247 A1.

Rosenfeld, Y. & Logcher, R. D., 1988. New Concepts for Deployable-Collapsable Structures. *International Journal of Space Structures,* 3(1), pp. 20-32.

Sánchez-Cuenca, L., 1996a. Geometric models for expandable structures. *Transactions on the Built Environment,* Volume 24, pp. 93-102.

Sánchez-Cuenca, L., 1996b. Geometría extensible para estructuras con barras en" X". *Scientia gerundensis,* Issue 22, pp. 153-159.

Sánchez-Cuenca, L., 1996c. Cúpula extensible. *RE: revista de edificación,* Volume 23, pp. 43-47.

Sánchez, J. & Escrig, F., 1997. Introducción general a la arquitectura móvil y de rápido montaje. *STAR: Structural Architecture,* Issue 1, pp. 5-23.

Sánchez, J., Escrig, F. & Valcárcel, J. P., 1996. The adventure of covering a swimming-pool with an X-frame structure. *WIT Transactions on the Built Environment,* Volume 24, pp. 113-122.

Singulark Arquitectura Y Estructuras Singulares Sl., 2014. *ArkiDes.* [Online]
Available at: http://arkides.es/
[Accessed 09 07 2019].

SL-Rasch GmbH Special & Lightweight Structures, 2018. *SL-Rasch - Seeking Excellence in Architecture.* [Online]
Available at: https://sl-rasch.de/
[Accessed 26 10 2019].

StructureLab GmbH, 2006-2010. *STRUCTURELAB® S1 Schirmsystem.* [Online]
Available at: sunshade.structurelab.com
[Accessed 20 11 2019].

Tagawa, H., Sugiura, N. & Kodama, S., 2015. *Structural Analysis of Deployable Structure with Scissor-like-element in Architectural Design Class.* Zurich, IABSE Symposium Report: Nara 2015, Elegance in Structures, pp. 1-8.

Tchako, A., 2008. *Union College Mechanical Engineering MER 312: Dynamics and Kinematics (of Mechanisms).* [Online]
Available at:
www.engineering.union.edu/~tchakoa/mer312/Lectures/Lecture%202.pdf
[Accessed 14 12 2019].

Technical Committee CEN/TC250, Structural Eurocode, 2005. *EN 1991-1-4 (English): Eurocode 1: Actions on Structures - Part 1-4: General Actions - Wind Actions.* Brussels: European Committee for Standardization CEN.

Technical Committee CEN/TC250, Structural Eurocodes, 2003. *EN 1991-1-3 (English): Eurocode 1: Actions on structures - Part 1-3: General actions - Snow loads.* Brussels: European Committee for Standardization CEN.

Technical Subcommittee B/525/1, Actions (loadings) and basis of design, 2010. *National Annex to BS EN 1991-1-4:2005, Eurocode 1 - Actions on structures. Part 1-4: General actions - Wind actions.* London: British Standards Institution BSi.

Technical Subcommittee B/525/1, Actions [loadings] and basis of design, 1997. *BS 6399-2 - Loading for buildings - Part 2: Code of practice for wind loads.* London: British Standards Institution BSi.

Ten Fold Engineering Limited, 2018. *Ten Fold Technology.* [Online]
Available at: http://tenfoldengineering.com/
[Accessed 09 07 2019].

Villate, M. C., 2008. *Estructuras no convencionales en arquitectura.* 1st ed. Bogotá: Universidad Nacional de Colombia.

Watkins, G. S. B. S., 1914. *Improvements in Supports for Tents, Marquees, Temporary Bridges and other Portable Structures.* United Kingdom, Patent No. 7755.

Willim, H.-D., Dr. Rasch, B. & Bär, F., 2004. *Foldable cover for large areas.* Europe, Patent No. 1,387,025.

Zeigler, T. R., 1976. *Collapsible self-supporting structure.* United States, Patent No. 3,968,808.

Zeigler, T. R., 1981. *Collapsible self supporting structures and panel and hub therefor.* United States, Patent No. 4,290,244.

Zeigler, T. R., 1985. *Display panel mounting clip.* United States, Patent No. 4,512,097.

Zeigler, T. R., 1987. *Portable shelter assemblies.* United States, Patent No. 4,689,932.

Zeigler, T. R., 2000. *Folding frame system with foldable leg assembly and method of erecting a folding frame system.* United States , Patent No. 6,141,934.

Zhao, J.-S., Chu, F. & Feng, Z.-J., 2009. The mechanism theory and application of deployable structures based on SLE. *Mechanism and Machine Theory,* 44(2), pp. 324-335.